Optimisation of high-value isoprenoid production in plants
Potential strategies and insight into carotenoid sequestration

Marilise Nogueira

This thesis was submitted for the degree of Doctor of Philosophy at

Royal Holloway University of London, September 2013

Declaration of Authorship

I hereby declare that the work presented in this thesis is the original work of the author unless otherwise stated. Original material used in the creation of this thesis has not been previously submitted either in part or whole for a degree of any description from any institution.

_____

Marilise Nogueira

Abstract

Carotenoids and ketocarotenoids are isoprenoid molecules, which represent one of the most widespread classes of natural pigments, found in animals, plants and microorganisms. Moreover, they have valuable antioxidant properties. Their health benefits and colorant aspects have led to attempts to elevate their level in foodstuffs.

In the present study, several metabolic engineering strategies were tested in order to enhance the levels of high-value carotenoid and ketocarotenoid compounds, such as lycopene, β-carotene, canthaxanthin and astaxanthin, in tomato and tobacco plants. Biosynthetic bacterial pathway genes have been overexpressed independently (GGPP synthase (*Crt*E), phytoene synthase (*Crt*B) and phytoene desaturase (*Crt*I)) and in combination (*Crt*E+B, *Crt*E+I, *Crt*B+I and β-carotene hydroxylase and ketolase (*Crt*Z+W)), with different promoters (for *Crt*B, *Crt*I and *Crt*B+I) or in association with transcription factors (Phytochrome-interacting factor 5 (*Crt*Z+W+PIF5) and Arabidopsis Response Regulator 14 (*Crt*Z+W+ARR14)). The effects of these different strategies on the plant metabolism and especially on carotenoid formation, sequestration and the activation of regulation mechanisms were studied.

The combination of the two genes *Crt*B and *Crt*I, in their hemizygous state, had a synergistic effect on the production of carotenoids and the expression of *Crt*Z+W+ARR14 increased the levels of ketocarotenoids in the plants. The important features for the design of metabolic engineering strategies were highlighted. Moreover, regulatory mechanisms that operate across multiple levels of cellular regulation, including transcription, protein localisation, metabolite levels, cell or tissue type, and organelle/sub-organelle structure and organisation were revealed. It was demonstrated how changes to chromoplast and sub-chromoplast structures, such as crystal formation, plastoglobule and membrane composition/structures can arise in response to changes in metabolites. A new carotenoid regulation mechanism at the sub-organellar level was discovered and a schematic model was proposed.

Acknowledgments

Finding the right PhD project was a rather long process, as I wanted it to be interesting, stimulating and ambitious. I do not regret the choice I made three years ago, as this PhD subject within Prof. Fraser's lab, gave me all the challenges and excitement I pursued.

I would like to thank my supervisor Prof. Paul Fraser for the opportunity to work within an exciting European project, METAPRO, in an excellent international lab. I am grateful for his enthusiasm and his involvement in my project. Our scientific conversations were the base of all the work produced in this study. Thank you for helping me, challenging and trusting me. I also thank Prof. Peter Bramley, my second supervisor, for his pertinent questions, which helped me broaden my horizons, and Dr Genny Enfissi for her guidance during these three years.
I would like to thank all the members of this lab from my 1st year to the last one, who all have, in different ways, made my journey easier.

I would also like to acknowledge Dr. Norihiko Misawa for providing research material and Dr Devoto, my adviser.

To the people in my life, who made this possible: My fiancé, Guillaume, who always supports and encourages me to pursue what I believe in, even for the hardest decision; my sisters, who always have faith in me; my parents, who gave me the opportunity to study for so long and the rest of my (extended) family for being such great people, I thank you all.

I am proud and glad of this achievement and I hope that is only the beginning...

Marilise

Table of contents

List of figures

11

13

List of tables

List of abbreviations

ABA	Abscisic acid
Abs	Absorbance
AC	Ailsa craig
APRR2	Two-component response regulator-like
ARR14	Arabidopsis Response Regulator 14
ATP	Adenosine-5'-triphosphate
BAP	6-Benzylaminopurine
BSA	Bovine serum albumin
Br	Breaker stage
C	Carbon
c	Celsius
Ca	Chlorophyll a concentration
CAR	Carotenoid
35S	Cauliflower mosaic virus 35S promoter
Cb	Chlorophyll b concentration
CCD	Carotenoid cleavage dioxygenase
^{3}Chl*	Triplet state chlorophyll
ChE	Chromoplast envelope
CHRC	chromoplast-specific carotenoid-associated protein C
CHRD	chromoplast-specific carotenoid-associated protein D
CoA	Coenzyme A
CRTB	Bacterial phytoene synthase
CRTE	Bacterial GGPP synthase
CRTI	Bacterial phytoene desaturase
CRTISO	Carotenoid isomerase
CRTO	Bacterial β-carotene hydroxylase
CRTR	Bacterial carotene hydroxylase
CRTR-B1	β-carotene hydroxylase 1
CRTR-B2	β-carotene hydroxylase 2
CRTW	Bacterial β-carotene ketolase
CRTZ	Bacterial β-carotene hydroxylase
CRTY	Bacterial lycopene cyclase
Ct	Cycle threshold
Cv	Cultivar
Cx+c	Total carotenoid concentration
CYC-B	Fruit specific lycopene β-cyclase
CYP175A1	Bacterial cytochrome P450 β-carotene hydroxylase
CYP97A	Haem-containing cytochrome P450 β-ring hydroxylase
CYP97C	Haem-containing cytochrome P450 ε-ring hydroxylase
DDB1	Damaged DNA binding protein 1
DET1	De-etiolated 1
DGDG	Digalactosyldiacylglycerol
dH$_2$O	Distilled water

DMAPP	Dimethylallyl diphosphate
DNA	Deoxyribonucleic acid
dsDNA	Double stranded DNA
DTT	Dithiothreitol
DW	Dry weight
DXP	1-Deoxy-D-xylulose 5-phosphate
DXS	1-Deoxy-d-xylulose 5-phosphate synthase
DXR	1-Deoxy-D-xylulose 5-phosphate reductoisomerase
EDTA	Ethylenediaminetetraacetic acid
EMS	Ethyl methane sulfonate
EPA	Environmental Protection Agency
F	Fraction
FAD	Flavin adenine dinucleotide
FAOSTAT	Food and Agriculture Organisation of the United Nations
FDA	Food and Drug Administration
FLIM	Fluorescence lifetime imaging microscopy
FPP	Farnesyl diphosphate
FRAP	Fluorescence recovery after photobleaching
FRET	Fluorescence resonance energy transfer
FW	Fresh weight
GA3P	Glyceraldehyde-3-phosphate
GA	Gibberellic acid
GC-MS	Gas Chromatography Mass Spectrometry
GFP	Green Fluorescent Protein
GGPP	Geranyl geranyl diphosphate
GGPPS	Geranyl geranyl diphosphate synthase
GM	Genetically modified
GMO	Genetically modified organism
GPP	Geranyl diphosphate
GPPS	Geranyl diphosphate synthase
GUS	β-Glucuronidase enzyme
h	Hour
H_2O_2	Hydrogen peroxide
HCl	Hydrochloric acid
HDS	1-Hydroxy-2-methyl-2-(E)-butenyl 4-phosphate synthase
HDR	4-Hydroxy-3-methylbut-2-enyl diphosphate reductase
HMG-CoA	3-Hydro-3-methylglutaryl Coenzyme A
HO˙	Hydroxyl radical
Hp-1	High pigment 1
Hp-2	High pigment 2
Hp-3	High pigment 3
HPLC	High performance liquid chromatography
HSP21	Heat shock protein 21
IPP	Isopentenyl diphosphate
IUPAC	International Union of Pure and Applied Chemistry

LB	Luria Broth medium
LCYE	Lycopene ε-cyclase
LCYB	Lycopene β-cyclase
LC-MS	Liquid chromatography mass spectrometry
MbS	Membranous sac
MEP	2-C-Methyl-D-erythritol 4-phosphate
MEcPP	Methylerythritol cyclodiphopshate
Min	Minute
MG	Mature green stage
MGDG	Monogalactosyldiacylglycerol
MVA	Mevalonate pathway
NAA	1-Naphthaleneacetic acid
NADPH	Nicotinamide Adenine Dinucleotide Phosphate Hydrogen
NCBI	National Centre for Biotechnology
NCED	9-*Cis*-epoxycarotenoid dioxygenase
NPQ	Non photochemical quenching
NXS	Neoxanthin synthase
$^1O2*$	Singlet oxygen
$O_2^{-\cdot}$	Superoxide anion
OD	Optical density
Pb	Lycopene cyclase promoter (*S. galapagense*)
PB	Phosphate buffer
PC	Phosphatidylcholine
PCR	Polymerase chain reaction
PDA	Photo-diode array
PDS	Phytoene desaturase
PE	Phosphatidylethanolamine
PG	Plastoglobule
PG promoter	Polygalacturonase promoter (*S. lycopersicum*)
PGL35	Plastoglobule PGL35 Plastoglobulin
PIF	Phytochrome-interacting factor family
PIF5	Phytochrome-interacting factor 5
PPPP	Pre-phytoene pyrophosphate
PS	Phosphatidylserine
PSI	Photosystem I
PSII	Photosystem II
PSBA	Photosystem II protein D1
PSY-1	Fruit specific phytoene synthase 1
PSY-2	Phytoene synthase 2
PVDF	Polyvinylidene fluoride
qPCR	Quantitative PCR
QTL	Quantitative trait loci
RAP2.2	Ethylene response transcription factor
RbcL	RuBisCO large subunit
RC	Remaining of crystals

RI	Retention index
RNA	Ribonucleic acid
RNAi	RNA interference
RO˙	Alkoxy radical
ROS	Reactive oxygen species
RP	Reverse phase
RT-PCR	Reverse transcription PCR
RTqPCR	Quantitative real time reverse transcription
RuBisCO	Ribulose 1,5-bisphosphate carboxylase/oxygenase
SAP	Shrimp Alkaline Phosphate
SD	Standard deviation
SDG8	Histone methyltransferase
SDS	Sodium dodecyl sulphate
SDS-PAGE	SDS polyacrylamide gel electrophoresis
Sec	Second
SIERF6	Ethylene response factor
SSU	Small subunit
sp	Species
T_0	Primary generation
T_1	Second generation
TAG	Triacylglycerol
TAP	Tandem Affinity Purification
TB	Transfer buffer
TEM	Transmission electron microscopy
Thp	Thylakoid plexus
TFA	Trifluoroacetic
TIC40	Chloroplast inner envelope membrane translocon complex protein
TILLING	Targeting Induced Local Lesions IN Genomes
TLC	Thin layer chromatography
Tm	Melting temperature
TOC75	Chloroplast outer envelope membrane translocon complex protein
Tris	Tris-hydroxymethyl-aminomethane
tp	Transit peptide
UPLC	Ultra High Performance Liquid Chromatography
USDA	U.S. Department of Agriculture
UTR	Untranslated regions
V	Volt
VDE-1	Violaxanthin de-epoxidase
WT	Wild-type
X-Gluc	5-Bromo-4-chloro-3-indolyl-β-D-glucuronic acid
ZEP-1	Zeaxanthin epoxidase
Z-ISO	15-C*is*-ζ-carotene isomerase

Chapter I: Introduction

1.1 Isoprenoids in plants

Isoprenoids are mainly designated as secondary metabolites, a wide group of compounds, which includes alkaloids and phenolics. Secondary metabolites were historically described as not directly essential for plant cell life (Theis and Lerdau, 2003), but can also be defined as compounds whose biosynthesis is restricted to selected plant groups (Pichersky and Gang, 2000). The majority of these compounds are involved in plant-environment interactions (Sheludko, 2010). It is considered that the ability to synthesise secondary metabolites has been selected in different lineages during evolution, when a specific metabolite or type of metabolites were required to address precise functions (Pichersky and Gang, 2000). Concurrently, it is also typically found that secondary metabolite formation is associated with a specialised type of tissue or cell within the tissues. Some other isoprenoids, such as phytohormones, are involved in essential plant functions and are therefore designated as primary metabolites.

The isoprenoids are the largest group of secondary metabolites (ca. 50,000 compounds) with a wide range of structural and functional diversity (Vranova et al., 2012). However, they are all biosynthetically derived from the same C_5 unit, isopentenyl diphosphate (IPP). IPP can be synthesised via two distinct pathways, the mevalonate (MVA) pathway in the cytosol and mitochondria and the 2-C-methyl-D-erythritol 4-phosphate (MEP) pathway in the plastid (Figure 1-1). The compartmentalisation of the isoprenoid pathway is unique to the plants and it is thought to be essential for the interactions of plants with their environment (Hemmerlin et al., 2012). The IPP is interconverted into dimethylallyl diphosphate (DMAPP) by isopentenyl diphosphate isomerase. DMAPP is then elongated into geranyl diphosphate (GPP), farnesyl diphosphate (FPP) and geranylgeranyl diphosphate (GGPP) by addition of one, two or three IPP units. Several isoprenoid families exist. They are distinguished by the number of carbons of the isoprenoid molecules and the identity of the precursor utilised for their biosynthesis. They consist of monoterpenes (C_{10}, built from GPP), sesquiterpenes (C_{15}, FPP), diterpenes (C_{20}, GGPP), triterpenes (C_{30}, FPP) and carotenoids (C_{40}, GGPP) (Figure 1-2). It is believed that GPP and all-*trans*-FPP biosynthesis occur exclusively in the plastid and

the cytosol, respectively. Exchanges between plastid and cytosol compartments have been described (Hemmerlin et al., 2012) and are represented in Figure 1-2.

Figure 1-1 Overview of isoprenoid biosynthesis and compartmentalisation in plant cells (adapted from Bouvier et al., 2005; Vranova et al., 2013)

Arrows indicate either single or multiple enzymatic steps. Solid-line arrows correspond to the main isoprenoid pathway, dashed-line arrows to related pathways, and red arrows to cross-membrane transport. HMG-CoA, 3-hydroxy-3-methylglutaryl CoA; MVA, mevalonate; IPP, isopentenyl diphosphate; DMAPP, dimethylallyl diphosphate; GPP, geranyl diphosphate; FPP, farnesyl

diphosphate; GGPP, geranylgeranyl diphosphate; GA3P, glyceraldehyde 3-phosphate; DXP, 1-deoxy-D-xylulose. Mitochondrion and chloroplast drawings were adapted from the websites http://www.rsc.org/chemistryworld/News/2010/August/27081001.asp and http://thebuildingblockof biology.wordpress.com/category/my-important-best-friend-the-plant-cell/chloroplast/, respectively.

Isoprenoids have an impressive scope of functions. They are involved in plant growth and survival via the phytohormones (gibberellic acid, abscisic acid, etc.); in photosynthesis via the carotenoids, chlorophylls and plastoquinones; in respiration via the ubiquinones; and in membrane structure via the phytosterols (Aharoni et al., 2005). Volatile isoprenoid compounds play an important role in defence, but also in attraction for the plants via plant-insect, plant-pathogen, and plant-plant interactions (Dudareva et al., 2004; Dudareva et al., 2013). Isoprenoids also include natural pigments, flavours and fragrances that are of commercial importance. One of the most commercially attractive roles of some isoprenoids is their medicinal properties, which are utilised by humans, as nutraceuticals, anti-carcinogenic and antimalarial medicines (Sinensky, 2000; Lewinsohn et al., 2001; Galili et al., 2002; Rodriguez-Concepion, 2004; Sun-Waterhouse, 2011). Carotenoid and ketocarotenoid compounds are of particular interest due to their natural pigmentation and their antioxidant activities (Fraser and Bramley, 2004; Krinsky and Johnson, 2005; Peñuelas and Munné-Bosch, 2005; Zhu et al., 2013).
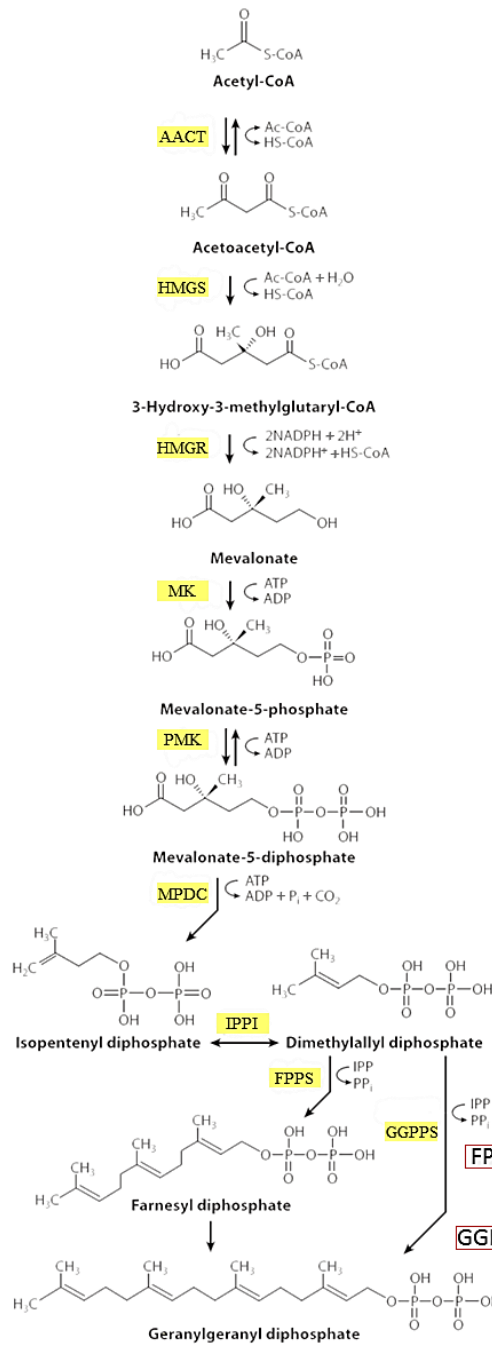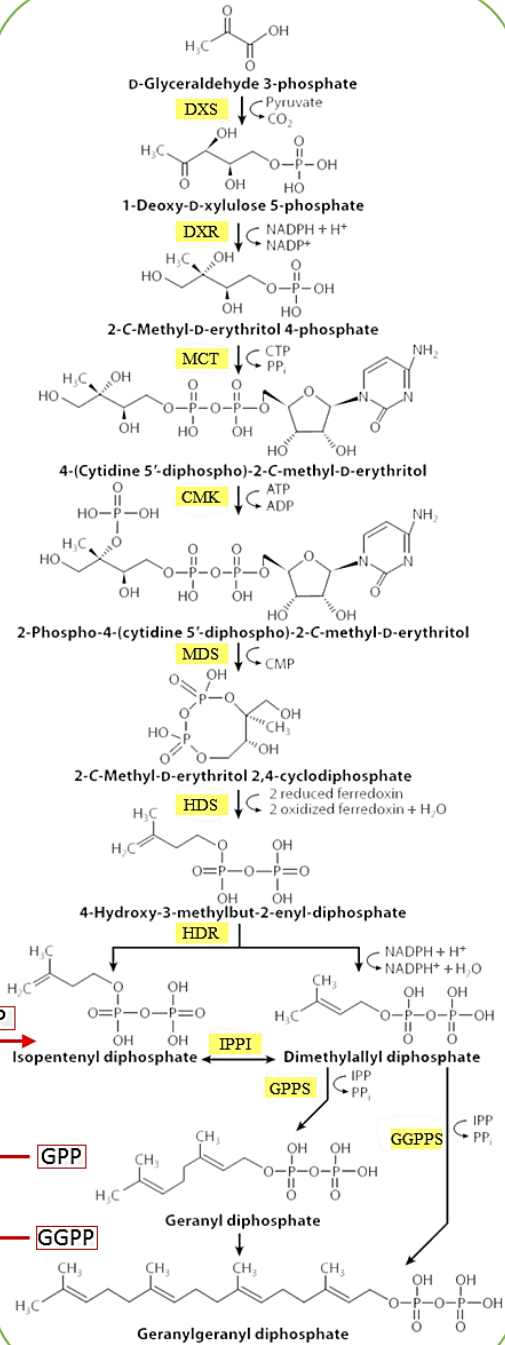
Figure 1-2 MVA and MEP pathways in plants (adapted from Hemmerlin, 2013; Vranova et al., 2013)

In plants, isopentenyl diphosphate (IPP) and its chemically active allylic isomer dimethylallyl diphosphate (DMAPP) are synthesised either by the cytosolic MVA pathway or by the plastidial MEP pathway. Substrates and enzymes of the MVA pathway are as follows: Ac-CoA, acetyl-coenzyme A;

HS-CoA, reduced coenzyme A; AACT, acetoacetyl-coenzyme A thiolase; HMGS, 3-hydroxy-3-methylglutaryl-coenzyme A synthase; HMGR, 3-hydroxy-3-methylglutaryl-coenzyme A reductase; MK, mevalonate kinase; PMK, phosphomevalonate kinase; MPDC, diphospho-mevalonate decarboxylase. Enzyme of the MEP pathway are as follows: DXS, 1-deoxy-D-xylulose 5-phosphate synthase; DXR, 1-deoxy-D-xylulose 5-phosphate reductoisomerase; MCT, 2C-methyl-D-erythritol 4-phosphate cytidyltransferase; CMK, 4-diphosphocytidyl-2C-methyl-D-erythritol kinase; MDS, 2C-methyl-D-erythritol 2,4-cyclodiphosphate synthase; HDS, 1-hydroxy-2-methyl-2-(E)-butenyl 4-diphosphate synthase; HDR, 1-hydroxy-2-methyl-2-(E)-butenyl 4-diphosphate reductase. IPPI, isopentenyl diphosphate isomerase; GPPS, geranyl diphosphate synthase; GGPPS, geranylgeranyl diphosphate synthase; Pi, orthophosphate; PPi, pyrophosphate. Red arrows correspond to cross-membrane transport and the transporters are depicted as red dots.

1.2 Carotenoids and ketocarotenoids

1.2.1 Structure and nomenclature

Carotenoids are biosynthesised in the plastids, by the tail-to-tail linkage of two geranylgeranyldiphosphate molecules (GGPP, C_{20}), which represent a total of eight IPP units. All carotenoids and ketocarotenoids are derived from this C_{40} skeleton molecule. It can be modified by (i) desaturation, (ii) cyclisation, (iii) addition of oxygen-containing functional groups (hydroxy (OH), epoxy, aldehyde (CHO), keto (C=O), carboxy (CO_2H), carbomethoxy (CO_2Me) and methoxy (OMe) groups), (iv) chain degradation or (v) chain extension. The acyclic carotenoids are called carotenes and those containing one or more oxygen functions are known as xanthophylls. The carotenoids harbouring a keto group are named ketocarotenoids and apocarotenoids are the cleavage products of carotenoid molecules catalysed by CCDs (carotenoid cleavage dioxygenases). Most commonly, carotenoids are described with their trivial names. However, it is recommended, as described in the IUPAC-IUB rules, to use the stem name carotene, preceded by the Greek-letter prefixes that designate the two end groups (Britton, 1995; Weedon and Moss, 1995). Seven possible end groups exist but only four are found in higher plants (ψ, β, ε, κ). The carotenoid hydrocarbon numbering scheme along with nomenclature examples of the acyclic lycopene and cyclic β-carotene, zeaxanthin and canthaxanthin are illustrated in Figure 1-3. In this study, trivial names will be used for the sake of clarity.
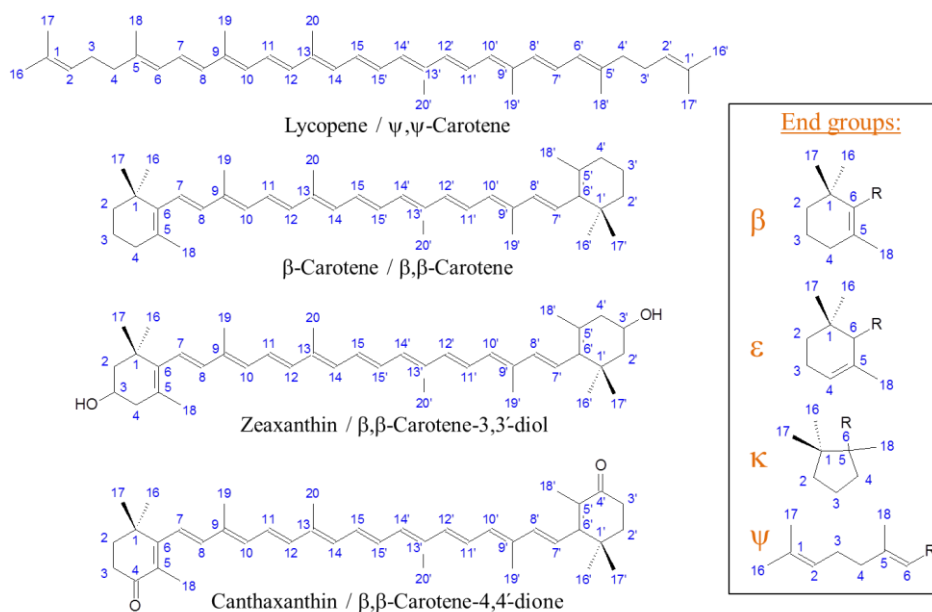
Figure 1-3 Nomenclature and numbering scheme of carotenoids

Names are given as following: trivial / IUPAC-IUB nomenclature. Only the end groups found in higher plants are represented.

Moreover, details of carotenoid structure (spatial orientation) are often given by specifying the geometrical isomer of the carbon-carbon double bonds of the molecule. Indeed, the four single bonds of each C=C double bond lie in the same plane. Consequently, each double bond of carotenoid polyene chains can exist in two forms, which are the *trans* (latin for "on the opposite side") and *cis* (latin for "on this side of") configurations. The *cis* configuration indicates that the substituent groups of the double bond are on the same side of the double bond. In a *trans* configuration, they are of each side of the double bond (Figure 1-4, a). The *cis* isomers are usually less stable thermodynamically compared to the *trans* form, since the presence of a *cis* double bond induces greater steric effects between hydrogen atoms and/or methyl groups. Therefore, most carotenoids in nature have predominantly an all-*trans* form (Britton, 1995). Another nomenclature is used to represent these spatial organisations: Z (from the German zusammen = together) and E (from the German entgegen = opposite). In this case, the Z and E configuration depend on the order of priority of the substituents on each carbon atom of the double bond. The highest priority corresponds to the substituent with the highest atomic numbers. If the two substituents with the highest priority are on the same side of the C=C bond, the geometry is assigned as Z. When they are at opposite sides, it corresponds to an E

26

configuration (Figure 1-4, b). In carotenoids, the *trans* and *cis* configurations are usually equivalent to E and Z, respectively, although some exceptions exist. (Britton, 1995; Weedon and Moss, 1995).
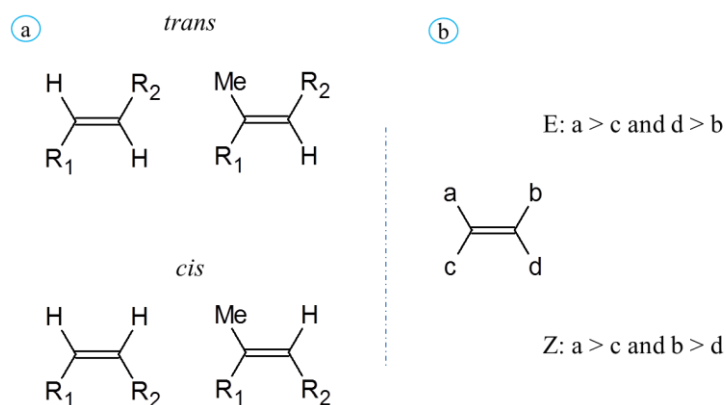
Figure 1-4 Geometric isomers

Trans/cis configurations are represented in a, E/Z configurations in b. Substituents priority order is indicated in b, as explained in section 2.1.

The central part of carotenoid molecules is characterised by a long system of alternating double and single bonds, which constitutes a conjugated system (Figure 1-3). The π-electrons are effectively delocalised over the entire length of the polyene chain, which makes it a highly reactive electro-rich system. This gives distinctive light-absorbing properties to the carotenoid molecules, which are influenced by the number of conjugated double bonds. Extending a conjugated system with more unsaturated bonds will tend to shift absorption to longer wavelengths. The polyene chain of carotenoids, composed of seven or more double bonds, delivers the ability to absorb light in the visible spectrum. Consequently, yellow, orange and red colours are produced (Britton, 1995; Weedon and Moss, 1995). When the polyene chain absorbs wavelengths in the visible range, it is termed a chromophore. The polyene chain also confers antioxidant properties to carotenoid molecules (Britton, 1995), which are further discussed in section 1.2.5.

1.2.2 Distribution of carotenoids

Carotenoid composition varies widely between plants and within plant tissues. The production of carotenoids occurs in almost all types of plastids, except in the

proplastid, which is the undifferentiated progenitor of plastids (Figure 1-5) (Howitt and Pogson, 2006).
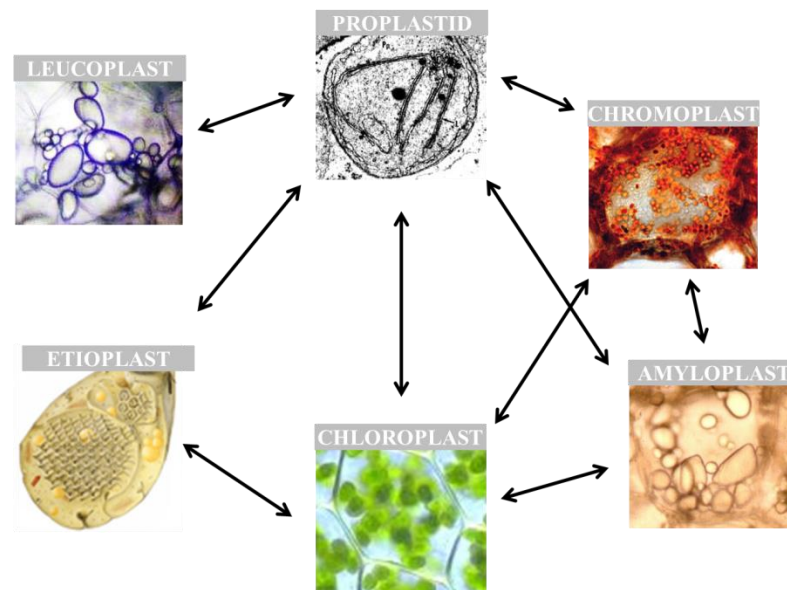
Figure 1-5 The plastid family (simplified)

The arrows represent a possible conversion/differentiation between two types of plastids. Proplastid (undifferentiated plastid), leucoplast (colourless plastid), chromoplast (pigment biosynthesis and storage plastids), amyloplast (starch-storing plastid), chloroplast (photosynthetic plastid) and etioplast (dark-grown precursor of the chloroplast). Pictures are not to scale, they were adapted from the following websites, respectively: www.skidmore.edu/academics/biology/plant_bio/photos /photos /cellbio.html; www.macroevolution.net/leucoplasts.html#.UfftC22YdX4; http://shivecellproj.weebly .com/chromoplast.html; www.biologie.uni-hamburg.de/b-online/library/webb/BOT410/anatweb/ pages /ORPlastids-1.htm; www. funsci. com/fun3_en/guide/guide3/micro3_en.htm; www.kmle.co.kr.

Chloroplasts are found in photosynthetic tissues. Their carotenoid composition consists of lutein (40-50% of the total), β-carotene (25-30%), violaxanthin (15%) and neoxanthin (15%). Small amounts of other carotenoids such as zeaxanthin and ζ-carotene can also be found (Young, 1993; Bramley, 2013). Mature green fruits are made of photosynthetic tissues and therefore contain chloroplasts, but with the onset of ripening, the chloroplasts differentiate into chromoplasts. This process activates many mechanisms such as degradation of the thylakoid membranes and chlorophylls, internal membrane remodelling, formation of carotenoid storing structures and often *de novo* synthesis of carotenoids (Egea et al., 2010; Figure 1-6).
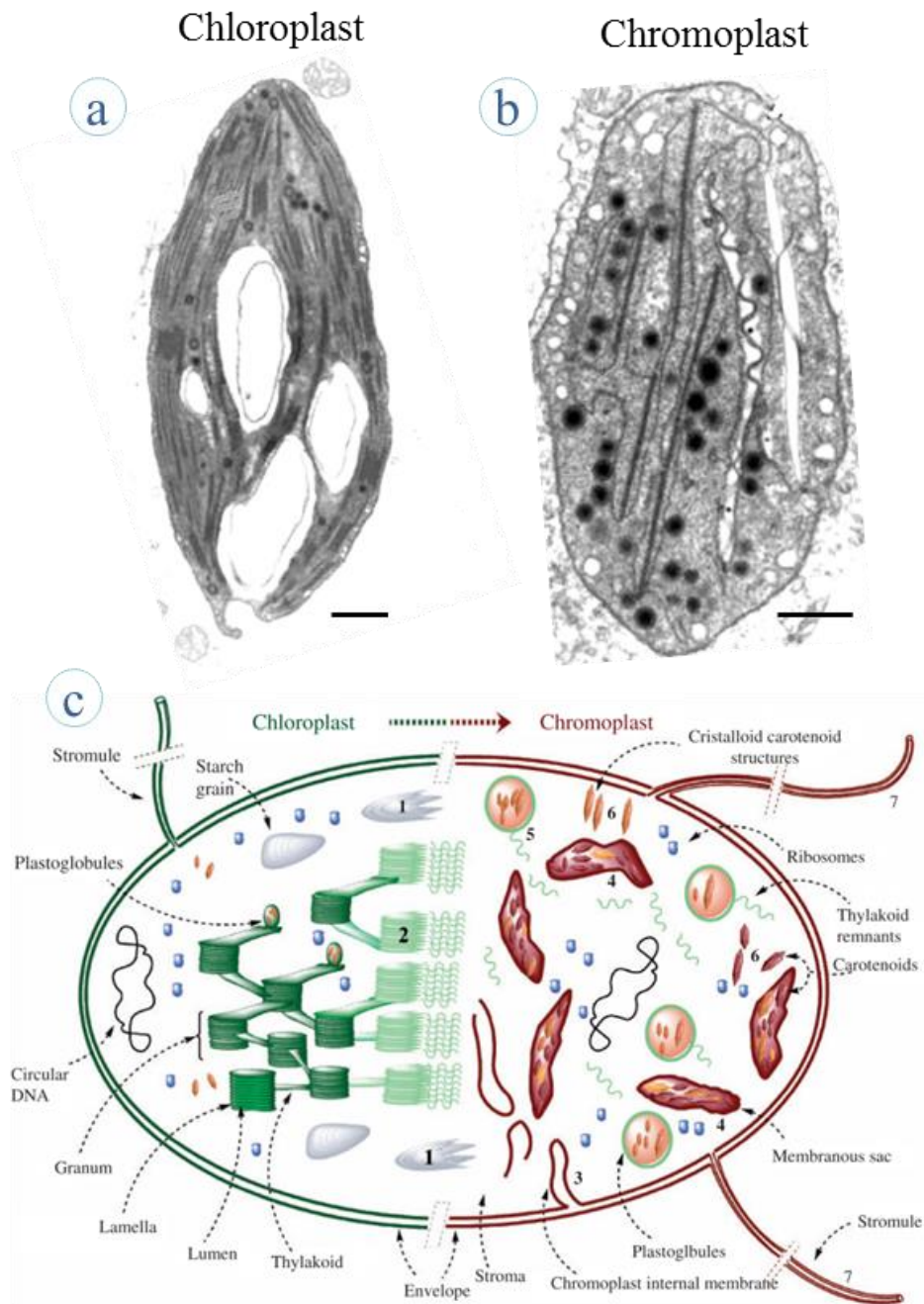
Figure 1-6 Chloroplast-chromoplast transition

a, electron micrograph of a tomato chloroplast; b, electron micrograph of a tomato chromoplast. Bar = 1μm (adapted from Simkin et al., 2007); c, schematic representation of the chloroplast–chromoplast transition. The scheme shows the breakdown of starch granules (1) and of grana and thylakoids (2); the synthesis of new membrane structures form the inner membrane envelope of the plastid (3) leading to the formation carotenoid-rich membranous sacs (4); the increase in the number and size of plastoglobules (5); the appearance of carotenoid-containing crystalloids (6); and the increase in the number of protrusions emanating from the plastid envelope, called stromules (7) (Egea et al., 2010).

The chromoplasts are the plastids of mature fruit, but also vegetable and flower tissues. They are capable of storing large quantities of carotenoids. The distribution of carotenoids is complex. The diversity (a few to over 50 carotenoids) and the quantities (insignificant to large amounts) of carotenoids are specific to species or even varieties (Howitt and Pogson, 2006; Bramley, 2013). For instance, strawberries contain low amount of carotenoids, whereas tomatoes have large quantities of lycopene, and peaches and mangoes contain large amounts of β-carotene. Unusual carotenoids, such as capsorubin and capsanthin, are found in peppers, poly-*cis*-carotenes are produced in tangerine tomatoes and apocarotenoids are found in large amounts in the peel and flavedo of Citrus species (Goodwin, 1980). Amyloplasts are the starch-storing plastids. However, they can also store carotenoids such as in the root tubers or seeds. Sweet potato contains mainly β-carotene, while potato accumulates β-cryptoxanthin or lutein. Amyloplasts are also found in starchy seeds such as wheat, rice and maize. Lutein and zeaxanthin are the main carotenoids found in seed amyloplasts (Howitt and Pogson, 2006).

1.2.3 Carotenoid interactions within the cell

Carotenoids are highly hydrophobic molecules, and therefore they have little or no solubility in an aqueous environment. Consequently, carotenoids are mainly found in the hydrophobic core of the membranes, except when they bind to other molecules that allow them to access aqueous areas. Carotenoids interact with other carotenoids, lipids and proteins. They associate with the hydrophobic part of the protein or with the lipid of the lipoprotein. Thus, carotenoids can also function and be transported in an aqueous environment. However, carotenoids have a tendency to crystallise in a hydrophilic environment. This alters their physical properties, such as light absorption and chemical reactivity (Britton, 1995). Moreover, carotenoid interaction with proteins allow them to maintain the optimal positions in order to interact with other molecules, such as in the case of the photosynthetic pigment-protein complexes, where the proteins hold the chlorophylls and carotenoids in proximity so that efficient energy transfer can occur (Britton, 1995).

The ability of carotenoids to fit in membrane structures depends on the shape, size and hydrophobicity of the carotenoid molecule. These features can be modified by, for instance, the polarity of the functional groups, the *trans* or *cis* configuration and

the cyclisation of the carotenoid molecule. Consequently, the sequestration of the carotenoids within the membrane depends on each individual carotenoid (Britton, 1995). All *trans* dipolar carotenoids, such as zeaxanthin, will tend to anchor in the two opposite polar regions of the bilayer (Subczynski et al., 1992; Havaux, 1998; Gruszecki and Strzalka, 2005). In the case of *cis* dipolar carotenoids, both polar ends are attached on the same side of the polar region of the membrane (Gruszecki and Strzalka, 2005). Non-polar carotenoids, such as lycopene and β-carotene, are distributed homogenously within the membrane without well-defined orientations, exclusively governed by van der Waals interactions with the hydrocarbon acyl chains of lipid molecules (Gabrielska and Gruszecki, 1996; Gruszecki and Strzalka, 2005). A schematic representation of the orientation of β-carotene, lutein, all *trans*-zeaxanthin and 13-*cis*-zeaxanthin in bilayer membranes is showed in Figure 1-7. The presence of carotenoids has an effect on the thickness, strength and fluidity of the membrane, but also on its effectiveness as a barrier to water and its permeability to oxygen and other molecules (Britton, 1995).
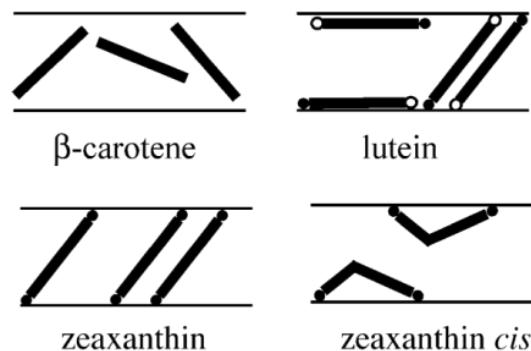
Figure 1-7 Schematic representation of orientation of carotenoids in the hydrophobic core of lipid membranes (Gruszecki and Strzalka, 2005)

Zeaxanthin, all *trans*-zeaxanthin; zeaxanthin *cis*, 13-*cis*-zeaxanthin.

1.2.4 Biosynthesis of carotenoids and ketocarotenoids

1.2.4.1 Carotenoid biosynthesis in plants

Since the 1950s, several approaches have been undertaken to elucidate the carotenoid biosynthetic pathway. Pioneering studies described the use of specific enzyme inhibitors and mutants of the carotenoid pathway (Porter and Lincoln, 1950;

(C_{10}), FPP (C_{15}) and GGPP (C_{20}) (Figure 1-9). These reactions involve the attack of a carbonium ion to the electron rich C3,4 double bond, associated with the loss of inorganic phosphate (Figure 1-2) (Fraser and Bramley, 2004). The condensation of two GGPP molecules in a head to head manner forms the intermediate pre-phytoene-pyrophosphate (PPPP). Phytoene (15-*cis*-phytoene) is obtained after elimination of the diphosphate group and stereospecific proton abstraction (Figure 1-9). Phytoene is the first carotenoid precursor of the pathway. It is colourless and its C_{40} skeleton is the basic structure from which all carotenoids are derived.
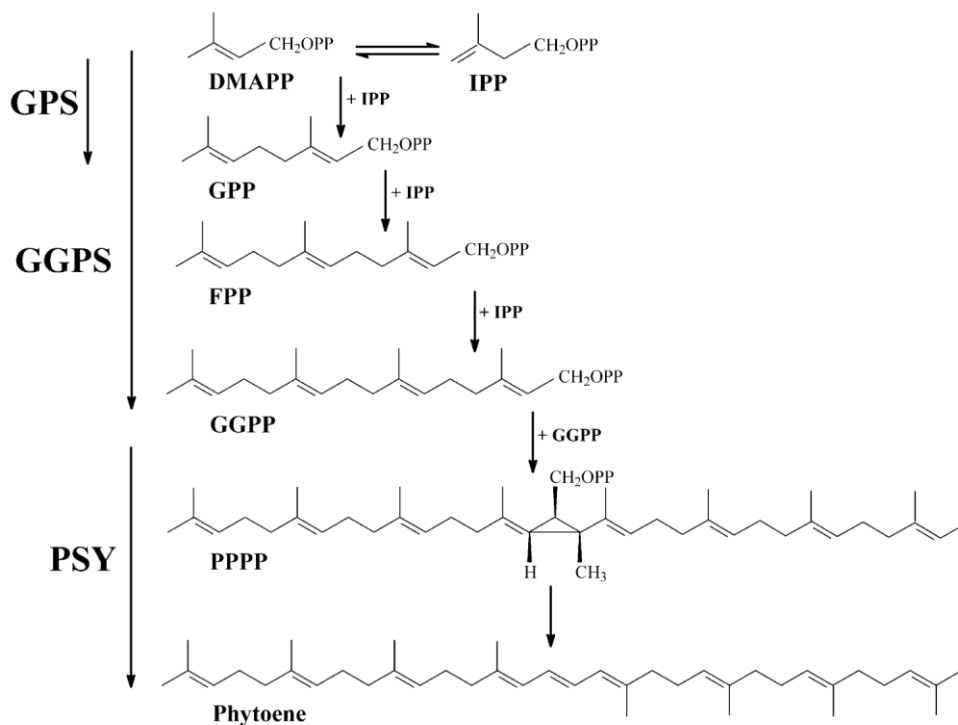
Figure 1-9 Phytoene synthesis from DMAPP and IPP

IPP, isopentenyl pyrophosphate; DMAPP, dimethylallyl pyrophosphate; GPP, geranyl diphosphate; FPP, farnesyl diphosphate; GGPP, geranylgeranyl diphosphate; PPPP, prephytoene diphosphate; GPS, geranyl diphosphate synthase; GGPS, geranylgeranyl diphosphate synthase and PSY, phytoene synthase (Fraser and Bramley, 2004).

The enzyme IPP isomerase catalyses the reversible isomerisation of IPP and DMAPP. GPP synthase (GPS) and GGPP synthase (GGPS) enzymes add a supplemental IPP unit to IPP or DMAPP and GPP, respectively. Phytoene synthase is responsible for the formation of the intermediate PPPP and phytoene. The corresponding gene(s) *Psy* have been identified and isolated from several species (for instance *Arabidopsis* (Lange and Ghassemian, 2003), maize (Buckner et al.,

33

Goodwin, 1955; Villoutreix, 1960). Then, *in vitro* approaches, using radioactive substrates were adopted (Williams et al., 1967; Bramley, 1985). Purification of enzymes from native and recombinant sources, gene cloning and expression in recombinant systems and transgenic plants and finally the use of the "omic" technologies are modern techniques used to pursue the study of the carotenoid biosynthesis pathway and its regulation (Bramley, 2013).

The description of the carotenoid pathway is divided in sections corresponding to different stages of the biosynthesis (Figure 1-8). The early stages of carotenoid formation were already illustrated in section 1, Figure 1-1 and 1-2. Carotenoids are synthesised in the plastids by nuclear encoded enzymes (Hirschberg, 2001). It involves IPP, which is synthesised mainly in the MEP pathway, but IPP from the MVA pathway could supposedly be also used, as exchanges of IPP between the MEP and MVA pathway do exist (Figure 1-2).
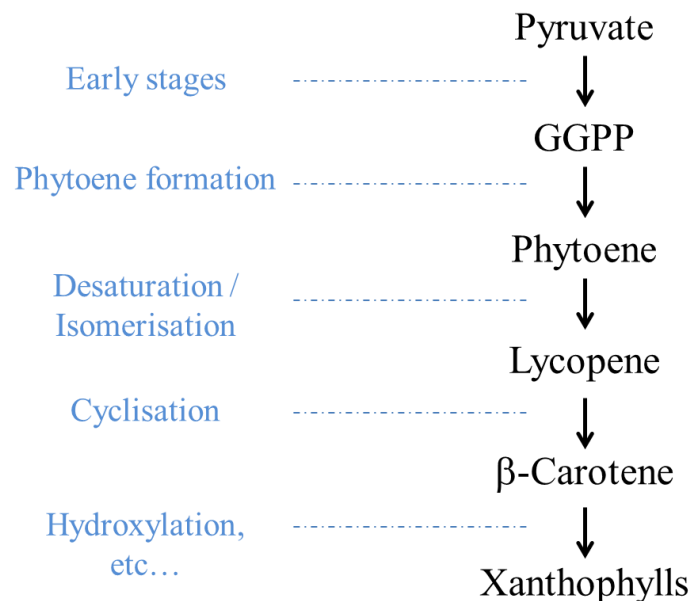
Figure 1-8 Summary of the stages of carotenoid biosynthesis

GGPP, geranylgeranyl diphosphate. Xantophylls can also be formed from lycopene. This step is not represented in this figure.

1.2.4.1.1 Formation of the first carotenoid, phytoene

The building unit IPP (C_5) is isomerised to its allylic isomer DMAPP in order to initiate chain elongation. Successive additions of IPP lead to the formation of GPP

1996), pepper (Kuntz et al., 1992)). In tomato, two variants of phytoene synthase (PSY-1 and PSY-2) have been identified and characterised. PSY-1 is a fruit and flower specific enzyme while PSY-2 is mainly active in chloroplasts (Fraser et al., 1999; Fraser et al., 2000a). The tomato phytoene synthases require ATP and Mn^{2+} (Fraser and Bramley, 2004).

1.2.4.1.2 Desaturation and isomerisation reactions leading to lycopene

The characteristic system of conjugated double bonds, the chromophore, is introduced via four sequential desaturation reactions. The extension of the polyene chain converts a colourless carotenoid (phytoene) into a red lycopene. Phytoene desaturase (PDS) catalyses two consecutives desaturation reactions to form ζ-carotene from phytoene (Figure 1-10). PDS activity is mainly membrane bound and requires FAD and oxidised quinones as cofactors (Fraser and Bramley, 2004). ζ-Carotene undergoes one desaturation reaction to become neurosporene and one more to lycopene (Figure 1-10). These last desaturations are catalysed by ζ-carotene desaturase, which requires FAD as a cofactor. Two isomerisation reactions occur in this pathway. The first one is catalysed by Z-ISO (Chen et al., 2010). The *tri-cis*-ζ-carotene is transformed in *di-cis* (Figure 1-10). The second one, through the activity of CRTISO, consists on the conversion of *tetra-cis*-lycopene to all-*trans*-lycopene (Isaacson, 2002; Isaacson et al., 2004). In green tissues, it is reported that the isomerisation steps occur only with the presence of light and chlorophyll (Isaacson, 2002; Bramley, 2013).
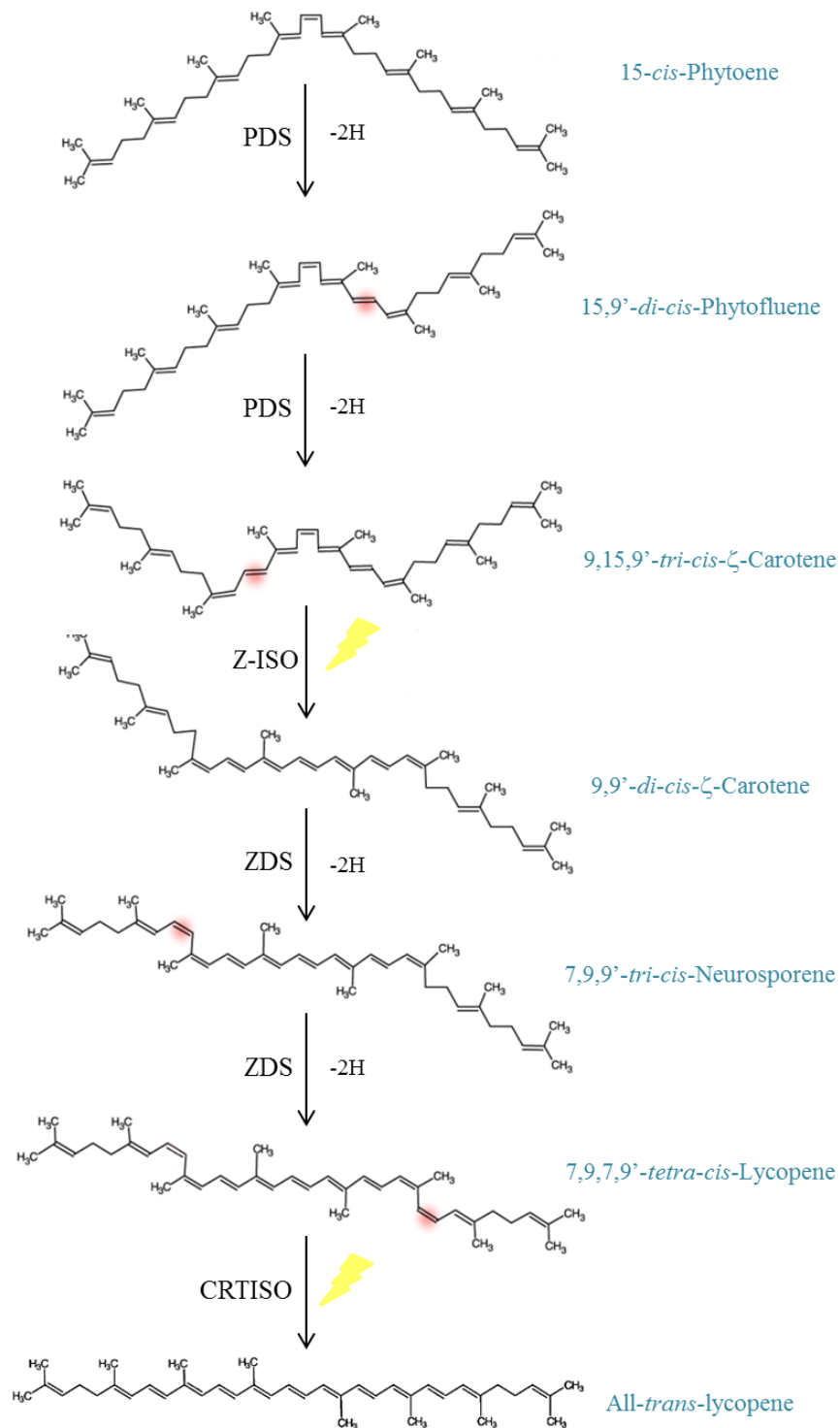
Figure 1-10 Desaturation and isomerisation reactions in the biosynthesis of lycopene
PDS, phytoene desaturase; Z-ISO, 15-*cis*-ζ-carotene isomerase; ZDS, ζ-carotene desaturase, CRTISO, carotene isomerase. Red shading indicates the position of newly formed double bonds. Yellow lightening symbols highlight reactions also mediated by light (adapted from Fraser and Bramley, 2004; Fraser et al., 2009).

1.2.4.1.3 Cyclisation reactions

All-*trans*-lycopene is at the junction of two distinct pathways, which are differentiated by the cyclic end groups that are formed from lycopene. Carotenoids of the β-pathway (γ-carotene and β-carotene) only contain β-rings, whereas carotenoids of the α-pathway (δ-carotene and α-carotene) have either only one ε-ring or ε- and β-rings (Figure 1-11). The ε-lycopene cyclase (LCY-E) and the β-lycopene cyclase (LCY-B) introduce ε- and β-rings, respectively. Both cyclases require NADPH as a cofactor (Fraser and Bramley, 2004). In tomato, a chromoplast specific β-lycopene cyclase (CYC-B) has also been identified (Ronen et al., 2000).
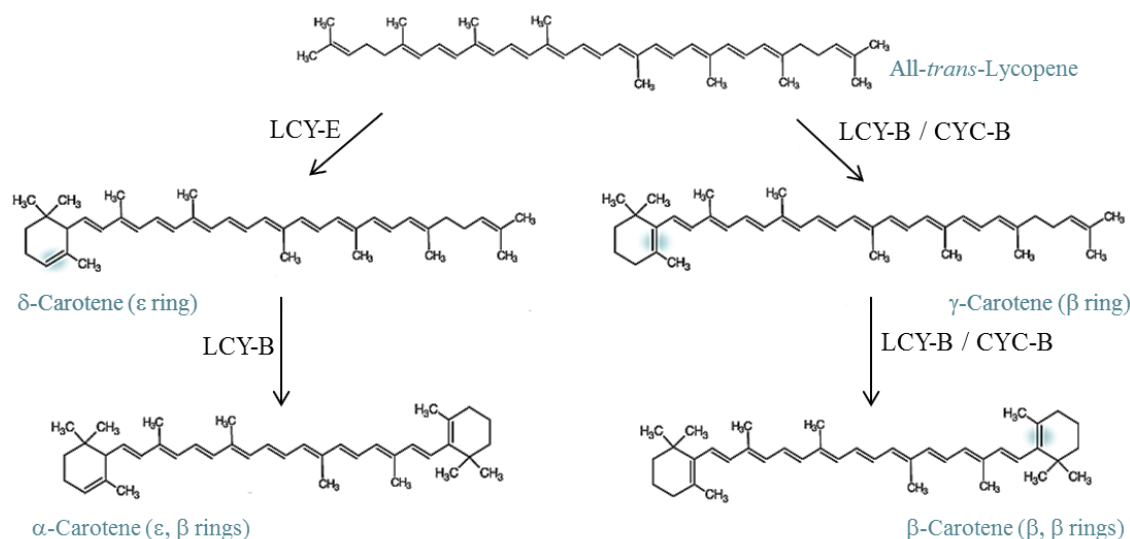
Figure 1-11 Cyclisation of lycopene

The characteristic double bond within the carotenoid end group is shown in blue. LCY-E, ε-lycopene cyclase; LCY-B, β-lycopene cyclase; CYC-B, fruit specific β-lycopene cyclase (adapted from Fraser and Bramley, 2004; Fraser et al., 2009).

1.2.4.1.4 Xanthophyll formation

In the later steps of the carotenoid pathway, oxygen atoms are introduced either as hydroxyl or epoxy groups (Figure 1-12). Hydroxylation of the C3 positions of the α-carotene and β-carotene result in α and β-cryptoxanthin, respectively. The hydroxylation of the C3′ positions leads then to the formation of lutein and zeaxanthin, respectively (Figure 1-12). The hydroxyl moieties are introduced at the β-rings by a haem-containing cytochrome P450 β-ring hydroxylase (CYP97A)

or/and the carotene β-hydroxylase 1 and 2 (CRTR-B1 and CRTR-B2), and at the ε-rings by a haem-containing cytochrome P450 ε-ring hydroxylase (CYP97C) (Sun et al., 1996; Tian and DellaPenna, 2001; Tian et al., 2003; Tian et al., 2004; Kim and DellaPenna, 2006) (Figure 1-12).
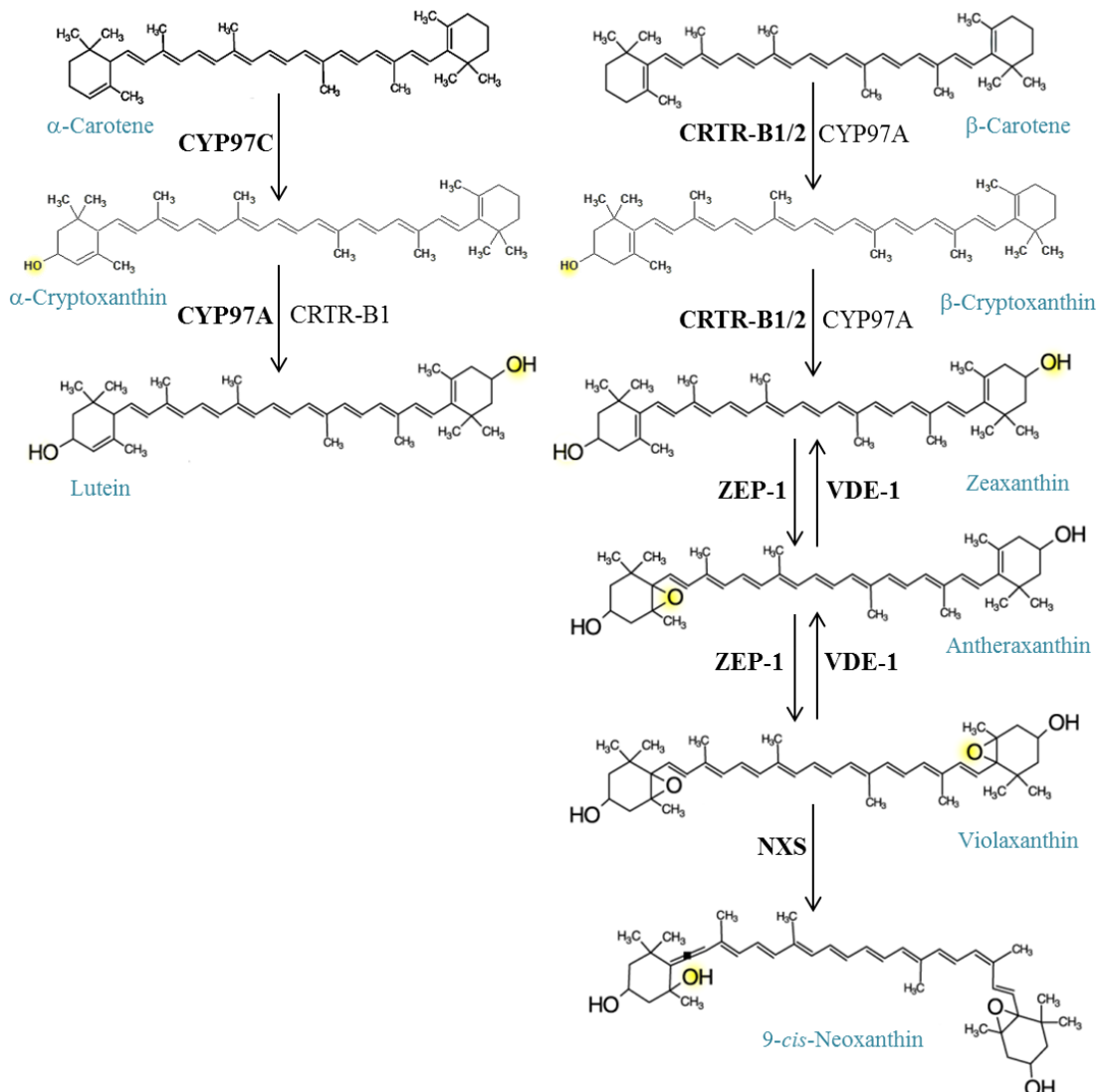
Figure 1-12 Xanthophyll biosynthesis

The oxygen/hydroxyl moieties introduced into the carotenoid skeleton are shaded in yellow. The enzymes encoding the major activity at each step are in bold. CYP97A, haem-containing cytochrome P450 β-ring hydroxylase; CYP97C, haem-containing cytochrome P450 ε-ring hydroxylase CRTR-B1, carotene β-hydroxylase 1; CRTR-B2, carotene β-hydroxylase 2 (flower specific); ZEP-1, zeaxanthin epoxidase; VDE-1, violaxanthin de-epoxidase; NXS, neoxanthin synthase.

Zeaxanthin epoxidase (ZEP-1) catalyses the β-ring epoxidation reaction of zeaxanthin, which is converted to antheraxanthin and which in turn forms

violaxanthin by the introduction of a second epoxy group (Figure 1-12). These reactions are reversible. Violaxanthin can be converted back to zeaxanthin, through the action of violaxanthin de-epoxidase (VDE-1). In order to protect thylakoid membrane lipids against photo-oxidation, which happens under excessive light, violaxanthin is rapidly and reversibly converted via antheraxanthin to zeaxanthin under the action of VDE (DemmigAdams and Adams, 1996). This is known as the xanthophyll cycle.

Violaxanthin is converted to neoxanthin by neoxanthin synthase (NXS), with the introduction of a single allenic end group. It is speculated that this group is formed by proton abstraction of C7, which has the consequence of converting the epoxy group into a hydroxyl group (Figure 1-12). In tomato, the deduced amino acid sequence of NXS is identical to that of CYC-B. Therefore, it is suggested that the enzyme is bi-functional under certain conditions (Fraser and Bramley, 2004).

1.2.4.2 Ketocarotenoid biosynthesis in bacteria

Ketocarotenoids are almost exclusively biosynthesised in microorganisms. The first carotenoid precursor of the ketocarotenoid pathway is β-carotene. As in plants, the formation of β-carotene in bacteria occurs from phytoene, which is formed by the condensation of two GGPP molecules (Figure 1-13). The GGPP synthase and phytoene synthase are called CRTE and CRTB, respectively. Contrary to the carotenoid pathway in plants, which requires four enzymes, only one bacterial enzyme (CRTI) is needed to convert phytoene to lycopene in bacteria (Figure 1-13). The formation of β-carotene is catalysed by the lycopene cyclase CRTY (Misawa et al., 1990; Misawa et al., 1995b).

Ketocarotenoids are biosynthesised from the carotenoids β-carotene, β-cryptoxanthin and zeaxanthin, via multiple and consecutive 3/3′-hydroxylation and 4/4′-ketolation reactions of the end groups. From β-carotene to the final product astaxanthin, there are eight intermediates (Figure 1-14). Several hydroxylases (CRTZ, CYP175A1 and CRTR) and ketolases (CRTW and CRTO), which are structurally different, have been functionally identified (Misawa et al., 1990; Misawa et al., 1995a; Misawa et al., 1995b; Fernandez-Gonzalez et al., 1997; Fraser et al., 1997; Fraser et al., 1998; Masamoto et al., 1998; Blasco et al., 2004; Misawa, 2009; Zhu et al., 2009). CRTZ

(hydroxylase) and CRTW (ketolase) are bi-functional, as they can act prior or after ketolation and hydroxylation of the β-rings, respectively. Since the intermediates of the pathway are found in relatively high proportions, it was postulated that the CRTZ and CRTW-type enzymes contain a reaction site, which can only introduce one hydroxyl or keto moiety at a time, respectively. *In vitro* characterisation of CRTZ and CRTW showed that these enzymes require O_2 and that Fe^{2+} is beneficial for their activities (Fraser et al., 1997).
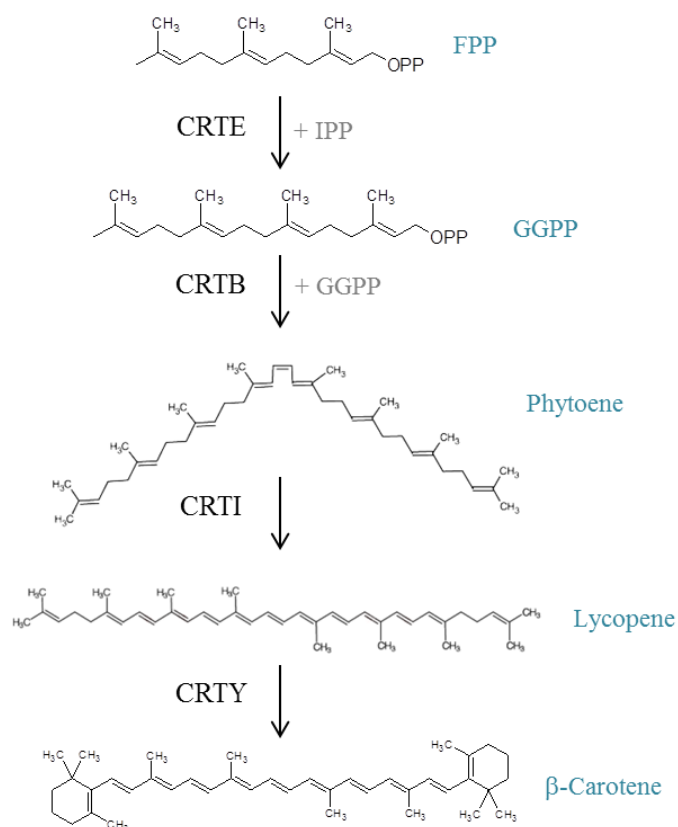
Figure 1-13 Formation of β-carotene in bacteria

FPP, farnesyl diphosphate; GGPP, geranylgeranyl diphosphate, IPP, isopentenyl pyrophosphate; CRTE, GGPP synthase; CRTB, phytoene synthase; CRTI, lycopene desaturase; CRTY, lycopene cyclase (adapted from Misawa et al., 1995b).

Most plants lack β-carotene ketolase enzymes and therefore are not able to synthesise ketocarotenoids. There are a few exceptions, such as the green algae *Haematococcus pluvialis* and the Adonis flower (Zhu et al., 2009). However, plants have endogenous β-carotene hydroxylases (as discussed in section 1.2.4.1.4).
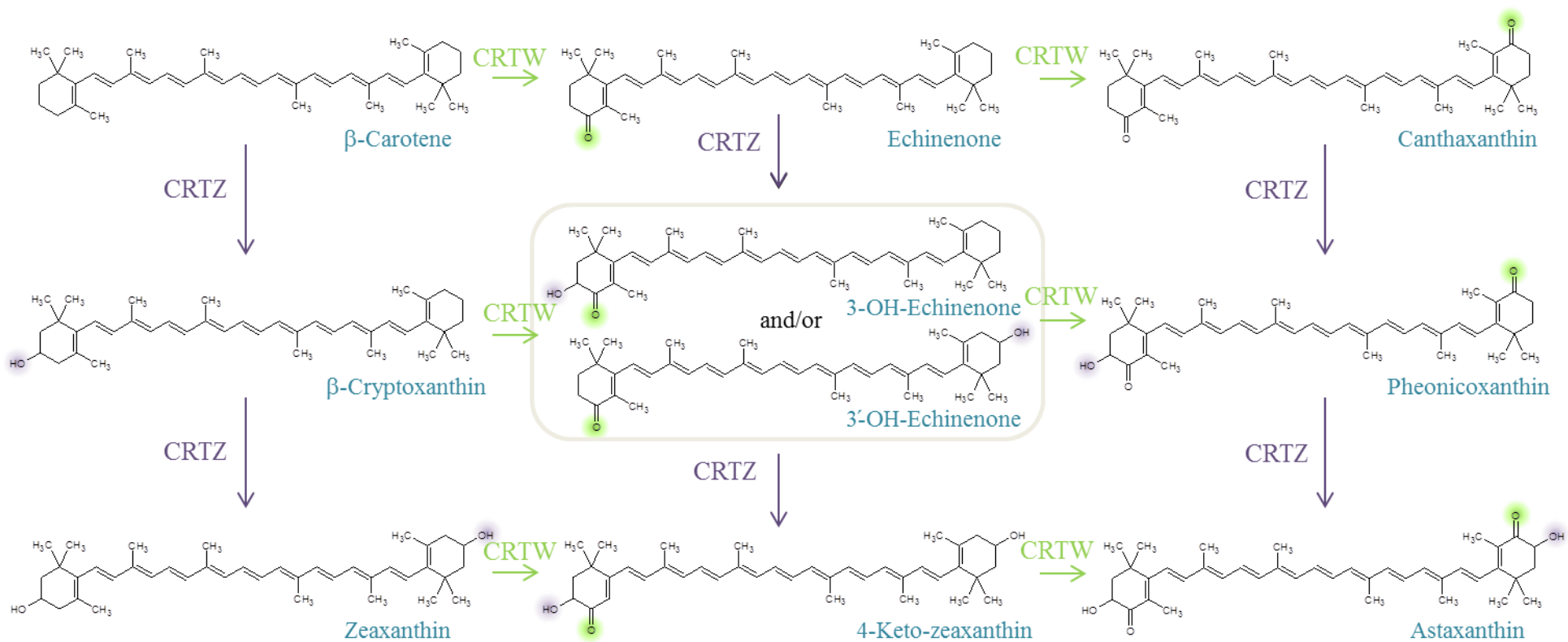
Figure 1-14 The ketocarotenoid biosynthetic pathway in bacteria

CRTZ, β-carotene hydroxylase; CRTW, β-carotene ketolase. Purple and green shadings indicate the position of newly introduced hydroxyl and keto groups, respectively. Other hydroxylases and ketolases, described in section 1.2.4.2, are not shown for the sake of clarity.

1.2.5 The roles of carotenoids and ketocarotenoids

1.2.5.1 In plants

Carotenoids are essential components of the light harvesting complexes, which allow photosynthetic organisms (plants, algae and photosynthetic bacteria) to collect light for photosynthesis. Carotenoids, especially xanthophylls (lutein, violaxanthin and zeaxanthin) are associated with chlorophylls within pigment-protein complexes (Figure 1-15). The carotenoids absorb light in the spectral region in which the sun emits, and transfer this energy to chlorophylls and subsequently to the reaction centre, initiating the first photochemical step of photosynthesis (Polivka and Frank, 2010). The advantage of having a variety of carotenoid and chlorophyll pigments is to increase the absorption range of light within the antenna and consequently the amount of energy transferred to the reaction centre.
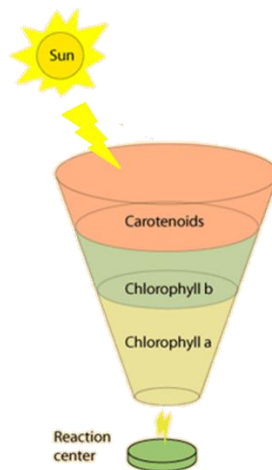
Figure 1-15 Antenna complex component of the light harvesting systems

Adapted from http://hyperphysics.phy-astr.gsu.edu/hbase/biology/antpho.html

Light is essential for the life of plants, however, excess light can cause photo-oxidative damage to membranes and proteins, via production of reactive oxygen and chlorophyll species. Carotenoids play an important role in photoprotection of the plant, via photochemical and non photochemical reactions. Firstly, carotenoids are able to quench the reactive triplet chlorophyll and reactive oxygen species (ROS), such as singlet oxygen and release the energy as heat (Frank and Cogdell, 1993). The photochemical quenching reactions are described in Figure 1-16.

41

$$\text{Chl} \longrightarrow {}^1\text{Chl*}$$

$$ {}^1\text{Chl} \longrightarrow {}^3\text{Chl*}$$

Quenching of triplet chlorphyll

$$ {}^3\text{Chl*} + \text{Car} \longrightarrow \text{Chl} + {}^3\text{Car*}$$

$$ {}^3\text{Car*} \longrightarrow \text{Car} + \text{Heat}$$
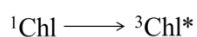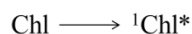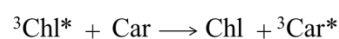
Quenching of singlet oxygen

$$ {}^3\text{Chl*} + \text{O}_2 \longrightarrow \text{Chl} + {}^1\Delta_g\text{O}_2\text{*}$$

$$ {}^1\Delta_g\text{O}_2\text{*} + \text{Car} \longrightarrow \text{O}_2 + {}^3\text{Car*}$$

$$ {}^3\text{Car*} \longrightarrow \text{Car} + \text{Heat}$$
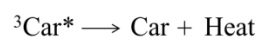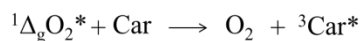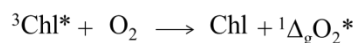
Figure 1-16 Photochemical quenching of triplet chlorophyll and singlet oxygen by carotenoids

Chl, chlorophyll; ^{3}Chl, triplet chlorphyll; Car, carotenoids; O_2, oxygen, $^1\Delta_g O_2$, singlet oxygen; *, denotes an excited state (adapted from Frank and Cogdell, 1993).

Ketocarotenoids were also shown to provide photoprotection in plants modified to synthesise ketocarotenoids. Transgenic carrot plants were more resistant to UV light and hydrogen peroxide treatment (H_2O_2), compared to wild type plants as ketocarotenoids helped to quench free radicals and ROS (Jayaraj et al., 2008).

Non photochemical quenching (NPQ) is provided by carotenoids via thermal dissipation processes (Havaux and Niyogi, 1999; Niyogi, 1999; Muller et al., 2001). The xanthophylls have a great capacity of energy dissipation since they have lower energy levels compared to those of chlorophylls and they undergo very rapid light-triggered concentration changes (DemmigAdams and Adams, 1996). Under excess light, violaxanthin is converted rapidly to zeaxanthin via the intermediate antheraxanthin. This reaction is reversed under low light levels. It is termed the xanthophyll cycle (Figure 1-17). The formation of zeaxanthin catalysed by violaxanthin de-epoxidase, which is located in the thylakoid lumen, is strictly regulated by pH of the lumen (Jahns et al., 2009). The exact role of zeaxanthin in non photochemical quenching is still under debate. It could have a direct function and/or a more indirect function, by strongly affecting the thermodynamic parameters of membranes (Jahns et al., 2009).
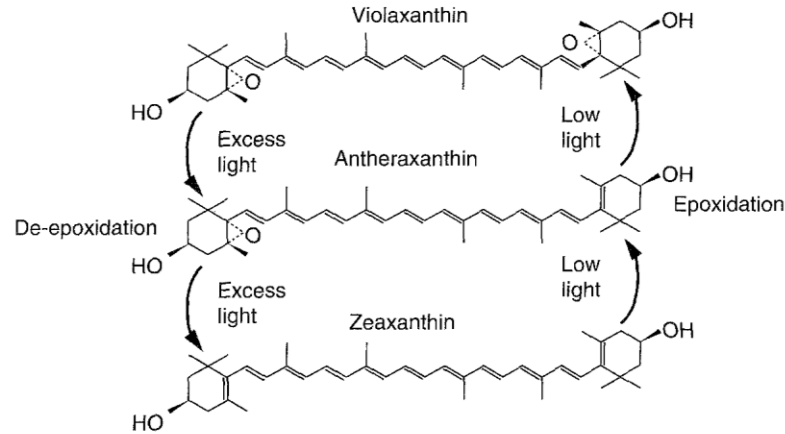
Figure 1-17 Xanthophyll cycle and regulation of excess of light (DemmigAdams and Adams, 1996)

Carotenoids and especially apocarotenoids or their products can be phytohormones, such as abscisic acid and volatile molecules, which play critical roles in the interactions between plants and their environments (Walter et al., 2010; Cazzonelli, 2011).

Another role of some carotenoids in plants is intrinsically linked with their light-absorbing properties, as they colour the fruits and flowers of plants. It is well known that colours of fruits and flowers play a role in attracting pollinators and favour seed dispersal (Cazzonelli, 2011).

1.2.5.2 In animals

Carotenoids are provided to animals through their diet and for humans, primarily from crop plants (roots, leaves, shoots, seeds, fruit and flowers), since they cannot synthesise carotenoids *de novo* (Fraser and Bramley, 2004). In animals, carotenoids play a role in reproduction, the determination of sexual behaviour, camouflage and avoiding predation and parasitism. However, they have many other functions, such as in fishes and birds, where they boost the immune system and promote health (McGraw, 2006; McGraw and Klasing, 2006; Cazzonelli, 2011).

Carotenoids and ketocarotenoids have been shown to be beneficial to human health probably due to their antioxidant activity (Krinsky, 1989; Krinsky and Johnson, 2005). Human diseases, such as cancers and heart diseases, always involve, at some

stage, oxidation processes mediated by free radicals, such as $O_2^{-\cdot}$ (superoxide anion), $HO^{\cdot}$ (hydroxyl radical), $RO^{\cdot}$ (alkoxy radical), $ROO^{\cdot}$ (peroxyl radical) (Britton, 1995a; Gulcin, 2012). Antioxidant molecules neutralize reactive oxygen species and thus prevent oxidative damage to cellular components. Consequently, the rate of cell death is reduced, along with the effects of ageing and ageing-related diseases (Gulcin, 2012; Zhu et al., 2013). The polyene chain, a highly reactive electron-rich system, is the important feature in relation with carotenoids' antioxidant activity. It stabilises the carotenoid radicals created by free radical quenching and acts as a prime target for the free radicals, removing them from the cellular environment (Britton, 1995; Krinsky and Yeum, 2003; Krinsky and Johnson, 2005). The three possible mechanisms of carotenoid interaction with free radicals are illustrated in Figure 1-18.

(a) $CAR + R\cdot \quad \text{-----}> R\text{-}CAR\cdot$

(b) $CAR + R\cdot \quad \text{------}> CAR\cdot^+ + R^-$

(c) $CAR + R\cdot \quad \text{------}> CAR\cdot + RH$
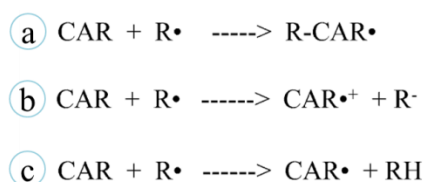
Figure 1-18 Carotenoid reactions with radicals

a, adduct formation; b, electron transfer; c, allylic hydrogen abstraction; CAR, carotenoid; R, radical (adapted from Krinsky and Yeum, 2003)

Since the 1970s, correlations between high intake of carotenoids and health benefits have been regularly published. The best-established carotenoid activity in terms of human health is provitamin A activity, which is conferred by 50 carotenoids with β-ring end groups, such as β-carotene and zeaxanthin. These carotenoids are cleaved symmetrically by an intestinal 15,15′-oxygenase to form retinal molecule(s) or asymmetrically by a 9,10′-oxygenase (Fraser and Bramley, 2004; Tang and Russell, 2009). Vitamin A deficiency has been linked with blindness and growth retardation, but also severe diseases including respiratory and urinary infections, dysentery and immune responses (Britton, 2009). A diet with provitamin A prevents deficiency related diseases and promotes human health by its immuno-stimulant and photo-protectant activities (Cazzonelli, 2011). Many studies have been reported on the health-promoting effects of these β-rings carotenoids, but also of other carotenoids and ketocarotenoids such as lutein, lycopene and astaxanthin, in cancers,

44

cardiovascular disease, eye disease and the prevention of cognitive decline (Johnson et al., 1995; Johnson, 2002; Fraser and Bramley, 2004; Krinsky and Johnson, 2005; Hussein et al., 2006; Voutilainen et al., 2006; Moeller et al., 2008; Johnson, 2010a; Johnson, 2010b; Naito, 2011; Yuan et al., 2011; Abdel-Aal et al., 2013; Bojorquez et al., 2013).

Awareness of the importance of carotenoid intake for health benefits has become predominant in the public domain. The population was recommended, by the World Health Organization, to eat at least five portions of fruits and vegetables (a minimum of 400g) a day in order to increase their intake of vitamins, fibre and carotenoids. Moreover, complementing daily diets with β-carotene, lutein, astaxanthin or lycopene nutraceuticals (food complement), has become very popular (as discussed in section 1.2.5).

1.2.6 Global market of carotenoids and ketocarotenoids

According to the most recent BBC research report (FOD025D, 2011), the global market for commercially used carotenoids (including ketocarotenoids) was $1.2 billion in 2010 and is estimated to reach $1.4 billion in 2018. The market is dominated by sales of β-carotene ($260 million), lutein ($230 million) and astaxanthin ($230 million). Canthaxanthin and lycopene have a global market of approximately $70-90 million.

These carotenoids and ketocarotenoids have large markets not only due to their health-benefits (as discussed in section 1.2.5.2), but also to their natural pigmentation. Indeed, they are used as industrial colourants, particularly in the aquaculture and poultry farming industries. Astaxanthin is the colour of choice for pigmenting fish and shrimp and canthaxanthin for introducing a red tone in egg yolk (Marz, 2011). Although the majority of carotenoids found in the market are chemically synthesised, the pressure for natural products keeps increasing and therefore changes of production are observed. Companies producing carotenoids from algae or by fermentation are starting to be competitive (Marz, 2011). For instance, β-carotene is also now produced from algae (COGNIS, Australia) and by fermentation (DSM, Holland and Vitatene, Spain).

The market is dominated by chemically synthesised carotenoids, because this type of production has low overall costs. Therefore, chemically synthesised carotenoids have lower prices than natural carotenoids. However, chemical synthesis has several disadvantages, such as the contamination with reaction intermediates, organic residues and the production of stereoisomers not found in Nature. Moreover, the general concept that natural products are healthier is prevalent in people's minds. Consequently, a greater majority of people are ready to pay more for natural products, enabling the natural carotenoid market to increase.

Although higher plants provide the majority of carotenoids to humans through their diet, almost none are industrially used to produce carotenoids. The only exception is marigold flowers (utilised by PIVEG company), which exist with a range of white to dark-orange petal colours.

Efforts to enhance high-value isoprenoid levels in plants have been undertaken for industrial purposes, but also to create biofortified crops, fruits and vegetables.

1.3 Enhancing high-value isoprenoid levels in plants

The functions and characteristics of the carotenoid and ketocarotenoid molecules (discussed in section 1.2.5) bring the attention of the scientific world and therefore, are attractive subjects for investigation. One of the critical tasks in the production of secondary metabolites is to find systems for high-scale generation of valuable natural products (Sheludko, 2010). Plants are essential providers of biologically active compounds. Moreover, they have several advantages compared to chemical synthesis, or the use of microorganisms: (i), Plants are ecologically and pharmacologically safe; (ii), they have high natural biosynthetic abilities, including multi-steps stereospecific synthesis of complex organic molecules and eukaryote-type biosynthesis; (iii), the natural potential of plant systems can be used to scale-up high-value compound production; (iv), they are of economic value; (v), they are renewable biosources, with no need for by-products of the petrochemical industry as precursors and no disposal of contaminated waste (Sheludko, 2010).

Field cultivation of medicinal plants was the first production system of valuable secondary metabolites. However, large-scale cultivation is often not straightforward, as medicinal plants are typically restricted to their local ecosystem and the pathogen sensitiveness increases in this scale of production (Bourgaud et al., 2001). This has led to the development of *in vitro* cultures, such as the culture of undifferentiated plant cells and tissue and organ cultures such as shoots (Bourgaud et al., 2001; Hussain et al., 2012). These techniques have been scaled-up through the usage of bioreactors. However, only a few commercial successes have been achieved, such as the production of ginseng (Ushiyama and Hibino, 1997). The major improvements in the production of plant secondary metabolites were accomplished following the development of molecular biology (Bourgaud et al., 2001). The possibility of optimising plant secondary metabolites, through molecular breeding and transgenic strategies, contributed to the success of these alternative approaches.

1.3.1 Conventional strategies

1.3.1.1 Breeding approach

Over thousands of years, humans have been selecting plants with interesting characteristics and crossing them in order to obtain plants, which suited their needs. Nowadays, breeding is still carried out in a similar way. The first step consists in generating a breeding population, by using parents that have different traits of interest. The second step is the selection of the segregating progeny for plants that combine the most useful traits of each parent and that are devoid of, or show minimal adverse effects (Manshardt, 2004). The selection can be assisted with molecular markers, such as AFLP (amplified fragment length polymorphism) or SSR (simple sequence repeat), which flank quantitative trait loci (QTL). Mapping of QTL for lycopene and fruit colour was studied in tomato (Chen et al., 1999; Liu et al., 2003). However, the complexity of the QTL, with a desirable influence on carotenoids levels, makes the process slow and laborious (Farre et al., 2010). The breeding approach was also chosen as one of the main strategies of the international project HarvestPlus, to develop staple food crops rich in micronutrients, especially provitamin A (β-carotene; Kimura et al., 2007; Ortiz-Monasterio et al., 2007). HPLC screening of several sweet potato, cassava and maize varieties has been undertaken

in order to select those that are naturally rich in provitamin A at harvest. Plant breeding trials were carried out with the selected lines (Kimura et al., 2007).

1.3.1.2 Plant mutants

Natural variants of plants with interesting carotenogenic properties have been previously described (Table 1-1). These mutants were subjected to natural, spontaneous mutation(s), which sometimes contributed to an increase or altered carotenoid levels, such as in the *beta* tomato mutant (Table 1-1). They are useful tools for complementation studies or to be subjected to further improvement through genetic engineering.

Mutant name	Phenotype	Enzyme (gene)	Carotenoid profile	References
white-flower (*wf*)	White to beige petals and pale anthers	CRTR-B2	Carotenoid analysis indicated a reduction of 80 to 84% in total carotenoids in petals of the various wf mutant alleles	Galpaz et al., 2006
yellow flesh (*r*)	Yellow fruit colour	PSY (*Psy1*)	Low carotenoid content in fruit	Fray and Grierson, 1993
delta	Orange fruit colour	LCY-E	Accumulation of δ-carotene at the expense of lycopene	Ronen et al., 1999
tangerine	Orange fruit colour	CRTISO	Accumulates pro-lycopene instead of all-*trans*-lycopene	Isaacson et al., 2002
beta	Orange fruit colour	LYC-B chromoplats	*Beta* is a dominant mutation that results in a 5-10% increase in fruit β-carotene levels, reflecting increased LYC-B activity, whereas *old gold* is a null allele at the same locus, which reduces the amount of β-carotene and increases lycopene in fruit	Ronen et al., 2000
old-gold (*og*)	Tawny orange flowers			
ghost	Poorly coloured petals compared with the yellow carotenoid-containing wild-type petals	PTOX (Plastid terminal oxidase gene)	Accumulates phytoene in fruits instead of lycopene	Josse et al., 2000
high-pigment 1 (*hp-1*)	Dark green leaves, deep red fruit, dark green immature fruit, increased leaf thickness and plastid compartment size	DDB1	Increases total carotenoid content in ripe fruit (1.8-fold); activity of phytoene synthase is increased (1.9-fold)	Cookson et al., 2003 Lieberman et al., 2004
high-pigment 2 (*hp-2*)	Dark green leaves, deep red fruit, dark green immature fruit	DET1	Increases total carotenoid content in ripe fruit, primarily lycopene	Mustilli et al., 1999 Kolotilin et al., 2007
high-pigment 3 (*hp-3*)	Dark green leaves, deep red fruit, dark green immature fruit	ZEP	30% more carotenoids in the mature fruit, leaves of the mutant lack violaxanthin and neoxanthin	Galpaz et al., 2008

Table 1-1 Carotenoid pathway mutants in tomato (*Solanum lycopersicum*) (adapted from Farre et al., 2010)

1.3.1.3 TILLING approach

Diversity can be introduced in plants via induced-mutation approaches, such as the ethyl methane sulfonate mutagenesis (EMS) method. Mutational screening at a specific locus can then be carried out to discover induced lesions. This method is called Targeting Induced Local Lesions IN Genomes (TILLING) (McCallum et al., 2000a, b). TILLING can be specifically used in an attempt to enhance carotenoid levels in tomato fruits. TILLING, when applied to study the lycopene cyclase locus of an EMS-Red Setter tomato population (Minoia et al., 2010), revealed one allele which conferred an increase in lycopene content (2-fold) in the red tomato fruit (Silletti et al., 2013). Mutations in genes encoding elements of the tomato light signal transduction pathway, such as *DEETIOLATED*1, resulted in increased total carotenoid levels (2.3-fold) of ripe tomato fruit (Jones et al., 2012). Therefore, it is another strategy to improve the content of valuable carotenoids in plants.

1.3.2 Metabolic engineering strategies

Metabolic engineering has been defined as the modification of intermediary metabolism using recombinant DNA techniques to produce new metabolites, improve the accumulation of existing metabolites or mediate the degradation of compounds. The introduction of genes of the carotenoid and ketocarotenoid pathways directly into plants provides a shortcut compared to the laborious breeding approaches exploiting natural diversity. Moreover, it allows introduction of genes from beyond the natural gene pool. It is the only strategy that can introduce the carotenoid pathway *de novo* in an organism or extend it beyond its natural endpoint via, for instance, the formation of ketocarotenoids (DellaPenna, 2001; Farre et al., 2010). Plant transformation can be executed via numerous techniques (Rao et al., 2009), but the most common are the indirect method with *Agrobacterium tumefaciens* or *rhizogenes* and the biolistic method. The first technique is based on the introduction of a plasmid-carrying gene construct into the genome by means of *Agrobacterium* (Chilton, 1979; Horsch et al., 1985). The second one is a direct delivery of DNA by microprojectile bombardment into intact cell tissues (Sanford, 2000). A plastid transformation technique has been developed more recently. It offers several advantages, including a high level of transgene expression and site-

specific integration by homologous recombination (Hasunuma et al., 2009). However, this approach is challenging and more difficult to establish.

The production of commercially valuable compounds in plants can be optimised using different engineering strategies (Figure 1-19). Strategies can focus on one or multiple steps of the pathway of interest, or on the surroundings of the pathway, upstream, to increase the levels of precursors, or downstream, to accumulate products. Entire parallel mini-pathways can also be created (Figure 1-19). Other strategies concentrate on the size, number and specialisation of plastids where the biosynthesis of the carotenoids occurs (Figure 1-19). All approaches are based on the expression of heterologous genes (recombinant DNA or RNAi), which encode a variety of molecular elements of the cell, such as enzymes, transcription factors, transporters, lipid associated proteins and light signal transduction components. These elements interact with the cell metabolism and that results in the accumulation or production of valuable carotenoids and ketocarotenoids (Figure 1-19).
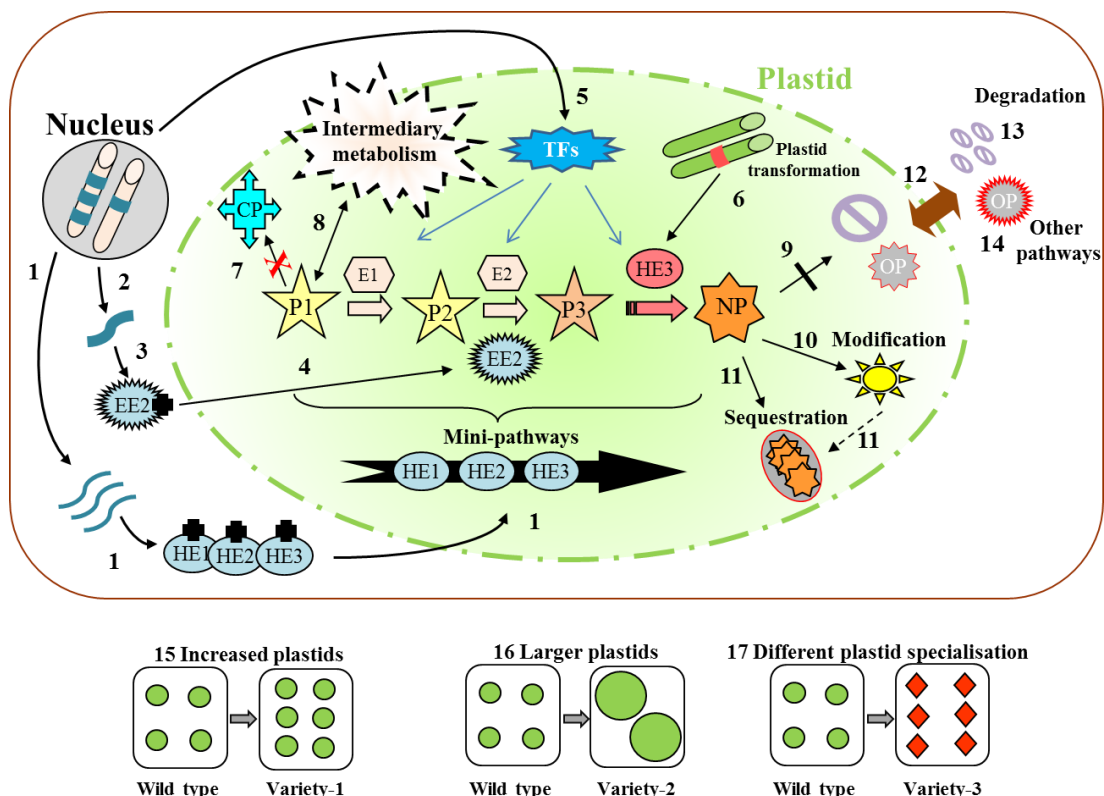
Figure 1-19 Diagrammatic representation of the potential strategies for metabolic engineering secondary metabolites (adapted from Fraser, personal communication)

P, product; E, enzyme; HE, heterologous enzyme; EE, enhanced enzyme (transcriptionally or/and translationally); NP, new product; OP; other products derived from the new product; CP, competing pathway; TFs, transcription factors. 1, Construction of a mini-pathway with heterologous enzymes; 2, improved transcription; 3, enhanced translation; 4, improved transcription and translation; 5 enhanced transcription via transcription factor expression; 6, plastid transformation; 7, restriction of the diversion of precursors; 8, interaction with intermediary metabolism and other plant processes; 9, minimising non-enzymatic degradation and the diversion of new products into other pathways; 10, metabolites plastidial modification; 11, sequestration of metabolites; 12, manipulating transport mechanisms; 13; controlling the rate of non-enzymatic degradation; 14, controlling the rate of diversion into other catabolic pathways.

A good example of the transcription factor approach (Figure 1-19, n°5) is the enhancement of anthocyanin production in tomato via the overexpression of two transcription factors (*Del* and *Ros1* from snapdragon *Antirrhinum majus*), which specifically induce anthocyanin synthesis (Butelli et al., 2008). Transgenic tomatoes containing the highest level of anthocyanin reported to date were obtained (2.8 mg/g FW). Such specific transcription factors of carotenoid synthesis have not been found yet. Sequestration strategies (Figure 1-19, n°11) can target lipid associated protein such as CHRD and fibrillin (Table 1-2), or the biosynthesis of the lipid linked with carotenoid sequestration to create a favourable hydrophobic environment. The latter approach builds on previous observations (Rabbani et al., 1998; Barsan et al., 2012). However, the most classical strategy is the overexpression of carotenogenic gene(s) from the target plant species or from another species into the target plant via nuclear transformation (Table 1-2). The collection of genes encoding carotenogenic enzymes isolated from bacteria, fungi and plants, including algae represent an important resource for carotenoid engineering (Table A1-1).

Table 1-2

Species	Genes (origin)	Function	Promoters	Carotenoid levels in transgenic plants	Engineering strategy	References
Arabidopsis thaliana	*Psy* (*Arabidopsis*)	phytoene synthase	Napin (seed specific)	260 µg/g FW β-carotene in seeds	tissue-specific overexpression of one carotenogenic gene	Lindgren et al., 2003
	Psy (*Arabidopsis*)	phytoene synthase	CaMV35S (constitutive)	1600 µg/g DW (10-fold) of total carotenoid in seed-derived calli, 500 µg/g DW (100-fold) in roots	overexpression of one carotenogenic gene	Maass et al., 2009
	Bkt1 (*H. pluvialis*)	β-carotene ketolase	Napin	4-keto-lutein, canthaxanthin and adonirubin seeds up to 13-fold	tissue-specific overexpression of one carotenogenic gene	Stalberg et al., 2003
	Chy-b (*Arabidopsis*)	β-carotene hydroxylase	CaMV35S	2274.8 nmol/g DW total carotenoid	overexpression of one carotenogenic gene	Cho et al., 2008
	Chy-b (*Arabidopsis*)	β-carotene hydroxylase	CaMV35S	285 mmol/chl a (mol) violaxanthin (2-fold) 728 mmol/chl a (mol) of total carotenoid	overexpression of one carotenogenic gene	Davison et al., 2002
	AtB1 (*Arabidopsis*)	β-ring hydroxylase	CaMV35S	38.2 µg/g β-carotene leaf tissue	overexpression of one carotenogenic gene	Kim et al., 2010
	CYP97A3 (*Arabidopsis*)	β-ring hydroxylase	CaMV35S	41.7 µg/g β-carotene leaf tissue	overexpression of one carotenogenic gene	Kim et al., 2010
	CYP97B3 (*Arabidopsis*)	β-ring hydroxylase	CaMV35S	36.7 µg/g β-carotene leaf tissue	overexpression of one carotenogenic gene	Kim et al., 2010
	CYP97C1 (*Arabidopsis*)	ε-ring hydroxylase	CaMV35S	41.3 µg/g β-carotene leaf tissue	overexpression of one carotenogenic gene	Kim et al., 2010
Canola (*Brassica napus*)	*Crt* B (*P. ananatis*)	phytoene synthase	Napin	1617 µg/g fresh weight (FW) total carotenoid in seeds (50-fold)	tissue-specific overexpression of one carotenogenic gene	Shewmaker et al., 1999
	Crt B (*P. ananatis*)	phytoene synthase	Napin	1341 µg/g FW total carotenoid in seeds	tissue-specific overexpression of one carotenogenic gene	Ravanello et al., 2003
	Crt E and *Crt* B (*P. ananatis*)	GGPP synthase and phytoene synthase	Napin	1023 µg/g FW total carotenoid in seeds	overexpression of several carotenogenic genes	Ravanello et al., 2003
	Crt B (*P. ananatis*) *Crt* I (*P. ananatis*)	phytoene synthase and lycopene desaturase	Napin	1412 µg/g FW total carotenoid in seeds	overexpression of several carotenogenic genes	Ravanello et al., 2003
	Crt B and *Crt* Y (*P. ananatis*)	phytoene synthase and lycopene cyclase	Napin	935 µg/g FW total carotenoid in seeds	overexpression of several carotenogenic genes	Ravanello et al., 2003
	Crt B and β-cyclase (*B. napus*)	phytoene synthase and lycopene desaturase	Napin	985 µg/g FW total carotenoid in seeds	overexpression of several carotenogenic genes	Ravanello et al., 2003

Table 1-2 (continued 2/8)

Species	Genes (origin)	Function	Promoters	Carotenoid levels in transgenic plants	Engineering strategy	References
Canola (*Brassica napus*)	*Crt* B, *Crt* I (*P. ananatis*) and CrtY (*P. ananatis*)	phytoene synthase, lycopene desaturase and lycopene cyclase	Napin	1229 µg/g FW total carotenoid in seeds	overexpression of several carotenogenic genes	Ravanello et al., 2003
	idi, *Crt* E, *Crt* B, *Crt* I and *Crt* Y (*P. ananatis*) *Crt* Z, *Crt* W (*Brevundimonas* sp.)	*idi*: isopentenyl diphosphate isomerase	CaMV35S, napin and *Arabidopsis* FAE1 (seed specific)	412-657 µg/g FW total carotenoid in seeds (30-fold)	overexpression of several carotenogenic genes	Fujisawa et al., 2009
				60–190 µg/g FW total ketocarotenoid in seeds		
Carrot (*Daucus carota*)	*Psy* (*Arabidopsis*)	phytoene synthase	CaMV35S	858.4 µg/g DW total carotenoid in roots	overexpression of one carotenogenic gene	Maass et al., 2009
	Bkt1 (*H. pluvialis*) *Chy-b* (*Arabidopsis*)	β-carotene ketolase and β-carotene hydroxylase	CaMV35S and *Agrobacterium rhizogenes* rolD (root specific)	345.5 µg/g FW total carotenoid in root	overexpression of several carotenogenic genes	Jayaraj et al., 2008
				240 µg/g root FW novel ketocarotenoid		
	Lcy-b (*Daucus carota*)	lycopene cyclase	CaMV35S	1250 µg/g DW total carotenoid in storage roots (1.6-fold)	overexpression of one carotenogenic gene	Moreno et al., 2013
				900 µg/g DW β-carotene in storage root (1.8-fold)		
Corn (*Zea mays*)	*Psy-1* (Z. mays) *Crt* I (P. ananatis)	phytoene synthase and lycopene desaturase	Wheat LMW glutelin and barley D-hordein	163.2 µg/g DW total carotenoid in seeds (112-fold)	overexpression of several carotenogenic genes	Naqvi et al., 2009
				59.32 µg/g DW β-carotene in seeds (169-fold)		
	Crt B and *Crt* I (*P. ananatis*)	phytoene synthase and lycopene desaturase	Super γ-zein	33.6 µg/g DW total carotenoid in seeds (34-fold)	overexpression of several carotenogenic genes	Aluru et al., 2008
	Psy-1 (*Z. mays*) *Crt* I (*P. ananatis*) *Crt* W (*Paracoccus spp.*) *Lyc-b* (*Gentiana lutea*)	phytoene synthase, lycopene desaturase, β-carotene ketolase and lycopene cyclase	Wheat LMW glutelin, barley D-hordein, corn γ-zein, rice prolamin (all endosperm-specific)	146.7 µg/g DW total carotenoid in seeds	overexpression of several carotenogenic genes	Zhu et al., 2008
				35.85 µg/g DW total ketocarotenoid in seeds		

53

Table 1-2 (continued 3/8)

Species	Genes (origin)	Function	Promoters	Carotenoid levels in transgenic plants	Engineering strategy	References
Lilly (*Lilium*)	*Crt* Z, *Crt* W, idi, *Crt* E, *Crt* B, *Crt* I and *Crt* Y	described in other lines	CaMV35S	133 μg/g FW total carotenoid and ketocarotenoid (26-fold) in calli, 135 μg/g FW (7.5-fold) in leaves	overexpression of several carotenogenic genes	Azadi et al., 2010
				17.7 μg/g FW β-carotene (59-fold) in calli, 44.6 μg/g FW (9-fold) in leaves		
Lotus (*Lotus japonicus*)	*Crt* W (*Agrobacterium aurantiacum*)	β-carotene ketolase	CaMV35S	387 mg/g FW total carotenoid in flower petals (1.5-fold)	overexpression of one carotenogenic gene	Suzuki et al., 2007
				89.9 μg/g FW total ketocarotenoid in flower petals (2.2-fold)		
Potato (*Solanum tuberosum*)	*Dxs* (*E. coli*)	DXP synthase	Patatin (tuber specific)	7 μg/g DW total carotenoid in tubers (2-fold)	tissue-specific overexpression of one carotenogenic gene	Morris et al., 2006a
	Crt B (*P. ananatis*)	phytoene synthase	Patatin	35 μg/g DW total carotenoid in tubers (6.3-fold)	tissue-specific overexpression of one carotenogenic gene	Ducreux et al., 2005
				11 μg/g DW β-carotene in tubers (19-fold)		
	Crt B (*P. ananatis*) *Bkt1* (*Haematococcus pluvialis*)	phytoene synthase and β-carotene ketolase	Patatin	5.2 μg/g DW total carotenoid in tubers	overexpression of several carotenogenic genes	Morris et al., 2006b
				1.1 μg/g DW total ketocarotenoid in tubers	overexpression of several carotenogenic genes	
	Crt B, *Crt* I and *Crt* Y (*P. ananatis*)	phytoene synthase, lycopene desaturase and lycopene cyclase	Patatin	114 μg/g DW total carotenoid in tubers (20-fold)	overexpression of several carotenogenic genes	Diretto et al., 2007a
				47 μg/g DW β-carotene in tubers (3600-fold)		
	Lyc-e (potato, antisense)	lycopene cyclase	Patatin	9.9 μg/g DW total carotenoid in tubers (2.5-fold)	tissue-specific overexpression of one carotenogenic gene	Diretto et al., 2006
				0.043 μg/g DW β-carotene in tubers (14-fold)		
	Zep (*Arabidopsis*)	zeaxanthin epoxidase	GBSS (tuber specific)	60.8 μg/g DW total carotenoid in tubers (5.7-fold)	tissue-specific overexpression of one carotenogenic gene	Romer et al., 2002

Table 1-2 (continued 4/8)

Species	Genes (origin)	Function	Promoters	Carotenoid levels in transgenic plants	Engineering strategy	References
Potato (*Solanum tuberosum*)	*Crt* O (*Synechocystis* sp.)	β-carotene ketolase	CaMV35S	39.76 μg/g DW total carotenoid in tubers Ketocarotenoid represented 10–12% of total carotenoid in tubers	overexpression of one carotenogenic gene	Gerjets and Sandmann, 2006
	Bkt 1 (*H. pluvialis*)	β-carotene ketolase	CaMV35S	30.4 μg/g DW total carotenoid in tubers 19.8 μg/g DW total ketocarotenoid in tubers	overexpression of one carotenogenic gene	Gerjets and Sandmann, 2006
	Bch (potato, antisense)	β-carotene hydroxylase	Patatin	9.3 μg/g DW total carotenoid in tubers (4.5-fold) 0.085 μg/g DW β-carotene in tubers (38-fold)	RNAi of carotenogenic gene	Diretto et al., 2007b
	Bch (potato, antisense)	β-carotene hydroxylase	GBSS and CaMV35S	3.31 μg/g DW β-carotene in tubers	RNAi of carotenogenic gene	Van Eck et al., 2007
	Crt W and *Crt* Z (*Brevundimonas* sp.)	β-carotene ketolase and β-carotene hydroxylase	CaMV35S	4260 μg/g DW total ketocarotenoid in leaves, 26.30 μg/g DW in tuber	overexpression of several carotenogenic genes	Mortimer et al., unpublished
	Or (*Brassica oleracea var botrytis*)	conversion of non-coloured plastid to chromoplasts	GBSS	25 μg/g DW total carotenoid (6-fold) in tubers	overexpression of non-carotenogenic genes	Lu et al., 2006
	Or (*Brassica oleracea var botrytis*)	conversion of non-coloured plastid to chromoplasts	GBSS	31 μg/g DW total carotenoid in tubers (5.7-fold)	overexpression of non-carotenogenic genes	Lopez et al., 2008
Rice (*Oryza sativa*)	*Psy-1* (daffodil)	phytoene synthase	CaMV35S	0.3 μg/g dry weight (DW) phytoene in seeds	tissue-specific overexpression of one carotenogenic gene	Burkhardt et al., 1997
			Gt1 (seed specific)	0.74 μg/g DW phytoene in seeds	overexpression of one carotenogenic gene	
	Psy-1 (*Zea mays*) *Crt* I (*Pantoea ananatis*)	phytoene synthase and lycopene desaturase	Gt1	37 μg/g DW total carotenoid in seeds	overexpression of several carotenogenic genes	Paine et al., 2005
	Psy-1 and *Lyc-b* (daffodil) *Crt* I (*Pantoea ananatis*)	phytoene synthase, lycopene cyclase and lycopene desaturase	Gt1 (*Psy* 1 and *Lyc-b*) and CaMV35S (*CrtI*)	1.6 μg/g DW total carotenoid in endosperm	overexpression of several carotenogenic genes	Ye al., 2000

Table 1-2 (continued 5/8)

Species	Genes (origin)	Function	Promoters	Carotenoid levels in transgenic plants	Engineering strategy	References
Sweet potato (*Ipomoea batatas L. Lam. cv.Yulmi*)	*Or* (*Ipomoea batatas L. Lam. cv. Sinhwangmi*)	conversion of non-coloured plastid to chromoplasts	CaMV35S	50 μg/g DW total carotenoid (10-fold)	overexpression of non-carotenogenic genes	Kim et al., 2013a
	Lcy- e (sweetpotato; antisense)	lycopene ε-cyclase	CaMV35S	20 μg/g DW β-carotene in calli (20-fold) 65 μg/g DW total carotenoid in calli (9-fold)	RNAi of carotenogenic gene	Kim et al., 2013b
	Chy-b (*Ipomoea batatas L. Lam. cv. Sinhwangmi* ; antisense)	β-carotene hydroxylase	CaMV35S	34.4 μg/g DW β-carotene in calli (38-fold) 117 μg/g DW total carotenoid in calli (18-fold)	RNAi of carotenogenic gene	Kim et al., 2012
Tobacco (*Nicotiana*)	LeLUT1 (tomato)	ε-hydroxylase	CaMV35S	ca. 100 μg/g FW lutein (1.6-fold increase)	overexpression of one carotenogenic gene	Zhou et al., 2013
	Crt W and *Crt* Z (*Paracoccus sp.*)	β-carotene ketolase and β-carotene hydroxylase	CaMV35S	1275 μg/g DW total carotenoid in leaves 64 μg/g DW total ketocarotenoid in leaves	overexpression of several carotenogenic genes	Ralley et al., 2004
	Crt W and *Crt* Z (*Brevundimonas* sp.)	β-carotene ketolase and β-carotene hydroxylase	Ribosomal RNA	7290 μg/g DW total ketocarotenoid in leaves	plastid transformation (overexpression of several carotenogenic genes)	Hasunuma et al., 2008
	Crt O (*Synechocystis* sp.) *Crt* Z (*P. ananatis*)	β-carotene ketolase and hydroxylase	CaMV35S	839 μg/g DW total carotenoid in leaves (2.5-fold) 342.4 μg/g DW total ketocarotenoid in leaves	overexpression of several carotenogenic genes	Gerjets et al., 2007
	Crt O (*Synechocystis* sp.)	β-carotene ketolase	CaMV35S	429 μg/g DW total carotenoid in leaves 156.1 μg/g DW total ketocarotenoid in leaves	overexpression of one carotenogenic gene	Zhu et al., 2007
	Crt O (*H. pluvialis*)	β-carotene ketolase	pds (fruit specific; tomato)	300 μg/g DW total ketocarotenoid in nectary (flower)	overexpression of one carotenogenic gene	Mann et al., 2000

Table 1-2 (continued 6/8)

Species	Genes (origin)	Function	Promoters	Carotenoid levels in transgenic plants	Engineering strategy	References
Tobacco (*Nicotiana*)	*Crt* W and *Crt* Z (*Brevundimonas* sp.)	β-carotene ketolase and β-carotene hydroxylase	CaMV35S	1910 µg/g DW total ketocarotenoid in leaves, 13970 µg/g DW in nectary/ovary, 5950 µg/g DW in petal	overexpression of several carotenogenic genes	Mortimer et al., unpublished
Tomato (*Solanum lycopersicum*)	*Dxs* (*Escherichia coli*)	DXP synthase	Fibrillin (pepper)	7200 µg/g DW total carotenoid in fruit (1.6-fold) 700 µg/g DW β-carotene (1.5-fold); 6700 µg/g DW lycopene (1.6-fold)	tissue-specific overexpression of one carotenogenic gene	Enfissi et al., 2005
	Psy-1 (tomato)	phytoene synthase	CaMV35S	3615 µg/g DW total carotenoid in vegetative tissue (1.14-fold) detection of lycopene (386 µg/g DW) and small increase of β-carotene	overexpression of one carotenogenic gene	Fray et al., 1995
	Psy-1 (tomato)	phytoene synthase	CaMV35S	2276.7 µg/g DW total carotenoid in ripe fruit (1.25-fold) 819 µg/g DW β-carotene in ripe fruit (1.4-fold)	overexpression of one carotenogenic gene	Fraser et al., 2007
	Crt B (*P. ananatis*)	phytoene synthase	Polygalacturonase (fruit specific)	5918 µg/g DW total carotenoid in ripe fruit (2-fold) 825 µg/g DW β-carotene (5-fold); 56 µg/g DW phytoene (1.6-fold); 5137 µg/g DW lycopene (1.8-fold)	tissue-specific overexpression of one carotenogenic gene	Fraser et al., 2002
	Crt I (*P. ananatis*)	lycopene desaturase	CaMV35S	520 µg/g DW (1.9-fold) β-carotene in fruit reduced lycopene and phytoene content	overexpression of one carotenogenic gene	Romer et al., 2000
	Lyc-b (*Arabidopsis*) *Chy-b* (*Capsicum annuum*)	lycopene cyclase β-carotene hydroxylase	pds (fruit specific; tomato)	63 µg/g FW β-carotene in fruit (12-fold) β-cryptoxanthin (11µg/g FW) and zeaxanthin (13 µg/g FW) were produced	tissue-specific overexpression of one carotenogenic gene	Dharmapuri et al., 2002
	Lyc-b (*Arabidopsis thaliana*)	lycopene cyclase	pds (fruit specific; tomato)	57 µg/g FW β-carotene in fruit (7-fold); no affect on lycopene	tissue-specific overexpression of one carotenogenic gene	Rosati et al., 2000

Table 1-2 (continued 7/8)

Species	Genes (origin)	Function	Promoters	Carotenoid levels in transgenic plants	Engineering strategy	References
Tomato (*Solanum lycopersicum*)	*Lyc-b* (antisense; *Arabidopsis thaliana*)	lycopene cyclase	pds (fruit specific; tomato)	85 μg/g FW lycopene in fruit (1.6-fold)	RNAi of carotenogenic gene	Rosati et al., 2000
	Lyc-b (tomato)	lycopene cyclase	CaMV35S	215.2 μg/g FW total carotenoid in fruit (2.3-fold)	overexpression of one carotenogenic gene	D'Ambrosio et al., 2004
	Lyc-b (citrus)	lycopene cyclase	CaMV35S	205 μg/g FW β-carotene in fruit (46-fold); almost no lycopene left	overexpression of one carotenogenic gene	Guo et al., 2012
				1105 μg/g DW β-carotene in fruit (4-fold)		
				30% increase of total carotenoid in fruit		
	Lyc-b (daffodil)	lycopene cyclase	Ribosomal RNA	950 μg/g DW β-carotene (4.5-fold) in fruit	plastid transformation (overexpression of one carotenogenic gene)	Apel and Bock, 2009
	Cyc-b (tomato)	lycopene cyclase	CaMV35S	increased % of β-carotene (6-fold)	overexpression of one carotenogenic gene	Ronen et al., 2000
	Cyc-b (antisense; tomato)	lycopene cyclase	CaMV35S	increased % of lycopene (1.1-fold)	RNAi of carotenogenic gene	
	Crt Y (*P. ananatis*)	lycopene cyclase	aptI	286 μg/g DW β-carotene in fruit (4-fold)	tissue-specific overexpression of one carotenogenic gene	Wurbs et al., 2007
	SINCED1	9-*cis*-epoxycarotenoid dioxygenase	E8 fruit-specific	210 μg/g FW lycopene in pulp (1.5-fold); 40 μg/g β-carotene (2.4-fold)	RNAi of carotenogenic gene	Sun et al., 2012
				275 μg/g FW total carotenoid in pulp (1.6-fold)		
	CrtR-b2 (tomato)	β-carotene hydroxylase	CaMV35S	1589 μg/g DW violaxanthin in leaf (3.5-fold)	overexpression of one carotenogenic gene	Giorio et al., 2012
				3453 μg/g DW total carotenoid in leaf (3.5-fold)		
	Crt W and *Crt* Z (*Paracoccus sp.*)	β-carotene ketolase and β-carotene hydroxylase	CaMV35S	Ketocarotenoid formation in leaves, low levels detected in the fruit	overexpression of several carotenogenic genes	Ralley et al., 2004
	Bkt (*Chlamdomonas reinhardtii*) and *Bhy* (*Haematococcus pluvialis*)	β-carotene ketolase and β-carotene hydroxylase	CaMV35S	5050 μg/g DW total ketocarotenoid in leaves	overexpression of several carotenogenic genes	Huang et al., 2013

Table 1-2 (continued 8/8)

Species	Genes (origin)	Function	Promoters	Carotenoid levels in transgenic plants	Engineering strategy	References
Tomato (*Solanum lycopersicum*)	Chrd (cucumber; antisense)	lipid associated protein	CaMV35S	Reduced carotenoid levels in flower	overexpression of non-carotenogenic genes	Leitner-Dagan et al., 2006
	Fibrillin (*Capsicum annuum*)	lipid associated protein	Fibrillin (pepper)	150 µg/g FW β-carotene (1.5-fold); 450 µg/g FW lycopene (2-fold); increased derived volatiles in fruit	overexpression of non-carotenogenic genes	Simkin et al., 2007
	Cry2 (tomato)	blue light photoreceptors	CaMV35S	1490 µg/g DW total carotenoid ripe fruit pericarps (1.7-fold) 101 µg/g DW β-carotene ripe fruit pericarps (1.3-fold)	overexpression of non-carotenogenic genes	Giliberto et al., 2005
	Det-1 (tomato, antisense)	light signal transduction	P119, 2A11 and TFM7 (ripening enhanced)	increased β-carotene (8.5-fold) and lycopene (2.2-fold) and increased flavonoid content in red-ripe fruit	RNAi of non-carotenogenic gene	Davuluri et al., 2005
	Det-1 (tomato, antisense)	light signal transduction	P119, 2A11 and TFM7 (ripening enhanced)	1455 µg/g DW β-carotene (15-fold); 1574 µg/g DW lycopene (5-fold); 4179 mg/g DW total carotenoid (6-fold) in ripe fruit	RNAi of non-carotenogenic gene	Enfissi et al., 2010
	Cul4	light signal transduction, DDB1 interacting protein	TMF7 (ripening enhanced)	59 µg/g FW β-carotene (2-fold); 310 µg/g FW lycopene (2-fold) in fruit	overexpression of non-carotenogenic genes	Wang et al., 2008
Wheat (*Triticum*)	*Psy-1* (*Z. mays*) *Crt* I (*P. ananatis*)	phytoene synthase and lycopene desaturase	CaMV35S and 1Dx5 (endosperm specific)	4.96 µg/g DW in seeds	overexpression of several carotenogenic genes	Cong et al., 2009

Table 1-2 Carotenoids and ketocarotenoid enhancement in transgenic plants (adapted from Farre et al., 2010)

A colour code differentiates each engineering strategy. Light pink, tissue-specific overexpression of one carotenogenic gene; light yellow, overexpression of one carotenogenic gene; green, overexpression of several carotenogenic genes; blue, RNAi of carotenogenic gene; dark blue, RNAi of non-carotenogenic gene; grey, overexpression of non-carotenogenic genes; yellow, plastid transformation. Highlighted cells correspond to the greatest levels of carotenoids and ketocarotenoids produced in plants.

The greatest amounts of β-carotene and lycopene were obtained in engineered tomato plants (Table 1-2) (Fraser et al., 2002; Enfissi et al., 2005; Enfissi et al., 2010; Guo et al., 2012). The same approach was chosen in three of these studies: Fraser et al., 2002, Enfissi et al., 2005 and Guo et al., 2012. It consisted of overexpressing a carotenogenic gene, *Crt*B, *dxs* and *Lcy-b*, respectively, from different species (*Pantoea ananatis*, *E. coli* and *Citrus*, respectively) in tomato. The fold change increase of carotenoid levels in these studies are not as spectacular compared to some other studies (1.5- to 5-fold increase compared to, for instance, 38-fold increase of β-carotene in sweet potatoes down-regulating β-hydroxylase (Kim et al., 2012)) (Table 1-2). However, tomato has high carotenoid basal levels and therefore, even a 1.5-fold increase has a substantial effect in terms of quantity of carotenoids. In the fourth study, the down regulation of a gene implicated in light signal transduction (*det1*) contributed to an increase of the plastid area in the fruit and consequently to an increased level of carotenoids (Enfissi et al., 2010). This work highlights the potential of an engineering strategy based on the alteration of carotenoid sequestration instead of their biosynthesis. The transgenic plants producing the highest levels of ketocarotenoids were engineered tobacco plants (Table 1-2; Hasunuma et al., 2008, Mortimer et al., unpublished). In these two studies, *Crt*Z and *Crt*W genes from *Brevundimonas* sp. were overexpressed in tobacco via plastid and nuclear transformation, respectively. The corresponding enzymes (CRTZ and CRTW) have been shown to be highly efficient in producing ketocarotenoids (Choi et al., 2005; Choi et al., 2006; Choi et al., 2007). Moreover, *Crt*Z and *Crt*W genes were transcriptionally optimised, since they were chemically synthesised with plant (rape) codon usage and, in the Mortimer et al. study, they were also translationally enhanced via the use of a potent *NtADH* 5′UTR (Satoh et al., 2004). Applying the strategy of overexpressing several carotenogenic genes, which are transcriptionally and translationally enhanced in tobacco, is the best combination so far, to produce ketocarotenoids in plants.

1.3.3 Plant platforms to engineer high levels of isoprenoids

Tomato is the most common fruit produced worldwide (FAOSTAT database 2011) and thus, it is amenable to modern agricultural practices, and could be produced in contained growth facilities as for GM perspectives. Tomato is a model plant well studied. As a consequence, genetic and genomic resources have been developed

(Zouine et al., 2012), advanced transcriptomic, metabolomic and proteomic platforms are established and efficient transformation protocols have been set up. Moreover, tomato is one of the plants with the highest basal level of carotenoids. It contains specialised storage tissues with cellular structures amenable to isoprenoid formation and accumulation. Tomato fruits are the best platform to engineer high amounts of carotenoids (as discussed in section 1.3.2). Additionally, tomato fruits are an essential component of our diet, as tomato fruits and tomato-based products provide at least 85% of our dietary lycopene (Fraser and Bramley, 2004). For all these reasons, tomato plants are an excellent system in which to engineer high level of carotenoids.

Tobacco plants, especially *Nicotiana benthamiana,* are also a plant model. Therefore, as for tomato, genomic resources are well developed. Methods for stable and transient transformation have been established. Moreover, previous studies showed that they are an excellent platform tested so far to engineer high level of ketocarotenoids (Table 1-2).

1.3.4 Genetically modified plants

Genetically modified plants have been grown commercially in the Americas and Asia for over 10 years and more recently in Africa. Regulation of GM plants differs between countries but it also depends on the intended use of the GM product. A crop not designed for human food use is not subjected to same regulations as the one for human consumption. Europe has the most stringent regulations in the world. All GMOs are subjected to extensive case-by-case evaluation by the European Food Safety Authority. GMOs authorised in Europe are mainly for animal feed. On the contrary, in the USA, although GM foods are under regulatory control of three agencies (the Food and Drug Administration (FDA), the Environmental Protection Agency (EPA) and the U.S. Department of Agriculture (USDA)), genetically modified tobacco, canola, corn, cotton, soybean, alfalfa and papaya are grown and commercialised for human consumption (Lemaux, 2008, 2009). Benefits of GM plants include the reduction of production costs and pesticide use, the increase of yields, resistance to insects, bacterial, fungal and viral diseases but also resistance to drought, salt and cold tolerance, the production of biopharmaceuticals, biofortified crops and biofuels (Yonekura-Sakakibara and Saito, 2006; Lemaux, 2008, 2009;

Clarke and Daniell, 2011). The slow pace of European approval has been criticized. Golden Rice, a crop containing a high level of provitamin A created to fight malnutrition in developing countries, may reach the market in the following years after 13 years of excessive regulations (Potrykus, 2010). This genetically engineered rice could have already saved many millions of humans from blindness and starvation. Although GM foods have been grown and consumed in other part of the world for years with no adverse environmental or health effects, in Europe, GM foods are still considered as a threat to human health by many. Some consumers avoid genetically engineered crops as they perceive them to be unnatural foods as opposed to the fruits and vegetables available in European supermarkets, which are perceived as natural. However, commercial varieties that are consumed by the public have also undergone genetic modifications during conventional breeding or selection (Manshardt, 2004; Rozin et al., 2012). This highlights the need for better communication with the public to ensure consumer understanding of the processes employed in the creation of both GM and non-GM products. This could be key to unlocking the excessive regulations applied in Europe.

1.4 Aim and objectives of the study

The aim of this project is the evaluation of potential engineering strategies to optimise the production of high-value isoprenoids in higher plants and especially, valuable carotenoids and ketocarotenoids. Additionally, mechanisms of the plant adaptation responses to increased carotenoid content were investigated most notably the process of carotenoid sequestration in the transgenic plants.

The metabolic engineering strategies assessed are described in the following objectives. The plant platforms chosen to test the different approaches are the tomato and tobacco plants for the reasons mentioned in section 1.3.3.

Objective 1: To evaluate the potential benefits of simultaneously overexpressing two bacterial carotenoid genes in tomato plants, compared to single independent expression, in terms of carotenoid content. The carotenogenic genes *Crt*E (geranylgeranyl diphosphate synthase), *Crt*B (phytoene synthase) and *Crt*I (phytoene desaturase) genes from the bacterium *Pantoea ananatis* were expressed

independently and in combination (*Crt*E+B, *Crt*E+I and *Crt*B+I) in Ailsa Craig tomato plants (Chapter III). The development of biofortified tomatoes, which contain more antioxidants and health-promoting compounds, is an attractive project for future perspectives.

Objective 2: To further our understanding of adaption mechanisms of the plants in response to perturbed carotenoid content at the level of the fruit, chromoplast but also at a sub-chromoplast level. The tomato *Crt*B+I line, which has a high level of carotenoids, was selected to fulfil this objective (Chapter IV). Knowledge on carotenoid sequestration mechanisms is of great importance as it could be utilised to generate new engineering strategies for the enhancement of carotenoid levels in plants.

Objective 3: To optimise the production of carotenoids in tomato via transcription enhancement of heterologous expression of bacterial genes. The chromoplast specific lycopene β-cyclase promoter from the orange fruited *Solanum galapagense* was chosen to control the expression of the *Crt*B and *Crt*I genes (Chapter V). The timing and strength of expression of this promoter is thought to be more appropriate for the carotenoid pathway compared than the ones utilised previously in the *Crt*B+I construct (objectives 1&2).

Objective 4: To optimise the production of high-value ketocarotenoids in plants via combining the expression of ketocarotenoid genes (*Crt*Z and *Crt*W), with transcription factors potentially related to carotenoid regulation (PIF5 and ARR14). The marine bacterial genes *Crt*Z (carotene hydroxylase) and *Crt*W (carotene ketolase) from *Brevundimonas* were selected as they were shown to be the most efficient at producing ketocarotenoids in plants (see section 1.3.2). They were transcriptionally and translationally enhanced via plant codon usage and a potent 5′ UTR, respectively. The potential of the transcription factors Phytochrome-Interacting Factor 5 (PIF5) and Arabidopsis Response Regulator 14 (ARR14) to enhance the formation of ketocarotenoids is assessed (Chapter VI). Industrial production of natural ketocarotenoids from plants, such as tobacco, could be a promising process to compete with chemical synthesis as the production method of choice for ketocarotenoid production.

A summary scheme representing the interactions of the bacterial enzymes used to achieve these objectives with the carotenoid pathway in plants is shown in Figure 1-20.
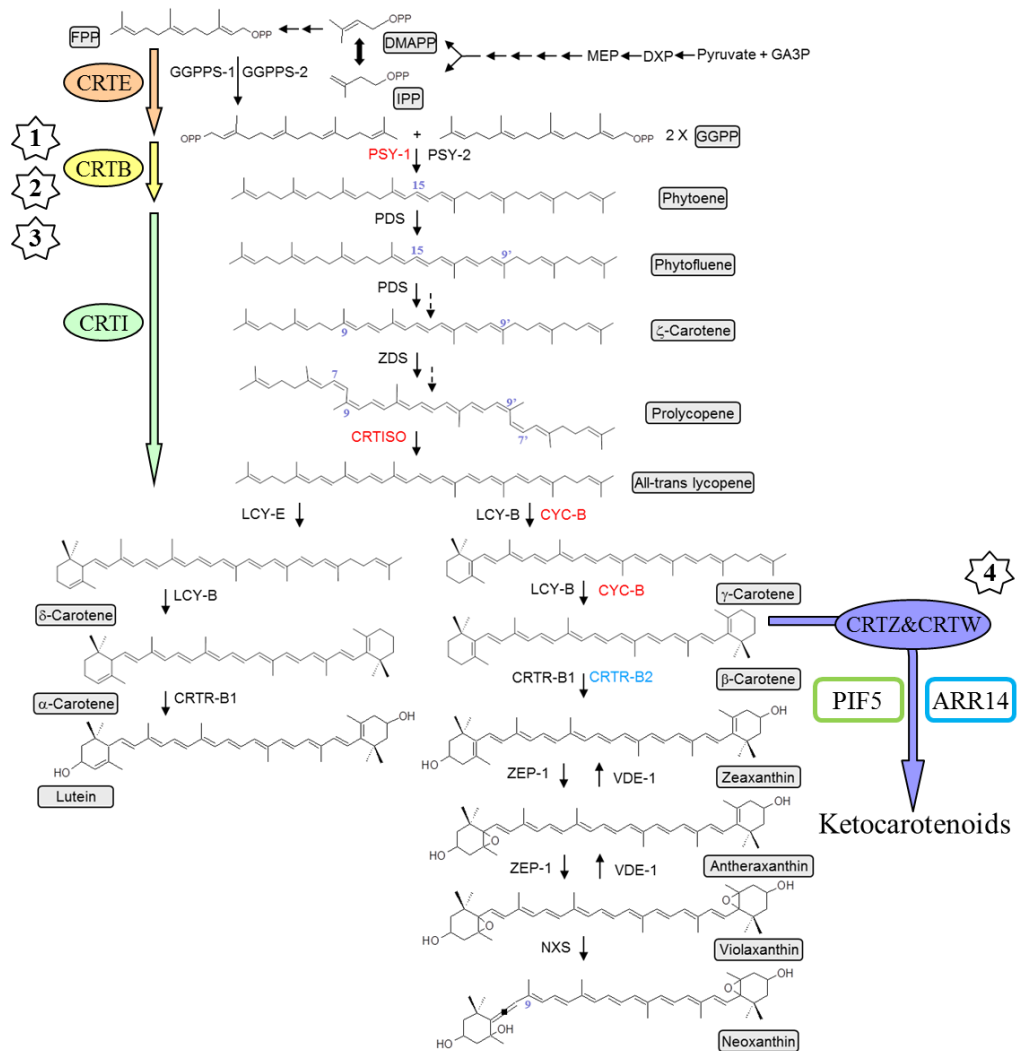
Figure 1-20 Summary scheme of the interactions of the bacterial carotenogenic enzymes within the carotenoid biosynthetic pathway in plants

Numbers in stars correspond to the number of the objective of this thesis. Enzymes: CRTE, geranylgeranyl diphosphate synthase; CRTB, phytoene synthase; CRTI, phytoene desaturase; CRTZ, carotene hydroxylase; CRTW, carotene ketolase. Transcription factors: PIF5, Phytochrome-Interacting Factor 5; ARR14, Arabidopsis Response Regulator 14. Enzymes in red are tomato fruit ripening specific or enhanced, those in blue are flower specific. GA3P, glyceraldehyde-3-phosphate; DXP, 1-deoxy-D-xylulose 5-phosphate; MEP, 2-C-methyl-D-erythritol 4-phosphate; IPP, isopentenyl diphosphate; DMAPP, dimethylallyl diphosphate; FPP, farnesyl diphosphate; GGPP, geranylgeranyl diphosphate; GGPPS-1 and -2, geranyl diphosphate synthase; PSY-1, fruit specific phytoene

synthase-1, PSY-2, phytoene synthase-2; PDS, phytoene desaturase; ZDS, ζ-carotene desaturase, CRTISO, carotene isomerase; LCY-E, ε–lycopene cyclase; LCY-B, β-lycopene cyclase; CYC-B, fruit specific β-lycopene cyclase; CRTR-B1, carotene β-hydroxylase 1; CRTR-B2, carotene β-hydroxylase 2 (flower specific); ZEP, zeaxanthin epoxidase; NXS, neoxanthin synthase; VDE, violaxanthin de-epoxidase. The *cis* configurations are not showed in all the molecules but they are represented with blue numbers. The dashed arrows illustrate biochemical steps which are not represented in this scheme.

Chapter II: Materials and methods

2.1 Plant cultivation and collection

2.1.1 Tomato and tobacco cultivation

Tomato (*Solanum lycopersicum* Mill. cv. Ailsa Craig) and tobacco (*Nicotiana benthamiana*) plants were grown in pots containing M3 professional growing medium (Scotts Levington®, UK). Plants were glasshouse-grown, with a daytime temperature of approximately 25°C and nocturnal temperature of 15°C. The light regime used was a 16 h light and 8 h dark. Tomato fruits were tagged at the breaker stage which was designated as the initiation of colour (orange/yellow) on predominantly green fruited tomatoes.

Transformed tomato plantlets received from UC Davis facility (USA) were carefully removed from the tubes with long forceps, taking care not to break off the roots. The agar was rinsed off from the roots with lukewarm tap water. Plants were placed in moist soil (M3 professional growing medium) in 2 inch pots. They were then placed in zip lock freezer bags and under 16 h light in a growth chamber. After 3 days, the bags were unsealed and after 24 to 36 h, they were fully opened. After an additional 24 h, the plants were removed from the bags and left in the growth chamber for an additional 7 days to acclimate before transferring to the greenhouse.

2.1.2 Cross pollination of tomato lines

Tomato *Crt*E, *Crt*B and *Crt*I lines were crossed to generate the *Crt*E+B, *Crt*E+I and *Crt*B+I lines. Cross pollination was performed by depositing the pollen of one line onto the stigma of the flowers of another line using a small paint brush or glass slide.

2.1.3 Tissue collection for DNA/RNA studies

Leaf and fruit tissues were harvested from *Ailsa Craig* tomato plants. Four expanding leaves (c.a. 3-4 cm) of each biological replicate plant were harvested. Younger leaves, at the top of the plants, were preferentially chosen. Leaves were flash frozen in liquid nitrogen and stored at -80°C prior to grinding. Fruits of each biological replicate plant at breaker + 3 days to breaker + 5 days were harvested. Seeds and jelly were quickly removed and the pericarp was cut in pieces (c.a. 2 cm^2). Pieces of pericarp were flash frozen in liquid nitrogen and stored at -80°C.

2.1.4 Tissue collection for metabolite analysis

Leaf and fruit tissues were harvested in a similar manner to that described in section 2.1.3, but these tissues were subsequently freeze dried for either one or three days, respectively, and then stored at -20°C. Fruits were harvested at several stages, depending on the experiments to be performed (mature green, breaker, breaker +3 days, breaker +7 days, breaker +14 days).

2.1.5 Seed collection

Seeds from harvested tomatoes were treated in a hydrochloric acid solution (1:1 HCl(32%)/dH$_2$O) within a plastic tray for 2 h. They were then rinsed with water and dried on filter paper for one day. Seeds were stored in small paper envelopes at room temperature.

2.2 Bacterial cultures

2.2.1 Maintenance of bacterial cultures

Escherichia coli strain DH5α and *Agrobacterium tumefaciens* strains LBA4404 and C58C1 were used. *E. coli* was used for plasmid amplification and vector construction and *Agrobacterium* for plant transformation. Bacterial growth was maintained on Luria Broth (LB; 1% (w/v) tryptone, 0.5 g % (w/v) yeast extract, 1% (w/v) NaCl) and YEB (0.5% (w/v) beef extract; 0.1% (w/v) yeast extract; 0.5% (w/v) peptone; 0.5 % (w/v) sucrose; 0.03% (w/v) MgSO$_4$.7H$_2$O) medium. Agar (1.5% w/v) was added to solidify media when necessary. Cooled media were supplemented with appropriate antibiotics for selection after autoclaving. *E. coli* and *Agrobacterium* were grown on solid and liquid media at 37°C and 28°C, respectively. Liquid cultures were shaken at 180 rpm. Glycerol stocks were made from each new liquid culture as described in section 2.2.2. Frozen bacterial cells were revived by scraping cells from the top of frozen cultures tubes, streaking onto LB-agar or YEB-agar plates, supplemented with appropriate antibiotics. Plates were incubated overnight to two days to establish colonies. Plates were sub-cultured by re-streaking one colony onto fresh plates.

2.2.2 Glycerol stocks

Screw-cap tubes (2 ml) containing 100% glycerol (500 µl) were autoclaved. An overnight culture of bacteria (1.5 ml) was added into the tube in a sterile manner and mixed thoroughly. The bacteria-glycerol solution was flash frozen in liquid nitrogen and placed at -80°C for long-term storage.

2.3 Extraction and analysis of nucleic acids

2.3.1 DNA extraction from plant tissues

Total cellular DNA was isolated, from plant tissues, using the Qiagen DNeasy® Plant Mini Kit, following the manufacturer's instructions. Frozen leaf tissue, collected as detailed in section 2.1.3, was ground using a TissueLyser LT (Qiagen, UK). The insert of the TissueLyser LT adapter was incubated on dry ice for 30 min. Frozen material (up to 100 mg) was placed in pre-cooled 2 ml sterile sample tube RB (Qiagen, UK) with one 0.5 mm stainless steel bead (Qiagen, UK). Leaf tissue was disrupted for 2 min at 50 Hz. Frozen fruit tissue, collected as detailed in section 2.1.3, was ground in liquid nitrogen, using a mortar and pestle. Frozen powder (up to 100 mg) was transferred into a pre-cooled 1.5 ml sterile microcentrifuge tube. Buffer AP1 (400 µl) and RNase A (4 µl) were added to the tubes containing the sample, and mixed vigorously by vortexing. The tubes were incubated for 10 min at 65°C and mixed three times during the incubation. Buffer AP2 (130 µl) was added to the lysate, mixed and the tubes were incubated for 5 min on ice. The lysate was placed into a QIAshredder Mini spin column in a 2 ml collection tube and centrifuged for 2 min at 14,000 rpm with an Eppendorf 5424 centrifuge. The flow-through was transferred to a new sterile microcentrifuge tube and buffer AP3 (1.5 volumes) was added. The sample was then transferred to a DNeasy Mini spin column and centrifuged for 1 min at 14,000 rpm. The flow-through was discarded. The column was transferred to a new 2 ml collection tube and washed twice with buffer AW (500 µl). The column was centrifuged for 1 min at 14,000 rpm for each wash. The column was transferred to a sterile 1.5 ml microcentrifuge tube and the DNA eluted with buffer AE (50 µl, twice), by centrifugation at 14,000 rpm for 1 min. DNA solutions were stored at -20°C.

2.3.2 RNA extraction from plant tissues

Total cellular RNA was extracted, from plant tissues, using the Qiagen RNeasy$^{®}$ Mini Kit and the RNase-Free DNase set (Qiagen, UK). Plant tissue, collected as detailed in section 2.1.3, was ground in liquid nitrogen, using a mortar and pestle. Frozen powder (up to 100 mg) was transferred to a pre-cooled 1.5 ml sterile microcentrifuge tube. Buffer RLT (450 μl) was added to the frozen material and mixed vigorously by vortexing. The lysate was placed into a QIAshredder Mini spin column in a 2 ml collection tube and centrifuged for 2 min at maximum speed with an Eppendorf 5424 centrifuge. The flow-through was transferred to a fresh sterile microcentrifuge tube to which 100% ethanol (0.5 volumes) was added and placed in an RNeasy Mini spin column in a 2 ml collection tube and centrifuged for 15 sec at 14,000 rpm. The flow-through was discarded. Buffer RW1 (350 μl) was added and the column centrifuged for 15 sec at 14,000 rpm, the flow-through was discarded. DNaseI incubation mixture (80 μl) was applied directly to the RNeasy spin column membrane and incubated at room temperature for 15 min. Buffer RW1 (350 μl) was added to wash the membrane, followed by another wash with buffer RPE (500 μl). The column was centrifuged for 15 sec at 14,000 rpm for each wash. A final wash with buffer RPE (500 μl) was performed and the column centrifuged for 2 min at 14,000 rpm. The flow-through of each wash was discarded. The column was placed into a new sterile microcentrifuge tube and the RNA eluted with RNase-free water (30 μl, twice) by centrifugation for 1 min at 14,000 rpm. RNA solutions were stored at -20°C.

2.3.3 Plasmid DNA purification from bacteria

Plasmid DNA was extracted from bacterial cultures using the Wizard$^{®}$ *Plus* SV Minipreps DNA Purification System reagents and protocol (Promega, UK). Bacterial overnight cultures (1 to 10 ml) were pelleted by centrifugation at 4,000 rpm for 5 min with the Eppendorf centrifuge 5810R. The pellet was resuspended in Cell Resuspension Solution (250 μl) and transferred to a 1.5 ml microcentrifuge tube. Cell Lysis Solution (250 μl) was added as well as Alkaline Protease Solution (10 μl). The sample was mixed by inverting the tube four times after each solution was added. The sample was incubated for 5 min at room temperature. Neutralization Solution (350μl) was added and the sample mixed by inverting the tube four times,

followed by centrifugation for 10 min at 14,000 rpm in an Eppendorf 5424 centrifuge. The cleared lysate was decanted into a Spin Column in a 2 ml collection tube and centrifuged at 14,000 rpm for 1 min. The flow-through was discarded. The spin column was washed twice by adding Wash Solution (750µl and 250µl respectively) followed by centrifugation for 2 min at 14,000 rpm and the flow-through was discarded. The column was transferred to a new sterile 1.5 ml microcentrifuge tube and the DNA eluted in Nuclease-Free Water (100µl) by centrifugation at 14,000 rpm for 1 minute. DNA solutions were stored at -20°C.

2.3.4 Quantification of nucleic acids

Spectrophotometric analysis of nucleic acids, using a NanoDrop 1000 spectrophotometer v3.7, was performed to determine the quantity of nucleic acids extracted and to provide an estimate of sample purity. Amongst the several application modules available, the module nucleic acids was chosen. When measuring DNA, the default setting was used (DNA-50), but for RNA, the option RNA-40 was selected. The spectrophotometer was zeroed using sterile deionised water at 260 nm. Absorbance (Abs) readings of samples (1µl) were taken at 260 nm. As quoted by the manufacturer, the detection limit is 2 ng/µl and the upper limit is 3,700 ng/µl for double strand DNA, 2,400 ng/µl for single strand DNA, and 3,000 ng/µl for RNA. A ratio of the absorbances at 260 and 280 nm was used to assess the purity of DNA and RNA samples. A ratio of ~1.8 and ~2 is accepted as pure for DNA and RNA, respectively. If the ratio is lower, it may indicate the presence of proteins or other contaminants, absorbing near 280 nm. A secondary measure of nucleic acid purity is given by the ratio of the absorbance at 260 and 230 nm. The ratio of pure samples is expected in the range of 1.8 to 2.2.

2.3.5 Construction of vectors

2.3.5.1 Restriction enzyme digestion

Restriction enzymes, such as AscI, PacI and EcoRI, were used in order to cleave DNA fragments from existing plasmids. The restriction enzymes were mainly purchased from Promega, UK and NEW ENGLAND Biolabs[®] Inc., UK. Each restriction enzyme was used according to the manufacturers' instructions. In general,

one unit of restriction enzyme is defined as the amount of enzyme required to digest 1 μg of lambda DNA in 1 h at a certain temperature (usually, 37°C or 65°C). Reactions were generally performed in a final volume of 20 μl, including 5 to 10 units of restriction enzyme, DNA (~1 μg), enzyme buffer (10X) and sterile deionised water. Sometimes, BSA (bovine serum albumin) was also required. Samples were incubated at the appropriate temperature for 1 to 4 h. Loading buffer (6X) was added to the sample and the DNA fragments were separated by agarose gel electrophoresis.

2.3.5.2 Agarose gel electrophoresis

Nucleic acid analysis by electrophoresis was performed on ~1% (w/v) agarose gels, depending on the size of the fragments of interest. Agarose was melted in TBE (Tris-hydroxymethyl-aminomethane (Tris) borate ethylenediamine tetra-acetic acid). GelRed[TM] (10,000X dilution of stock) nucleic acid gel stain (Biotium, UK) was added to the mixture before it was poured in one compartment of a gel electrophoresis tank with a gel comb and left to set for 20 min. The agarose gel was transferred in the electrophoresis tank filled with TBE. Samples were loaded in the gel wells with Blue/Orange Loading Dye (6X; Promega, UK). DNA ladder (100bp or 1kb; Promega) depending on the sizes of the DNA) was run alongside with the samples, for DNA size comparison. Gels were run 10-15 min at 50-100 volts. DNA bands were visualized using a U:Genius[3] gel imaging system (Syngene, UK).

2.3.5.3 DNA purification

Purification of DNA from (i), PCR amplification and (ii), agarose gel was performed using the Wizard® SV Gel and PCR Clean-Up System (Promega, UK). An equal volume of Membrane Binding Solution was added to the PCR amplification product. In the case of DNA purification from an agarose gel, a ratio of 10 μl of Membrane Binding Solution per 10 mg of agarose slice gel, containing the DNA fragment of interest, was added in a sterile 1.5 ml microcentrifuge tube. The sample mixture was mixed vigorously with a vortex and incubated at 50-65°C for 10 min until the gel slice was completely dissolved. The tube was mixed vigorously every few minutes during the incubation time. From here, the same protocol was followed for DNA purification from PCR amplification or agarose gel. The mixture of DNA with Membrane Binding Solution was placed in a SV Minicolumn in a collection tube and

incubated for 1 min at room temperature, followed by centrifugation at 14,000 rpm for 1 min in Eppendorf 5424 centrifuge. The flow-through was discarded. The SV Minicolumn was washed twice by adding Membrane Wash Solution (700 µl and 500 µl, respectively), followed by centrifugation for 1 min and 5 min, respectively, at 14,000 rpm. At each step, the flow-through was discarded. An additional centrifugation at 14,000 rpm for one min was performed. The SV Minicolumn was transferred into a sterile 1.5 ml microcentrifuge tube. Nuclease-Free Water (50 µl) was directly placed at the centre of the column, followed by a one min incubation at room temperature and by centrifugation for 1 min at 14,000 rpm. The eluted DNA was kept at -20°C.

2.3.5.4 Dephosphorylation of 5′ phosphates from DNA or RNA

Dephosphorylation of linearised plasmids is employed to prevent the plasmids recircularising during the ligation step when cloning the DNA of interest. It is especially useful when both ends of the linearised plasmid have been cleaved with the same restriction enzyme. Shrimp Alkaline phosphate (SAP, Promega, UK) was utilised to catalyse the dephosphorylation of 5′ phosphates from DNA. SAP (1 unit per µg DNA) was incubated with cleaned restriction-digested vector at 37°C for 15 min in 1X SAP reaction buffer in a final volume of 30-50 µl. SAP was inactivated by heating at 65°C for 15 min, followed by centrifugation at 14,000 rpm for a few seconds.

2.3.5.5 Ligation

The ligation of two strands of DNA is necessary to form plasmid from different DNA fragments. The T4 DNA Ligase (Promega, UK) was utilised to catalyse this reaction. A 1:3 molar ratio of vector:insert DNA was used to clone a fragment into a plasmid vector. The following formula was used to calculate the amount (ng) of insert to be used.

$$\frac{\text{ng of vector x kb size of insert}}{\text{kb size of vector}} \times \text{molar ratio of} \frac{\text{insert}}{\text{vector}} = \text{ng of insert}$$

In a sterile microcentrifuge tube, the appropriate amount of vector DNA and insert was added, together with 1 unit of T4 DNA ligase, ligase buffer (10X) and Nuclease-

Free Water to a final volume of 10 µl. The reaction was incubated at room temperature for 3 h or overnight at 4°C.

2.3.5.6 Description of vectors used in this work

The vectors used in this work are described in Table 2-1. A representative scheme of the vectors is shown in appendix Figure A2-1.

| Name of vectors | Description | Antibiotic resistance in | | | References |
		Escherichia coli (DH5α)	*Agrobacterium* (LBA4404 or C58C1)	Plant	
CrtE	Geranylgeranyl diphosphate synthase gene (*P. ananatis*)	Kanamycin	Rifampicin, Kanamycin	Kanamycin	Fraser et al.
CrtB	Phytoene synthase gene (*P. ananatis*)	Kanamycin	Rifampicin, Kanamycin	Kanamycin	Fraser et al., 2002
CrtI	Phytoene desaturase gene (*P. ananatis*)	Kanamycin	Rifampicin, Kanamycin	Kanamycin	Romer et al., 2000
CrtB*	Phytoene synthase gene (*P. ananatis*)	Ampicillin	Rifampicin, Ampicillin	Kanamycin	Misawa et al., perso. com.
CrtI*	Phytoene desaturase gene (*P. ananatis*)	Ampicillin	Rifampicin, Ampicillin	Kanamycin	Misawa et al., perso. com.
pb	Lycopene β-cyclase promoter (*S. galapagense*)	Kanamycin	Rifampicin, Kanamycin	Kanamycin	Heldt et al., perso. com.
pbCrtB	Phytoene synthase gene (*P. ananatis*)	Ampicillin	Rifampicin, Ampicillin	Kanamycin	Nogueira, PhD study
pbCrtI	Phytoene desaturase gene (*P. ananatis*)	Ampicillin	Rifampicin, Ampicillin	Kanamycin	Nogueira, PhD study
pbCrtB+I	Phytoene synthase and desaturase genes (*P. ananatis*)	Ampicillin	Rifampicin, Ampicillin	Kanamycin	Nogueira, PhD study
ZW	Carotene hydroxylase (*Crt* Z) and ketolase (*Crt* W) (*Brevundimonas*) with plant codon usage	Spectinomycin	Rifampicin, Spectinomycin	Kanamycin	Misawa et al., perso. com.
PIF5	Phytochrome-Interacting Factor 5 transcription factor	Spectinomycin	Rifampicin, Spectinomycin	Kanamycin	Misawa et al., perso. com.
ARR14	Arabidopsis Response Regulator 14 transcription factor	Ampicillin	Rifampicin, Ampicillin	Kanamycin	Misawa et al., perso. com.
ZW-PIF5	*Crt* Z+*Crt* W+PIF5	Spectinomycin	Rifampicin, Spectinomycin	Kanamycin	Misawa et al., perso. com.
ZW-ARR14	*Crt* Z+*Crt* W+ARR14	Spectinomycin	Rifampicin, Spectinomycin	Kanamycin	Misawa et al., perso. com.
GUS	β-glucuronidase gene	Spectinomycin	Rifampicin, Spectinomycin	Kanamycin	Laboratory stocks
p19	p19 Suppressor of gene silencing gene	Kanamycin, Chloramphenicol	Rifampicin, Kanamycin, Chloramphenicol	Kanamycin	Laboratory stocks
pBINPLUS	Binary vector for plant transformation	Kanamycin	Rifampicin, Kanamycin	Kanamycin	Laboratory stocks
pZK3B	Empty vector for cloning	Spectinomycin	Rifampicin, Spectinomycin	Kanamycin	Misawa et al., perso. com.

Table 2-1 Description of the vectors used in this study

Kanamycin, ampicillin and rifampicin were utilised at 50 mg/µl, spectinomycin at 100 mg/µl and chloramphenicol at 36 mg/µl.

All the plant transformations, using the vectors described in Table 2-1, were carried out during this thesis except for the *Crt*E, *Crt*B and *Crt*I tomato lines, which were created prior this work.

2.3.6 Testing the presence of transgenes

2.3.6.1 Designing primers

Primers were designed using the open-source program Primer3web version 4.0.0 (http://primer3.ut.ee/) and the sequence of the genes of interest mainly obtained from the National Centre for Biotechnology (NCBI) website (www.ncbi.nlm.nih.gov). Primers for PCR analysis were designed to the following specifications: 18-23bp (optimal 20bp) for primer length, Tm of 57-62°C (optimal 59°C), maximum Tm difference, 5°C and a percentage of GC content of 30-70% (optimal 50%). Primers for real-time PCR analysis, using the SYBR® Green system, were designed with different specifications: amplicon length: 100-150bp, primer length: 10-30bp, GC content: ideally 40-60%, Tm: 55-60°C and the maximal Tm difference between primers, 4°C. For both PCR and real-time PCR primers, mismatches between primers and target, especially towards the 3′ end of the primer should be avoided, as well as 3′ end with Ts, complementarities within the primers to avoid hairpins, complementarities between the primers to avoid primer dimers, especially of 2 or more bases at the 3′ ends of the primers. Primers were supplied by Eurofins MWG Operon, UK. The sequences of the primers used in this work are listed in the appendix Table A2-2.

2.3.6.2 PCR

The presence of the *Crt* genes in the crossed lines was detected by PCR, using sets of primers shown in Table A2-2. PCR reactions were performed using IllustraTM puReTaq Ready-to-go PCR beads (GE Healthcare, UK), with reagents prepared following the manufacturer's guidelines. Reactions contained 10 pmol of each of the respective forward (5′ 3′) and reverse (3′ 5′) primers, ~50 ng of plant genomic DNA, extracted from the leaves, as described in section 2.3.1, and sterile molecular water (Sigma-Aldrich, UK) to a final volume of 25 µl. Tubes were incubated at 95°C for 5 min to denature the DNA template, followed by 30 cycles of PCR amplification, which consisted of a denaturation step at 94°C for 30 sec, an annealing step at 50°C

for 30 sec and an extension step at 72°C for 30 sec. A final incubation of 5 min at 72°C was performed to complete the reaction. Reactions were carried out using a Techgene thermo cycler (Techne, UK). The temperature of annealing varied depending on the set of primers. The annealing temperature corresponds to approximately the Tm of the primers minus 5°C. PCR products were analysed by agarose gel electrophoresis (described in section 2.3.5.2).

2.3.7 Determination of genes' zygosity in plants

2.3.7.1 Cloning DNA in TOPO® vector

PCR products were cloned into pCR®2.1 TOPO® cloning vectors for quantitative real-time PCR (section 2.3.7.2), using the TOPO-TA DNA cloning® kit (Invitrogen, UK). The PCR product (2 μl) was added to a salt solution (1 μl), TOPO® vector (1 μl) and sterile water to a final volume of 6 μl. The mixture was incubated for 5 min at room temperature to allow the ligation reaction to proceed. The reaction (TOPO® Cloning reaction) was placed on ice. TOPO® Cloning reaction (2 μl) was added to a vial of One Shot® TOP10 chemically competent *E.coli* cells, which were previously thawed on ice. One Shot® TOP10 competent cells were transformed by heat shock treatment at 42°C for 30 sec, followed by immediate incubation on ice. Room temperature S.O.C. medium (250 μl) was added to the transformation reaction and the tubes incubated at 200 rpm, horizontally at 37°C for 1 h in a shaking incubator. The transformed cells were selected with ampicillin. The transformation reaction (50-150 μl) was spread on pre-warmed LB agar plates supplemented with ampicillin (50 μg/ml) and incubated overnight at 37°C. The resulting colonies were used to inoculate LB medium (5 ml) supplemented with ampicillin (50 μg/ml). Liquid cultures were incubated overnight at 37°C in a shaking incubator. Plasmid DNA was isolated using the Wizard® *Plus* SV Miniprep DNA Purification System (section 2.3.3). Presence of the cloned product was confirmed by PCR and agarose gel electrophoresis (sections 2.3.6.2 and 2.3.5.2).

2.3.7.2 Quantitative real-time PCR

Quantitative real-time PCR (qPCR) was used to determine the zygosity of the transgenes *Crt*B and *Crt*I in plants, and relied upon the comparison of the relative

amplification of the transgenes in these plants and in the *Crt*B and *Crt*I plants with known zygosity. The endogenous single-copy gene, phytoene desaturase was utilised as a normaliser. Real-time qPCR analysis was performed using a QuantiFast SYBR® Green PCR kit (Qiagen, UK) and a Research Rotor-Gene RG-3000 thermal cycler (Corbett Life Sciences). DNA was extracted from plant leaves (section 2.3.1) and quantified (section 2.3.4). DNA solutions were diluted to a concentration of 25 ng/μl. Per reaction, DNA (25 ng) was used, the relevant primers (forward and reverse) at a final concentration of 1 μM were added, as well as 2X QuantiFast SYBR® Green PCR Master Mix (10 μl) and RNA-free water to final volume of 20 μl. Thermocycling conditions were, 95°C for 15 min, followed by 40 cycles of 15 sec at 94°C, 30 sec at 50°C, and 15 sec at 72°C. Melt curve analysis was performed to verify the specificity of the reactions. Calibration curves for each gene were run simultaneously with experimental samples. Calibration curves covered the complete range of expected expression, with 4 or 5 points of dilution of TOPO® plasmids containing the DNA amplicon of interest (2.3.7.1). Triplicates of each reaction were run. The standard curve determined the linearity, reaction efficiency, sensitivity and reproducibility of the assay. The qPCR reaction was considered acceptable when the PCR efficiency, given by the Rotor-Gene software, was between 90 and 110% and the R^2, which indicates how well the data points lie on a line, higher than 0.985.

2.3.7.3 Delta Delta Ct (ΔΔCt) method

A direct comparison of Ct values between the target gene and the reference gene, given by the Rotor-Gene software, allows a relative quantification of the amount of DNA of interest in the experimental sample compared to the calibrator sample. PCR efficiencies of both the target and of the reference gene were between 90 and 110% and did not differ by more than 10%. Only the initial experiment requires a standard curve to compare the PCR efficiency of the target and control gene. In the case of the determination of the zygosity of *Crt*B genes in new plants, the target gene was *Crt*B, the reference gene was phytoene desaturase (endogenous single-copy gene), the experimental samples corresponded to the *Crt*B plants with unknown zygosity and the calibrator samples were the hemizygous *Crt*B plants previously determined.

$$\Delta Ct = Ct \text{ target} - Ct \text{ reference gene}$$

$$\Delta\Delta Ct = (Ct \text{ target} - Ct \text{ reference}) \text{ calibrator} - (Ct \text{ target} - Ct \text{ reference}) \text{ sample}$$

The normalized target amount in the sample was then equal to $2^{-\Delta\Delta Ct}$ and this value could be used to compare expression levels in samples. When the amount of *Crt*B DNA in the new plants was twice that of the *Crt*B hemizygous plant, it meant that the *Crt*B gene was homozygous. On the contrary, when the $2^{-\Delta\Delta Ct}$ equalled one, it meant that the *Crt*B gene was hemizygous.

2.3.8 Determination of number of transgenes in plants

2.3.8.1 Southern blot

Southern blotting was used to determine the number of inserts of the transgene of interest in tomato plants. DNA from plants with unknown numbers of insert (pb*Crt*B, pb*Crt*I and pb*Crt*B+I), as well as DNA of the control Ailsa Craig (untransformed plant) was extracted from the tomato leaves (section 2.3.1). Probes for the genes of interest (*Crt*B and *Crt*I), labelled with DIG-dUTP, were created by a polymerase chain reaction, using the PCR DIG Probe synthesis kit (Roche, UK). The instructions of the manufacturer were followed to perform this step. DNA from the experimental samples, a positive and negative control, were digested by a restriction enzyme, which cleaves only once between the left and right border of the insert, but not in the gene of interest. This restriction enzyme also needed to be a high frequency enzyme. The digestion was performed with EcoRI (Promega, UK) in 100 μl (section 2.3.5.1). Isopropanol was used to precipitate the DNA. The salt concentration was adjusted with sodium acetate pH 5.2, to 0.3 M. Isopropanol (0.6 volumes) was added to the digestion reaction, followed by centrifugation at maximum speed for 10 to 30 min at 4ºC. The supernatant was discarded and the DNA pellet was washed with 1 to 10 ml of room temperature 70% ethanol, followed by centrifugation at maximum speed for 5 to 15 min at 4ºC in the Eppendorf 5424 centrifuge. The pellet was air-dried for 5 to 20 min. DNA was dissolved in buffer AE (15 μl; Qiagen). A thin 0.8% agarose gel (16.7x11.2cm) was made (section 2.3.5.2) and loaded with genomic DNA (~10 μg), plasmid (~1 ng; positive control), as well as a ladder (1 kb; Promega). The gel was electrophoresed overnight at 25 V for an

optimum separation of the DNA bands (section 2.3.5.2). The gel was submerged in Denaturation solution (0.5 M NaOH, 1.5 M NaCl) for 15 min, twice, at room temperature and with gentle shaking. It was then rinsed with sterile distilled water and submerged in Neutralisation solution (0.5 Tris-HCl, pH 7.5, 1.5M NaCl) for 15 min, twice, at room temperature with gentle shaking. Each gel was equilibrated in 20X SSC buffer (3M NaCl, 300mM sodium citrate, pH 7.0) for a minimum of 10 min. The blot transfer apparatus was then assembled and 20X SSC buffer was placed in the reservoir. A glass plate was placed on top of that and a long sheet of Whatman paper (3MM paper; Whatman international Ltd) was placed on top of it with its ends in contact with the buffer. The gel was laid on the soaked sheet of Whatman paper and on top of it a positively charged nylon membrane (1417240.1; Roche, UK) was placed, followed by a layer of Whatman paper, a stack of paper towels, a glass plate and weights (200 to 500 g). The transfer of DNA from the gel to the membrane was carried out overnight. The apparatus was dismantled and the wet membrane exposed to UV light for 1 min at 120 mJ in a transilluminator (UVItec, UK). It was then briefly washed in molecular water, and air-dried. Membrane, in a mesh, was placed in Hybaid tubes (Thermo Scientific, UK), containing pre-warmed pre-hybridisation buffer (20 ml of DIG Easy Hyb; Roche, UK) and then incubated in the Hybaid oven for at least 30 min at 45ºC (temperature depends on the sequence of the probe used). A second Hybaid tube was incubated with hybridisation solution (DIG Easy Hyb (7 ml), with the appropriate PCR probe (21 µl)) for 10 min at 68ºC in the oven. The pre-hybridisation solution was discarded from the first Hybaid tube and replaced by the pre-warmed hybridisation solution. The tube was incubated in the Hybaid oven, under rotation, for 6 to 16 h at 45ºC. The hybridisation solution was replaced with low stringency buffer (100 ml; 2X SSC (0.3 M NaCl, 30 mM sodium citrate, pH 7.0)) containing 0.1% (w/v) SDS and incubated at room temperature for 5 min, twice. Low stringency buffer was discarded and pre-warmed high stringency buffer (100 ml; 0.1X SSC + 0.1% (w/v) SDS) was added in the Hybaid tube and incubated 15 min at 68ºC, twice, in the Hybaid oven, under rotation. The membrane was washed in washing solution (100 ml; 0.1 M maleic acid, 0.15 M NaCl, pH 7.5, 0.3% Tween 20) for 2 min at room temperature. The washing solution was discarded and blocking solution (100 ml; Roche) was added, and incubated for 30 min, and then discarded. The membrane was then incubated in antibody solution (Anti-

Digoxigenin-AP (Roche), 1:10,000 in blocking solution) for 30 min. It was rinsed with molecular water, followed by two washes of washing buffer (0.1 M maleic acid, 0.15 M NaCl, pH 7.5, 0.3% (v/v) Tween 20) for 15 min each time. After equilibration for 3 min in detection buffer (20 ml; 0.1M Tris-HCl, 0.1M NaCl, pH 9.5), the membrane was placed in a plastic bag with CSPD solution (1:100 in detection buffer; Roche; 4 ml) and incubated 5 min at room temperature. The plastic bag was sealed after squeezing the excess CSPD solution out and incubated for 10 min at 37 ºC in an incubator (Memmert, UK), to enhance the luminescence reaction. The bag containing the membrane was placed in a cassette (Curix AGFA, UK) together with a Lumi-Film Chemiluminescent Detection Film (Roche, UK) and left for 30 min to 90 min. The film was developed using a developer (Photon Imaging Systems, UK). The number of bands on the developed film corresponded to the number of inserts of transgenes in the plants.

2.3.8.2 Verification by real-time qPCR

The number of insert was verified by qPCR in a similar way to that for the zygosity of plants (section 2.3.7.2), using the $\Delta\Delta Ct$ method (section 2.3.7.3). A hemizygous plant with only one insert of gene of interest was used as the comparator. The value of $2^{-\Delta\Delta Ct}$ corresponds to the number of transgene inserts, because all the inserts in the plant tested were hemizygous, as they all belonged to the first generation of transgenic plants.

2.3.9 Determination of transcript levels

2.3.9.1 RT-PCR

Reverse-transcription PCR (RTPCR) was used to create a complementary DNA (cDNA) template of the genes of interest. RT-PCR amplification was performed using illustra^{TM} Ready-to-go^{TM} RTPCR beads (GE Healthcare, UK). RNA was extracted from tomato plant as described in sections 2.1.3 and 2.3.2. Reactions contained oligo (dT) primer (2.5 pmol), each of the respective forward and reverse primers (5 pmol) and template RNA (~200 ng). Molecular water was added to a final volume of 50 µl. Tubes were incubated at 55°C for 5 min to denature the template, followed by a reverse transcription reaction at 65°C for 30 min and 5 min incubation at 95°C to denature the reverse transcriptase. This was followed by 30 cycles of PCR

amplification (denaturation 94°C for 30 sec; annealing 52°C for 30 sec; extension 72°C for 30 sec). A final incubation of 5 min at 72°C completed the reaction. Reactions were carried out using a Techgene thermo cycler (Techne, UK). PCR products were analysed by agarose gel electrophoresis (section 2.3.5.2) and cloned in to TOPO® vectors (section 2.3.7.1) for real-time RT-qPCR.

2.3.9.2 RT-qPCR

Real-time qRT-PCR was performed to measure the expression of genes of interest. It was performed using a QuantiFast™ SYBR® Green RT-PCR kit (Qiagen, UK) and a Research Rotor-Gene RG-3000 thermal cycler (Corbett Life Sciences, UK). DNA was extracted from plant leaves (section 2.3.1) and quantified (section 2.3.4). RNA solutions were diluted to a concentration of 25 ng/μl. Per reaction, RNA (25 ng) was used, the relevant primers (forward and reverse) at a final concentration of 1 μM were added, as well as 2X QuantiFast SYBR Green RT-PCR Master Mix (10 μl), QuantiFast RT Mix (0.2 μl) and RNA-free water to final volume of 20 μl. Thermo-cycling conditions were 10 min at 55°C for reverse transcription, 5 min at 95°C for PCR activation, followed by 35 cycles of 5 sec at 95°C and 10 sec at 60°C for PCR amplification. Melt curve analysis was performed to verify the specificity of the reactions. Calibration curves for each gene were run simultaneously with experimental samples. Calibration curves covered the complete range of expected expression, with 4 or 5 points of dilution of TOPO® plasmids containing the RNA amplicon of interest (sections 2.3.9.1 and 2.3.7.1). The actin gene was used as the normaliser (Table A2-2). Triplicates of each reaction were analysed. The standard curve determined the linearity, reaction efficiency, sensitivity and reproducibility of the assay. The RT-qPCR run was considered acceptable when the PCR efficiency, given by the Rotor-Gene software, was between 90 and 110% and the R^2, which indicates how well the data points lie on line, higher than 0.985.

2.4 Transformation of plants and bacteria

2.4.1 Plant transformation

2.4.1.1 Tomatoes and *Nicotiana benthamiana* transient transformation

Tomato cultivars Moneymaker and Micro-Tom were transformed with several constructs (GUS (control); ZW; ZW-PIF5 and ZW-ARR14 as described in appendix Figure A2-1) by *Agrobacterium tumefaciens* C58C1-mediated transient transformation. The protocol was based on that developed by Orzaez et al. (2006). Overnight cultures (5 ml) of *Agrobacterium* harbouring the plasmid of interest were transferred into 50 ml of induction media (yeast extract 1 g/l, beef extract 5 g/l, peptone 5 g/l, sucrose 5 g/l, 2 mM $MgSO_4$, 20 μM acetosyringone, 10 mM MES, pH 5.6) and grown again overnight at 28°C, with shaking at 220 rpm. Overnight cultures (50 ml) were then centrifuged for 10 min at 4,000 rpm in an Eppendorf centrifuge 5810R. The supernatant was discarded and the pellet was resuspended in induction medium (5 ml). The centrifugation step was repeated and the pellets were resuspended in infiltration media (10 mM $MgCl_2$, 10 mM MES stock, 200 μM acetosyringone; 10 ml; pH 5.6) to an OD_{600} of 0.5. The culture was then left at room temperature for a minimum of 3 h, with gentle agitation (50 rpm). Equal volumes of *Agrobacterium* strain with the plasmid expressing the gene of interest, along with *Agrobacterium* strain harbouring p19 plasmid (to maximize protein production by suppression of gene silencing (Voinnet et al., 2003)) cultures were combined. The *Agrobacterium* culture mix was collected and injected in the tomato fruit as subsequently described. Tomato fruits were infiltrated using a 1ml syringe with a 0.5x16 mm needle (BD Plastipack). The syringe was introduced 3 to 4 mm in depth into the fruit tissue through the stylar apex and the *Agrobacterium* culture was gently injected into the mature green fruit tomato. The total volume injected varied with the size of the fruit (~600 μl for the Micro-Tom fruit; ~ 1.5 ml for the Moneymaker tomato fruits). The progress of the process could be followed by a slight change in colour in the infiltrated areas. Once the entire fruit surface has been infiltrated, some drops of infiltration solution begin to show running off the hydathodes at the tip of the sepals. Fruits were collected between 4 to 9 days after infiltration. Histochemical detection of GUS activity was carried out on the tomato fruits transiently transformed by *Agrobacterium* harbouring the GUS vector.

Nicotiana benthamiana plants (6 week old) were transformed with several constructs (GUS (control); ZW; ZW-PIF5 and ZW-ARR14, as described in Appendix A2-1) by *Agrobacterium tumefaciens* C58C1-mediated transient transformation. The protocol was based on that of developed by Sparkes et al. (2006). Overnight cultures (5 ml) of *Agrobacterium* harbouring the plasmid of interest were transferred into 50 ml of induction media (yeast extract 1 g/l, beef extract 5 g/l, peptone 5 g/l, sucrose 5 g/l, 2 mM Mg SO_4, 20 μM acetosyringone, 10 mM MES, pH 5.6) and grown again overnight at 28°C, shaking at 220 rpm. Overnight cultures (50 ml) were then centrifuged for 10 min at 4,000 rpm in an Eppendorf centrifuge 5810R. The supernatants were discarded and the pellets were resuspended in induction medium (5 ml). The centrifugation step was repeated and the pellets were resuspended in infiltration medium (10 mM MES buffer, 10 mM $MgCl_2$, 100 μM acetosyringone, pH 5.6; 10 ml) to an OD_{600} of 0.5. The culture was then left at room temperature for a minimum of 3 h with gentle agitation (50 rpm) applied. Equal volumes of culture were combined (*Agrobacterium strain* with the plasmid containing the gene of interest with *Agrobacterium* strain harbouring p19 plasmid to maximize protein production by suppression of gene silencing (Voinnet et al. 2003)). The mix was collected and injected in the tobacco epidermal cells as described below. The tobacco plants were placed under a white fluorescent lamp for 1 h before infiltration to open the stomata fully as an aid to infiltration. The leaves to be infiltrated were chosen in the middle of the plant (neither the youngest nor oldest). The region of the leaf was prepared to be infiltrated by gently rubbing the underside of the leaf in order to remove the wax cuticle. A 1 ml syringe (without needle) was used to collect the resuspended *Agrobacterium* culture. The tip of the syringe was placed against the underside of the leaf over the rubbed region and the plunger was gently pressed down while directly supporting the upperside of the leaf with a finger. Diffusion of the *Agrobacterium* culture through the leaf, as it filled the mesophyllar air spaces could be followed. This step was repeated in order to fill all the chosen leaf material. Leaves were collected and frozen in liquid nitrogen at 9 days after infiltration. Histochemical detection of GUS activity was carried out on the tobacco leaves transiently transformed by *Agrobacterium* harbouring the GUS vector as described in section 2.4.1.2.

2.4.1.2 Histochemical detection of GUS activity

The β-glucuronidase (GUS) enzyme from *E. coli* was used as the marker gene in transformed plants. Thin slices of tomato fruits or whole tobacco leaves transiently transformed by *Agrobacterium* harbouring the GUS plasmid were covered with GUS buffer (0.1 M of sodium phosphate buffer pH 7, 25 ml; 0.5M EDTA, pH 8, 1 ml; 5% Triton X-100 (1 ml), 1 ml of 25 mg of X-GlcA (5-bromo-4-chloro-3-indolyl-β-D-glucuronic acid; Melford) dissolved in dimethylforamide (1 ml), and water (22 ml)) in a petri dish and incubated overnight at 37°C, shaking at 100 rpm. The tissues were thus put in contact with 5-bromo-4-chloro-3-indolyl glucuronide (X-Gluc), which is the substrate of the β-glucuronidase enzyme. If the enzyme was present in the tissue, its product was synthesised and then dimerised through its reaction with oxygen resulting in a blue dye being produced. The tomato slices or tobacco leaves were washed in methanol for one day to give rise to the blue colouration representing GUS enzyme activity.

2.4.1.3 Stable transformation

Nicotiana glauca was transformed with several constructs (ZW and ZW-ARR14 as described in Appendix A2-1) by *Agrobacterium* LBA4404-mediated transformation. Plants were transformed following the protocol based on the leaf disc method developed for *N. tabacum* by Horsch et al. (1985). Tobacco seeds were sterilised. A first wash in 95% (v/v) EtOH for 1 minute was followed by a 10 min wash in 20% (v/v) bleach with 0.01% Tween 20 (Sigma-Aldrich, UK) and five consecutive washes with sterile water. Seeds were sown in Magenta pots (Sigma-Aldrich, UK) on Murishage and Skoog medium (MS media; 0.44% (w/v) MS salts (Melford laboratories, UK), 0.1% (v/v) Gamborgs vitamin solution (Sigma-Aldrich, UK), 3% (w/v) sucrose) solidified with 0.8% (w/v) agar. Medium was autoclaved prior to use and hormones and antibiotics added, if necessary, when cooled. Explants, 0.5-1.0 cm^2, were excised from *in vitro* grown plantlets. Explants were pre-cultured for 24 h on plates of MS-agar medium supplemented with 6-benzylaminopurine (BAP, 1 mg/l) and 1-naphthaleneacetic acid (NAA, 0.1 mg/l). Plates were sealed with Parafilm$^®$ (Sigma-Aldrich, UK). Overnight cultures (50 ml) of *Agrobacterium* harbouring the plasmids of interest were centrifuged for 5 min at 4,000 rpm in an Eppendorf centrifuge 5810R. Bacterial pellets were resuspended to an OD$_{600}$ of 1.0

(but also 0.5 and 0.1) in liquid MS medium. Pre-cultured explants were immersed in the *Agrobacterium* suspension for 3 to 5 min, blotted on sterile filter paper, and placed upside down on fresh MS-agar plates. Explants were co-cultured with *Agrobacterium* for four days on the same media at 26°C, under low light conditions (7-11 μmol/m^2/s). Following co-culture, explants were transferred to MS-agar plates supplemented with plant hormones as before plus antibiotics; carbenicillin (500 μg/ml) was used to inhibit *Agrobacterium* growth and kanamycin (100 μg/ml) to select recombinant plants. Explants were sub-cultured every two weeks. After four weeks, the carbenicillin concentration in the medium was halved (250 μg/ml). Well defined shoots were excised from the explants and transferred to Magenta pots (Sigma-Aldrich, UK) on MS-agar as before, but without hormones, to induce root growth. Plants were regenerated at 26°C under a 16 h light (45-70 μmol/m^2/s) and 8 h darkness cycle.

2.4.2 Bacterial transformation

2.4.2.1 Preparation of *Escherichia coli* heat shock competent cells

Overnight cultures were prepared by inoculating liquid LB (5 ml) with a single colony of *Escherichia coli* stain DH5α from a LB-agar plate. The cultures were incubated overnight at 37°C in a shaker. Overnight cultures (200 μl) were used to inoculate fresh LB medium cultures (20 ml). The *E.coli* cultures were incubated with gentle agitation (200 rpm) until the cell densities, determined with a DU$^{\circledR}$800 Spectrophotometer (Beckman Coulter), reached an optical density OD_{578} of 0.6 to 0.85. The cultures were transferred in sterile 50 ml Falcon tubes (BD Biosciences) and incubated on ice for 10 min, prior to centrifugation for 10 min at 4,000 rpm and 4°C in an Eppendorf centrifuge 5810R. The supernatants were discarded. The bacterial pellets were washed by re-suspending the pellet in 4 ml of ice cold $CaCl_2$/glycerol solution (0.1 M/10% glycerol, filter-sterilised 0.2 μm), incubated on ice for a minimum of 15 min and followed by centrifugation for 10 min at 4,000 rpm and 4°C. The supernatants were discarded. Bacterial pellets were re-suspended in ice cold $CaCl_2$/glycerol solution (400 μl) and separated into aliquots (25 μl) in pre-chilled autoclaved 1.5 ml microcentrifuge tubes. The bacterial cells were then flash frozen in liquid nitrogen and kept as -80°C prior to transformation by heat shock method.

2.4.2.2 Heat shock transformation of *Escherichia coli*

Escherichia coli competent cells, prepared as detailed in section 2.4.2.1, were transformed with selected plasmids by the heat shock method. *E. coli* competent cells (25 μl) were thawed on ice. Plasmid DNA (1μl) was mixed gently with the cells. The mixture was incubated on ice for 30 min and then transferred into a water bath at 42°C for 45 sec followed by incubation on ice for 2 min. SOC media (2% w/v bacto-tryptone, 0.5% w/v bacto-yeast extract, 8.56 mM NaCl or 10 mM NaCl, 2.5 mM KCl, 10 mM $MgCl_2$ or 20 mM $MgSO_4$ and 20 mM glucose; 250 μl) was added. The mixture was incubated at 37°C for 1 h, gently shaking at 180 rpm. Cells were plated on fresh LB-agar plates, supplemented with appropriate antibiotic selection and incubated overnight at 37°C. Positive transformants were identified by antibiotic resistance.

2.4.2.3 Preparation of *Agrobacterium* competent cells

Overnight cultures were prepared by inoculating liquid YEB (5 ml) with a single colony of *Agrobacterium* from a YEB-agar plate. The cultures were incubated overnight at 28°C in a shaker. An aliquot from overnight cultures (500 μl) was used to inoculate fresh YEB media cultures (50 ml). The *Agrobacterium* cultures were incubated with gentle agitation (200 rpm) until the cell densities, determined with a DU®800 Spectrophotometer (Beckman Coulter, UK), reached an optical density OD_{600} of 1 to1.5. The cultures were split into two aliquots (25 ml) in sterile 50 ml Falcon tubes (BD Biosciences, UK) and incubated on ice for 20 min, prior to centrifugation for 15 min at 4,000 rpm and 4°C in an Eppendorf centrifuge 5810R. The supernatants were discarded. The bacterial pellets were washed by re-suspending the pellet in pre-chilled sterile water (25 ml) followed by centrifugation for 20 min at 4,000 rpm and 4°C. The resulting supernatants were discarded. Washing was repeated four times. Following washing the bacterial pellets were re-suspended in pre-chilled sterile 10% (v/v) glycerol (2.5 ml) and cells from the same original cultures re-combined in a sterile 50 ml Falcon tube. This was followed by centrifugation at 4,000 rpm and 4°C for 10 min. The supernatants were discarded. Bacterial pellets were re-suspended in pre-chilled sterile 10% (v/v) glycerol (200 μl) and separated into aliquots (40 μl) in pre-chilled 2 ml screw-cap microcentrifuge

tubes. The bacterial cells were then flash frozen in liquid nitrogen and kept at -80°C prior to transformation by electroporation.

2.4.2.4 Electroporation transformation of *Agrobacterium*

Electrocompetent *Agrobacterium* cells, prepared as detailed in section 2.4.2.3, were transformed with selected plasmids by electroporation with a Muliporator® Electroporator 2510 (Eppendorf, UK). Electrocompetent cells (40 µl) were thawed on ice. Plasmid DNA (1 µl) was mixed gently with the cells. The mixture was transferred to a pre-chilled sterile electroporation cuvette in a pre-chilled cuvette holder. The mixtures were subjected to five milliseconds electrical pulses of 1440V. Liquid YEB medium (400 µl) was added to *Agrobacterium* cells. The mixtures were transferred to sterile 1.5 ml microcentrifuge tubes and incubated for 1 h at room temperature with gentle agitation (200 rpm). Cells were plated on fresh YEB-agar plates supplemented with appropriate antibiotic selection and incubated overnight at 28°C. Positive transformants were identified by antibiotic resistance.

2.5 Extraction and analysis of metabolites

2.5.1 Carotenoids, chlorophylls and lipids from freeze dried plant material

Carotenoids, tocopherols, chlorophylls and lipids were extracted from freeze dried fruit and leaf tissues. Extractions were made from sample powder (15 mg) in 1.5 ml microcentrifuge tubes. Metabolites were extracted by the addition of chloroform and methanol (2:1). Samples were stored for 20 min on ice. Subsequently, water (1 vol.) was added. Samples were centrifuged for 5 min at top speed in an Eppendorf 5424 centrifuge. The organic phase, containing the pigment extract, was placed in a fresh centrifuge tube and the aqueous phase re-extracted with chloroform (x2 by volume). Organic phases were pooled and dried using a GeneVac Ez-2 Plus rotatory evaporator (UK). Dried samples were stored at -20°C and resuspended in ethyl acetate prior to spectrophotometric and chromatographic analysis (sections 2.5.2, 2.5.3 and 2.5.4).

2.5.2 Spectrophotometric quantification of carotenoids and chlorophylls

Specific absorption coefficients for an absorbance of a 1% sample in a 1 cm path-width cuvette have been determined and published for most carotenoids ($A^{1\%}$ in a 1 cm light path) (Britton et al., 1995). Using these coefficients, the weight (X; mg) of carotenoid in a sample solution (Y; ml) can be calculated using the equation below.

$$X = (Abs \times Y \times 1000)/ \text{absorbance coefficient} \times 100)$$

Purified carotenoids, suspended in the appropriate solvents, were quantified using the equation above. The absorbance (Abs) of the sample was measured at the wavelength corresponding to the absorbance maximum (λ) of the carotenoid in the given solvent. Absorbance values were determined using a DU$^{®}$800 Spectrophotometer (Beckman Coulter, UK).

The equations below derived, by Wellburn (1994) enable the calculation of chlorophyll a (Ca), chlorophyll b (Cb) and total carotenoids concentrations (µg/ml) in a mixed sample. The equations utilise the absorbance coefficient values of chlorophylls and carotenoids suspended in chloroform and the Abs of a mixed sample measured at the λ of Ca, Cb and Cx+c (666 nm, 648 nm and 480 nm respectively).

$$Ca \text{ (chlorophyll a)} = (10.91 \ast Abs_{666}) - (1.2 \ast A_{648})$$

$$Cb \text{ (chlorophyll b)} = (16.38 \ast Abs_{648}) - (4.57 \ast Abs_{666})$$

$$Cx+c \text{ (total carotenoids)} = (1000 \ast Abs_{480} - 1.42 \ast Ca - 46.09 \ast Cb)/ 202$$

Samples obtained from leaf extraction (section 2.5.1), were used for the quantification of Ca, Cb and Cx+c. Sample (1 µl) was suspended in chloroform (1 ml). Abs_{480}, Abs_{648} and Abs_{666} were measured using Beckman Coulter DU$^{®}$800 spectrophotometer and used to quantify Ca, Cb and Cx+c, using the equations above.

2.5.3 Ultra High Performance Liquid Chromatography

Carotenoids were separated and identified by Ultra High Performance Liquid Chromatography (reverse phase) with photo diode array detection (UPLC-PDA). An Acquity™ UPLC (Waters, UK) was used with a BEH C18 column (2.1 x 100 mm, 1.7 µm) with a BEH C18 VanGuard pre-column (2.1 x 50 mm, 1.7 µm). The mobile

phase used was A, MeOH/H$_2$O (50/50 by volume) and B, ACN (acetonitrile)/ethyl acetate (75:25 by volume). All solvents used were HPLC grade and filtered prior to use through a 0.2 μm filter. The gradient was 30% A: 70% B for 0.5 min and then stepped to 0.1% A: 99.9% B for 5.5 min and then to 30% A: 70% B for the last 2 min. The column temperature was maintained at 30°C and the temperature of samples at 8°C. On-line scanning across the UV/Vis range was performed in a continuous manner from 250 to 600 nm, using an extended wavelength PDA (Waters, UK). Carotenoids were identified by their spectra (Figure A2-2) and quantified from dose-response curves (Figure A2-3). Ketocarotenoid analysis was performed using the method described previously, except for the gradient of solvent, which was 50% A: 50% B for 0.5 min and then stepped to 30% A: 70% B for 4.5 min, to 0% A: 100% B for 2 min, back to 30% A: 70% B for 1 min and to 50% A: 50% B for the two last minutes.

2.5.4 High Performance Liquid Chromatography

Carotenoids extracted from plant tissues, as described in section 2.5.1, were separated and identified by High Performance Liquid Chromatography with photo diode array (HPLC-PDA). An Agilent HPLC (UK) was used with a C30 reverse-phase (RP) 5 μm column (150 x 4.6 mm) coupled to a C30 guard column (50 x 4.6 mm, 5 μm) (YMC Inc., USA). For screening analysis, the mobile phases used were A, methanol; B water/methanol (20/80 by volume), containing 0.2% ammonium acetate, and C, tert-methyl butyl ether. The gradient was 95% A: 5% B for 2 min stepped to 80% A: 5% B: 15% C, from which a linear gradient to 30% A: 5% B: 65% C over 23 min was performed. For detailed analysis mobile phases used were A, methanol; B, water/methanol (50/50 by volume), containing 0.2% ammonium acetate and C, tert-methyl butyl ether. The gradient was 95% A: 5% B for 6 min stepped to 80% A: 5% B: 15% C, from which a linear gradient to 30% A: 5% B: 65%C over 42 min was performed. A Waters Alliance HPLC system was used (Waters 600S controller, Waters 610 pump, Waters 996 photodiode array detector and Waters 717plus auto-sampler). The column temperature was maintained at 25°C during screening and 12°C during detailed analysis, with a Jones Chromatography column heater/cooler. Detection was performed continuously from 220 to 700 nm with an online photodiode array detector. Carotenoids were analysed at a wavelength of 450 nm. Component identification was performed by co-chromatography and

comparison of spectral properties and retention times with authentic standards and reference spectra (Britton et al., 2004). The HPLC separation, detection and quantification of carotenoids, tocopherols and chlorophylls have been described in detail previously (Fraser et al., 2000b).

2.5.5 Thin Layer Chromatography

Metabolite extracts (6 μl) obtained from freeze-dried tomato tissues (mix of three biological replicates), as described in section 2.5.1, were loaded at the bottom of HPTLC silica gel 60 F254 plates (Merck, UK). Lipids were separated using a solvent system of acetone/toluene/water (91:30:7). They were visualized with iodine vapour and identified by co-chromatography with lipids of known composition.

2.5.6 Lipid extraction and derivatisation for GC-MS analysis

For quantitative analysis, individual lipids were isolated from TLC plates (section 2.5.5) and extracted in chloroform/methanol (1:1). Then, internal standard (myristic acid-D27; 50 μg) was added to the extract prior drying. To transmethylate the lipids, the samples were resuspended in hexane (2 ml), methanol (4 ml), plus 1% sulphuric acid and incubated at 85°C for 2 h. Hexane (2 ml) and water (1 ml) plus 5% of KCl were then added. The hexane phase was dried and resuspended in methanol (20 μl) for quantification by GC-MS (section 2.5.8).

2.5.7 Metabolite extraction and derivatisation for GC-MS analysis

Methanol (400 μl) and water (400 μl) were added to freeze-dried (10 mg) tomato fruit powder mix of three biological replicates. Six technical replicates were utilised. Samples were mixed vigorously with a vortex and incubated at room temperature for 1 h with continuous agitation. Chloroform (800 μl) was added and mixed vigorously followed by centrifugation at 10,000 rpm for 5 min to remove cell debris. The upper phase of the supernatant, containing methanol and water, was collected in a fresh microcentrifuge tube. The internal standard ribitol (10 μg) was added in an aliquot of the collected fraction (20 μl) and dried using a GeneVac Ez-2 Plus rotary evaporator (UK). At this point, samples could be derivatised immediately or stored without degradation at -20°C. Derivatisation was performed by the addition of methoxyamine-HCl (30 μl; Sigma-Aldrich, UK) prepared at a concentration of 20 mg/ml in pyridine. After incubation in glass screw-capped tubes at 40°C for 1 h, N-

methyltrimethylsilytrifluoroacetaminde (70 µl; Sigma-Aldrich, UK) was added and incubated for 2 h at 40°C before GC-MS analysis (section 2.5.8).

2.5.8 Gas chromatography-mass spectrometry

Gas chromatography-mass spectrometry analysis was performed, as previously described (Enfissi et al., 2010), on an Agilent HP6890 (UK) gas chromatograph with a 5973MSD. Typically, samples (1 µl) were injected with a split/splitless injector at 290°C with a 20:1 split. Retention time locking to the internal standard was used. The gas chromatography oven was held for 4 min at 70°C before ramping at 5°C/min to 310°C. This final temperature was held for a further 10 min, making a total time of 60 min. The interface with the MS was set at 290°C and MS performed in full scan mode using 70 eV EI+ and scanned from 10 to 800 D. To identify chromatogram components found in the tomato profiles, a mass spectral (MS) library was constructed from in-house standards, as well as the NIST08 MS library. Retention time calibration was performed on all standards to facilitate the determination of retention indices (RIs). Using the retention indices and MS, identification was performed by comparison with the MS library. Relative quantification to the internal standard was performed.

2.6 Extraction and analysis of proteins

2.6.1 Protein extraction

Following carotenoid extraction and removal of the organic phase (section 2.5.1), a volume of methanol, equal to the organic phase removed, was added. The sample was mixed vigorously using a vortex mixer and centrifuged for 5 min at 14,000 rpm in an Eppendorf 5424 centrifuge (UK). The supernatants were discarded. Protein pellets were air dried and stored at -20°C prior to analysis.

2.6.2 Protein quantification

Protein quantification was carried out using a Quick Start Bradford Microassay (Bio-Rad). Bovine Serum Albumin (BSA) (Sigma-Aldrich, UK) standards were prepared at concentrations of 0, 0.2, 0.4, 0.6 and 0.8 µg/µl in 1.5 ml microcentrifuge tubes. Proteins (section 2.6.1) were resuspended in 0.5 M Tris-HCl. Aliquots (20 µl) were

added in fresh microcentrifuge tubes. Bradford dye reagent (1 ml) (Bio-Rad) was added to each tube and mixed with a vortex. Tubes were incubated for 15 min at room temperature. The OD_{595} of each mixture was measured with a $DU^{®}800$ Spectrophotometer (Beckman Coulter, UK). Absorbance measurements for BSA standards were used to create a standard curve. The protein concentration was calculated by comparison of the sample OD_{595} with the BSA standard curve.

2.6.3 Separation of proteins on SDS-PAGE

The precipitated protein pellets (section 2.6.1), were resuspended in SDS loading buffer (30-100 μl; 0.5 M Tris-HCl (pH 6.8) 10% (v/v) glycerol, 10% (w/v) SDS, 0.05% (w/v) bromophenol blue, 1.4% (v/v) β-mercaptoethanol) and transferred to 1.5 ml microcentrifuge tubes. Tubes were incubated for 5 min in boiling water. Solubilised proteins were separated by sodium dodecyl sulphate polacrylamide gel electrophoresis (SDS-PAGE). Aliquots (5 μl), of solubilised proteins in SDS loading buffer, were loaded in 0.5 cm wells in 12.5% SDS-PAGE gels. The stacking gel was composed of acrylamide/bis-acrylamide solution (16.7% v/v) (National Diagnostics), Tris-HCl (0.5 M; 12.6% v/v; pH 6.8), SDS (0.1% w/v), ammonium persulphate (0.1% w/v), and tetramethylethylenediamine (temed) (0.1% v/v). The running gel comprised acrylamide/bis-acrylamide solution (40% v/v), SDS (0.1% w/v), Tris-HCl (1.5 M; 25% v/v; pH 8.8), ammonium persulphate (0.1% w/v) and temed (0.1% v/v). Gels were cast in Hoefer Scientific Instrument gel-casting apparatus. The running buffer was Tris (0.25 M), glycine (1.92 M), and SDS (1% w/v). High-Range Rainbow Molecular Weight Markers (RPN756E, GE Healthcare) were run alongside the protein samples. Gels were run at 80V per gel for c.a. 3 h in Hoefer protein-electrophoreses apparatus.

2.6.4 Gel staining

Protein gels were silver stained using a ProteoSilverTM Plus Silver Stain Kit (Sigma-Aldrich, UK). Gels were incubated in fixing solution (50% (v/v) ethanol 10% (v/v) acetic acid) for 20 min, followed by two washes (each for 10 min), the first in 30% (v/v) ethanol and the second in distilled water. Gels were sensitized for 10 min in Sensitizer solution (1% v/v of ProteoSilver Sensitizer), followed by two 10 min washes in distilled water. Gels were equilibrated in Silver solution (1% v/v of ProteoSilver Solution) for 10 min. A final wash in distilled water was performed for

1.5 min before gel development. Gels were developed with Developer solution (5% v/v of ProteoSilver Developer 1 and 0.1% v/v of ProteoSilver Developer 2). ProteoSilver Stop Solution (5 ml) was added to stop the development of the gels when the required colour intensity was obtained. Gels were scanned with an image scanner (Amersham Biosciences).

2.6.5 Western blotting

SDS-PAGE gels (section 2.6.3) were used for Western blotting using a Mini Trans-Blot Electrophoretic Transfer Cell and PowerPac 300 (Bio-Rad). An ImmobilonTM-P transfer membrane (polyvinylidene fluoride (PVDF) membrane with 0.45 μm pore size; Millipore) and two pieces of filter paper (3 mm thick) were cut to match the size of the selected gel. The transfer membrane and filter papers were equilibrated in methanol (20%) for 10 sec, followed by Transfer Buffer (TB; 25 mM Tris, 192 mM glycine, and 20% (v/v) methanol) for a minimum of 10 min, prior to blotting. The SDS-PAGE gels were rinsed in TB and overlaid with equilibrated transfer membranes. The gels and transfer membranes were sandwiched between 2 pieces of equilibrated filter paper and two TB soaked foam pads, in a gel holding cassette. The cassette was inserted into a Mini Trans-Blot Electrophoretic Transfer Cell (Bio-Rad), together with a cooling unit filled with frozen sterile water. The cell was filled with TB and run for ~1 h at 100V, to transfer the proteins from the gel to the transfer membrane. The membranes were incubated in BSA (1% w/v), overnight at 4°C with gentle agitation (200 rpm), in order to block protein binding sites. Primary antibodies solutions were prepared by diluting the antiserum in TBST (5 mM TrisHCl pH 7.5, 15 mM NaCl, 0.01% v/v Tween20) with 0.1% (w/v) of BSA. Primary antibodies were used to target the following proteins (values in parenthesis are the v/v dilutions): CRTI (1/5,000), CRTB (1/1,000), plastoglobulin 35 (PGL35) (1:3,000), PsbA D1 protein of PSII, C terminal (1:10,000), RuBisCO large subunit (RbcL), form I and II (1:10,000), chloroplast inner envelope membrane translocon complex protein (TIC40) (1:5,000) and chloroplast outer envelope membrane translocon complex OEP75 protein (TOC75) (1:1,000). The appropriate primary antibody was bound to the membrane by incubation for 1 h, with gentle agitation (200 rpm). Membranes were washed three times for 10 min with gentle agitation (200 rpm) in TBST. The secondary antibody was bound to the membranes by incubation for 2 h. The secondary antibody used was Anti-Rabbit IgG Alkaline Phosphatase Conjugate

(Promega, UK) at a 1:5000 (v/v) dilution. Membranes were washed three times for 5 min in TBST and twice for 1 min in TBT (5 mM TrisHCl pH 7.5, 15 mM NaCl), with gentle agitation (200 rpm). Visualization of the immunoreactions was performed with *FAST*TM BCIP®/NBT (5-bromo-4chloro-3-indlyl phosphate/nitro blue tetrazolium tablets; Sigma-Aldrich, UK). One tablet was dissolved in 20 ml of distilled water. Membranes were incubated in this solution until the desired density of colour was obtained. The reaction was stopped by washing the membranes in distilled water twice for 2 min. Molecular weights of the proteins were determined by comparison with parallel lanes of High-Range Rainbow Molecular Weight Markers (GE Healthcare, UK).

2.6.6 Liquid Chromatography-mass spectrometry

2.6.6.1 In-Gel Digestion of Protein Bands

Stained bands corresponding to the proteins of interest were excised from the SDS-PAGE gels (section 2.6.3) using a scalpel, cut into 1 mm cubes, and placed in microcentrifuge tubes (0.5 ml). Gel sections were washed three times for 10 min with 50 mM ammonium bicarbonate, pH 8.0 (50 μl). Washed gel sections were dried 3 times with acetonitrile (50 μl) for 10 min. Once the gel pieces shrank and turned opaque, 12.5 ng/μl trypsin (10 μl) dissolved in 50 mM ammonium bicarbonate, pH 8.0, were added. An additional 15 μl of 50 mM ammonium bicarbonate was added to each tube in order to cover the gel pieces. The tubes were incubated at 37°C overnight and the supernatant was transferred to a fresh microcentrifuge tube. Tryptic peptides were sequentially extracted with ACN/H_2O (25 μl; 50:50, v/v) with 0.1% (v/v) of trifluoroacetic acid (TFA) sonicating for 10 min (twice). The peptide extracts were combined and dried using a GeneVac Ez-2 Plus rotary evaporator (Ipswich) and reconstituted in 5 μl of 0.1% v/v TFA. The peptide samples were cleaned with ZipTip C18 (Millipore, USA), prior to the nano-LC-MS/MS analysis and peptides were eluted with H_2O:ACN (10 μl; 50:50, v/v) with 0.1% of formic acid.

2.6.6.2 Nano-LC/MS/MS conditions

The nano LC-MS/MS analyses were performed using an Ultimate 3000 RSLC nano system from Dionex (Thermo Fisher Scientific Ltd, UK), coupled to an AmaZon

ETD ion-trap mass spectrometer, equipped with a nanoelectrospray ionization source (Bruker Daltonik, Germany). Loading buffer (20 μl; H_2O:acetonitrile, 98:2, v/v with 0.1% of formic acid) were added to the sample and were injected (2 μl) into the LC-MS system by using the autosampler. Sample was pre-concentrated on a Dionex Acclaim® PepMap 100 column (100 μm x 2 cm, C18, 5 μm, 100Å) (Dionex Corporation, LC Packings) at a flow rate of 4 μl /min and using 0.1% (v/v) of TFA as mobile phase. After 3 min of pre-concentration, the trap column was automatically switched in-line with a Dionex Acclaim® PepMap RSLC nano-column (75 μm x 15cm, C18, 2 μm, 100Å) (Dionex Corporation, LC Packings). Mobile phases consisted of solvent A, containing 0.1% formic acid in water, and solvent B, containing 0.1% formic acid in 100% acetonitrile. Chromatographic conditions were a linear gradient from 95 to 60% solvent A in 45 min at a flow rate of 0.250 μl/min at 30ºC. The column outlet was directly coupled to a nano eletrospray ion source. The positive mass spectrum was recorded for a mass range m/z 300-2000, followed by MS/MS scans of the three most intense peaks. Typical ion spray voltage was in the range of 2.5-3.0 kV, and nitrogen was used as collision gas. The ion trap was used in Ultrascan mode with a maximum accumulation time of 200 ms and an average of 5 ms. Other source parameters and spray position were optimized with a tryptic digest of BSA protein.

2.6.6.3 Database search

Automated spectral processing and peak list generation was performed using Mascot Distiller v2.4.2.0 software (Matrix Science, USA) (hppt://www.matrixscience.com). The database search was done through Mascot Daemon software in combination with the Mascot interface 2.2 (Matrix Science, USA) (hppt://www.matrixscience.com). Mascot searches were done with no enzymatic specificity and a peptide tolerance on the mass measurement of 100 ppm and 0.6 Da for MS/MS ions. Carbamidomethylation (C) and oxidation of Met were used as variable modifications. Identification of the protein origin of the identified peptides was done using UniProt protein database. BLAST was used as a basic local alignment search tool to find regions of local similarities between the identified proteins and the protein sequences of *Solanum lycopersicum* (http://blast.ncbi.nlm.nih.gov/Blast.cgi).

95

2.7 Isolation and fractionation of organelles

2.7.1 Chromoplast fractionation (system 1)

Chromoplast extraction was undertaken in a cold room at 4°C. Fresh tomato fruits, ca. 10, (breaker + 3 to + 5 days, 90 to 150 g) were harvested from selected plants, cut into pieces of ~1 cm^2, covered in foil and stored at 4°C overnight, to reduce starch content. Tomato tissue was homogenised in pre-chilled chromoplast extraction buffer (0.4 M sucrose, 50 mM Tris, 1 mM DTT, 1 mM EDTA, pH 7.8), twice for 3 sec in a small laboratory blender (Waring Products, UK). The resulting slurry was filtered through 4 layers of muslin cloth and the liquid decanted into a 500 ml screw cap centrifuge tube. Subsequently, tubes were centrifuged for 10 min at 5,000 g and 4°C in a Sorval RC5C centrifuge (Thermo Scientific, UK), with a GSA-3 rotor. The supernatant was discarded, the pellet resuspended in extraction buffer and transferred into 50 ml centrifuge tubes. The tubes were centrifuged for 10 min at 9,000 g and 4°C with the GSA-5 rotor. The supernatants were discarded. Pellets were resuspended in 45% sucrose buffer (45% w/v sucrose, 50 mM Tricine, 2 mM EDTA, 2 mM DTT, 5 mM sodium bisulphite, pH 7.9; 3 ml). The chromoplasts were physically broken by using a hand held potter homogenizer (VWR, UK). The solutions were then resuspended in 45% sucrose buffer (5 ml) and the 8 ml were placed in a 38.5 ml Ultra-Clear^{TM} centrifuge tube (Beckmann Coulter, UK). Subsequently, other layers of discontinuous sucrose gradient were overlaid, consisting of 38% w/v sucrose buffer (6 ml), then 20% w/v sucrose buffer (6 ml), 15% w/v sucrose buffer (4 ml) and 5% w/v sucrose buffer (8 ml). Three gradients were prepared concurrently. Gradients were centrifuged for 17 h at 100,000 g and 4°C, using an L7 ultracentrifuge with an SW28 swing out rotor (Beckman Coulter, UK). Fractions (1 ml) were collected, from the top of the gradients using a Minipuls$^®$3 peristaltic pump and FC203B fraction collector (Gilson, UK). Carotenoids were extracted using the same method detailed in section 2.5.1. Dried extracts were stored at -20°C prior to UPLC-PDA analysis (section 2.5.3). Proteins remaining in the aqueous phases were precipitated, as described in section 2.6.1 for TEM analysis (2.8.2), samples were dialysed overnight against phosphate buffer (50 mM, pH 7.5).

2.7.2 Chromoplast fractionation (system 2)

Chromoplasts were isolated as in system one (section 2.7.1). However, instead of resuspending the pellets obtained after the centrifugation step at 9,000 *g* (section 2.7.1), they were resuspended in 0.6 M sucrose buffer (0.6 M sucrose, 50 mM Tris,1 mM DTT,1 mM EDTA, pH 7.8; 3 ml) and homogenised using a hand held Potter homogenizer (VWR) in order to break the chromoplasts. The solution was then resuspended in 0.6 M sucrose buffer to a final volume of 35 ml in 38.5 ml Ultra-Clear^{TM} centrifuge tubes (Beckmann Coulter, UK). Tubes were centrifuged for 1 h at 100,000 *g* and 4°C, using an L7 ultracentrifuge with an SW28 swing out rotor (Beckman Coulter, UK). The red-coloured supernatants, which correspond to the chromoplast crystals and plastoglobules were transferred in microcentrifuge tubes and stored at -20°C. The pellets were resuspended in 45% sucrose buffer (8 ml) and placed in a 38.5 ml Ultra-Clear^{TM} centrifuge tube (Beckmann Coulter, UK). The same gradient and protocol, as that of system one (section 2.7.1) was used. The two systems are represented in Figure A2-4.

2.7.3 Separation of chromoplast type by sucrose gradient centrifugation

Chromoplast extraction was undertaken in a cold room at 4°C. Fresh tomato fruits (200 g) were harvested from selected plants, cut into pieces of ~1cm^2, covered in foil and stored at 4°C overnight, to reduce starch content. Tomato tissue was homogenised in pre-chilled chromoplast buffer A (100 mM Tris-HCl pH 8.2, 0.33 M sorbitol, 2 mM $MgCl_2$, 10 mM KCl, 8 mM EDTA,10 mM ascorbic acid, 5 mM L-cysteine,1 mM PMSF, 1% PVPP, 1 mM DTT), twice for three sec in a small laboratory blender (Waring Products). The resulting slurry was filtered through 4 layers of muslin cloth and the liquid decanted into a 500 ml screw cap centrifuge tube. Subsequently, tubes were centrifuged for 15 min at 5,000 *g* and 4°C in a Sorval RC5C centrifuge (Thermo Scientific, UK), with a GSA-3 rotor. The supernatants were discarded. The pellets were resuspended in buffer B (buffer A without PVPP) and transferred into 50 ml centrifuge tubes. The tubes were centrifuged for 15 min at 5,000 *g* and 4°C with the GSA-5 rotor. The supernatants were discarded. The pellets were resuspended in buffer B (4 ml). In 38.5 ml Ultra-Clear^{TM} centrifuge tubes, a discontinuous sucrose gradient (sucrose w/v in 50 mM Tris-HCl pH 7.4 supplemented with 1 mM DTT) with the following steps was constituted: 50% (9

ml), 40% (7 ml), 30% (7 ml) and 15% (7 ml) of sucrose. The chromoplast solutions (4 ml) were placed on top of the gradients. Gradients were centrifuged for 1 h at 100,000 g and 4°C, using an L7 ultracentrifuge with an SW28 swing out rotor (Beckman Coulter, UK). The chromoplast fractions were recovered with a Pasteur pipette in microcentrifuge tube, washed in one volume of buffer B followed by centrifugation at 6,000 g for 10 min. The supernatants were discarded and the pellets of chromoplasts stored at -20°C.

2.8 Transmission electron microscopy (TEM)

2.8.1 TEM of tomato pericarp

Tomato fruit were cut into 2 mm cubes using a new sharp razor blade in a drop of cold fixative (CAB; 2.5% glutaraldehyde in 100 mM sodium cacodylate buffer, pH 7.2) on dental wax. Pieces of tissue were transferred into a glass vial (with a cocktail stick) containing cold fixative (~2 ml). Lids were placed on the vials and tissue was fixed in the fridge (4˚C) overnight. Tissue was washed twice in CAB for 10 min each time and then post fixed in 1% osmium tetroxide in CAB for 1 h at room temperature (20˚C). Tissue was washed twice for 10 min each time in milliQ water. Tissue was dehydrated in increasing concentrations of ethanol 50, 70, 90% (10 min) and three times with ethanol 100% (15 min). Tissue was then washed (10 min) in the transition solvent propylene oxide. Tissue was then transferred into 50% propylene oxide 50% agar low viscosity resin (ALVR) (Agar Scientific) for 30 min. Tissue was then placed in 100% ALVR, twice, 1.5 h, with vacuum applied four times during the incubation. Tissue pieces were then placed in labelled silicone moulds and polymerised in the oven (60˚C) for 24 h. Polymerised blocks were sectioned (70 nm) on a RMC MTXL ultramicrotome and sections were collected on 400 mesh copper grids. Sections were counterstained with 4.5% uranyl acetate in 1% acetic acid for 45 min and Reynolds lead citrate for 7 min. Sections were viewed in a Jeol 1230 TEM, with an accelerating voltage of 80 kV. Images were recorded with a Gatan digital camera.

2.8.2 TEM of sub-chromoplast fractions

Two previous methods were combined (De Camilli et al., 1983; Angaman et al., 2012). Dialysed sub-chromoplast fractions (section 2.7.1) were pelleted in microcentrifuge tubes and fixed in 2.5% (v/v) glutaraldehyde in 100 mM phosphate buffer (PB) (pH 7.4) for 1 h at room temperature. Fixed sub-chromoplast components were pelleted in a microfuge tube and washed 2 x 10 min in PB. After the final wash components were resuspended in PB (100 ml). Aliquots (100 μl) of fixed component were added to tubes immersed in a 54°C water bath. After a 15 sec interval, which allowed the suspension to warm up, 100 ml of a solution (at 54°C) containing 3% agarose in 5 mM PB was added to the sub-chromoplast suspension. The suspension obtained was quickly mixed, while still immersed in the warm water bath, by forcing it up and down through a Pasteur pipette pre-warmed in a 60°C oven. Care was taken to prevent foaming. Immediately afterwards, the agarose-sub-chromoplast suspension was transferred by pipetting into a frame made from two glass slides separated by a shaped acetate gasket and held together by bull dog clips. The frame had also been pre-warmed in a 60°C oven. The agarose mixture was then allowed to cool and solidify. At this point, the two glass slides were separated and the agarose gel, attached to one of the glass slides, was cut into 2 mm squares with a razorblade. The gel squares were then washed off the glass slide into a petri dish by a stream of 0.1% Alcian blue in 1% acetic acid from a Pasteur pipette. These agarose squares were then transferred to glass vials and washed (2 x 10 min) in PB to remove stain. The Alcian blue stain made the agarose squares visible and aided subsequent processing and resin embedding. Samples were post-fixed in 1% osmium tetroxide (OsO$_4$) containing potassium ferricyanide (K$_3$Fe(CN)$_6$, 0.8% (w/v)) in the same phosphate buffer for 1 h at room temperature. Then, after washes in milliQ water, TEM was carried out, as described in section 2.8.1.

2.9 Statistical analysis

A minimum of three biological and three technical replicates were analysed for every experiment unless stated otherwise. Metabolite levels from the different technology platforms were combined. PCA was performed on these data matrices. SIMCA-P+ software v. 13.0.2 (Umetrics, UK) was used to carry out and display clusters derived

from PCA analysis. GraphPadPrism software v.5 (GraphPad Software, UK) or Excel (Microsoft) embedded algorithms were used to calculate student's t-tests or Dunnett's test in order to determine significant differences between the transgenic lines and the control AC. Where appropriate, $P < 0.05$, $P < 0.01$, and $P < 0.001$ are indicated by *, **, and ***, respectively. The term significant was used in this manuscript to indicate statistical significant differences.

Chapter III: Characterisation of tomato lines expressing different carotenoid gene combinations

3.1 Introduction

Optimising the production of carotenoids in tomato plants through expression of heterologous genes is a strategy that has been used successfully to genetically engineer the carotenoid pathway (Romer et al., 2000; Enfissi et al., 2005; Wurbs et al., 2007). Contrary to the overexpression of endogenous genes in plants, expression of heterologous genes such as those derived from bacteria can be advantageous in avoiding cosuppression and gene silencing (Fray et al., 1995; Fraser et al., 2002) as well as alleviating the impact of endogenous regulatory mechanisms. In this study, three tomato lines expressing the bacterial genes: (i), geranylgeranyl diphosphate synthase (*Crt*E); (ii), phytoene synthase (*Crt*B) and (iii), phytoene desaturase (*Crt*I) independently were chosen (details on the constructs are given in Appendix FA2-1; and the catalytic action of the enzymes is described in Figure 1-20) and genetically crossed in order to investigate the potential effect of coordinate expression of multiple bacterial genes on carotenoid production.

3.2 Results

3.2.1 Generation and selection of lines with different carotenoid gene combinations produced by genetic crossing

Tomato varieties containing the *Pantoea ananatis* (i), geranylgeranyl diphosphate synthase (*Crt*E); (ii), phytoene synthase (*Crt*B) both under the control of the tomato polygalacturonase fruit specific promoter and (iii), phytoene desaturase (*Crt*I) under the control of the CaMV 35S constitutive promoter were used as parental lines for stacking the transgenes by genetic crossing (section 2.1.2). These parental lines were all homozygous for the transgenes of interest and showed inheritable phenotypes/genotypes beyond the F_5 generation. Genetic crosses were performed in a complementary manner, with the pollen of one transgenic parent placed onto the stigma of another after emasculation and vice versa. A minimum of six complementary crossing events were carried out to establish combinations of the following heterologous carotenoid genes *Crt*E+B, *Crt*E+I, and *Crt*B+I. From these crosses, ten F_1 plants per crossing event were generated and screened by PCR for the presence of transgenes (Figure 3-1). Four PCR positive lines for each combination

were selected for further analysis. No changes in the phenotype of the crosses were observed compared to the Ailsa Craig (wild type), when grown concurrently. The only exceptions were the lines containing the *Crt*I gene which had slight altered fruit morphology (e.g. globe shaped fruit).
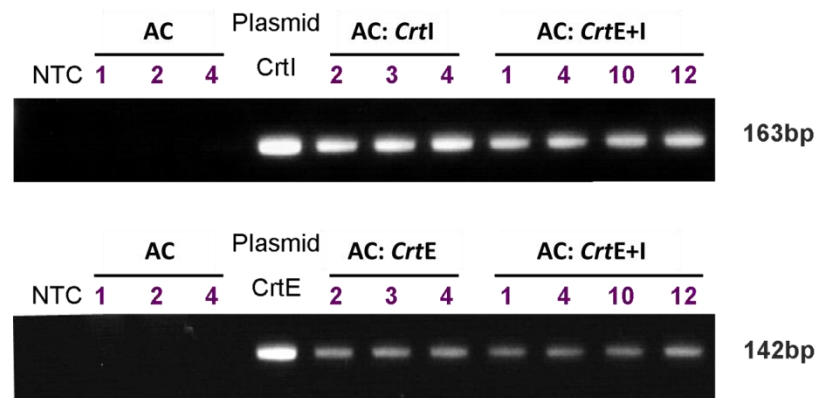
Figure 3-1 PCR confirmation of the presence of *Crt*E and *Crt*I genes in the *Crt*E+I lines

Amplification of the genes *Crt*I (163bp) and *Crt*E (142bp) was performed by PCR on four plants of the *Crt*E+I genetic cross and visualised under UV light. DNA was extracted from a pool of 4 representative leaves of each genotype. NTC: non template control; AC: Ailsa Craig tomato variety (wild type). Numbers (purple) indicate different biological replicates. The same approach was undertaken for *Crt*E+B and *Crt*B+I lines.

The lines were screened for total pigment content and those exhibiting the highest or altered carotenoid contents were taken to mature plants in the F_2 generation. The generation of a double homozygous *Crt*B+I line was also undertaken as the *Crt*B+I hemizygous line showed an interesting increase in carotenoids. The selection of this *Crt*B+I homozygous line is described in section 2.3.7.

3.2.2 Assessment of carotenoid profiles in tomato fruits and leaves of all transgenic lines

In order to fully assess the *Crt* gene combinations and the effects of gene dosage, detailed analysis of carotenoids, chlorophylls and tocopherols were performed on lines, both in the hemizygous and homozygous states. Leaf and fruit tissue extracts of tomato plants, were screened by Ultra and High Performance Liquid Chromatography with on-line photo-diode array detection (UPLC-PDA and HPLC-PDA) to enable the estimation of the level of carotenoids being produced in each transgenic plant and their control Ailsa Craig (AC). The UPLC and HPLC methods are described in sections 2.5.3 and 2.5.4. Chromatogram profiles of carotenoids, chlorophylls and α-tocopherol and their spectral characteristics are showed in Figure 3-2.

The HPLC/UPLC profiles of the leaf pigments revealed significant qualitative differences that could be attributed to the presence of the *Crt*I gene (Figure 3-2). Quantification indicated that β-carotene had increased 1.5- to almost 2-fold and other β-ring derived carotenoids such as violaxanthin (and its isomers) displayed similar increases (Table 3-1). The total carotenoid content was also increased (~1.4-fold), which contributed to a decreased chlorophyll:carotenoid ratio (Table 3-1). In comparison to the wild type, no significant differences in carotenoid contents were found in the lines expressing the *Crt*E and *Crt*B genes.

Figure 3-2 Chromatographic profiles of carotenoids, chlorophylls and α-tocopherol of AC and *Crt*B+I lines (a), with the chromatographic annotations and spectral characteristics (recorded from 250 to 600 nm) (b), obtained by HPLC analysis
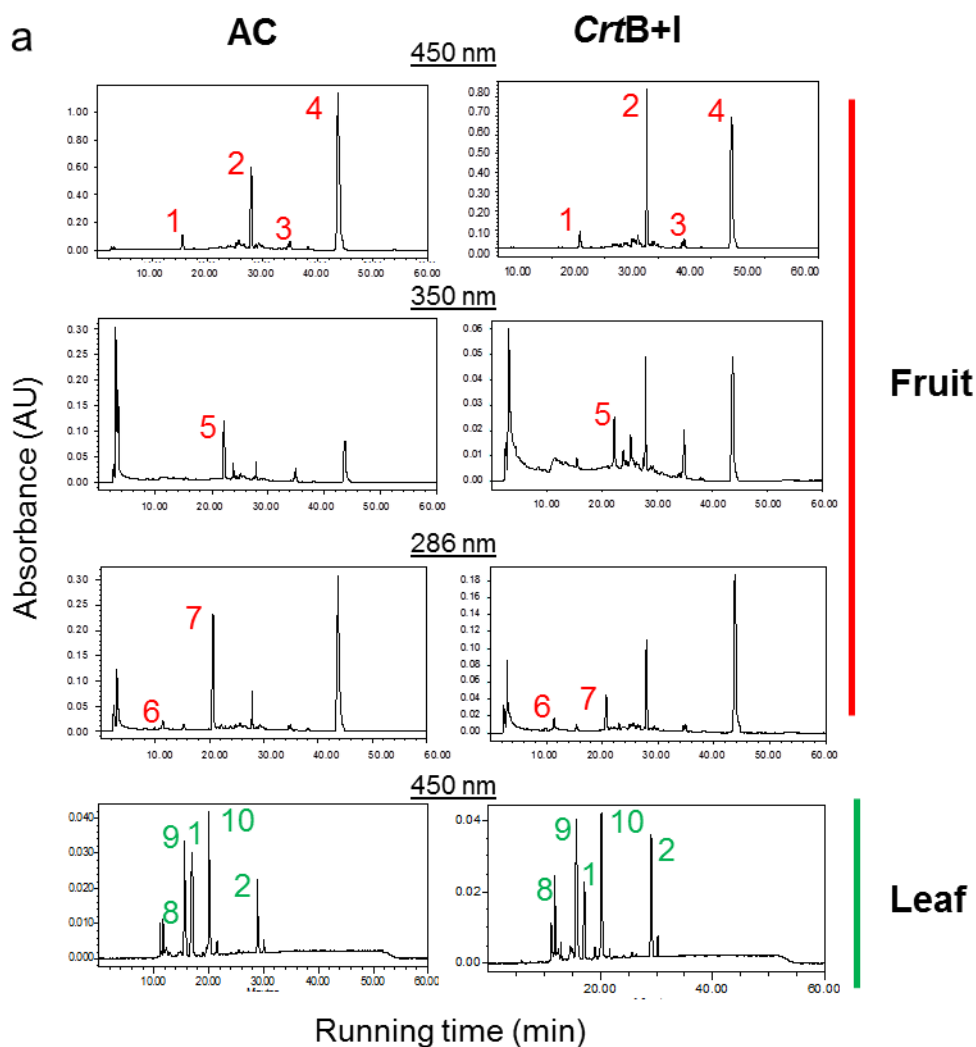
NAMES	Peak number	Retention time (min)	Spectra λ_{max} (nm)
Lutein	1	15.44	(420.2), 445.1, 474.1
β-Carotene	2	27.90	- , 452.4, 480.2
γ-Carotene	3	34.87	(440.3), 465.7, 497.1
Lycopene	4	44.01	(446.3), 472.9, 504.4
Phytofluene	5	22.18	(330.1), 348.2, 365.8
α-Tocopherol	6	11.39	292.3
Phytoene	7	20.67	286.4
Violaxanthin	8	11.33	(417.9), 436.7, 464.5
Chlorophyll b	9	15.67	469.3
Chlorophyll a	10	20.12	431.9

A similar situation occurred in the tomato fruit, where the presence of the *Crt*I gene in the ripe tomato fruit confers the greatest changes in carotenoid and tocopherol levels compared to the other genes, *Crt*E and *Crt*B (Table 3-1). Indeed, in comparison to the wild type, the hemizygous and homozygous *Crt*E lines showed a similar carotenoid profile, and only a significant increase of phytoene level (1.2-fold) is noticeable in the hemizygous *Crt*B line. However, there was a significant increase of lycopene level in the *Crt*E+B line (1.4-fold) as well as in the homozygous *Crt*B line (2.2-fold). The hemizygous *Crt*I line was characterised by a high level of β-carotene (2.3-fold increase compared to AC), a greater content of γ-carotene, lutein and α-tocopherol, and a substantial decrease of phytoene and phytofluene (0.4-fold). The presence of an early step carotenoid gene (*Crt*E or *Crt*B) in the hemizygous *Crt*E+I and *Crt*B+I lines alleviated the decrease of phytoene and phytofluene. Moreover, an increase of lycopene content (1.4 fold) was also observed in the hemizygous *Crt*B+I line. The homozygous *Crt*I line had a similar carotenoid profile to the hemizygous *Crt*B+I line. Surprisingly, the level of lycopene in the homozygous CrtB+I line was comparable with the wild type. However, the β-carotene content of this line was the highest compared to all the *Crt*I lines studied (e.g. *Crt*I gene on its own, or in combination).

Analysis of ripe fruit pigments derived from the various *Crt* gene combinations indicated that the CRTI enzyme solely or in combination with the CRTE and CRTB enzymes, conferred the greatest effects on lycopene and β-carotene contents compared to the wild type, either in the hemizygous or homozygous states (Table 3-1). Analysis of carotenoid pigments among the genotypes of the different *Crt* gene combinations revealed *Crt*B+I as the best line for fruit carotenoid content. Therefore, further characterisation was performed to ascertain the underlying mechanisms associated with the effects of this gene combination.

LEAF

Genotype	AC	*Crt*E	*Crt*B	*Crt*I	*Crt*E+B	*Crt*E+I	*Crt*B+I
Zygosity	-	homozygous			hemizygous		
β-Carotene	219 ± 15	331 ± 7	217 ± 7	**298 ± 6***	228 ± 4	**361 ± 32***	**319 ± 13***
Violaxanthin∗	335 ± 16	347 ± 10	322 ± 9	**535 ± 4****	344 ± 4	**552 ± 22***	**549 ± 14****
Lutein	303 ± 20	316 ± 8	311 ± 7	294 ± 9	310 ± 11	280 ± 16	253 ± 8
Total CAR	856 ± 51	894 ± 24	851 ± 23	**1127 ± 18***	881 ± 19	**1193 ± 69***	**1120 ± 26***
Chlorophyll a	9433 ± 2210	10825 ± 642	11005 ± 448	8107 ± 213	9534 ± 1264	7501 ± 422	7301 ± 507
Chlorophyll b	1346 ± 598	1817 ± 289	2217. ± 93	589 ± 190	1468 ± 429	426 ± 274	519 ± 70
CHL: CAR	13 ± 3	15 ± 1	15 ± 1	8 ± 1	13 ± 2	7 ± 1	7 ± 1

FRUIT

Genotype	AC	*Crt*E	*Crt*B	*Crt*I	*Crt*E+B	*Crt*E+I	*Crt*B+I	*Crt*E	*Crt*B	*Crt*I	*Crt*B+I
Zygosity	-	hemizygous						homozygous			
Phytoene	133 ± 16	136 ± 4	**160 ± 4***	**52 ± 7****	143 ± 8	**70 ± 7****	**56 ± 8****	149 ± 15	124 ± 12	**41 ± 1****	**42 ± 3****
Phytofluene	134 ± 24	141 ± 4	146 ± 11	**55 ± 13****	138 ± 5	**84 ± 2****	**81 ± 2****	153 ± 11	134 ± 8	**79 ± 1****	**40 ± 1****
Lycopene	1224 ± 255	1434 ± 55	1352 ± 108	1191 ± 10	**1681 ± 258***	1285 ± 168	**1656 ± 6***	1602 ± 21	**2696 ± 146****	**1780 ± 74***	1109 ± 113
β-Carotene	321 ± 32	322 ± 10	**220 ± 19****	**785 ± 11****	296 ± 18	**560 ± 39****	**665 ± 55****	286 ± 8	377 ± 40	**680 ± 93****	**803 ± 40****
γ-Carotene	62 ± 7	56 ± 2	**48 ± 2***	**93 ± 14***	61 ± 3	71 ± 3	**74 ± 2***	66 ± 4	71 ± 5	**81 ± 6****	69 ± 3
Lutein	122 ± 15	**132 ± 3****	117 ± 9	**155 ± 5***	116 ± 2	120 ± 2	122 ± 1	120 ± 4	**114 ± 1***	**114 ± 2***	117 ± 5
Total CAR	1995 ± 327	2220 ± 73	2042 ± 136	2330 ± 26	2435 ± 251	2190 ± 177	**2649 ± 117****	2376 ± 328	**3517 ± 179****	**2775 ± 368***	2179 ± 140
α-Tocopherol	256 ± 39	283 ± 10	229 ± 8	**319 ± 8****	232 ± 21	**336 ± 19****	**385 ± 42****	**334 ± 40***	331 ± 63	**378 ± 24****	**343 ± 16****

Table 3-1 Carotenoid, chlorophyll and tocopherol contents in the leaves and fruits of the transgenic lines

Table 3-1 Carotenoid, chlorophyll and tocopherol contents in the leaves and fruits of the transgenic lines

Carotenoid, chlorophyll, and tocopherol contents are presented as µg/g DW. Four representative leaves and three representative fruits from a minimum of three plants were used. The leaves and fruits were pooled and three determinations were made per sample, making a minimum of three biological and three technical replicates. Methods used for these determinations are described in section 2.5. The mean data are presented ± SD, with n=9. Violaxanthin∗ indicates the presence of violaxanthin and isomers; CHL, chlorophyll and CAR, carotenoid. Dunnett's test was used to determine significant differences between the wild type background (AC) and the transgenic varieties. Values in bold indicate where significant differences have been found. P<0.05, P<0.01 and P<0.001 are designated by *****, ******, and *******, respectively.

3.2.3 Biochemical and molecular characterisation of the *Crt*B+I line

3.2.3.1 Spatial repartition of carotenoids within the different tissues of the tomato fruit

In ripe fruit, carotenoids and tocopherols were quantified (by UPLC analysis) in the pericarp, jelly and columella tissues of the homozygous *Crt*B, *Crt*I and *Crt*B+I lines and compared to the same material in wild type background (Table 3-2 and Figure 3-3). Carotenoids and α-tocopherol were found in all the fruit tissues, but not in the same proportion. Analysis of wild type tissues showed that, on a DW basis per unit mass, pericarp tissue contained the most carotenoids, with about 50% of total carotenoid present. The columella sequestrated 30% of total carotenoids, while the jelly tissue contained about 20%. In the transgenic lines *Crt*B, *Crt*I and *Crt*B+I, the distribution of total carotenoid within the fruit compartments was comparable to that of the control, although quantitative increases were evident in the different tomato tissues. For example, total carotenoid content was elevated in the pericarp and columella by 1.3- and 1.4-fold, respectively in the *Crt*B line. In the *Crt*I line, the columella tissue had a 1.2-fold increase.

Lycopene and β-carotene are the predominant carotenoids in the tomato fruit and of the most biotechnological interest. Therefore, for clarity, analysis focused only on these two carotenoids (Figure 3-3). Lycopene was mainly found in the pericarp of the control and all the transgenic lines while β-carotene was the most abundant carotenoid in the jelly of all lines. However, the predominant carotenoid in the

columella varied among the different lines. Lycopene was the main carotenoid in the columella tissue of the wild type and the *Crt*B lines, whereas β-carotene predominated in *Crt*I and *Crt*B+I lines. In order to understand how the changes in carotenoid contents were distributed in the fruit tissues, the changes arising have been represented as relative fold changes for each carotenoid analysed. Although the lycopene levels increased in the pericarp and in the columella tissues of *Crt*B (homozygous) line, the greatest increase occurred in the columella (2.3-fold increase). The β-carotene levels increased in all the fruit tissues of *Crt*I and *Crt*B+I (homozygous) but the greatest change was seen in the columella (2.2- and 2.5-fold increase, respectively for *Crt*I and *Crt*B+I lines). The carotenoids, lycopene and β-carotene, were preferentially stored in the pericarp of the fruit for all lines. However, when their level varied significantly due to the expression of heterologous genes, the greatest accumulation of these carotenoids occurred in the columella.

	Pericarp				Jelly				Columella			
Line	AC	*Crt* B	*Crt* I	*Crt* B+I	AC	*Crt* B	*Crt* I	*Crt* B+I	AC	*Crt* B	*Crt* I	*Crt* B+I
Lutein	154.6 ± 4.6	**132.6 ± 0.9***	150.6 ± 1.4	158.4 ± 3.1	150.8 ± 0.6	142.5 ± 2.2	142.7 ± 5.6	143.6 ± 6.1	127.5 ± 0.7	**123.0 ± 0.9***	135.2 ± 4.1	133.3 ± 3.6
Lycopene	1154.8 ± 120.1	**2021 ± 67.2***	**1358 ± 58.2***	1201.7 ± 14.4	226.2 ± 31.2	248.4 ± 28.4	184.3 ± 10.6	192.0 ± 47.4	526.9 ± 25.8	**1191.0 ± 22*****	491.8 ± 48.3	416.7 ± 60.1
γ-Carotene	99.1 ± 4.4	85.2 ± 10.1	88.7 ± 9.7	87.5 ± 3.9	70.3 ± 5.5	60.5 ± 1.7	71.7 ± 5.3	69.5 ± 5.5	89.7 ± 1.9	**68.3 ± 1.7****	**80.5 ± 1.7***	76.7 ± 5.7
β-Carotene	344.1 ± 21.1	**246.1 ± 7.6***	**685.2 ± 37.8***	**825.6 ± 69.3***	341.8 ± 27.7	302.2 ± 16.9	**505.2 ± 44.6***	**541.4 ± 43.6***	303.7 ± 19.5	230.7 ± 12.1	**658.4 ± 18*****	**775.0 ± 70*****
Phytofluene	187.6 ± 5.5	197.9 ± 16.4	**66.5 ± 3.2*****	**67.2 ± 1.3****	0.0 ± 0.0	0.0 ± 0.0	0.0 ± 0.0	0.0 ± 0.0	112.5 ± 2.2	**142.8 ± 6.0 ***	**66.2 ± 3.2*****	**67.2 ± 11.6***
Phytoene	177.4 ± 4.9	144.9 ± 8.5	**53.6 ± 4.5*****	**59.5 ± 5.3*****	21.6 ± 1.6	20.5 ± 1.7	18.2 ± 1.2	18.6 ± 1.6	98.7 ± 1.7	89.3 ± 11.6	**40.2 ± 7.4***	**40.0 ± 15.6***
Total CAR	2117.6 ± 138.1	**2828 ± 99.1***	2402.9 ± 235.2	2399.9 ± 81.1	810.6 ± 103.1	774.1 ± 16.3	922.1 ± 57.0	965.1 ± 62.0	1259.0 ± 34.0	**1846 ± 39.1***	**1472 ± 35.2***	1509.0 ± 62.0
α-Tocopherol	309.1 ± 15.9	308.8 ± 5.3	377.8 ± 60.9	**420.8 ± 6.2***	209.1 ± 17.2	250.4 ± 7.7	274.1 ± 33.8	239.1 ± 20.3	291.0 ± 9.3	248.1 ± 15.4	313.2 ± 59.1	282.4 ± 25.2

Table 3-2 Carotenoid content found in the pericarp, jelly and columella tissues of ripe fruit derived from the genetic crosses containing different gene combinations

Carotenoid contents are presented as µg/g DW. Methods used for this determination are described in section 2.5. Determinations were made from three independent pools of three fruits, each pool with three technical replicates. The mean data are presented with ± SD. Dunnett's test was used to determine significant differences between the wild type background (AC) and the transgenic varieties for each compound. Values in bold indicate where significant differences have been found. P<0.05, P<0.01 and P<0.001 are designated by *****, ******, and *******, respectively. CAR, carotenoid.

Figure 3-3 Lycopene and β-carotene contents found in the pericarp, jelly and columella tissues of the tomato fruits of the genetic crosses

Carotenoid contents are given as μg/g DW. Methods used for determinations are described in the experimental section. Three representative fruits were used for a minimum of three plants. Three determinations were made per fruit, making three biological and three technical replicates. The bars represent the mean ± SD. Dunnett's tests were used to determine significant differences between the wild type background (AC) and the transgenic lines for each compartment. Bars with stars indicate where significant differences have been found. P<0.05, P<0.01 and P<0.001 are designated by *****, ******, and *******, respectively.

It is also interesting to notice that in the *Crt*I line, which showed a small increase of lycopene in the fruit (1.1-fold increase compared to AC), this increase was only seen in the pericarp. However, when there was an increase of almost 2-fold of lycopene in the fruit such as in the *Crt*B line, the changes occurred in the pericarp and the columella.

Overall, these results demonstrate that the transgenic lines had an altered intra fruit carotenoid composition compared to the wild type (AC).

3.2.3.2 The effect of the *Crt*B+I (homozygous) combination on carotenoid composition during fruit development and ripening

Pigment analysis of the pericarp of tomato fruit was carried out at mature green, breaker, breaker + 3 days, breaker + 7 days and breaker + 14 days in both *Crt*B+I line and its comparator (AC). Carotenoids (phytoene, phytofluene, violaxanthin, lycopene, β-carotene, γ-carotene, and lutein) and α-tocopherol were quantified by UPLC (Table 3-3). Changes of these metabolite levels in *Crt*B+I occurred at different time points during ripening, depending on the identity of the metabolite. In general, differences in the carotenoid composition of *Crt*B+I were observed at each time point, although a greater number of metabolites levels were affected in *Crt*B+I from the breaker + 3 days ripening stage.

For clarity, a figure representing only the carotenoids with greatest altered levels (phytoene, β-carotene and lycopene) in *Crt*B+I during ripening is displayed (Figure 3-4). With the onset of ripening at the breaker stage, the phytoene content decreased, while β-carotene content increased in *Crt*B+I line. These significant differences remained throughout fruit ripening. The difference of phytoene levels between AC and *Crt*B+I lines continuously increased through ripening. In the case of β-carotene, the difference of levels between AC and *Crt*B+I also increased, but only until the breaker + 7 days ripening stage. A difference in lycopene content did occur in *Crt*B+I line compared to AC, but only at the breaker + 3 days stage, when there was a decrease. The lycopene content in all the other stages was not significantly different from that in AC at the same ripening stages.

Significant changes were observed in the carotenoid composition of CrtB+I compared to the wild type (AC) during the ripening process.

	Stage of fruit development and ripening									
	Mature green		Breaker		Breaker + 3 days		Breaker + 7 days		Breaker + 14 days	
	AC	*Crt* B+I	AC	*Crt* B+I	AC	*Crt* B+I	AC	*Crt* B+I	AC	*Crt* B+I
Phytoene	0 ± 0	0 ± 0	13 ± 1	**9 ± 0*****	42 ± 0	**19 ± 0*****	130 ± 2	**34 ± 2*****	209 ± 25	**28 ± 1****
Phytofluene	0 ± 0	0 ± 0	0 ± 0	0 ± 0	59 ± 1	**34 ± 1*****	129 ± 2	**57 ± 2*****	199 ± 21	**35 ± 1****
Violaxanthin*	67 ± 6	65 ± 3	44 ± 2	**51 ± 3***	0 ± 0	0 ± 0	0 ± 0	0 ± 0	0 ± 0	0 ± 0
Lycopene	0 ± 0	0 ± 0	40 ± 1	41 ± 4	336 ± 5	**222 ± 8*****	995 ± 16	1021 ± 42	1197 ± 186	1029 ± 14
β-Carotene	105 ± 8	93 ± 4	114 ± 5	**157 ± 1****	156 ± 2	**280 ± 11****	282 ± 2	**555 ± 15*****	284 ± 29	**520 ± 7****
γ-Carotene	0 ± 0	0 ± 0	24 ± 1	24 ± 1	23 ± 1	24 ± 0	24 ± 1	24 ± 1	23 ± 1	24 ± 1
Lutein	105 ± 8	**87 ± 4***	89 ± 4	90 ± 2	91 ± 3	**98 ± 3***	96 ± 3	95 ± 3	90 ± 4	94 ± 1
α-Tocopherol	99 ± 12	122 ± 4	102 ± 6	**181 ± 9*****	156 ± 4	**195 ± 4*****	185 ± 6	**203 ± 6***	201 ± 22	207 ± 4

Table 3-3 Carotenoid and α-tocopherol contents in AC and *Crt*B+I throughout ripening

Carotenoid and α-tocopherol contents are presented as μg/g DW. Methods used for these determinations are described in section 2.5. Determinations were made from three independent pools of three fruits, each pool with three technical replicates. The mean data are presented with ± SD. Dunnett's test was used to determine significant differences between the wild type background (AC) and the transgenic variety for each compound. Values in bold indicate where significant differences have been found. $P<0.05$, $P<0.01$ and $P<0.001$ are designated by *, **, and ***, respectively. Violaxanthin*, indicates violaxanthin and isomers.
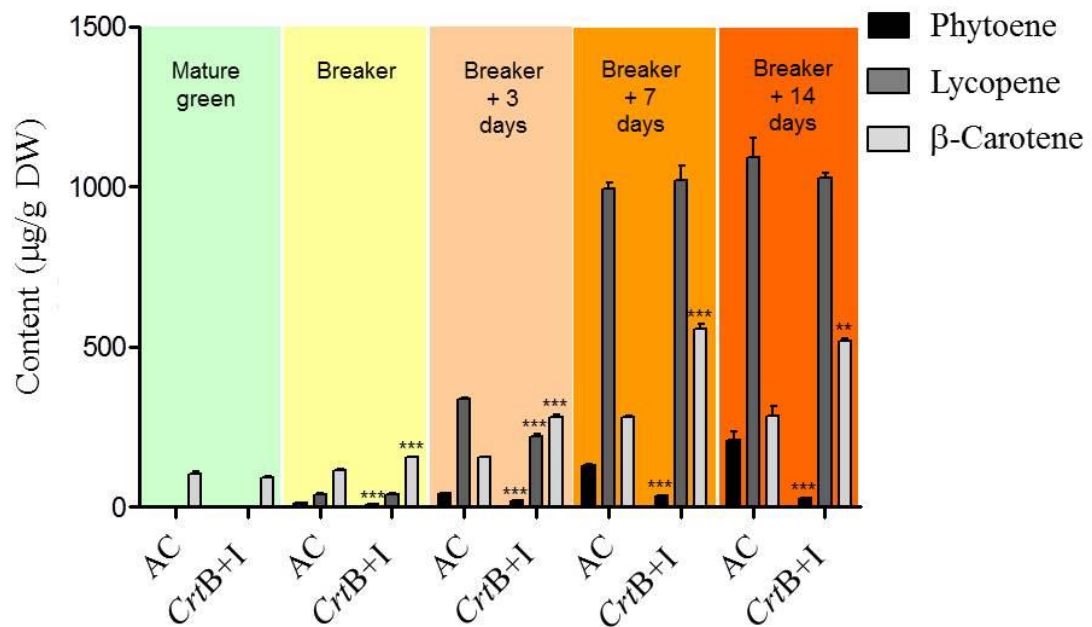
Figure 3-4 The changes in carotenoid composition in the fruit of *Crt*B+I through ripening, compared to AC

Lycopene, β-carotene and phytoene contents are given as μg/g DW. Methods used for determinations are described in section 2.5. Three representative fruits were used. Three determinations were made per fruit, making three biological and three technical replicates. The bars represent the mean ± SD. Student's t-test was used to determine significant differences between the wild type background (AC) and the *Crt*B+I line for ripening stage. Bars with stars indicate where significant differences have been found. $P<0.05$, $P<0.01$ and $P<0.001$ are designated by *****, ******, and *******, respectively.

3.2.3.3 Transcriptional changes of the carotenoid/isoprenoid pathway in the *Crt*B+I line

The *Crt*B+I combination modified the carotenoid profile of both leaf and fruit tissues (Table 3-1). To ascertain how these effects arose, transcriptional analysis of carotenoid biosynthetic pathway genes was carried out. Quantitative real-time RT-PCR was performed on leaf and tomato fruit (at breaker + 3 days) from the *Crt*B, *Crt*I, *Crt*B+I lines and the wild type (AC) as described in section 2.3.9.

Overall, only the expression of a few transcripts for carotenoid biosynthesis genes was affected by the heterologous expression of *Crt*B and *Crt*I genes in the tomato tissues (Figure 3-5). Although these variations in gene expression between AC and *Crt*B+I were significant, they remained modest (only 0.5- to 3- fold change).
In the leaf, only the level of the fruit specific lycopene β-cyclase (*Cyc-B*) and the flower specific carotene β-hydroxylase (*CrtR-b2*) transcripts were significantly different in the *Crt*I containing lines, showing a 2- to 3-fold increase, in comparison with the wild type levels.

In the fruit, there was an upregulation of the expression of the geranylgeranyl diphosphate synthase-2 (*Ggpps-2*), the zeaxanthin epoxidase-1 (*Zep-1*), the ε-lycopene cyclase (*Lcy-E*) and the lycopene β-cyclase (*Lcy-B*) with a 2- to 2.5-fold increase of the *Ggpps-2* transcript level in the *Crt*I and *Crt*B+I lines, a 2-fold increase of the *Zep-1* transcript level in *Crt*B+I, a similar increase of *Lcy-E* transcripts in *Crt*B line and a 1.3-fold increase of *Lcy-B* transcripts in the *Crt*B+I line, all compared to the wild type levels. Moreover, the *Crt*B and *Crt*B+I lines had reduced levels of *Psy-1* and 2 transcripts (~0.7-fold) compared to their control. However, the *Crt*I line only exhibited a significant reduction in *Psy-2*. The carotene β-hydroxylase (*CrtR-b1*) transcripts were reduced in all transgenic lines, whereas the phytoene and ζ-carotene desaturase (*Pds* and *Zds*) transcripts were only lower in the *Crt*B line.
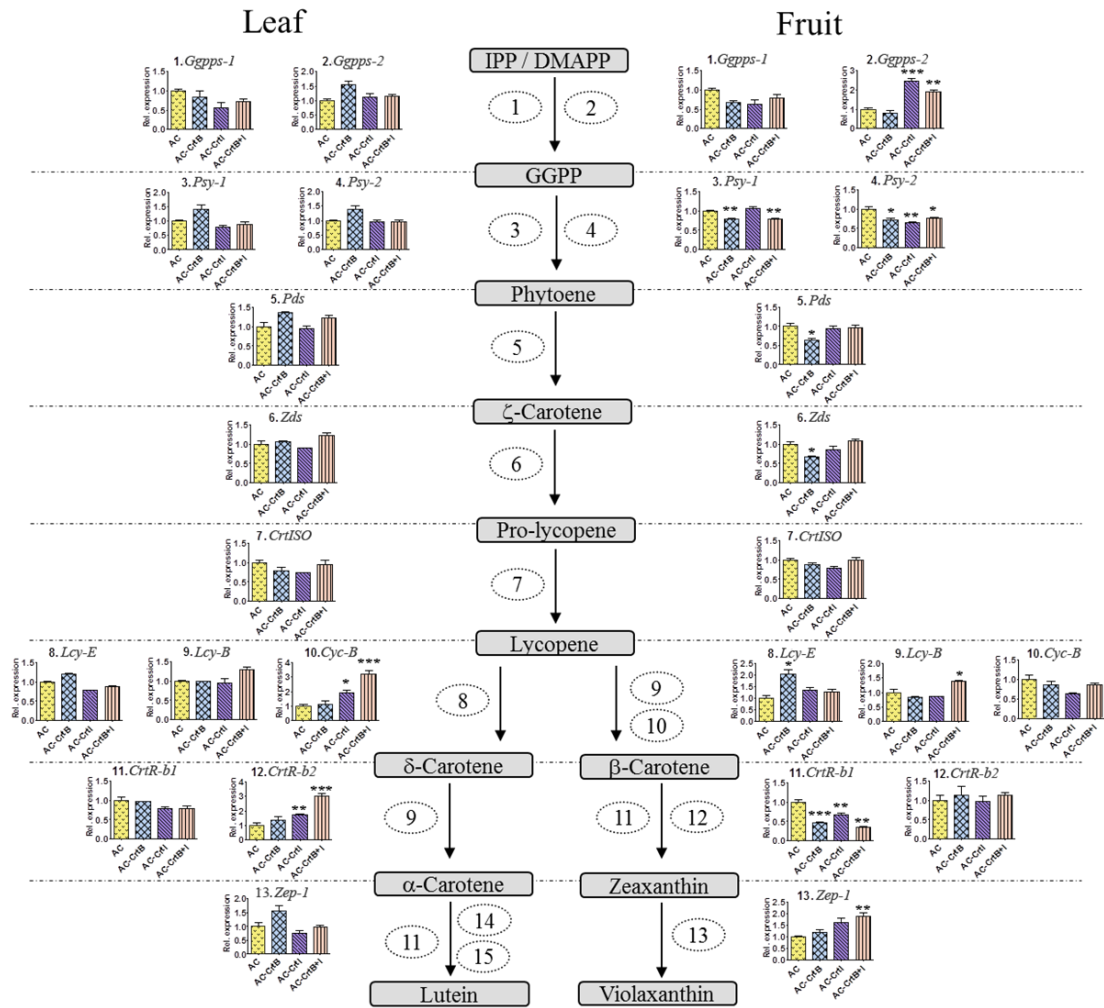
Figure 3-5 Changes in the transcript levels of carotenoid biosynthetic genes in response to changes in carotenoid content resulting from the expression of *Crt*B, *Crt*I and *Crt*B+I genes in tomato

Pooled fruit originating from 3 plants per genotypes (AC; AC-*Crt*B; AC-*Crt*I; AC-*Crt*B+I) were ground in liquid nitrogen to provide a homogenous powder as described in section 2.3.9. Total RNA was then extracted from an aliquot of this material. Quantitative real time RT-PCR was performed with gene-specific primers for (1) *Ggpps-1*, geranylgeranyl diphosphate synthase-1; (2) *Ggpps-2*, geranylgeranyl diphosphate synthase-2; (3) *Psy-1*, phytoene synthase-1; (4) *Psy-2*, phytoene synthase 2; (5) *Pds*, phytoene desaturase; (6) *Zds*. ζ-carotene desaturase; (7) *CrtISO*, carotene isomerase; (8) *Lcy-E*, ε-lycopene cyclase; (9) *Lcy-B*, β-lycopene cyclase; (10), *Cyc-B*, β-lycopene cyclase; (11) *CrtR-b1*, carotene β- hydroxylase 1; (12) *CrtR-b2*, carotene β-hydroxylase 2; (13) *Zep-1*, zeaxanthin epoxidase-1. The expression data shown have been normalized to the expression of actin. Data are represented as relative levels found in the three varieties compared to the wild-type AC (Ailsa Craig). Statistical determinations are shown as mean $\pm$ SD values, where n= 3. Dunnetts's test established statistically significant differences (*, $p<0.05$; **, $p<0.01$; ***, $p<0.001$) from the wild-type levels. The yellow bars of the histogram indicate levels in the wild-type AC, the blue bars in AC-*Crt*B, the

purple bars in AC-*Crt*I and the pink bars in AC-*Crt*B+I. IPP, isopentenyl pyrophosphate; DMAPP, demethylallyl diphosphate; GGPP, gerenaylgeranyl diphosphate; (14), CYP97A, P450 β-ring hydroxylase; (15),CYP97C, P450 hydroxylase.

3.2.3.4 Cellular changes occurring in the *Crt*B+I line

To observe potential ultrastructural changes at the cellular level, Transmission Electron Microscopy (TEM) was performed on ripening fruit (pericarp tissue) from the *Crt*B+I and the wild type lines, as described in section 2.8.1. Characteristic features of chromoplast structures were observed, such as plastoglobules and (remnants of) lycopene crystals, in both AC and *Crt*B+I electron micrographs (Figure 3-6). However altered plastid parameters were also apparent. Firstly, the chromoplasts in the *Crt*B+I were larger in volume (9.1 ± 1.3 μm^2) compared to the wild type (3.12 ± 0.5 μm^2). In addition, the *Crt*B+I plastids contained significantly more plastoglobules (2.8-fold) (Figure 3-6, electron micrographs C and D). Some of these plastoglobules were larger (c.a. 2-fold) and had different staining characteristics, which could correspond to crystal-like structures. Structures termed "thylakoid plexus" and "membranous sacs" were identified and were more abundant in the chromoplasts derived from the *Crt*B+I line. The formation of the membranous sacs from the inner envelope of the chromoplast have been visualised in *Crt*B+I line (Figure 3-6, electron micrograph E).

Among the different lines, the electron micrographs showed very similar types of chromoplasts. As a complementary experiment, and to verify that no heterogeneity in chromoplast structure and carotenoid content existed, the separation of potential chromoplast types (from the pericarp of tomato fruits) was performed by sucrose density gradient centrifugation (described in section 2.7.3). The intact chromoplasts accumulating at the different densities on the gradient, all appeared to have similar ultrastructure and carotenoid profiles (Figure 3-7). The only difference between the *Crt*B+I line and control was the quantitative difference in carotenoids; a feature reflecting the carotenoid content of the intact fruit tissue.
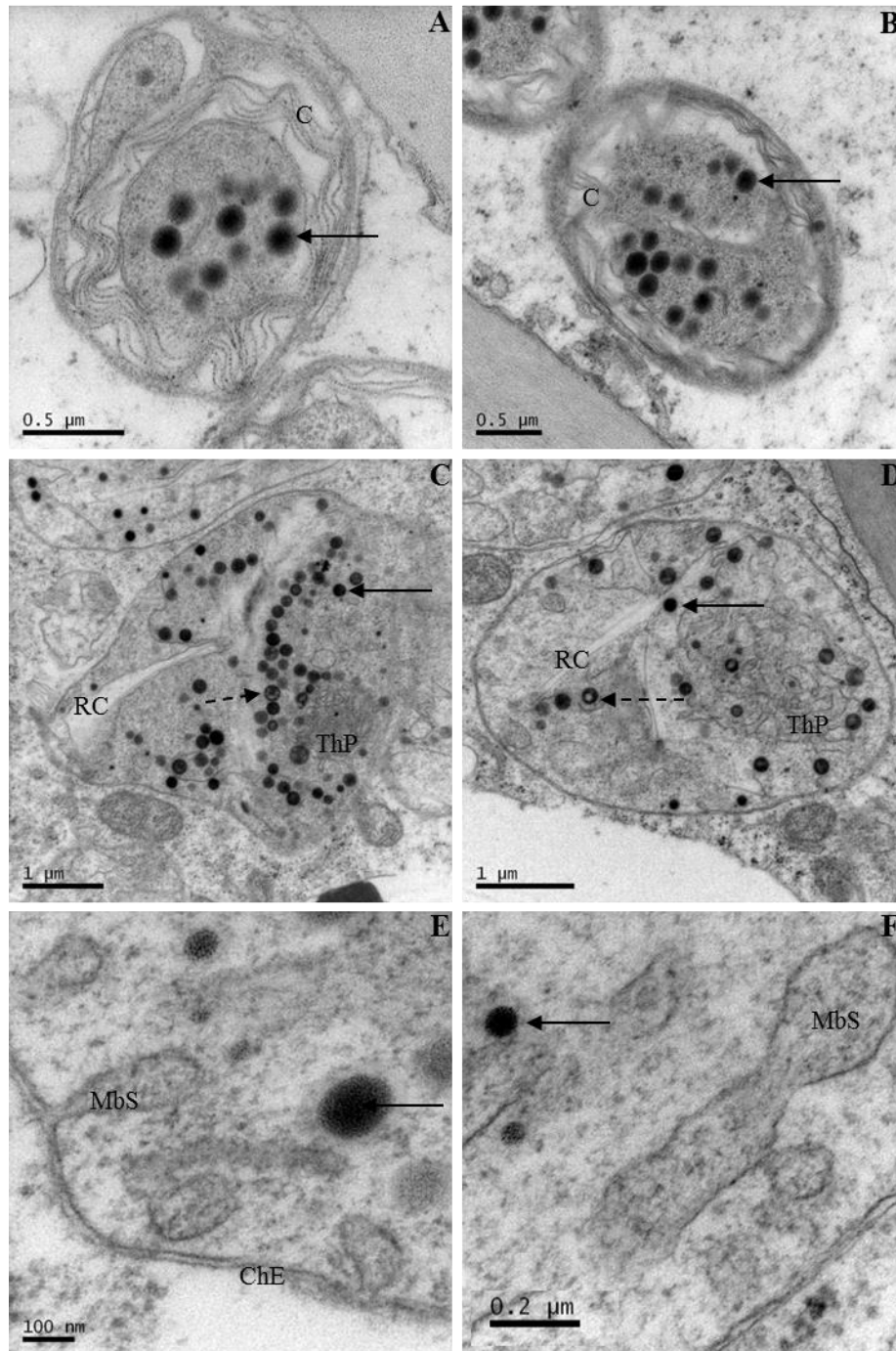
Figure 3-6 Electron micrographs of chromoplasts and substructures of the *Crt*B+I line and the AC control

(A-B), Chromoplasts found in Ailsa Craig (control); (C-D), Chromoplasts of the *Crt*B+I line; (E-F), Substructures of the CrtB+I chromoplasts. Arrows show plastoglobules; dashed arrows show plastoglobules containing another structure (possibly a crystal); C, lycopene crystal; RC, remains of crystal; ThP, thylakoid plexus-like; MbS, membranous sac; ChE, chromoplast envelope. Methods used to obtain the electron micrographs are described in section 2.8.1.
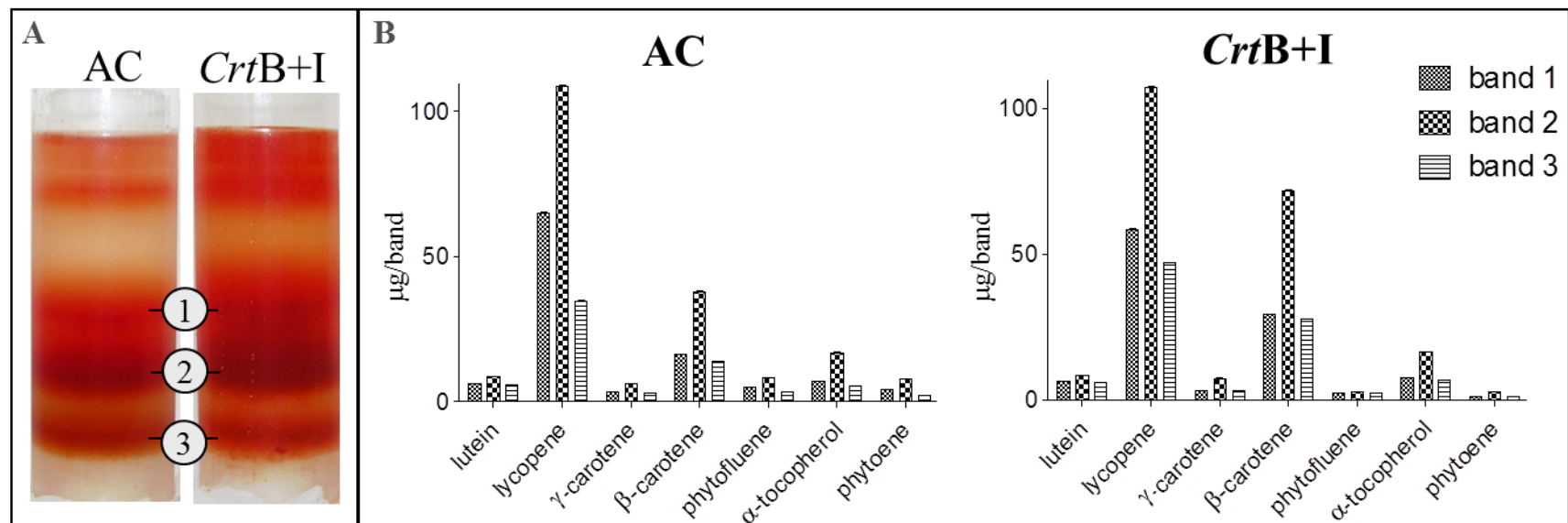
Figure 3-7 Separation of chromoplast type by sucrose gradient centrifugation

(A) Photograph of the sucrose gradient. The numbers 1, 2 and 3 represent the bands of separated chromoplasts

(B) Carotenoid profile of AC and *Crt*B+I bands 1, 2 and 3. Carotenoids contents are given as µg/band. The volume of band 1&3 was +/- 0.5ml and the volume of band 2 was +/- 1ml. Methods used for determinations are described in sections 2.5 and 2.7.3. Eight representative fruits were used. Three determinations were made per fruit, making eight biological and three technical replicates. The bars represent the mean ± SD.

3.2.3.5 Metabolite perturbations arising from the expression of *Crt*B+I genes

The distinct changes at the cellular level suggested that metabolite perturbations beyond the isoprenoid pathway have arisen in the *Crt*B+I line. To assess the broader effects across metabolism, metabolite profiling was performed. Using a combination of analytical platforms, over 50 metabolites were identified and quantified in a relative or absolute manner in the tomato leaf and fruit of *Crt*B+I line and in the wild type. To investigate the changes in the metabolome of the *Crt*B+I line, metabolite changes relative to their control (AC) levels were determined (as described in sections 2.5.7 and 2.5.8) and statistical analysis performed to assess the differences (as described in section 2.9). Significant (p-value <0.05) changes of metabolite levels were found in all the class of compounds analysed (Table 3-4). Alteration of isoprenoid levels in the leaf and fruit of *Crt*B+I line have been described in section 3.2.2. In the fruit of *Crt*B+I, all amino acids and most of the sugars levels were significantly greater, compared to their levels in AC, while the majority of the organic acids detected were significantly decreased in *Crt*B+I. The results in the leaf were more varied although similar conclusions for the amino acids could be drawn. The levels of several lipid classes were also assessed in the tomato fruit of AC and *Crt*B+I (as described in sections 2.5.5, 2.5.6 and 2.5.8). Interestingly, only the level of monogalactosyldiacylglycerol lipid (MGDG) showed a 3.6-fold increase in *Crt*B+I compared to its level in AC. No significant differences were observed in the total amounts of fatty acids for all other lipid classes analysed.

	Ratio *Crt*B+I to AC	
Metabolite	Leaf	Fruit
Amino acid		
Alanine	**1.43 ± 0.08**	-
Aspartic acid	**10***	**2.10 ± 0.53**
β-Alanine	**10***	-
γ-Aminobutyric acid	1.03 ± 0.06	**2.44 ± 0.11**
Leucine	**10***	-
Proline	**10***	-
Glutamine	**1.98 ± 0.2**	**1.41 ± 0.33**
Serine	**10***	**1.73 ± 0.29**
Threonine	1.32 ± 0.39	**10***
Valine	1.34 ± 0.37	-
Isoprenoid		
α-Tocopherol	-	**1.34 ± 0.12**
Violaxanthin	**1.64 ± 0.08**	-
Lutein	0.83 ± 0.06	0.97 ± 0.07
β-Carotene	**1.46 ± 0.21**	**2.50 ± 0.25**
Chlorophyll a	0.77 ± 0.35	-
Chlorophyll b	0.39 ± 0.32	-
γ-Carotene	-	1.11 ± 0.11
Lutein	-	0.96 ± 0.07
Lycopene	-	0.91 ± 0.19
Phytoene	-	**0.31 ± 0.04**
Phytofluene	-	**0.30 ± 0.02**
Non amino acid N-Containing compound		
Putrescine	**10***	-
Lipid		
DGDG	ND	1.05 ± 0.50
MGDG	ND	**3.61 ± 1.03**
PE	ND	1.09 ± 1.12
PS/PC	ND	0.75 ± 0.22
Triglycerides	ND	0.99 ± 0.10
Organic acid		
Aconitic acid	-	**0.01#**
Citric acid	**1.13 ± 0.09**	0.98 ± 0.14
Erythronic acid	**6.80 ± 1.01**	-
Fumaric acid	**0.61 ± 0.09**	**0.01#**
Glucaric acid	**8.88 ± 1.57**	1.53 ± 0.10
Gluconic acid	**0.29 ± 0.09**	**0.76 ± 0.15**
Glycerate	**0.01#**	-
Itaconic acid	-	**0.28 ± 0.04**
Isocitrate	**0.01#**	-
Lactic acid	**10***	-
Maleic acid	**0.61 ± 0.06**	**0.01#**
Malic acid	**1.49 ± 0.17**	1.05 ± 0.14
Succinic acid	0.96 ± 0.07	**0.89 ± 0.07**
Phosphate		
Glucose-6-phosphate	**10***	**0.01#**
Glycerol-3-phosphate	**10***	-
Phosphate	**8.87 ± 1.91**	0.99 ± 0.06
Polyol		
Glycerol	**10***	-

Inositol	**0.74 ± 0.14**	**1.96 ± 0.20**
Sugar		
Arabinose	**0.58 ± 0.23**	**3.45 ± 0.88**
Fructose	**0.90 ± 0.06**	1.10 ± 0.21
Glucose	**1.90 ± 0.18**	**1.15 ± 0.20**
Ribose	**0.58 ± 0.23**	**3.45 ± 0.88**
Sedoheptulose	**0.18 ± 0.05**	0.95 ± 0.17
Xylose	**0.58 ± 0.23**	**3.45 ± 0.88**
Xylulose	-	**0.01#**

Table 3-4 Metabolite changes occurring in tomato leaf and fruit in the *Crt*B+I line compared to the control AC

Data have been compiled from multiple analytical platforms. The ratio data are presented as mean ± SD. Student's t-test was carried out. Significant changes are represented in bold (p-value < 0.05). **10***, theoretical value when a metabolite is unique to *Crt*B+I at the concentration used**; 0.01#**, theoretical value when a metabolite is unique to AC at the sample concentration used, - indicates metabolite not detected in both *Crt*B+I and AC at the sample concentration used; ND indicates metabolite not determined ; PS/PC, phosphatidylserine/phosphatidylcholine; PE, phosphatidylethanolamine; DGDG; digalactosyldiacylglycerol; MGDG, monogalactosyldiacylglycerol

Multivariate principal component analysis (PCA) was used to assess the overall variance in chemical composition among AC and *Crt*B+I lines and to identify the contributions of each metabolite in the leaves and tomato fruits to the overall variance. A scatter plot representing the score values for the fruit PCA (Figure 3-8) showed two statistically different clusters, corresponding to AC and *Crt*B+I fruits. The two lines are clearly separated in the score scatter plot. The same result was observed for the score scatter plot of the leaf PCA (Figure 3-9). The loading scatter plot of the fruit and leaf PCAs indicated that numerous metabolites have significant weightings and the clusters were due to multiple metabolites. In the fruit, MGDG, β-carotene and some amino acids such as threonine and aspartic acid had the highest loading in *Crt*B+I whereas phytoene, phytofluene and some organic acids like aconitic acid, fumaric acid and itaconic acid had the highest loading in AC.

Figure 3-8 Principal component analysis of isoprenoids, lipids and polar compounds of AC and *Crt*B+I tomato fruits

A minimum of three biological and three technical replicates were analysed for every experiment. Metabolite levels from the different analytical platforms were combined. Lipid values correspond to the sum of the total fatty acid values obtained by GC-MS. PS PC, phosphatidylserine/phosphatidylcholine; PE, phosphatidylethanolamine; DGDG, digalactosyldiacylglycerol; MGDG, monogalactosyldiacylglycerol; TAG; triacylglycerides. The methods used to analyse isoprenoids, and polar metabolites are described in sections 2.5 and 2.9 along with the treatment and processing of data.

In the leaf, the loading scatter plot demonstrated that the variables with the greatest loading were serine, proline, glycerol, phosphate and glucaric acid, which were all influencing *Crt*B+I. Violaxanthin and its isomers, plus β-carotene, were also found close to the previous metabolites described but with a smaller weight.

To compare visually alterations in sectors of metabolism and interactions between metabolites, the relative changes in metabolite levels compared with their respective controls were painted onto biochemical pathway displays (Figure 3-10). The variables with the greatest loading in *Crt*B+I leaf and fruit (enumerated previously) are not linked to closely associated biochemical pathways, but a common feature is that they all have their levels increased in *Crt*B+I line.
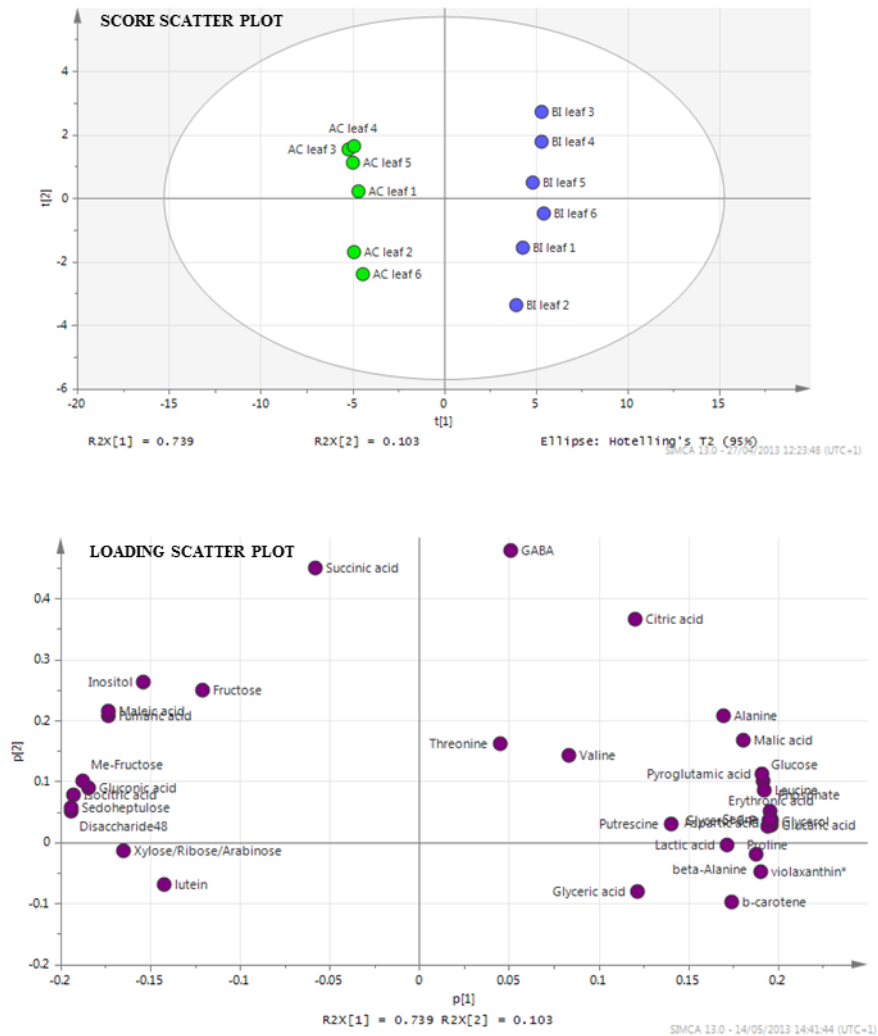
Figure 3-9 Principal component analysis of isoprenoids, lipids and polar compounds of AC and *Crt*B+I tomato leaves

A minimum of three biological and three technical replicates were analysed for every experiment. Metabolite levels from the different technology platforms were combined. Lipid values correspond to the sum of the total fatty acid values obtained by GC-MS. The methods used to analyse isoprenoids, and polar metabolites are described in sections 2.5 and 2.9 along with the treatment and processing of data.

A

Phosphate

Sucrose

Glucaric acid — Rhamnose — Threonic acid — Tartaric acid — Oxalic acid — Galactonic acid

Trehalose

Glucose — Fructose — Mannose — Ascorbic acid — Galacturonic acid — Ribose

Maltose

Glucose-6-phosphate — Gluconic acid — Xylose — Gentiobiose — Stigmasterol

Erythritol — Mannitol — Arabinose — Melizitose — Sitosterol — Campesterol

Galactose

Sedoheptulose — Fructose-6-phosphate — Sorbitol — Sorbitol-6-phosphate — Benzoic acid — Cycloartenol

Xylulose

Glycine

Dehydroascorbic acid — Quercetin derivatives

Serine — Glycolate — 3PGA — Inositol — Inositol-6-phosphate — Glycerol-3-phosphate — Squalene — Amyrin

Glycerate — Glycerol — 5-Hydroytryptamine — Kaempherol

Lactic acid — PEP — TRP — PHE — TYR

Asparagine — Leucine — Valine — ILE — Alanine — Pyr — Shikimate — Naringenin-chalcone — FPP — Ubiquinone

Quinic acid — Chlorogenic acid

3-Caffeoylquinic — Mevalonate

Itaconic acid — Ac-CoA

b-Alanine — Aspartic acid — Oxaloacetate

Lysine — Citric acid — Citramalic acid

MET — H-SER — Aconitic acid

Cysteine — Fumaric acid — Isocitrate

Threonine — Succinic acid — 2-Oxoglutaric acid

Malic acid — SuccCoA

Putrescine — ARG — Glutamic acid — Glutamine

PRO — g-aminobutyric acid

5-oxo-proline

PLASTID

Deoxyxylulose-5-phosphate — MEP — IPP/DMAPP — GPP — FPP — GGPP

Phylloquinone — Phytyl-PP — Phytoene

Phytol — Phytofluene

g-Tocopherol — z-carotene

a-Tocopherol — Neurosporene

Chlorophyll b — Pro-lycopene

Chlorophyll a — d-Carotene — Lycopene — g-Carotene

a-Carotene — b-Carotene

a-cryptoxanthin — b-cryptoxanthin

Zeaxanthin

Lutein — Neoxanthin — Violaxanthin

lipids species

PS/PC — PE

DGDG — MGDG

triglycerides

Fatty acids

Palmitic acid — Linoleic acid

Stearic acid — Oleic acid

Red, decreased levels
Fold increase:
- to 5
- over 5

Green, elevated levels
Fold increase:
- to 5
- over 5
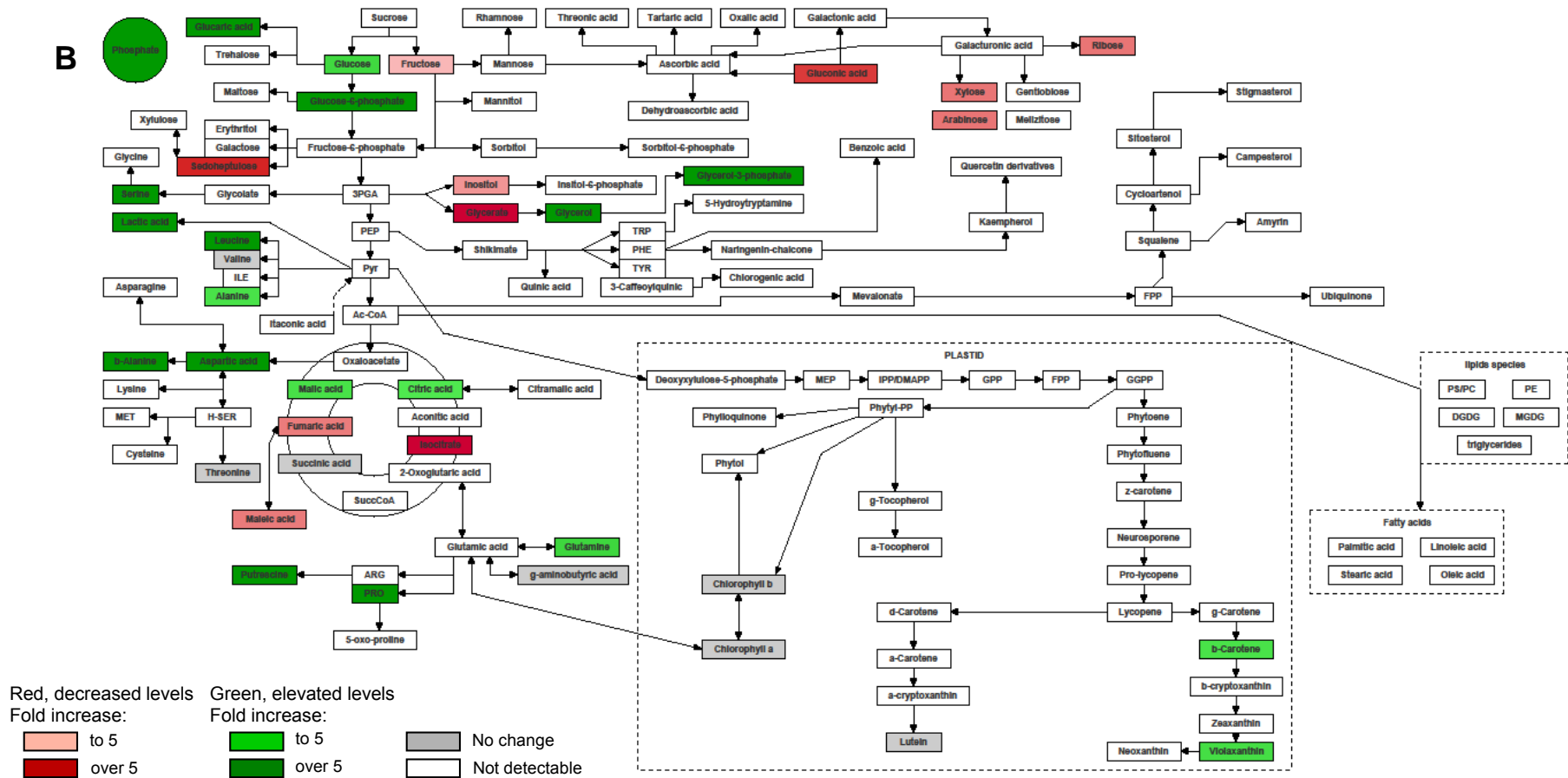
No change

Not detectable

Figure 3-10 Metabolite changes in tomato leaf and fruit as a result of the expression of the *Crt*B+I genes

Figure 3-10 Metabolite changes in tomato leaf and fruit as a result of the expression of the *Crt*B+I genes

A. Fruit; B. Leaf. The metabolomic data are displayed quantitatively over schematic representations of biochemical pathways produced with BioSynLab software (www.biosynlab.com). False colour scale is used to display the quantity of each metabolite in *Crt*B+I line relative to that in the control AC. Green indicates a significant 3-fold increase, to 5-fold increase is pale green, and >5-fold is dark green. Red colouration has been used to represent decreased metabolite levels; dark red is over 5-fold, light red is to 5-fold. Grey indicates no significant change, whereas white indicates that the metabolite was not detected in the samples either because it is not present in the sample or because the compound cannot be detected using the analytical platforms available. 3PGA, glyceraldehyde-3-phosphate; Ac-CoA, acetyl-coenzyme A; ARG, arginine; DGDG; digalactosyldiacylglycerol; DMAPP, dimethylallyl pyrophosphate; FPP, farnesyl diphosphate; GGPP, geranylgeranyl-pyrophosphate; GPP, geranyl diphosphate; H-SER, homo serine; ILE, isoleucine; MEP, 2-C-methyl-D-erythritol 4-phosphate; MET, methionine; MGDG, monogalactosyldiacylglycerol; PE, phosphatidylethanolamine; PEP, phosphoenolpyruvate; PHE, phenylalanine ; PRO, proline; PS/PC, phosphatidylserine/phosphatidylcholine; Pyr, pyruvate; SuccCoA, succinyl-coenzyme A; TRP, tryptophan; TYR, tyrosine.

Multivariate principal component analysis was then performed on the same data set but excluding the isoprenoid data, which represents the target compounds expected to be affected by the expression of the *Crt*B and *Crt*I genes. The analyses in fruit and leaf tissues of AC and *Crt*B+I are shown in Figure 3-11 and Figure 3-12, respectively. In the scatter plots of the score plot for AC and *Crt*B+I lines, distinct clustering occurred. The same variables, as those occurring when the isoprenoid data were included within the PCA, appeared to contribute the most to the separation of AC and *Crt*B+I, such as MGDG in the fruit.
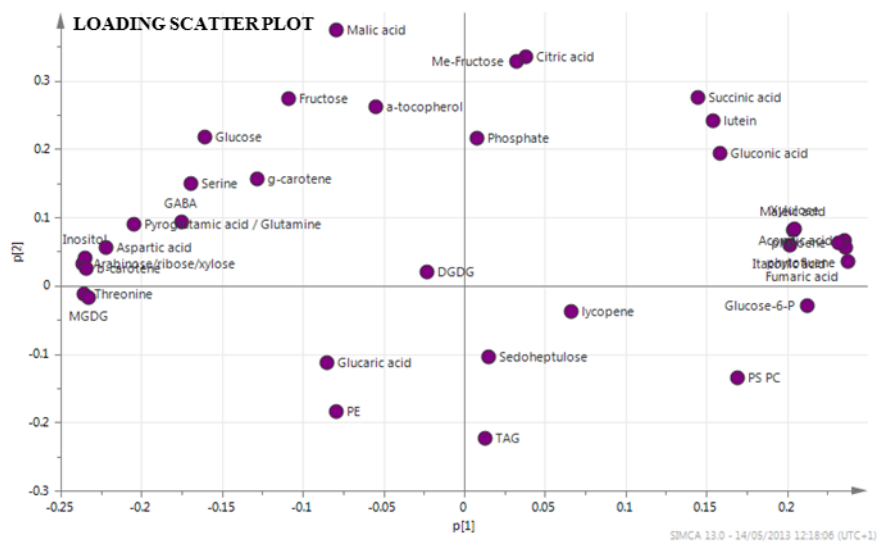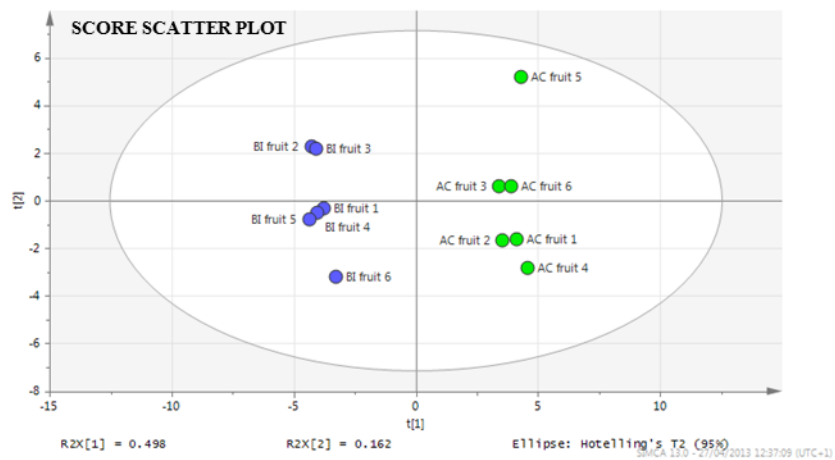
Figure 3-11 Principal component analysis of the metabolites detected by GC-MS in AC and *Crt*B+I tomato fruits, with the metabolites derived from the targeted carotenoid pathway excluded from the data matrix

Three biological and six technical replicates were performed. The methods used to analyse the polar metabolites are described in sections 2.5 and 2.9, along with the treatment and processing of data.
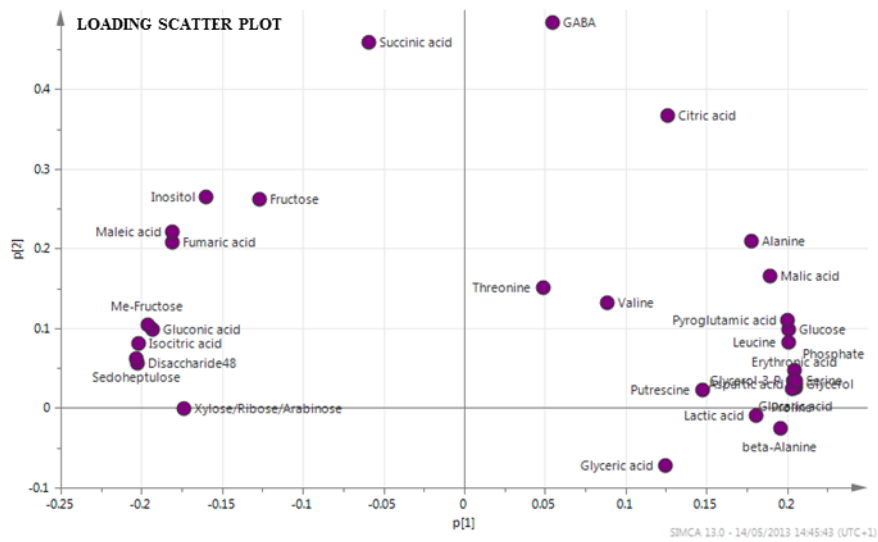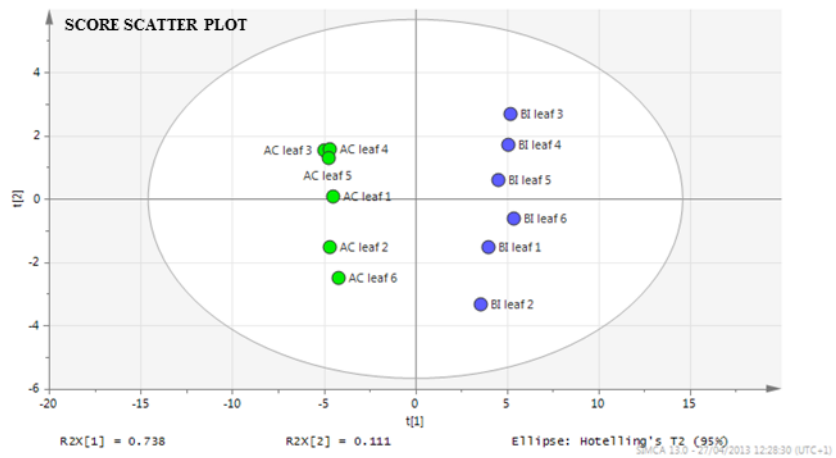
Figure 3-12 Principal component analysis of the metabolites detected by GC-MS in AC and *Crt*B+I tomato leaves, with the metabolites derived from the targeted carotenoid pathway excluded from the data matrix

Three biological and six technical replicates were analysed. The methods used to analyse isoprenoids, and polar metabolites are described in sections 2.5 and 2.9, along with the treatment and processing of data.

In order to have a better understanding of the lipid modification in *Crt*B+I fruits, the fatty acids composition of each lipid class was analysed (Table 3-5) and the fold change increase of the percentage of each fatty acid in a particular lipid of *Crt*B+I compared to its percentage in AC was calculated (Table 3-6). The predominant fatty acids found in most of the lipid classes of AC are the C16 and C18 fatty acids as in *Crt*B+I. It is interesting to notice that, in the MGDG of AC, the two predominant fatty acids are C18 fatty acids and that no C16 fatty acids were detected at the sample concentration used. However, in *Crt*B+I line, the two predominant fatty acids are C16 and C18.

MGDG is the only class of lipid whose level significantly varied in *Crt*B+I compared to AC. It seems that the main changes in MGDG are due to an increase of the quantity of 16:0 and 16:1 cis-9 fatty acid in *Crt*B+I line (Table 3-6).

Multivariate principal component analysis was performed on the fatty acids solely derived from all the lipid classes in order to identify and understand the contribution of each fatty acid in AC and *Crt*B+I. The AC and *Crt*B+I fruits can be grouped as two distinct clusters in the scatter plot of the PCA score values (Figure 3-13). The 16:0 and 16:1 *cis*-9 fatty acids seem to have an influential loading, but they are not the only metabolites with influence. Several fatty acids seem to contribute to the separation of *Crt*B+I to AC, mainly 18:1 and 16:1 fatty acids for most of the lipid classes analysed.

fatty acid (%)	PS / PC AC	PS / PC *Crt* B+I	PE AC	PE *Crt* B+I	DGDG AC	DGDG *Crt* B+I	MGDG AC	MGDG *Crt* B+I	Triglycerides AC	Triglycerides *Crt* B+I
12:0	-	-	-	-	-	-	0.4 ± 0.4	0.2 ± 0.2	0.4 ± 0.1	0.6 ± 0.3
14:0	0.8 ± 0.8	0.3 ± 0.1	0.5 ± 0.5	0.4 ± 0.1	1.8 ± 0.8	1.2 ± 0.2	3.5 ± 1.6	1.6 ± 0.3	0.6 ± 0.2	1.1 ± 0.9
16:0	32.4 ± 0.6	34.7 ± 1.1	27.5 ± 2.8	28.2 ± 1.5	52.5 ± 6.7	57.0 ± 3.6	-	41.9 ± 8.5	15.8 ± 2.8	11.4 ± 3.9
16:1 *cis* -9	3.7 ± 6.1	-	2.0 ± 1.8	-	-	-	-	3.3 ± 1.1	0.3 ± 0.1	2.0 ± 3.2
18:0	6.7 ± 0.8	6.7 ± 1.4	7.1 ± 0.2	8.6 ± 3.2	35.5 ± 15.1	29.7 ± 1.5	64.4 ± 9.3	34.8 ± 11.7	7.1 ± 0.8	10.0 ± 3.2
18:1 *cis* -9	8.6 ± 4.6	5.4 ± 4.7	-	1.7 ± 2.4	-	-	2.8 ± 2.4	11.1 ± 18.0	24.2 ± 0.6	23.9 ± 9.1
18:1 *trans* -9	-	3.2 ± 2.8	-	2.5 ± 2.2	-	-	-	-	-	-
18:2 *trans* -9,12	45.9 ± 13.0	48.7 ± 2.7	60.9 ± 4.7	57.3 ± 3.9	9.8 ± 8.7	11.7 ± 2.2	27.1 ± 10.2	6.6 ± 4.0	49.4 ± 3.0	47.1 ± 5.7
20:0	0.8 ± 0.1	0.7 ± 0.1	1.0 ± 0.1	0.7 ± 0.1	0.5 ± 0.4	0.4 ± 0.4	0.4 ± 0.6	0.4 ± 0.4	0.9 ± 0.1	1.3 ± 0.3
22:0	-	-	-	-	-	-	-	-	0.6 ± 0.1	1.3 ± 0.2
22:2 *cis* -13,16	-	-	-	-	-	-	-	-	0.1 ± 0.0	0.2 ± 0.2
24:0	1.1 ± 0.4	0.3 ± 0.0	0.9 ± 0.2	0.5 ± 0.1	-	-	1.4 ± 2.5	-	0.7 ± 0.1	1.0 ± 0.3

Table 3-5 Fatty acids composition of the lipid classes in *Crt*B+I and control AC

Values represent the percentage of each fatty acid in *Crt*B+I and the AC background. The data are presented as ± SD. Three biological and three technical replicates were used. - indicates fatty acids not detected at the concentration used, Values highlighted in blue correspond to the predominant fatty acids for each lipid class; PS/PC, phosphatidylserine/phosphatidylcholine; PE, phosphatidylethanolamine; DGDG; digalactosyldiacylglycerol; MGDG, monogalactosyldiacylglycerol.

Fatty acid	Ratio % in *Crt* B+I to % in AC				
	PS/PC	PE	DGDG	MGDG	Triglycerides
12:0	-	-	-	0.48 ± 0.08	1.42 ± 0.61
14:0	0.45 ± 0.07	0.77 ± 0.10	0.68 ± 0.10	0.46 ± 0.08	1.70 ± 1.37
16:0	**1.08 ± 0.03**	1.02 ± 0.05	1.07 ± 0.07	**10***	0.72 ± 0.24
16:1 *cis* -9	**0.01#**	**0.01#**	-	**10***	7.69 ± 0.48
18:0	1.00 ± 0.20	1.20 ± 0.45	0.83 ± 0.04	0.54 ± 0.18	1.42 ± 0.45
18:1 *cis* -9	0.64 ± 0.55	**10***	-	3.96 ± 1.92	0.99 ± 0.38
18:1 *trans* -9	**10***	**10***	-	-	-
18:2 *trans* -9,12	1.06 ± 0.06	0.94 ± 0.06	1.17 ± 0.22	0.24 ± 0.14	0.95 ± 0.11
20:0	0.86 ± 0.09	**0.67 ± 0.09**	0.89 ± 0.79	1.23 ± 0.98	**1.51 ± 0.39**
22:0	-	-	-	-	2.10 ± 0.37
22:2 *cis* -13,16	-	-	-	-	1.45 ± 0.05
24:0	0.31 ± 0.03	**0.52 ± 0.10**	-	**0.01#**	1.51 ± 0.46
TOTAL*	0.75 ± 0.22	1.09 ± 0.12	1.05 ± 0.50	**3.61 ± 1.03**	0.99 ± 0.10

Table 3-6 Changes in the composition (in percentage) of fatty acids present in the lipids species found in *Crt*B+I and control AC

Values represent the percentage ratio of each fatty acid in *Crt*B+I compared to the AC background. The ratio data are presented as ± SD. Student's t-test was carried out. The significant changes are shown in bold (p-value < 0.05). Lipids were extracted from a mix of 3 ripe tomato fruits. Lipids were then separated on a TLC plate. Three technical replicates were used. **10*** is a theoretical value used when a fatty acid is unique to *Crt*B+I**; 0.01#** is a theoretical value used when a fatty acid is unique to AC, - indicates fatty acids not detected in both *Crt*B+I and AC at the concentration used, * corresponds to the ratio (*Crt*B+I to AC) of the sum of fatty acid contents for each lipid species; PS/PC, phosphatidylserine/phosphatidylcholine; PE, phosphatidylethanolamine; DGDG; digalactosyldiacylglycerol; MGDG, monogalactosyldiacylglycerol.
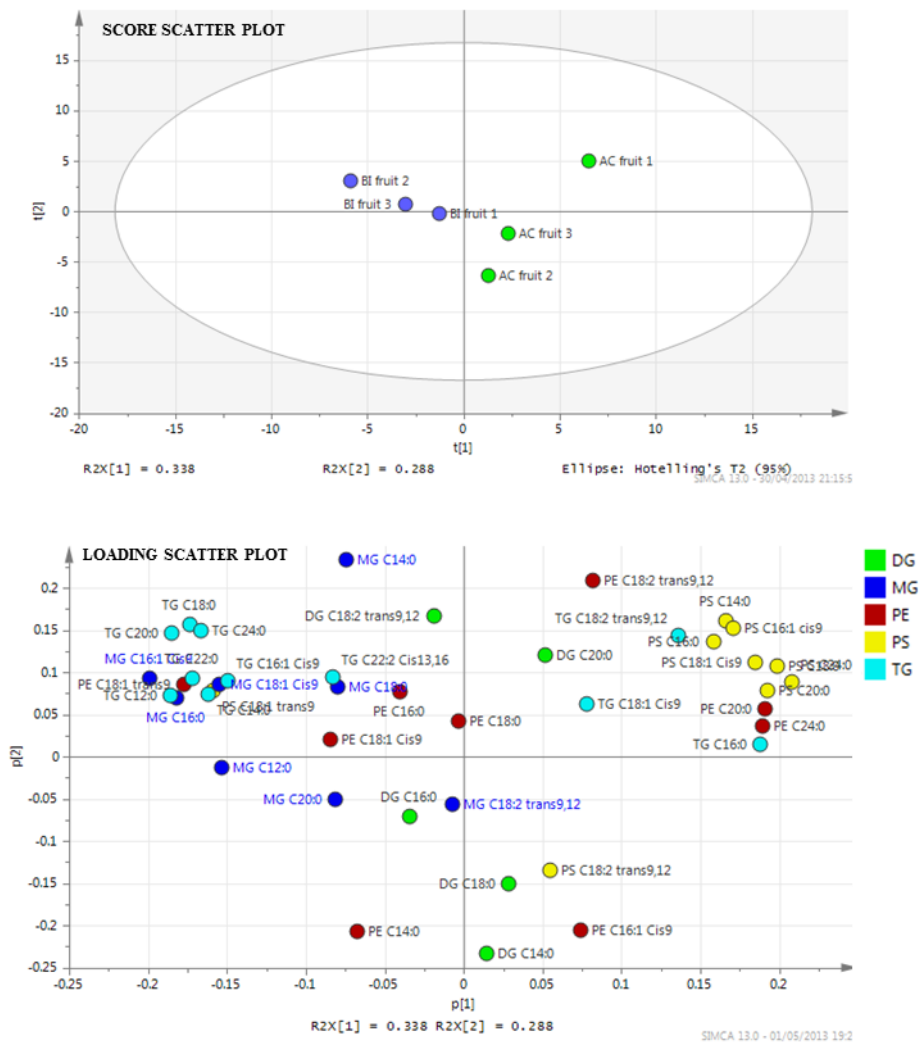
Figure 3-13 Principal component analysis of the fatty acids of AC and *Crt*B+I tomato fruits

Lipid classes: PS, (PS and PC) phosphatidylserine/phosphatidylcholine; PE, phosphatidylethanolamine; DG, (DGDG) digalactosyldiacylglycerol; MG, (MGDG) monogalactosyldiacylglycerol and TG; triglycerides. These compounds were isolated by TLC and their fatty acids were analysed by GC-MS. Three biological and three technical replicates were analysed.

3.3 Discussion

3.3.1 Expression of several carotenoid genes can have synergistic effects on carotenoid formation

The *Pantoea Crt* genes have proven useful tools in the enhancement of carotenoids in bacterial, fungal, and plant systems (Misawa et al., 1991; Shimada et al., 1998; Ravanello et al., 2003). The carotenoid profiles of homozygous *Crt*B and *Crt*I tomato lines have been studied previously (Romer et al., 2000; Fraser et al., 2002). The results generated in this study correlate with the previous description of these lines, with the exception that no difference in total carotenoid content in the *Crt*I line was detected (Table 3-1). This could reflect the different generations used, or more precise sampling. The carotenoid profile of the *Crt*E tomato line is described for the first time in this thesis. Although the reaction catalysed by CRTE was the least effective in increasing the level of carotenoids, the presence of transcripts and the changes in pigments showed that this enzyme was active upon expression. This is significant as the bacterial CRTE enzyme uses FPP predominantly as a precursor (Sandmann and Misawa, 1992), whereas the plant GGPP synthase enzyme utilises IPP or DMAPP as precursors (Laferriere and Beyer, 1991). Thus, despite altered precursor specificity, it seems that the CRTE step can still act or be influential on the pathway flux.

As expected, the individual expression of the three *Crt* genes (*Crt*E, *Crt*B and *Crt*I) in tomato plants led to different carotenoid/isoprenoid phenotypes (Table 3-1). It seems logical as each enzyme (CRTE, CRTB and CRTI) has a different precursor and a different product compared to the other enzymes. However, it is interesting to note that the precursor-product relationship was not always observed. Indeed, the decrease of the precursor and the increase of the product did not always correlate. For instance, in the hemizygous *Crt*I plants, there was a decrease of phytoene but an increase of β-carotene instead of an expected increase of lycopene. In the homozygous *Crt*B plants, there was an increase of lycopene but not of phytoene. There was also an increase of α-tocopherol in all the *Crt*I containing lines, which was not expected as it is a metabolite synthesised upstream of the carotenoid pathway. This reveals that there is a high level of regulation within the carotenoid

pathway that leads to unpredicted carotenoid/isoprenoid phenotypes. Other carotenoid engineering studies in other plant species encountered similar situations (e.g. an increase of β-carotene instead of lycopene). For instance, in rice ("Golden rice") an engineering approach initially utilised a construct harbouring three genes, phytoene synthase (*Psy*), *Crt*I and lycopene β-cyclase, but it was later realised that the lycopene β-cyclase gene was not necessary as *Psy* and *Crt*I alone were able to drive β-carotene synthesis (Beyer et al., 2002). However, it has been suggested that in tomato a feedback regulatory loop exists from β-carotene, or its derivative (Al-Babili et al., 1999; Romer et al., 2000), which is different from the rice mechanism that relies on the expression of constitutively expressed intrinsic carotenoid rice genes (Schaub et al., 2005).

The strategy of a coordinate expression of multiple bacterial carotenoid genes in order to improve carotenoid formation has been utilised previously in canola seeds (Ravanello et al., 2003) and potato tuber (Diretto et al., 2007a). The decrease of phytoene and increase in lycopene/β-carotene levels while expressing the *Crt*I gene seems to be a constant effect in both these studies and, in part, supported by our findings in tomato fruit (Table 3-1). In contrast to potato and canola, tomato fruit have a high basal level of endogenous carotenoids. In the present study, a genetic crossing approach has been used, whereby the highest producers were selected for subsequent crossing. The coordinate expression of two hemizygous carotenoid genes in tomato highlights synergistic effects on carotenoid formation, which are not observed in the lines expressing only one carotenoid gene. For instance, there is no significant increase in the lycopene level of the hemizygous *Crt*E, *Crt*B and *Crt*I lines, compared to the control. However, there is a significant increase in the hemizygous *Crt*E+B and *Crt*B+I lines compared to the control, and to the hemizygous *Crt*E, *Crt*B and *Crt*I lines (p-value < 0.5). The production of lycopene, which was not enhanced by the expression of only one bacterial carotenoid gene, is positively affected when two bacterial carotenoid genes are expressed. It suggests that there is an interaction between the CRTE and CRTB enzymes and the CRTB and CRTI enzymes. It is interesting to notice that there is no such synergistic effect on the lycopene formation in *Crt*E+I line. The CRTE and CRTI enzymes may not be able to interact through the endogenous phytoene synthase. Only the bacterial

136

enzymes representing consecutive steps of the carotenoid pathway have been able to produce a synergistic effect on the carotenoid formation. It may indicate that the CRTE, CRTB, and CRTI enzymes need to form an aggregate complex (termed metabolon; Jorgensen et al., 2005)) to be able to interact together, or be sequestrated into a common microenvironment within the plastid. Previous work also suggested that a complex of the bacterial phytoene synthase, phytoene desaturase and the lycopene cyclase enzymes allowed *in vivo* activity of all three proteins through substrate channelling (Ravanello et al., 2003). Another example of synergistic interactions between carotenoid pathway enzymes, driving the formation of lutein, have been reported (Quinlan et al., 2012).

Although the strategy of combining expression of bacterial hemizygous carotenoid genes allows the increase of some carotenoid levels, the dose of the heterologous gene seems to also have a similar impact on the carotenoid levels. For instance, while the level of lycopene was not significantly increased in the *Crt*B and *Crt*I hemizygous lines compared to the wild type, it was in the *Crt*B and *Crt*I homozygous lines, as it is in the *Crt*E+B and *Crt*B+I hemizygous lines. Surprisingly, the homozygous *Crt*B+I line did not have a significant increase in lycopene and total carotenoid levels. However, it contained the highest level of β-carotene produced in all the lines studied. Consequently, the hemizygous *Crt*B+I line appears to be a more appropriate option than the homozygous line in regard to increasing the entirety of the carotenoid molecules.

It is important to note that the dose of gene (hemizygous or homozygous) affects the carotenoid phenotype in the plant, as discussed in the previous paragraph. In most cases, the dose of gene will be positively linked with the quantity of product synthesised by the enzyme. Consequently, it means that different levels of the carotenoid synthesised by the heterologous enzyme will lead to different carotenoid/isoprenoid phenotypes. A similar phenomenon had been reported in tobacco overexpressing the tobacco *Psy-1* gene (Busch et al., 2002). This reveals that the level of one carotenoid can trigger different regulatory mechanisms in the carotenoid pathway. Thus, it implies that there are sensors in the plants that can recognise the identity of a carotenoid and its level in order to trigger signaling in the plant, which will lead to the regulation of the flux in the carotenoid pathway.

The aim of this work was to study the strategy of the coordinate expression of multiple bacterial carotenoid genes in order to increase carotenoid production. It seems that it is an efficient strategy, but only with specific carotenoid gene combinations (*Crt*B+I or *Crt*E+B). The tomato plant has a high basal level of carotenoids and although changes in carotenoids of interest were moderate (2- to 3-fold increase), these increases are really substantial. Tomato lines producing up to 2700 μg/g DW of lycopene and 800μg/g DW of β-carotene were engineered which is 4 to 20 times more β-carotene synthesised than in engineered maize (Naqvi et al., 2009), potato (Diretto et al., 2007a), cassava (Welsch et al., 2010) and carrot (Maass et al., 2009). However, this work shows that the coordinate expression of multiple bacterial genes is not the only aspect to be considered. The choice of the heterologous carotenoid genes, their combination and the dose of genes are all criteria with a potential impact on carotenoid formation that need to be assessed in order to manipulate the pathway. Other criteria such as the choice of the promoter and the subcellular location of the carotenoids and their enzymes will be discussed in chapters IV and V of this thesis.

3.3.2 The effects of *Crt*B+I expression go beyond the carotenoid pathway

Transcriptional regulation of the carotenoid pathway has been well documented (Fraser and Bramley, 2004; Fraser et al., 2009). In the present study, it has been observed that the small changes detected at the transcriptional level correlate with the changes in carotenoids (Figure 3-5). Of particular interest was the observation that, those transcripts affected the most, correspond to genes associated with alternative tissue specific expression. For example, in the leaf, it is the transcripts of the fruit specific lycopene cyclase (*Cyc-b*) and the flower specific carotene β-hydroxylase (*CrtR-b2*) genes that were altered. This finding suggests that the transcription of carotenoid genes is tightly regulated for those genes expressed in a certain tissue but genes not usually expressed in a given tissue are not under the same regulatory mechanisms (Fray et al., 1995). Overall, the changes of the transcript levels of the carotenoid genes in *Crt*B+I, compared to AC, remained modest. This may be due to the fact that the tomatoes used for this experiment were

at the breaker + 3 days stage of ripening. It is possible that greater modification of the transcripts levels could appear in a later ripening stage, especially under the control of the polygalacturonase promoter (Atkinson et al., 1998).

The presence of CRTB and CRTI also affected the spatial accumulation of pigments over fruit development and ripening, as well as the partitioning of the carotenoids within the fruit tissues. For example, comparisons between the pericarp of the homozygous *Crt*B+I line with its control AC, at different ripening stages, showed that the timing of carotenoid formation is altered in the *Crt*B+I line (Figure 3-4 and Table 3-3). From the breaker stage, the *Crt*B+I line contained significantly more β-carotene and less phytoene compared to AC, but lycopene level was significantly lower in the *Crt*B+I line at the breaker + 3 days ripening stage. These changes in carotenoids reflect the expression of the different promoters controlling the *Crt*B and *Crt*I genes, the *Crt*I gene being under constitutive control and the *Crt*B gene ripening specific promoter control (Atkinson et al., 1998). The earlier presence of the CRTI enzyme influences the level of β-carotene and phytoene from the breaker stage, and the CRTB enzyme appearing later in the ripening process affects the level of lycopene. The choice of the promoter is always a determinant in engineering carotenoid production in plants, but it becomes crucial when overexpressing two bacterial genes, which enzymes may need to interact, or be in the same tissue, in order to create a synergistic effect on carotenoid production.

Another effect of altered pigment content resulting from CRTB and CRTI is the intra-fruit partitioning of carotenoids in the pericarp, jelly and columella fruit tissues (Figure 3-3 and Table 3-2). The pericarp seems to be the most amenable fruit compartment to store carotenoids (i.e. the highest levels), but the greatest changes resulting in the increased lycopene level in the *Crt*B line and β-carotene level in the *Crt*I and *Crt*B+I lines were associated with the columella tissue. This suggests that the accumulation of the carotenoid in the tomato fruit depends on several tissue related factors, such as the type of cells, the type and quantity of membranes, and perhaps the water content of each tissue/cell type. The factor revealed is the saturation of a tissue with a specific carotenoid. It would appear that a saturation limit for a specific carotenoid exists in a given tissue and beyond this point another

region of the fruit must be utilised. In the case of the *Crt*I line, there was a small increase of total lycopene level (1.2-fold), which was only noticeable in the pericarp compartment. However, in the *Crt*B line, which had a 2-fold increase of total lycopene level, an increase in the pericarp (1.7-fold) was observed, but also in the columella (2.3-fold). There is already evidence that spatio-temporal specificity in the accumulation of endogenous carotenoid from tomato fruit exists (Moco et al., 2007). The work presented here highlights the presence of a saturation threshold specific to individual carotenoids, which leads in the case of an increased carotenoid level to a modification of the spatial sequestration of the carotenoids within the fruit.

In addition to the altered tissue distribution, structural differences at the chromoplast level have also been observed (Figure 3-6). The chromoplasts from the *Crt*B+I line appeared to be greater in size and contain more membranes (previously described as thylakoid plexus by Harris and Spurr, 1969a). The thylakoid plexus had also been identified in the chromoplast of the full ripe fruit of the high β-mutant tomato (Harris and Spurr, 1969b). The presence of the thylakoid-like membranes could allow a greater storage environment for the carotenoids. In *Crt*B+I, most of the plastoglobules were the same size as in AC. However, some of them appeared to be much greater and seemed to contain a crystal-like structure. Plastoglobules containing crystals have previously been reported in another *Solanum* species (*Solanum capsicastrum*; Wrischer et al., 2007). Therefore, the mechanism of storing crystals in the plastoglobules of the *Crt*B+I chromoplasts seems plausible. Another striking difference was the number of membranous sacs. In the *Crt*B+I line, the formation of multiple membranous sacs from the inner envelope of the chromoplasts was observed (Figure 3-6, E and F). This is the first time that a clear image of the formation process of the membranous sacs has been shown. The hypothetical role of the membranous sacs (also described as carotenoid-containing-structure or newly synthesised membrane) is to contain crystals of carotenoids (Cheung et al., 1993; Deruere et al., 1994; Simkin et al., 2007; Egea et al., 2010). The structure of the chromoplasts found in *Crt*B+I seem to have been altered in order to accommodate more (crystals of) carotenoids. The chromoplast structure can be affected by the type of carotenoids that are accumulating (Harris and Spurr, 1969a). It seems that in the *Crt*B+I line, which has an increased level of lycopene, but a more substantial

increase in β-carotene, only have one type of chromoplast structure in the pericarp (Figure 3-7).

Metabolite profiling illustrated that, in addition to cellular changes the expression of *Crt*B+I genes in the tomato fruit had effects across the metabolome (Table 3-4). As expected, the carotenoid/isoprenoid levels were affected. Moreover, primary metabolism, including the lipid content, was modified in *Crt*B+I. The PCA performed on the whole dataset of metabolites and on the dataset without the isoprenoid compounds showed that AC and *Crt*B+I could still cluster apart, even when the isoprenoids were not present (Figure 3-8 to Figure 3-12). This suggests that differences within primary metabolism are significant enough to differentiate these two lines. The precise biochemical/molecular links with the increased sugars and amino acid levels and decrease of organics acids levels in response to altered carotenoids awaits further systematic analysis. However, it could be that perturbations in fruit ripening via phytohormone imbalances could have arisen. Such changes in sugars, amino acids and organic acids have the potential to alter taste, which is an important industrial attribute. Among the lipids analysed a significant increase of monogalactosyldiacylglycerol (MGDG) content (3.6-fold increase) was determined in the transgenic lines containing *Crt*I; Specifically a significant increase of 16:0 and 16:1 *cis*-9 fatty acids and a slight augmentation of 18:1 fatty acid. It is not the first time that an associated increase of carotenoid and MGDG lipid levels has been observed. A marine bacterium (cyanobacterium *Synechococcus* sp), showed a similar effect in carotenoid and MGDG lipid levels, especially the 16:0 and 18:3 fatty acids, during high light acclimation (Montero et al., 2012). It seems that it is the prokaryotic pool of MGDG (16:0 plus 18:1, from plastids) that is positively regulated, in parallel with the carotenoid level in the *Crt*B+I line. MGDG is found in abundance in the inner envelope and in the thylakoid membranes of the chloroplast/chromoplast (Marechal et al., 1997). The reason why the quantity of MGDG increased in relation to an elevated carotenoid content is the fact that MGDG has a high propensity for interfacial curvature (Szilagyi et al., 2007), allowing the membrane to adapt to a greater quantity of β-carotene. This membrane curvature property of MGDG has been proposed to be essential for the conversion of violaxanthin to zeaxanthin, by allowing the conical-shaped violaxanthin de-

141

epoxidase enzyme to bind to the curved thylakoid membranes and act on violaxanthin molecules (Figure 3-14). In the transgenic line, it appears that the plasticity of the membrane to accumulate lipids is increased to accommodate the extra carotenoid produced.
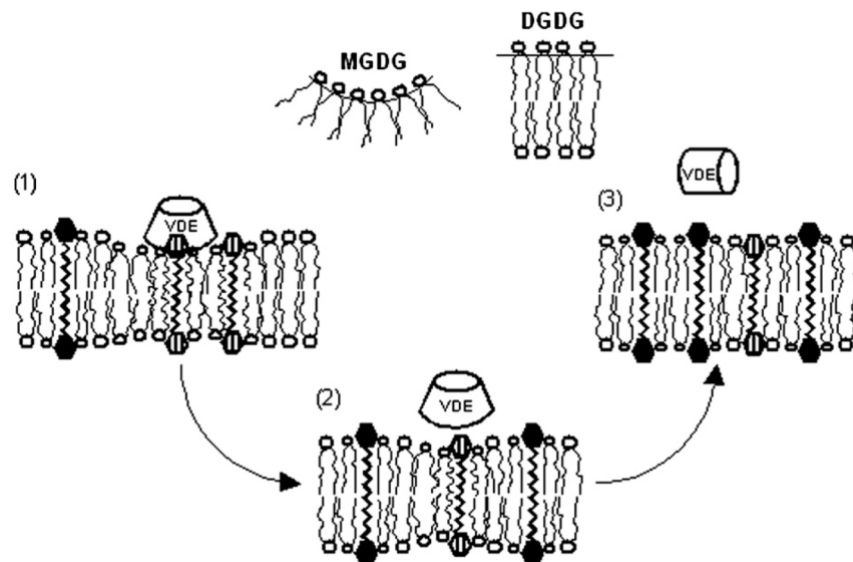
Figure 3-14 Schematic model of the effect of curvature stress on the xanthophyll cycle (from Szilagyi et al., 2007)

Upon high light, the formation of the MGDG-rich regions gives rise to curvature stress in the bilayer. MGDG serves as an efficient host for violaxanthin (hatched hexagon) and is also required by the violaxantin de-epoxidase enzyme, VDE (truncated cone). (1), The enzyme binds to the membrane and converts violaxanthin to zeaxanthin (filled hexagon); (2), As the conversion proceeds more hydrophobic and stretched zeaxanthin is formed; (3), The membrane expands and brings about a release of curvature stress, leading to a less favoured lipid environment for VDE (cylinder).

Chapter IV: Sub-plastidial sequestration of carotenoids in response to elevated synthesis

4.1 Introduction

The heterologous expression of the bacterial *Crt*B and *Crt*I gene combination in tomato plants resulted in an increase of carotenoid content in the fruit. Changes at multiple levels (transcription, primary and secondary metabolites, chromoplast ultrastructure, and fruit tissue) in the plant were observed, as described in Chapter III. The sub-plastidial components of the *Crt*B+I chromoplasts had also been altered, with the increased content of carotenoids in the fruit. In this chapter, the following questions are addressed: (i), where in the plastid are the pigments sequestrated? and (ii), whether adaptation to increased levels arises within the sub-plastidial component of the chromoplasts. Sucrose density gradient centrifugation was performed to fractionate chromoplasts from the wild type and the *Crt*B+I line and then sub-plastidial structures were isolated. Characterisation of the AC and *Crt*B+I chromoplasts sub-structure was then achieved.

4.2 Results

4.2.1 Fractionation and identification of sub-plastidial components of the chromoplasts from AC (wild type) and *Crt*B+I lines

The sub-plastidial components of AC and *Crt*B+I chromoplasts from breaker + 3 to 5 days ripening stage tomato fruits were isolated in a 5 steps discontinuous sucrose density gradient (as described in section 2.7.1 and Figure A2-4). The separation of the sub-chromoplast structures in the sucrose gradients is shown in Figure 4-1. Two distinct coloured sectors in the gradient of AC and *Crt*B+I were observed, the first occurring at the top of the gradient in fractions 1 and 2 and the second in the middle, lower part of the gradient from fractions 16 to 24. The red/orange colour intensity of all these fractions was greater in the *Crt*B+I preparations compared to AC. The lower coloured sector of the gradient was characterised by the presence of crystal-like structures. A greater intensity of crystal-like aggregates was found in the upper phase of this sector derived from the wild type (fractions 16 to 20), compared with relatively fewer structures in its lower phase (fractions 21 to 24). In contrast, the *Crt*B+I line exhibited a greater intensity of crystalline aggregates over both parts of the coloured sector. It is interesting to note that in the *Crt*B+I preparation, a clear

separation of the two crystalline phases was observed with fraction 20/21 containing no crystal-like structures.
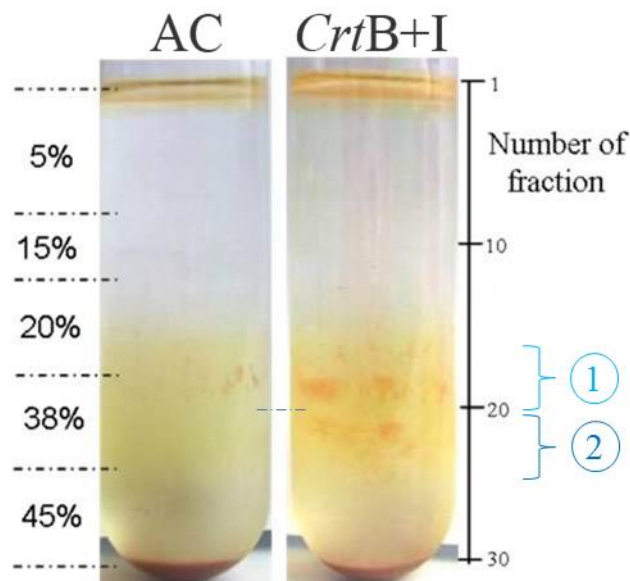
Figure 4-1 Fractionation of sub-plastidial components of the chromoplasts from AC (wild type) and *Crt*B+I lines

Chromoplasts were extracted from breaker + 3 to 5 days fruits (90 g), broken with a hand held Potter-type homogeniser and separated in a discontinuous sucrose gradient of 5%, 15%, 20%, 38% and 45% sucrose w/v. Encircled 1 and 2 correspond to sub-membrane compartments I and II, respectively. Fractions (1 ml) were collected for further analysis. Typically, a total of 30 or 31 fractions were collected per centrifuge tube.

Fractions (F, 1 ml) were collected from top to bottom of the gradients and sixteen fractions throughout the gradient (mainly from coloured sections) have been thoroughly analysed to identify and designate the different sub-compartments of the chromoplasts. The protein profiles of these fractions have been determined and identification of individual proteins undertaken (Figure 4-2 and Table 4-1).

The protein profiles of AC and *Crt*B+I were similar. F1 and F2 were characterised by two major proteins. These proteins have been identified as plastoglobulin-1 and the plastid lipid associated protein, CHRC (Table 4-1). These two proteins are known to be localised in the plastoglobule (Kessler et al., 1999; Ytterberg et al., 2006; Kessler and Vidi, 2007). The amount of protein present in F7 and F12 was too low for detection on SDS-PAGE stained with silver reagents. Fractions 17 to F30 in the gradient contained a comparatively higher protein intensity compared to earlier

fractions, with prominent bands displaying Gaussian distribution across adjacent fractions (Figure 4-2). In the F17 to F24, all the prominent proteins identified were derived from the photosynthetic systems present in the thylakoid membrane, as for example, ATP synthase subunit β, photosystem I reaction centre subunit II, Photosystem II 22 kDa protein, and the oxygen evolving enhancer proteins 1 and 2. In F24 to F30, thylakoid proteins were still identified, but additional proteins were found, such as the heat shock cognate 70 kDa protein. This protein has been attributed to the chromoplast envelope (Ko et al., 1992). RuBisCO protein, from the chromoplast stroma, was mainly detected in F28 and F30. Further details on the proteins identified are provided in Table 4-1.

In order to complement the proteomic approach, immuno-detection of key biomarker proteins of known sub-plastid location were used. The immuno-localisation of PGL35 (plastoglobulin 35), PSBA (photosystem II protein D1), TIC40 (translocon at the inner envelope of chloroplasts), TOC75 (translocon at the outer envelope of chloroplasts) and the stromal RBCL (RuBisCo large subunit) proteins was carried out across the gradient (Figure 4-2). The PGL protein was detected in F1 and F2, but also in F18 to F30. Following comparative protein loading of wild type and *Crt*B+I samples, a greater quantity of PGL was prevalent in the *Crt*B+I derived fractions. The PSBA protein was mainly detected in the 17 to 26 fractions and at low level in control F1 and F2. The TIC protein was found principally in F28 and F30 in AC and in F24, F25 and F26 in *Crt*B+I. As expected, TOC75, specific to the chloroplast envelope, was not detected in the fractions. The RBCL protein was mainly discovered at the bottom of the gradient in F26 to F30 in AC and F25 to F30 in *Crt*B+I.

According to these results, it seems that F1 and F2 correspond to the free plastoglobules of the chromoplasts (displayed in yellow in Figure 4-2), while F17 to F23 represent the subcompartment structure with thylakoid membrane (represented in green in Figure 4-2). Fractions 24 to F26/28 appear to be a mix of thylakoid membrane and envelope membrane structure (dark green in Figure 4-2) and the last fractions (F25 to F30) represents enriched stromal proteins (orange in Figure 4-2). This colour code will be used for all the figures of this chapter.
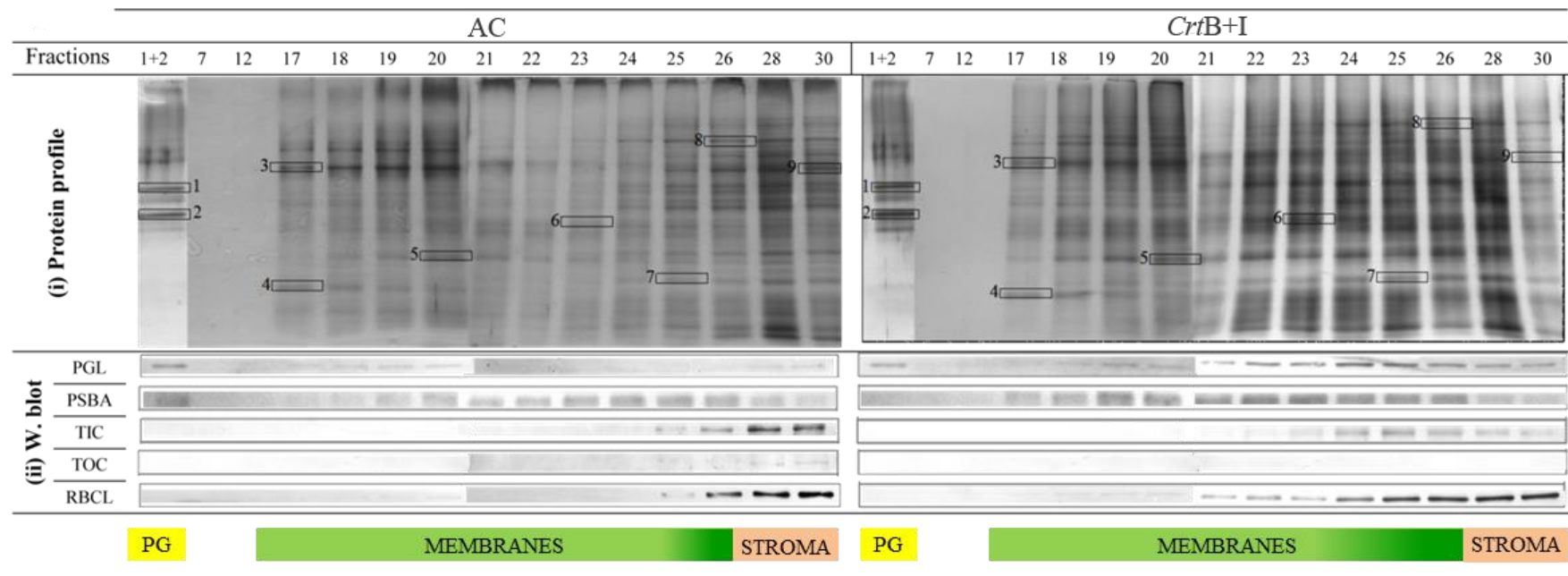
Figure 4-2 Identification of sub-chromoplast components within the fractions

(i). Protein profile. Proteins, extracted from each fraction, were separated and visualised using SDS-PAGE, followed by silver staining. Selected proteins have been identified by LC-MS-MS: 1. plastoglobulin-1; 2. plastid lipid associated protein CHRC; 3. ATP synthase subunit b; 4. photosystem I reaction centre subunit II; 5. photosystem II 22 kDa protein; 6. oxygen evolving enhancer protein1; 7. oxygen evolving enhancer protein 2; 8. heat shock cognate 70 kDa protein-1; 9. RuBisCO large subunit-binding protein subunit b. Details of the identification of these proteins are showed in Table 4-1. (ii). Western blot. Immuno localisation of biomarker proteins (plastoglobulin (PGL, 35 kDa); Photosystem II protein D1 (PSBA, 28 kDa); Translocon at the inner envelope of chloroplasts (TIC, 45 kDa); Translocon at the outer envelope of chloroplasts (TOC, 75 kDa); and RuBisCo large subunit (RBCL, 52 kDa) in the fractions was determined by western blotting. The colour scheme represents the different sub-chromoplast components. PG, plastoglobules. Dark green corresponds to the envelope membrane location.

Band number[1]	Acc.No[2]	Protein Name	Score[3]	Location[4]
1	PG1_PEA	Plastoglobulin-1, chloroplastic	73	Chloroplast › plastoglobules periphery
2	LIPC_SOLTU	Light-induced protein, chloroplastic	750	Chloroplast thylakoid membrane
97% similarity with	Q0ZPA3_SOLLC	Plastid lipid associated protein CHRC		Chloroplast
3	ATPB_SOLLC	ATP synthase subunit β	750	Chloroplast thylakoid membrane; Peripheral membrane protein
4	PSAD_SOLLC	Photosystem I reaction center subunit II	187	Chloroplast thylakoid membrane
5	PSBS_SOLLC	Photosystem II 22 kDa protein	331	Chloroplast thylakoid membrane
6	PSBO_SOLLC	Oxygen-evolving enhancer protein 1	170	Chloroplast thylakoid membrane
7	PSBP_SOLLC	Oxygen-evolving enhancer protein 2	853	Chloroplast thylakoid membrane
8	HSP72_SOLLC	Heat shock cognate 70 kDa protein 2	1003	N/A
94% similarity with	HSP7E_SPIOL	70 kDa heat shock-related protein		Chloroplast envelope
9	RUBB_BRANA	RuBisCO large subunit-binding protein subunit β	501	Chloroplast

Table 4-1 Identification of proteins from the isolated fractions by nESI-LC-MS/MS

The protein band number refers to the number shown in Figure 4-2(i).[1] The homology of bands 2 and 8 with *Solanum lycopersicum* species was studied and the percentage of similarity and accession number of the closest protein are shown. [2] Accession number according to SwissProt protein database. [3] Score obtained in Mascot (v2.4.2.0) search. Scores higher than 51 indicate identity or extensive homology (p<0.001).[4] According to UniProt (http://www.uniprot.org/).

4.2.2 Biochemical characterisation of AC and *Crt*B+I sub-chromoplast fractions

Carotenoids and α-tocopherol were profiled by UPLC (section 2.5.3), in most of the fractions (25 out of 31 fractions) derived from the separation of the sub-chromoplast components of AC and *Crt*B+I from the sucrose gradient. The distribution of the isoprenoids within the gradient was investigated and the percentage of each metabolite per fraction was represented (Figure 4-3). The profile of quantity of metabolite (μg/fraction) within the gradient was similar to the profile of percentage.

The percentage of each compound varied through the gradient and was dependent on the line analysed. However, a common feature was that all compounds accumulated mainly in the membranes (F15 to F28) and that phytoene, phytofluene and α-tocopherol were also found in a large percentage in the plastoglobules (F1&2). Two sectors of dense pigmentation, forming peaks of metabolite intensity were observed for lycopene, β-carotene, lutein, and α-tocopherol, derived from the fractionation of the *Crt*B+I fruit. The first peak of pigmentation, related to F16 to F21, has been designated as the sub-membrane compartment I (see also Figure 4-1). The second peak, located in F21 to F26, is termed sub-membrane compartment II. Lycopene, β-carotene and lutein had similar profiles through the gradient. In AC, they mainly accumulated in the sub-membrane I. The *Crt*B+I line is characterised by an increase of lycopene, β-carotene and lutein. The accumulation of these carotenoids was greater in both sub-membrane compartment I and II in *Crt*B+I line, compared to the control. The ratio of the sub-membrane compartment I to II percentage of content of these carotenoids was altered in the *Crt*B+I line. It decreased in *Crt*B+I compared to AC. On a percentage basis the relative increase in carotenoids in *Crt*B+I, compared to AC, was greater in sub-membrane compartment II. One of the differences between sub-membrane compartment I and II was the ratio of β-carotene to lycopene, which was higher in sub-membrane compartment II. The profile of α-tocopherol through the gradient was similar to that of lutein, with the exception that α-tocopherol was also found in the plastoglobules (14% of the total content in AC and 9% in *Crt*B+I).
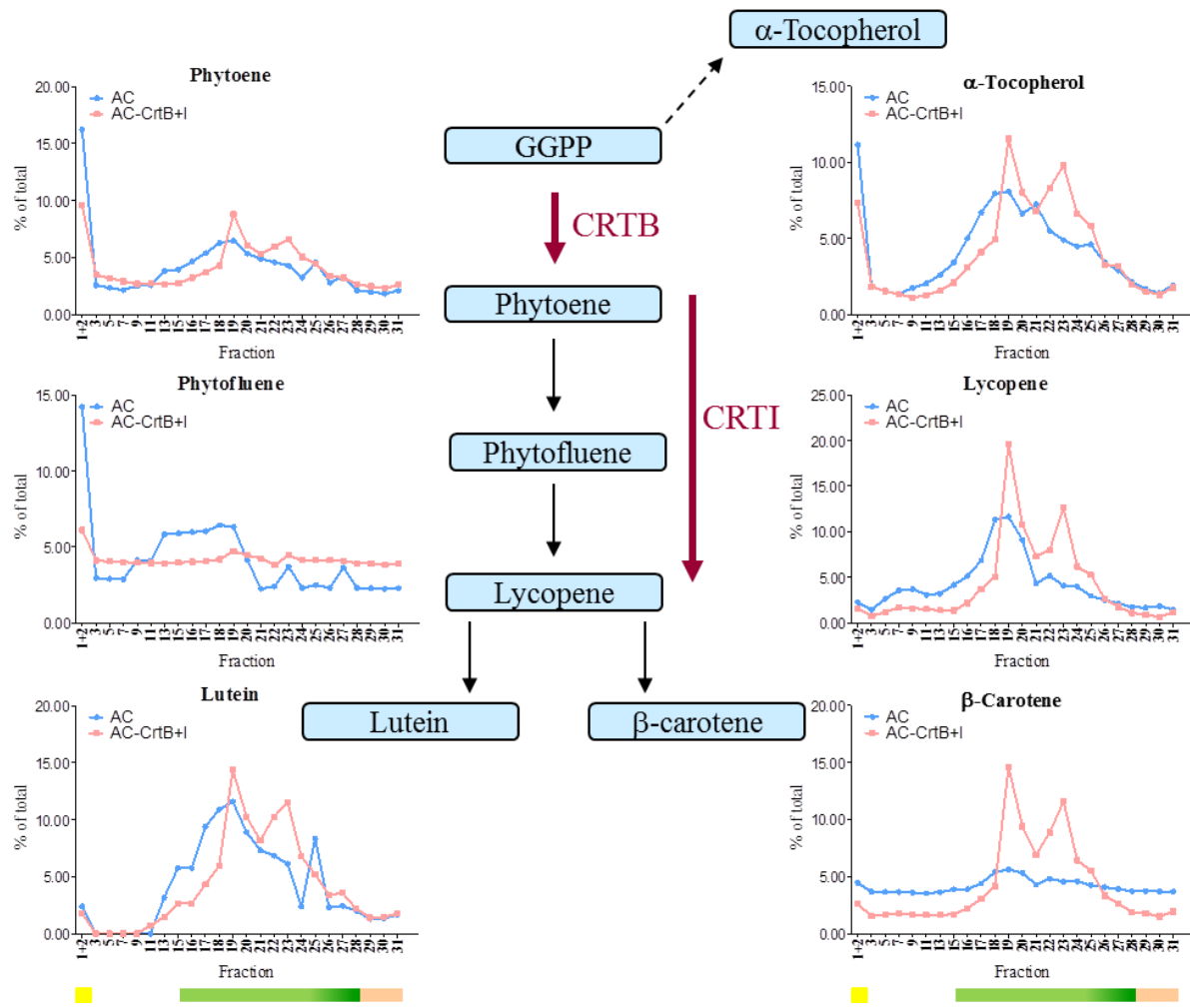
Figure 4-3 Percentage of carotenoids and α-tocopherol in sub-chromoplast fractions

Metabolites were extracted from each fraction. Contents are given as % in a fraction compared to the total content in the gradient. Simplified carotenoid pathway is displayed. Black arrows correspond to one or more carotenoid step(s) and dashed arrow to isoprenoid enzymes(s). The heterologous enzymes are showed in red. CRTB, phytoene synthase; CRTI, phytoene desaturase; GGPP, geranylgeranyldiphosphate. Colour scheme represents the different sub-chromoplast components. Yellow indicates the plastoglobules; green corresponds to the membranes and dark green the envelope membrane; orange displays the stroma. Total amounts (in AC, *Crt*B+I; μg/fraction) of α-tocopherol (7.8, 12.5); phytoene (2.3, 1.3); phytofluene (2.4, 1.3); lycopene (7.5, 14.2); β-carotene (7.1, 18.9) and lutein (1.3, 1.9).

150

In the control chromoplasts, phytoene and phytofluene accumulated in the plastoglobules (15%) and then mainly in the sub-membrane compartment I. In the *Crt*B+I line, the levels of phytoene and phytofluene were lower with only 6 to 9% of these carotenoids accumulating in the plastoglobules. The percentage of phytoene and phytofluene was comparable in the sub-membrane compartments I and II of *Crt*B+I line.

The lipid composition in AC and *Crt*B+I chromoplasts was also investigated, as membrane structures had been revealed to be altered in *Crt*B+I line. Lipids were extracted from the tomato fruits and separated by thin layer chromatography (as described in section 2.5.5). The lipid profile of AC and *Crt*B+I fractions were qualitatively comparable (Figure 4-4). All the fractions contained triglycerides. However, MGDG (monogalactodiacylglycerol), DGDG (digalactodiacylglycerol), PE (phosphatidylethanolamine), PS (phosphatidylserine) and PC (phosphatidylcholine) were found only in the F17 to F26/28 (the membrane region). Similarly, no major qualitative differences were found when comparing the protein profiles of AC and *Crt*B+I (Figure 4-2).
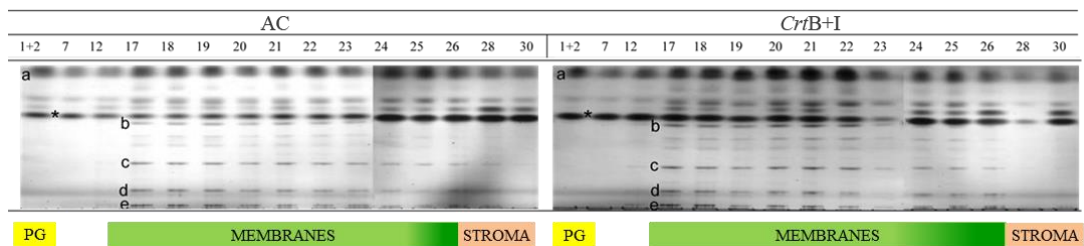
Figure 4-4 Lipid profiles in the sub-chromoplast fractions of AC and *Crt*B+I

Lipids derived from the fractions were separated in a TLC silica plate with a mixture of acetone:toluene:water (91:30:7). Standards for lipid species were used for identification: a, triglycerides b, monogalactodiacylglycerol; c, digalactodiacylglycerol; d, phosphatidylethanolamine; e. phophatidylserine / phosphatidylcholine; *, contaminant. Colour scheme represents the different sub-chromoplast components. PG, plastoglobules. Dark green corresponds to the envelope membrane location.

4.2.3 Cellular characterisation of AC and *Crt*B+I sub-chromoplast fractions

Structural differences of the sub-chromoplast components between AC and *Crt*B+I were investigated. Electron microscopy was used to visualise the structures fractionated through the gradient (Figure 4-5). Plastoglobule structures were found in F1 and F2 of both the wild type and the *Crt*B+I line. Membranous structures with varying degrees of complexity and aggregation were seen in F16, F18 to F22, and F24, although, clear vesicle-like structures predominated in these fractions. The structures varied in the thickness of the membrane, as judged by the intensity of staining and membrane size, with some vesicles embedded in larger membrane structures (ca. 2-fold larger). In addition, some vesicles appeared to retain plastoglobules and/or dense staining amorphous material associated with these membranes. The different electron density level throughout the membranes suggests a variability of the carotenoids, and/or lipoproteins of the membrane. The contents of fractions lower in the gradient (e.g. F24) appeared to be enriched with larger vesicles, containing electron dense material.
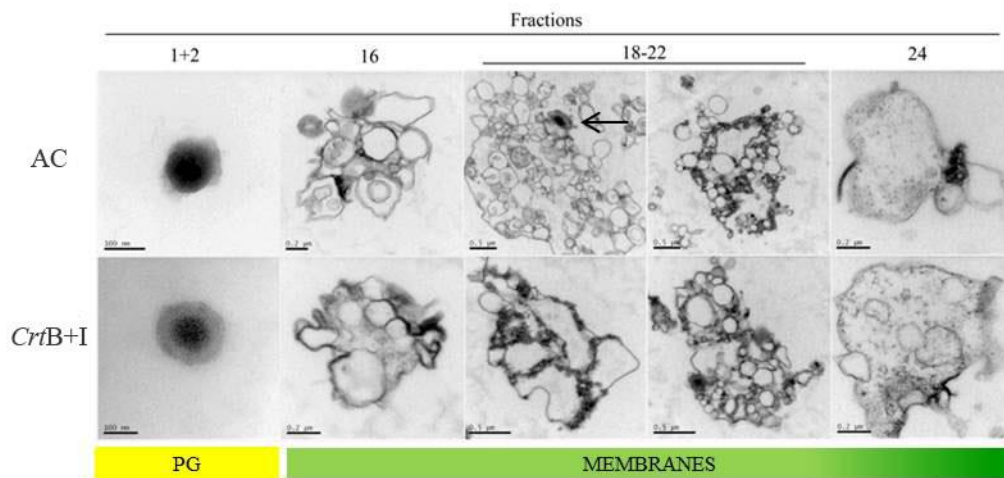
Figure 4-5 Ultrastructure of the sub-chromoplast fractions of AC and *Crt*B+I

After collection, the fractions (1+2, fraction 1 and 2 pooled together; 16, fraction 16; 18-22, fractions 18 to 22 pooled together; 24, fraction 24) were dialysed against phosphate buffer, fixed in osmium tetroxide and visualised by TEM. Colour scheme represents the different sub-chromoplast components. PG, plastoglobules. Dark green corresponds to the envelope membrane location. The arrow shows a plastoglobule. The bar scale represent 100 nm for F1+2 pictures, 0.2 μm for F16 and F24, and 0.5 μm for F18-22.

4.2.4 Localisation of the endogenous and heterologous enzymes within the sub-chromoplast fractions

The localisation of the heterologous enzymes (CRTB and CRTI) within the sub-chromoplast fractions was studied in comparison with the location of the endogenous phytoene synthase (PSY-1) in order to give an insight into spatial and biosynthetic aspects of the carotenoid pathway. Immuno detection of these enzymes (CRTB, CRTI and PSY-1) was performed using specific antibodies (Figure 4-6). As expected, CRTB and CRTI were only found in the *Crt*B+I line. They appeared to be strongly associated with the thylakoid-related fractions and mainly in the sub-membrane compartment II. However, PSY-1 was observed mainly in the stroma of both the control and *Crt*B+I lines as showing in Figure 4-6.

Figure 4-6 Phytoene synthase and desaturase enzymes localised within the sub-chromoplast fraction of AC and *Crt*B+I

CRTB, heterologous phytoene synthase enzyme (38 kDa); CRTI, heterologous phytoene desaturase enzyme (56 kDa); PSY-1, endogenous phytoene synthase enzyme (35 kDa). Specific antibodies were used for the immuno detection of these enzymes in each fraction collected. The coloured bars at the bottom of the figure display a scheme that represents the different sub-chromoplast components. Yellow indicates the plastoglobules; green corresponds to the membranes and dark green the envelope membrane; orange displays the stroma.

4.2.5 Carotenoid crystals are located within the chromoplast membranes

An experiment was performed to ascertain if the carotenoid crystals, visualised in the sub-membrane compartment I and II of the *Crt*B+I gradient, are actually attached/embedded into the membrane (Figure 4-7).

Light microscopy of the sub-chromoplast components before separation on sucrose gradient (section 2.7.1 and Figure A2-4) showed crystals embedded in membranous-like structures (Figure 4-7, a). Similar pictures were obtained when observing the fractions containing crystal-like structures (in sub-compartment I and II) in the sucrose gradient after separation (Figure 4-7, b).

A different fractionation protocol was also used (system 2, section 2.7.2 and Figure A2-4). The sub-compartments of the chromoplasts were first separated in a 0.6 M sucrose step. At the top of the gradient, a large red area was observed after centrifugation (and collected in microcentrifuge tubes), while the membranes pelleted at the bottom of the gradient. The membranes were then separated in the system 1 gradient. No crystals were observed in the sub-membrane compartment I and II (Figure 4-7). However, membrane-free crystals were observed by light microscopy when analysing the red sector obtained in the first step gradient of the system 2 (Figure 4-7, c). It seems that when using system 2, the crystals separate from the membrane. Therefore, it appears that the carotenoid crystals are normally attached/embedded into the membrane, but can be separated during the fractionation.
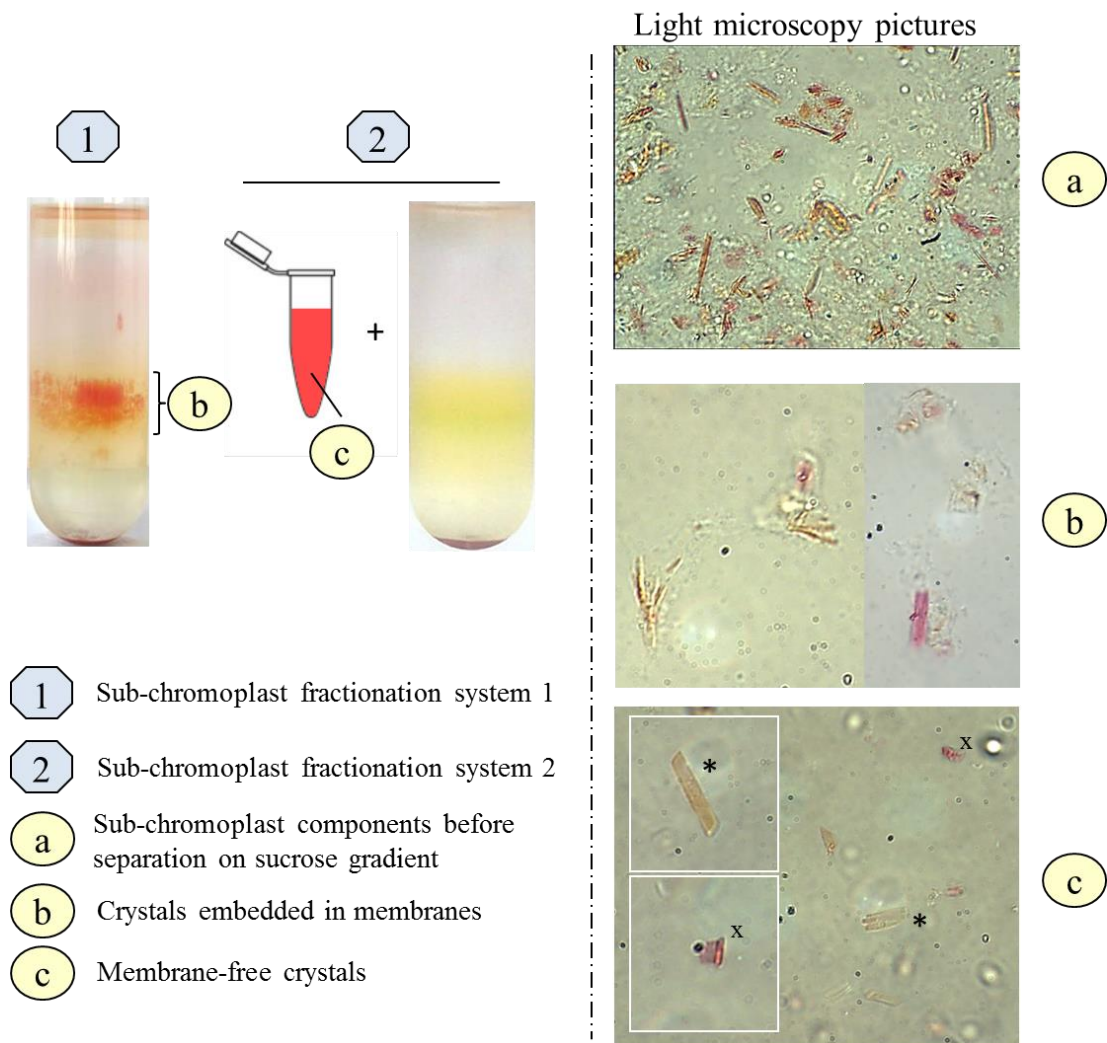
Figure 4-7 Evidence of the carotenoids crystals embedded in the chromoplast membranes

The sub-compartments of *Crt*B+I chromoplasts were separated on a discontinuous sucrose gradient in system 1(picture tube 1; section 2.7.1 and Figure A2-4). In system 2 (described in section 2.7.2 and Figure A2-4), before separation on the same sucrose gradient, the chromoplast sub-compartments were spun in a 0.6 M sucrose solution. A red sector was created at the top of the gradient (tube not showed here) and collected in microcentrifuge tubes (represented) while the chromoplast membranes pelleted. Only the membranes were separated on the second gradient (picture tube 2). For both experiments, 150 g of breaker + 3 to 5 days tomatoes were used. Light microscopy photographs were taken at magnification 600X. x, membrane free red crystal (possibly lycopene crystal); *, membrane free orange crystal (possibly β-carotene crystal).

4.3 Discussion

4.3.1 Separation and characterisation of sub-chromoplast compartments

Chromoplast components were separated and analysed (Figure 4-1) to determine where carotenoids were sequestrated within AC and *Crt*B+I chromoplasts. SDS-PAGE and subsequent Western blot analysis of sub-plastid fractions, using key biomarker proteins of known sub-plastid location, were performed to identify the different compartments of the chromoplasts (Figure 4-2). The discontinuous sucrose gradient resulted in a broad and partially overlapping area of biomarker proteins. The plastoglobule fractions were found at the top of the gradient (F 1&2). However, the plastoglobule biomarker protein PGL also appeared in the thylakoid membrane fractions (F16/17 to F26). This correlates with the fact that plastoglobules arise from thylakoid membrane at areas of high curvature by a membrane-blistering mechanism. Then, they remain physically coupled to the thylakoids throughout their life span (Austin et al., 2006). In this study, tomatoes at the breaker + 3 to 5 days ripening stage were used. During chromoplast biogenesis, structural changes occur, such as the degradation of thylakoid membranes (Spurr and Harris, 1968) and the increase in size and number of plastoglobules (Harris and Spurr, 1969a). At the ripening stage studied, thylakoid membranes are expected to be in the process of disintegration and consequently plastoglobules are then found in a membrane-free form. The plastoglobule fractions (F1&2) correspond to the membrane-free plastoglobules. Thylakoid membranes were still present in the chromoplasts studied because the PSBA thylakoid biomarker protein was detected. This was confirmed with the TEM pictures (Figure 4-5), where membranous structures were visualised. Occasionally, plastoglobules were also found attached to these membranes (Figure 4-5, arrow), which validates the presence of the PGL biomarker protein in the membrane fractions, especially in *Crt*B+I. The greater intensity of the thylakoid biomarker protein in the *Crt*B+I immuno-blots suggests that the *Crt*B+I chromoplasts contained more thylakoid membranes than AC chromoplasts. The thylakoid membranes and envelope membranes were not separated in the sucrose gradient, as the envelope biomarker protein TIC was found at the bottom of the thylakoid membranes fractions area in *Crt*B+I. Although most of the biomarker proteins were detected in similar location in AC and *Crt*B+I gradients, it was not the case for TIC (inner envelope marker). In AC, the TIC protein was found at the

bottom of the thylakoid fractions, but mainly in what corresponds to stromal fractions (F28-30). The shift of location of the TIC protein in AC and *Crt*B+I gradients reveals a difference in the envelope density and therefore structure in the chromoplasts of these two lines. The other envelope biomarker protein, TOC (from the outer envelope), was not detected in AC and *Crt*B+I chromoplasts sub-compartments which correlates with previous study showing that the TOC75 protein is lost during the chloroplast to chromoplast conversion (Barsan et al., 2010). The TOC and TIC proteins were detected in the samples derived from the fractionation of chloroplasts by sucrose density centrifugation (Enfissi et al. unpublished). The localisation of the envelope was different in the chloroplast gradient compared to the chromoplast. That correlates with the changes occurring within the envelope during the ripening process.

The identification of the different sub-chromoplast compartments of AC and *Crt*B+I also revealed qualitative differences of plastoglobules and thylakoid membranes and structural differences of the envelope between AC and *Crt*B+I. This finding correlates with the description of AC and *Crt*B+I chromoplasts ultrastructure in Chapter III, Figure 3-6, where more membranes linked with plastoglobules were visualised in *Crt*B+I chromoplasts.

4.3.2 Sequestration of carotenoids and enzymes in the sub-compartments of AC and *Crt*B+I chromoplasts

The majority of studies quantifying carotenoid levels in tomato plants are completed at a fruit tissue level (Fraser et al., 2009; Enfissi et al., 2010) or chromoplast level (Camara et al., 1983; Angaman et al., 2012). However, understanding the dynamic nature of the carotenoid pathway at a sub-chromoplast level seems crucial to improve predictive metabolic engineering of this complex pathway as it was suggested in recent carotenoid reviews (Cazzonelli and Pogson, 2010; Shumskaya and Wurtzela, 2013). In this study, the analysis of the sequestration of carotenoid metabolites and enzymes in AC and *Crt*B+I sub-chromoplast compartments was undertaken.

The isoprenoids studied were sequestrated mainly in the membranes (thylakoid and envelope) but also in the plastoglobules (Figure 4-3). The profile of percentage of metabolite per fraction along the gradient was different in CrtB+I, compared to the profile in AC. While in the thylakoid membrane of AC there was only one main peak of isoprenoid accumulation (for lycopene, β-carotene, lutein and α-tocopherol) at the sub-membrane compartment I (F16 to F21), there was a supplementary peak at the sub-membrane compartment II (F21 to F26) in CrtB+I. No differences were found in the protein and lipid profiles of these two sub-membrane compartments (Figure 4-2 and 4-4). They both corresponded to the location of crystal-like structures in the CrtB+I sucrose gradient (Figure 4-1). The only variance found was that the sub-membrane compartment II contained a greater ratio of β-carotene to lycopene compared to compartment I. The main characteristic of the CrtB+I tomatoes used for this experiment is an increased level of β-carotene compared to AC. So, a greater content of β-carotene in the sub-membrane compartment II seems plausible. It may be that the two groups of crystals (at the sub-membrane compartment I and II) are separated in the sucrose gradient due to their different composition in carotenoid crystals and that they are then responsible for the differentiation between the two sub-membrane compartments. Carotenoid crystals have been shown to be embedded into the membranes (Figure 4-7). In other studies, carotenoid crystals are found enclosed in a membrane (Simkin et al., 2007), which correlates with this finding. This supports the hypothesis of the crystals being the cause of the distinction between the two sub-membrane compartments in the thylakoid membranes. The question that arises is: Why a similar type of membrane accumulates different proportions of carotenoid crystals? One possibility is that it is the way the crystal forms in the membrane and how the thylakoid membranes break during the centrifugation. During the formation of the lycopene crystal, lycopene seems to predominate in long areas of the thylakoid membrane (Figure 4-8). It is difficult to imagine β-carotene crystals forming within lycopene crystals. Consequently, β-carotene crystals are plausibly formed in other parts of the thylakoid membranes which are lycopene crystal-free. It is possible that lycopene and β-carotene crystals have different densities. So, that could result in the fractionation of the thylakoid membranes during the centrifugation separating thylakoid membranes with different percentages of lycopene and β-carotene.

158
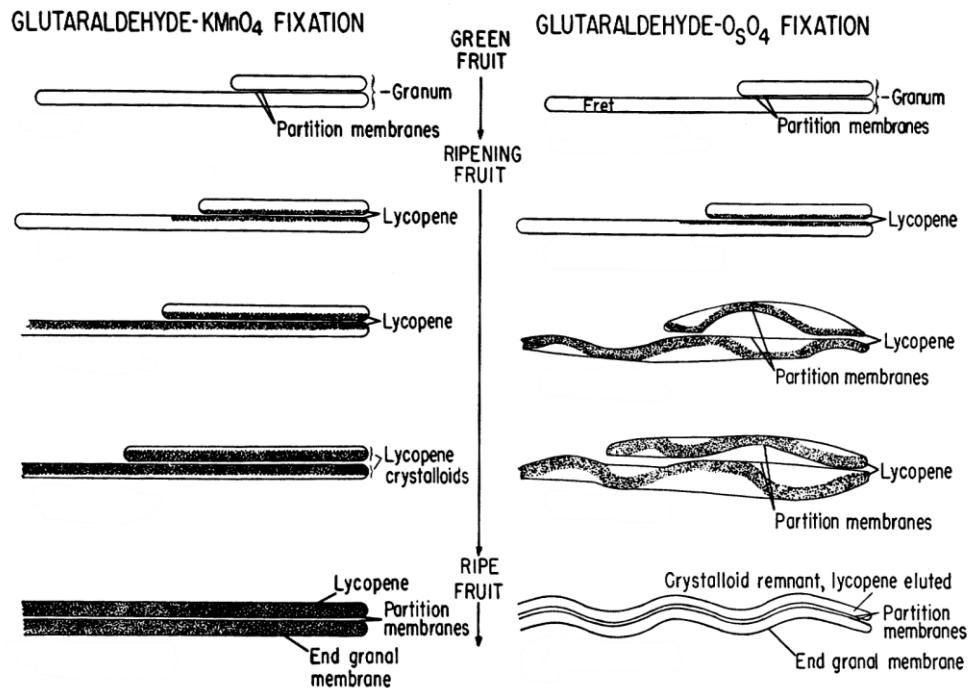
Figure 4-8 Diagrammatic interpretation of lycopene crystalloid development as revealed with two different fixatives (glutaraldehyde -$KMnO_4$ or -O_SO_4). Adapted from Harris and Spurr, (1969a).

These diagrams are based on electron micrographs observed in Harris and Spurr, (1969a). Lycopene often first appears with the partition and then spreads throughout the thylakoid membrane. After O_SO_4 fixation, the lycopene crystalloids appear as undulating dark lines (visible in TEM of AC chromoplasts; Figure 3-6); with $KMnO_4$, they appear relatively straight. As lycopene continues to increase in the thylakoids, the pigment crystalloids and the associated membranes increase in length. Individual crystalloids lamellae can join to form a multiple crystalloids.

In AC, the lutein profile had an extra peak, located at the end of the subcompartment II (Fractions 24 to 26; Figure 4-3). That could correspond to lutein stored in the envelope membrane. Lutein has been previously reported in the chloroplast envelope membrane (Block et al., 1983), so it is plausible to find it as well in the chromoplast envelope membrane. The reason why a similar peak was not present in *Crt*B+I is unclear, especially as the presence of the *Crt*I gene increases lutein. Perhaps, the lutein derived from the presence of *Crt*I is sequestered in a different sub-plastidial environment away from the endogenous pool. Phytoene and phytofluene had

159

atypical profiles, compared to the other isoprenoids studied, due to a high percentage of these metabolites in the plastoglobules. Phytoene has also been detected in plastoglobules of *Arabidopsis thaliana* (Lundquist et al., 2013). In the *Crt*B+I gradient, the percentage of these carotenoids in the plastoglobules decreases considerably (1.7- to 2.5-fold decrease). *Crt*B+I line contains significantly less phytoene and phytofluene (1.6- to 3-fold decrease), compared to AC. This decreased content seems to mainly have an impact on the sequestration of phytoene and phytofluene in the plastoglobules. It suggests that either less phytoene and phytofluene were stored in the plastoglobules because they were utilised in the up-regulated carotenoid pathway in *Crt*B+I, or that the pool of phytoene and phytofluene in the plastoglobules has been required for the biosynthesis of the carotenoid pathway, which was also up-regulated due to the presence of the CRTB and CRTI enzymes. The isoprenoids studied were almost not detected in the stromal fractions, suggesting that they are not part of soluble protein complexes.

The localisation of carotenoid pathway enzymes has been mainly based on proteomics studies. Enzyme location varies a lot depending on the plant species and the type of organelle studied (Ytterberg et al., 2006; Joyard et al., 2009; Wang et al., 2013). The localisations also seem to change during the chloroplast to chromoplast conversion (Shumskaya and Wurtzela, 2013). Therefore, enzyme location within the plastid is very inconsistent in the literature and this is why it is important to do the specific localisation studies of the carotenoid enzymes within the chromoplasts of tomato. The heterologous enzymes phytoene synthase (CRTB) and phytoene desaturase (CRTI) have been found in the same location which is in the (thylakoid) membranes of the *Crt*B+I chromoplast (Figure 4-6). This finding correlates with a previous study which describes CRTI as a membrane-peripheral FAD-dependent oxidase/isomerase (Fraser et al., 1992; Schaub et al., 2012). It strengthens as well the hypothesis that the enzymes can interact with each other (as a metabolon) and have a synergistic effect on the carotenoid production. However, the endogenous phytoene synthase (PSY-1) enzyme was mainly located in the stroma of AC and *Crt*B+I. This correlates with results found in the literature (Fraser et al., 1994; Fraser et al., 2002). These results bring to light the interesting aspect that CRTB and PSY-1 are not found in the same sub-chromoplast compartments, although they catalyse the same step in the carotenoid pathway. A previous study reported an altered sub-organelle

localisation of PSY enzymes only due to the variation of one amino acid in the sequence (Shumskaya et al., 2012). The phytoene synthase enzymes described in this chapter have more than one amino acid differences since they belong to two diverse sources (appendix Figure A4-1), so it seems conceivable that their localisations within the chromoplast vary. An alternative is that, upon over-expression, enzymes do not necessarily reside in their normal endogenous position. Moreover, CRTB and PSY-1 are not in the sub-chromoplast compartment sequestrating the highest content of their product phytoene and CRTI is not present in the same compartment as its precursor. Consequently, what could be thought as an inefficient process for carotenoid biosynthesis could actually represent a novel means of regulation. These data also reveal the importance of signaling and transporters within the chromoplasts. This aspect will be further discussed in the general discussion Chapter VII.

4.3.3 Identification of carotenoid sequestration mechanisms

The *Crt*B+I line has increased carotenoid levels compared to AC. In this study, investigations were focused on the differences between *Crt*B+I and its control at the sub-chromoplast level. The assessments made led to the identification of carotenoid sequestration mechanisms.

A comparison between subcompartments of the fruit chromoplasts from control and *Crt*B+I lines showed a number of important differences. Firstly, an increased number of β-carotene and lycopene crystal-like structures arose in the thylakoid-like membrane fractions of the *Crt*B+I line (Figure 4-1 and 4-3). Storage of endogenous carotenoid in crystal-like structures has been reported in other plant species such as mango (Vasquez-Caicedo et al., 2006) and red papaya (Schweiggert et al., 2011), as well as in tomato (Rosso, 1967, 1968). It seems that this sequestration mechanism has been positively regulated in the transgenic line containing an excess of carotenoid. This phenomenon has also been reported in *Arabidopsis* and carrot roots (Maass et al., 2009) and embryogenic calli from citrus (Cao et al., 2012), overexpressing the phytoene synthase gene. Altogether, the data shown in this chapter, plus the images of AC and *Crt*B+I chromoplasts (Figure 3-6), indicate that membranes of the chromoplast (envelope and thylakoid-like membrane) also appear

to play an important role in carotenoid sequestration. The inner envelope of the *Crt*B+I chromoplasts seemed to be actively producing vesicles (membranous sacs), which were visible in the electromicrographs of the *Crt*B+I chromoplasts (Figure 3-6). The thylakoid-like membranes appeared in greater quantity and electron density in the *Crt*B+I chromoplasts, compared to those in AC (Figure 3-6, Figure 4-2 and Figure 4-5). The darker and thicker membranes could be caused by a high number of lipids, proteins and carotenoids. A previous study had highlighted similar characteristics of the chromoplast compartments of the tomato high β-mutant (Harris and Spurr, 1969b). They described invagination of the internal membrane of the plastid envelope and a swollen grana and intergrana lamaella. Finally, the presence of phytoene at a high level in the plastoglobules (Figure 4-3) shows that a significant quantity of the substrate for phytoene desaturase (and carotene formation) is partitioned away from the enzyme. Collectively these data suggest that sub-plastidial compartmentalisation of precursors and enzymes represent a new regulatory mechanism for the carotenoid pathway.

The study of transgenic lines with modest carotenoid changes (2- to 3-fold increase compared to the control) allowed the identification of several carotenoid sequestration processes, which respond to the elevated content of carotenoids. A comparable study of a transgenic line with a large increase of carotenoid content may not help further our understanding of the sub-plastidic location of carotenoids and their enzymes, since such increases would be too disruptive. The separation of the sub-chromoplast compartments on a sucrose gradient, together with immuno-detection of proteins and chromatographic analysis of carotenoids give a more accurate view of the localisation of the constituents of the carotenoid pathway within the chromoplast, compared to the studies of proteins which have been fused to reporter like GFP and consequently modified (Shumskaya et al., 2012).

Chapter V: Evaluation of a *Solanum galapagense* promoter to regulate the expression of bacterial carotenoid genes in *Solanum lycopersicum*

5.1 Introduction

In the search for potential strategies to increase carotenoid levels in plants, tomato plants coordinately overexpressing bacterial carotenoid genes, *Crt*B and *Crt*I, were studied and described in Chapters III and IV. These two genes were under the control of the polygalacturonase ripening specific promoter (PG) and the CaMV 35S constitutive promoter (35S), respectively. The PG promoter was chosen since tomato plants overexpressing the *Crt*B gene or other phytoene synthases under the control of 35S showed pleiotropic effects (Fray et al., 1995). Polygalacturonase is a major cell wall polyuronide degrading enzyme of tomato fruit (Gray et al., 1992), which is synthesised *de novo* at the onset of ripening (Tucker and Grierson, 1982), but the highest activity of this enzyme is at a late stage in the ripening process (Nicholass et al., 1995). The hypothesis is that an earlier ripening stage promoter may have a greater impact on carotenoid levels when controlling the expression of *Crt*B. The focus of the work in this chapter is to investigate the effect of timing of expression of carotenoid genes on carotenoid production in plants. The lycopene β-cyclase (*Cyc-B*) promoter (pb) from the orange fruited *Solanum galapagense* was chosen for further investigation on the basis of two criteria. Firstly, the pb promoter is an early fruit ripening stage promoter (Enfissi et al., unpublished; Heldt et al., unpublished). Secondly, the transcript levels of *Cyc-B* are 100 times greater in *S. galapagense* compared to *S. lycopersicum* (Enfissi et al. unpublished), which is the tomato species used in all the studies in this thesis. Here, the generation and characterisation of three new transgenic tomato lines pb-*Crt*B, pb-*Crt*I and pb-*Crt*B+I in *S. lycopersicum* is reported. The carotenoid contents of the T_0 and T_1 generation of tomato plants were analysed and the pb promoter was further characterised.

5.2 Results

5.2.1 Construction of vectors and generation of transgenic tomato plants

Vectors harbouring the *Crt*B gene and *Crt*I, solely or in combination, with the lycopene β-cyclase promoter (pb) were constructed from vectors kindly provided by Dr N. Misawa (Ishikawa Prefectural University, Japan), which were 35S-*Crt*B (CrtB*) and 35S-*Crt*I (CrtI*) (described in appendix Figure A2-1). All these vectors

carried the alcohol dehydrogenase 5′ untranslated region of *Nicotiana tabacum*, the RuBisCO small subunit transit peptide of *Pisum sativum* L., the heat shock protein 18.2 gene terminator of *Arabidospsis thaliana* and the nopaline synthase gene terminator of *Agrobacterium tumefaciens* (Figure 5-1). In order to create the new vectors, the 35S promoters of the 35S-*Crt*B and 35S-*Crt*I vectors were replaced with the pb promoter and then the sequence of interest of the newly constructed pb-*Crt*B vector was cut (using AscI and PacI restriction enzymes) and pasted into the newly constructed pb-*Crt*I vectors to form pb-*Crt*B+I (=pb-*Crt*B+pb*Crt*I) as illustrated in Figure 5-1. The sequence of the pb promoter and the primers used to create these vectors are described in Figure A5-1 (appendices) and Table A2-2. The sequences of interest were then inserted in pBINplus binary vector (Vanengelen et al., 1995) between the left and right T-DNA borders, using the AscI and EcoRI restriction enzymes. For the pb-*Crt*B+I vector, a partial digestion was necessary in order to get the whole B+I fragment.

pb-*Crt*B:
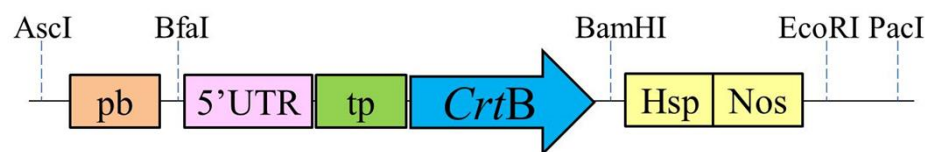
pb-*Crt*I:
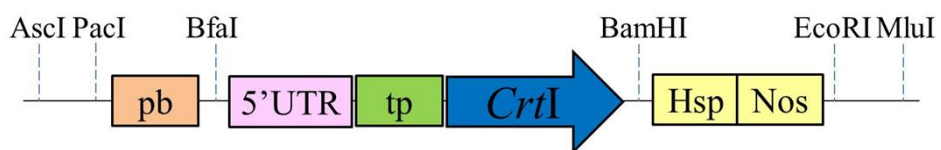
pb-*Crt*B+I:
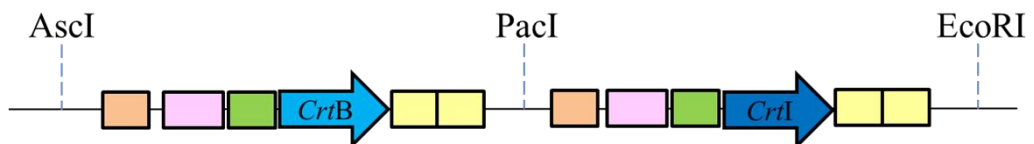
Figure 5-1 Structure of the pb-*Crt*B, pb-*Crt*I and pb-*Crt*B+I constructs containing the lycopene β-cyclase promoter from *Solanum galapagense*

Locations of the restriction sites are shown by the blue dashed line. pb, lycopene β-cyclase promoter from *Solanum galapagense*; 5′ UTR, untranslated region of *Nicotiana tabacum* alcohol dehydrogenase; tp, transit peptide of the *Pisum sativum* L. RuBisCO small subunit; Hsp, terminator of

the *Arabidospsis thaliana* heat shock protein 18.2 gene; Nos, terminator of nopaline synthase gene from *Agrobacterium tumefaciens*.

The vectors were then sent to the transformation facility at UC Davis (Plant transformation Facility, 192 Robbins Hall, University of California Davis, CA 95616, USA), where the transformations of cv. Ailsa Craig tomato plants (*S. lycopersicum*) with the three pb-*Crt* vectors were performed. Eleven transgenic seedlings per pb-*Crt* line were received and transferred into soil following an acclimation protocol (described in section 2.1.1). However, two plantlets of each of pb-*Crt*I and pb-*Crt*B+I lines did not survive.

5.2.2 Analysis of the transgenic primary (T$_0$) generation

5.2.2.1 Characterisation of T$_0$ plants

The presence of the *Crt*B and *Crt*I genes was verified by PCR (section 2.3.6.2 and primers are described in Table A2-2), in young tomato plants (30 cm high), to confirm that the transgenic lines corresponded to their predicted genotype (Figure 5-2). No escapes were found. Moreover, the absence of the *Crt*B gene was verified in the pb-*Crt*I plants and the absence of *Crt*I in the pb-*Crt*B lines was verified to confirm that no contamination had occurred. The results were all negative (data not shown).
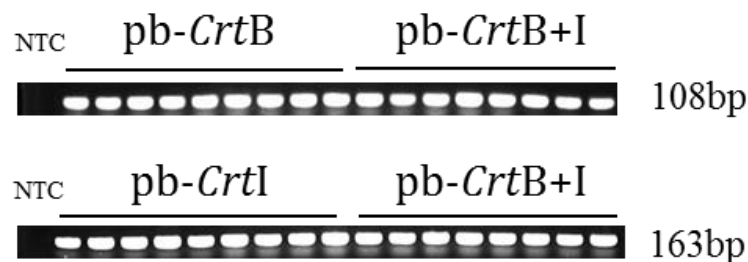
Figure 5-2 PCR confirmation of the presence of *Crt*B and *Crt*I genes in the pb-*Crt* transgenic lines

Amplication of the genes *Crt*B (108bp) and *Crt*I (163bp) was performed by PCR on all pb-*Crt*B, pb-*Crt*I and pb-*Crt*B+I transgenic plants and visualised under UV light. DNA was extracted from a pool of 4 representative leaves of each line. NTC: non template control.

The number of inserts for each plant of the three pb-*Crt* lines was determined by Southern blot, using *Crt*B and *Crt*I probes (method is described in section 2.3.8.1). First, the probes were created and tested (*Crt*B, 108bp; *Crt*I, 163bp), the DNA from all the transgenic plants was extracted and then southern blots were performed using the DNA cut by the EcoRI restriction enzyme. The resulting autoradiograms, obtained from the Southern blot, displayed band(s) of different sizes. The number of bands corresponded to the number of *Crt* gene inserts in the transgenic plant. The autoradiogram obtained for the determination of the number of inserts in pb-*Crt*I plants using the *Crt*I probe is shown in Figure 5-3. There is only one plant (n°5) harbouring one *Crt*I insert; and plants n°1 & 2 have two inserts. All the other pb-*Crt*I plants have a high number (>4) of *Crt*I inserts (Figure 5-3).
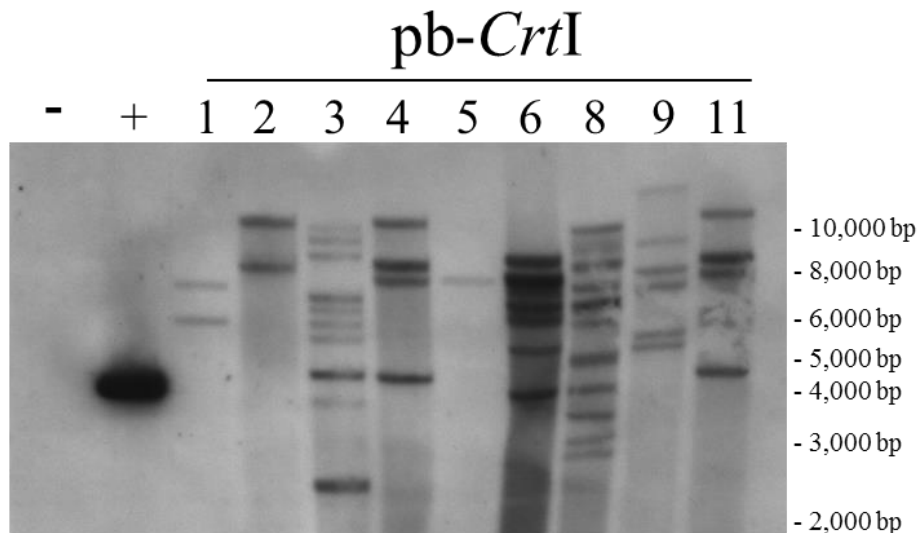
Figure 5-3 Autoradiograms of Southern blot obtained from DNA of pb-*Crt*I lines digested by EcoRI and hybridised to *Crt*I probes

Numbers correspond to the different pb-*Crt*I plants.-, negative control (DNA from the AC control); +, positive control (DNA from the plasmid *Crt*I).

The *Crt*B probe was utilised for the determination of the number of inserts in pb-*Crt*B and pb-*Crt*B+I plants. Overall, an unexpectedly high number of inserts was found in some of the pb-*Crt* transgenic lines (Table 5-1). In order to confirm some of the results found by Southern blot, real-time qPCR was performed to quantify the level of *Crt* genes and therefore determine the number of inserts in each transgenic plant (method is described in section 2.3.8.2). Table 5-1 summarises the number of

inserts found in each plant of the three pb-*Crt* lines using the two distinct methods (Southern blot and qPCR). The qPCR results for the plant tested confirmed most of the Southern blot results (14 from 15).

line	pb-*Crt* B		pb-*Crt* I		pb-*Crt* B+I	
	Southern blot	qPCR	Southern blot	qPCR	Southern blot	qPCR
1	4		2	1 or 2	< 6	
2	6		2	2		
3	6		< 5	6	1	1
4	1	1	4	4	2	2
5	2	2	1	1	< 10	
6	3		< 6	10	6	
7	1	1			< 9	
8	3		10 or 11	10 or 11	1 or 2	2
9	< 2		6	8	4	
10	3					
11	3		6	6	3	

Number of inserts

Table 5-1 Number of *Cr*t inserts in the T_0 pb-*Crt* transgenic lines, analysed by Southern blot and checked by qPCR

The yellow cells represent plants which died at the seedling stage. qPCR analysis was only performed on selected lines using the primers described in Table A2-2. No number means that the number of inserts was not determined by qPCR. Southern blot and qPCR methods are described in section 2.3.8.

5.2.2.2 Isoprenoid profiles of the pb-*Cr*t lines of the T_0 generation

The isoprenoid profiles of the tomato fruits (pericarp) from all the T_0 plants of the three pb-*Crt* lines were analysed in order to select the plants to grow for T_1 generation, depending on their level of carotenoids and α-tocopherol (method is described in section 2.5.3). The contents of isoprenoids in the three different T_0 transgenic lines are displayed Table 5-2 (A-C). The pb-*Crt*B plant n°5 as well as the pb-*Crt*I n°8 and the pb*Crt*B+I n°1 and 11 did not produce fruits, preventing analysis of isoprenoids.

The ten T_0 pb-*Crt*B plants had variable isoprenoid profiles, but common features can be highlighted. Compared to the AC control, the phytoene levels were increased up to 2.3-fold, the phytofluene levels up to 1.6-fold, and the lycopene levels up to 1.5-

fold, while the total carotenoid content increased up to 1.4-fold, depending on the plant (Table 5-2, A). Changes in β-carotene, γ-carotene, lutein and α-tocopherol levels occurred only in a few plants. The selection of the plants to be grown for a T_1 generation was based on the number of inserts and the levels of isoprenoids. The pb-CrtB7 plant was selected as it contained only one insert and the levels of isoprenoids were the highest.

Although the eight T_0 pb-CrtI plants had different isoprenoid profiles, the main characteristics of these plants were an increase of phytoene levels, up to 2-fold compared to the control and an increase of phytofluene and lycopene up to 1.5-fold. The total carotenoid content increased from 1.2- to 1.4-fold, compared to AC (Table 5-2, B). The levels of β-carotene are quite variable as they can be lower or greater compared to the control (0.8- to 1.7- fold). Some plants, for example pb-CrtI6, had an increase in β-carotene content, but not of lycopene. Other transformants such as pb-CrtI4 and 9 had a contrasting profile with increased lycopene content but not of β-carotene, while others showed an increase in both carotenoids (for instance, pb-CrtI3 and 5). In certain lines, changes were also observed in γ-carotene, lutein and α-tocopherol. The plant selected, for further investigations, was pb-CrtI2 as it contained only 2 inserts and high levels of phytoene, lycopene and α-tocopherol. Although the pb-CrtI6 plant had multiple inserts (ca.10), it was also sown for the T_1 generation, because its level of β-carotene was the greatest amongst the pb-CrtI plants.

The seven pb-CrtB+I plants were defined by an increased level of phytoene (1.3- to 3.4-fold), phytofluene (1.1- to 2.1-fold), lycopene and γ-carotene (up to 1.6-fold), lutein and α-tocopherol (up to 1.3-fold) and total carotenoid content (1.1- to 1.6-fold), compared to AC (Table 5-2, C). The level of β-carotene varied depending on the plant (0.9- to 2-fold change). There was a positive correlation between the level of β-carotene and the number of CrtB+I inserts in the plants. The plants with one or two inserts had ca. 250 μg/g DW of β-carotene, those with 4 to 6 inserts showed a β-carotene level of ca. 400 μg/g DW and the plants with the greatest number of inserts (ca. 10) had ca. 550 μg/g DW of β-carotene. This correlation was not found for the other isoprenoids.

The pb-*Crt*B+I3 line, which harboured one insert, was selected on the basis of increased phytoene, phytofluene and lycopene contents. The pb-*Crt*B+I6 and 7 plants were also sown, as they had a higher level of phytoene/lycopene and β-carotene, respectively, but did contain more than 6 inserts.

A.

	AC	1	2	3	4	6	7	8	9	10	11
							pb-*Crt* B				
Phytoene	98 ± 2	**186 ± 6*****	**200 ± 1*****	**221 ± 3*****	**183 ± 6*****	**185 ± 3*****	**201 ± 5*****	124 ± 4	**211 ± 2*****	**224 ± 23*****	**167 ± 1*****
Phytofluene	135 ± 2	**190 ± 4*****	**187 ± 1*****	**215 ± 2*****	**187 ± 6*****	**183 ± 3*****	**208 ± 3*****	156 ± 5	**203 ± 2*****	**201 ± 17*****	**177 ± 1****
Lycopene	1412 ± 22	**2026 ± 37*****	**2180 ± 24*****	**2291 ± 23*****	1570 ± 57	**1751 ± 24*****	**2209 ± 29*****	1328 ± 11	**1736 ± 29*****	**2032 ± 43*****	**1847 ± 95*****
β-Carotene	281 ± 3	**229 ± 3****	**242 ± 1***	249 ± 1	302 ± 7	279 ± 2	270 ± 4	313 ± 6	250 ± 1	275 ± 20	264 ± 2
γ-Carotene	76 ± 1	87 ± 4	**95 ± 6****	**93 ± 4***	76 ± 2	**94 ± 4***	**103 ± 1*****	79 ± 2	78 ± 1	83 ± 4	74 ± 1
Lutein	142 ± 1	**155 ± 1***	151 ± 1	152 ± 2	142 ± 3	154 ± 1	148 ± 1	138 ± 1	145 ± 1	148 ± 7	144 ± 1
Total CAR	2143 ± 27	**2874 ± 54*****	**3054 ± 20*****	**3219 ± 32*****	**2459 ± 80***	**2647 ± 35*****	**3139 ± 38*****	2138 ± 21	**2621 ± 28*****	**2963 ± 103****	**2673 ± 99*****
α-Tocopherol	280 ± 6	311 ± 7	304 ± 2	**332 ± 6***	301 ± 10	286 ± 5	305 ± 7	309 ± 11	297 ± 5	296 ± 28	293 ± 1

B.

	AC	1	2	3	4	5	6	9	11
					pb-*Crt* I				
Phytoene	98 ± 2	**184 ± 7*****	**194 ± 5*****	**141 ± 2*****	**161 ± 2*****	90 ± 1	**178 ± 2*****	**166 ± 1*****	**120 ± 1****
Phytofluene	135 ± 2	**189 ± 6*****	**194 ± 4*****	**166 ± 2*****	**166 ± 1*****	**118 ± 1****	**206 ± 2*****	**173 ± 1*****	146 ± 2
Lycopene	1412 ± 22	**1791 ± 60*****	**2116 ± 37*****	**1662 ± 24*****	**2067 ± 21*****	**1848 ± 11*****	1506 ± 3	**1735 ± 17*****	**1746 ± 33*****
β-Carotene	281 ± 3	**231 ± 4*****	**245 ± 4*****	**310 ± 7*****	296 ± 1	**302 ± 1***	**467 ± 3*****	269 ± 2	**245 ± 1*****
γ-Carotene	76 ± 1	74 ± 1	**102 ± 7****	92 ± 1	**126 ± 7*****	87 ± 6	**133 ± 2*****	80 ± 3	73 ± 2
Lutein	142 ± 1	142 ± 3	**154 ± 2****	141 ± 3	147 ± 1	144 ± 1	140 ± 1	**159 ± 1*****	150 ± 1
Total CAR	2143 ± 27	**2610 ± 77*****	**3005 ± 37*****	**2511 ± 39*****	**2964 ± 26*****	**2589 ± 12*****	**2630 ± 10*****	**2581 ± 16*****	**2480 ± 32*****
α-Tocopherol	280 ± 6	258 ± 5	**341 ± 8*****	288 ± 5	**337 ± 3*****	279 ± 3	**246 ± 3***	300 ± 12	**319 ± 8***

C.

	AC	3	4	5	6	7	8	9
				pb-*Crt* B+I				
Phytoene	98 ± 2	**231 ± 1**∗∗∗	**162 ± 1**∗∗∗	**236 ± 2**∗∗∗	**337 ± 3**∗∗∗	**163 ± 1**∗∗∗	**129 ± 4**∗∗∗	**159 ± 2**∗∗∗
Phytofluene	135 ± 2	**213 ± 1**∗∗∗	**175 ± 1**∗∗∗	**243 ± 2**∗∗∗	**287 ± 2**∗∗∗	**179 ± 1**∗∗∗	**154 ± 4**∗∗∗	**166 ± 2**∗∗∗
Lycopene	1412 ± 22	**2036 ± 17**∗∗∗	**2094 ± 45**∗∗∗	1538 ± 38	**2176 ± 12**∗∗∗	**1154 ± 6**∗∗∗	**1779 ± 46**∗∗∗	**1809 ± 19**∗∗∗
β-Carotene	281 ± 3	**226 ± 1**∗∗∗	**257 ± 1**∗∗	**558 ± 3**∗∗∗	**338 ± 1**∗∗∗	**563 ± 3**∗∗∗	280 ± 5	**445 ± 5**∗∗∗
γ-Carotene	76 ± 1	79 ± 1	**88 ± 3**∗∗	**125 ± 1**∗∗∗	**111 ± 2**∗∗∗	**115 ± 1**∗∗∗	77 ± 2	**129 ± 1**∗∗∗
Lutein	142 ± 1	143 ± 1	**168 ± 1**∗∗∗	**137 ± 1**∗	**155 ± 1**∗∗∗	145 ± 1	**148 ± 1**∗∗	**151 ± 1**∗∗∗
Total CAR	2143 ± 27	**2928 ± 20**∗∗∗	**2944 ± 49**∗∗∗	**2836 ± 46**∗∗∗	**3404 ± 16**∗∗∗	**2319 ± 5**∗	**2566 ± 61**∗∗∗	**2859 ± 29**∗∗∗
α-Tocopherol	280 ± 6	271 ± 3	**389 ± 4**∗∗∗	285 ± 8	**331 ± 1**∗∗	**344 ± 10**∗∗∗	310 ± 9	302 ± 6

Table 5-2 Carotenoid and tocopherol contents in the pericarp tissue of all lines of pb-*Crt* transgenic (T_0) tomato plants

A, pb-*Crt*B; B, pb-*Crt*I; C, pb-*Crt*B+I. Tomato used (pericarp) were at breaker + 7 days ripening stage. Isoprenoid contents are presented as µg/g DW. Methods used for this determination are described in section 2.5. Determinations were made from at least three biological replicates and three technical replicates. The mean data are presented with ± SD. Dunnett's test was used to determine significant differences between the wild type background (AC) and the transgenic varieties for each compound. Values in bold indicate where significant differences have been found. P<0.05, P<0.01 and P<0.001 are designated by **∗**, **∗∗,** and **∗∗∗**, respectively. CAR, carotenoid. Numbers represents the different events for each pb-*Crt* variety.

5.2.3 Analysis of transgenic T_1 generation

5.2.3.1 Characterisation of the T_1 pb-*Cr*t plants

The inheritance of the *Crt* gene(s) in the pb-*Crt*B7, pb-*Crt*I2 and pb-*Crt*B+I3 T_1 lines was determined by real-time qPCR (section 2.3.7). Twenty plants were grown from the T_0 seeds and their zygosity analysed in order to select, ideally, three of azygous, hemizygous and homozygous plants. The ratio of azygous, hemizygous and homozygous plants found for each T_1 pb-*Cr*t line are represented in Table 5-3. Mendelian inheritance was expected as 5/10/5 ratio for the lines with one insert and 1/4/6/4/1 for pb-*Crt*I2, which had 2 inserts (Table 5-3). However, when the qPCR results were ambiguous, they were not included and were then classified as "others" (see Table 5-3). Consequently, without having the whole dataset, it is impossible to conclude on a Mendelian inheritance.

	Number of *Crt* copies			
	0 copy	1 copy	2 copies	other*
pb-*Crt* B7	3	2	6	8
pb-*Crt* B+I3	1	12	5	1
Mendelian	5	10	5	

	Number of *Crt* copies				
	0 copy	1 copy	2 copies	3 copies	4 copies	other*
pb-*Crt* I2	6	0	9	2	1	2
Mendelian	1	4	6	4	1	

Table 5-3 Inheritance of the *Crt* genes in the T_1 generation of pb-*Cr*t plants

Twenty plants were screened by line. Other*, plants excluded of the analysis due to ambiguous results. In this table, *Crt*B+I3 (=*Crt*B+*Crt*I) is considered as only one *Crt* copy, not two. Mendelian represents the expected distribution of 20 plants in the case of Mendelian inheritance.

For the pb-*Crt*I2 lines, further investigation was necessary. The pb-*Crt*I2 line harboured two inserts in the T_0 generation, so when two copies of the *Crt*I gene were found in the T_1 generation, it could correspond to two hemizygous inserts, or one homozygous insert, associated with the loss of the second insert. In order to determine the inheritance of the *Crt*I gene in the T_1 pb-*Crt*I2 lines, which contained two copies of the gene, a Southern blot experiment was performed (Figure 5-4). Two

bands were found in all the tested pb-*Crt*I2 lines. Therefore, it was concluded that all the lines were hemizygous for two *Crt*I inserts.
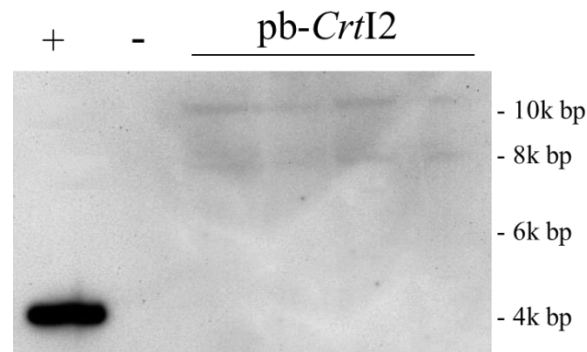
Figure 5-4 Autoradiogram of Southern blot obtained from DNA of pb-*Crt*I2 (T_1) lines with two copies of *Crt*I, digested with EcoRI and hybridised to *Crt*I probes

Multiple pb-*Crt*I2 plants were tested. +, positive control (DNA from the plasmid *Crt*I); -, negative control (DNA from the AC control).

5.2.3.2 Isoprenoid profiles in the pb-*Crt* lines of the T1 generation

5.2.3.2.1 Ripening series in pb-*Crt*I2 and pb-*Crt*B+I3 lines

Profiles of isoprenoids in the pericarp of the transgenic pb-*Crt* T_1 tomato fruits were determined by UPLC (method described in section 2.5.3). The isoprenoid contents in pb-*Crt*I2 and pb-*Crt*B+I3 lines were analysed in 5 developmental and ripening tomato stages (mature green, breaker, breaker + 3 days, breaker + 7 days, breaker + 14 days). Homozygous (2 copies) and double homozygous (4 copies) lines were studied for pb-*Crt*I2 and a hemizygous (1 copy) and homozygous lines (2 copies) for pb-*Crt*B+I3 (Table 5-4).

Mature Green		pb-*Crt* I2		pb-*Crt* B+I3	
	Azygous	Homozygous	Double homozygous	Hemizygous	Homozygous
β-Carotene	149 ± 1	**142 ± 1***	151 ± 1	150 ± 1	144 ± 1
Lutein	171 ± 1	**161 ± 1****	**182 ± 2*****	170 ± 1	**155 ± 1*****
Neo / viola	93 ± 1	**88 ± 1****	**102 ± 1*****	92 ± 1	**83 ± 1*****
Total CAR	412 ± 1	**392 ± 2****	**435 ± 3***	411 ± 2	**382 ± 2*****

Breaker		pb-*Crt* I2		pb-*Crt* B+I3	
	Azygous	Homozygous	Double homozygous	Hemizygous	Homozygous
Phytoene	23 ± 1	**19 ± 1*****	25 ± 1	21 ± 1	21 ± 0
Lycopene	58 ± 1	**62 ± 1***	**73 ± 1*****	60 ± 1	**65 ± 1*****
β-Carotene	154 ± 1	**172 ± 1*****	**171 ± 2*****	**162 ± 1***	**162 ± 2***
γ-Carotene	40 ± 1	42 ± 1	**42 ± 1***	40 ± 1	42 ± 1
Lutein	148 ± 1	**165 ± 1*****	**172 ± 1*****	**161 ± 1*****	152 ± 2
Neo / viola	68 ± 1	**75 ± 1****	71 ± 1	73 ± 1	71 ± 1
Total CAR	492 ± 3	**535 ± 1****	**555 ± 5****	**516 ± 2***	**514 ± 5***
α-Tocopherol	156 ± 2	169 ± 1	**208 ± 2*****	166 ± 1	144 ± 2

Br + 3d		pb-*Crt* I2		pb-*Crt* B+I3	
	Azygous	Homozygous	Double homozygous	Hemizygous	Homozygous
Phytoene	132 ± 3	**95 ± 1*****	**80 ± 1*****	**80 ± 3*****	**88 ± 2*****
Phytofluene	134 ± 1	**110 ± 2*****	**97 ± 1*****	**102 ± 2*****	**109 ± 1*****
Lycopene	655 ± 13	690 ± 13	**431 ± 5*****	**405 ± 9*****	**579 ± 12****
β-Carotene	195 ± 3	**219 ± 1****	204 ± 3	209 ± 1	**213 ± 1***
γ-Carotene	55 ± 1	**59 ± 1***	53 ± 1	54 ± 1	56 ± 1
Lutein	153 ± 2	**168 ± 1*****	161 ± 2	**166 ± 1****	153 ± 1
Total CAR	1324 ± 15	1342 ± 16	**1024 ± 13*****	**1015 ± 12*****	**1198 ± 17****
α-Tocopherol	195 ± 1	**220 ± 1*****	**212 ± 3***	183 ± 2	**178 ± 2***

Br + 7d		pb-*Crt* I2		pb-*Crt* B+I3	
	Azygous	Homozygous	Double homozygous	Hemizygous	Homozygous
Phytoene	315 ± 12	305 ± 27	**165 ± 5*****	262 ± 23	**195 ± 22*****
Phytofluene	251 ± 6	257 ± 21	**158 ± 3****	220 ± 14	**184 ± 17*****
Lycopene	1119 ± 80	**1422 ± 38*****	**749 ± 33*****	1043 ± 67	1200 ± 82
β-Carotene	188 ± 4	**224 ± 13***	207 ± 2	202 ± 8	**244 ± 10*****
γ-Carotene	51 ± 1	**56 ± 2***	49 ± 1	53 ± 2	**61 ± 2*****
Lutein	149 ± 2	**170 ± 7****	156 ± 2	145 ± 2	155 ± 6
Total CAR	2072 ± 87	**2434 ± 68*****	**1484 ± 43*****	1924 ± 91	2039 ± 136
α-Tocopherol	182 ± 8	**276 ± 30*****	202 ± 4	184 ± 6	193 ± 9

Br + 14d		pb-*Crt* I2		pb-*Crt* B+I3	
	Azygous	Homozygous	Double homozygous	Hemizygous	Homozygous
Phytoene	433 ± 9	399 ± 3	-	466 ± 8	**297 ± 2*****
Phytofluene	356 ± 7	338 ± 11	-	381 ± 3	**272 ± 2*****
Lycopene	1729 ± 42	1614 ± 23	-	1772 ± 16	1755 ± 29
β-Carotene	193 ± 3	**255 ± 3*****	-	**224 ± 1****	**226 ± 5*****
γ-Carotene	54 ± 1	**62 ± 1***	-	61 ± 1	**61 ± 2***
Lutein	138 ± 3	**153 ± 2****	-	147 ± 1	142 ± 2
Total CAR	2905 ± 64	2820 ± 40	-	3053 ± 15	2752 ± 37
α-Tocopherol	244 ± 1	**336 ± 1*****	-	223 ± 6	226 ± 12

Table 5-4 Carotenoid and α-tocopherol contents in pb-*Crt*I2 and pb-*Crt*B+I3 lines of T$_1$ generation during fruit developmental and ripening stages

Isoprenoid contents are presented as µg/g DW. Methods used for this determination are described in the section 2.5. Determinations were made from at least three biological replicates and three technical replicates. The mean data are presented with ± SD. Dunnett's test was used to determine significant differences between the control (azygous) and the transgenic lines for each compound. Values in bold indicate where significant differences have been found. P<0.05, P<0.01 and P<0.001 are designated by *, **, and ***, respectively. CAR, carotenoid; Neo / viola, neoxanthin and violaxanthin; -, not determined; MG, mature green; Br; breaker; Br+3d; breaker + 3 days; Br+7d; breaker + 7 days; Br+14d; breaker + 14 days.

Contents of isoprenoids varied depending on the line and the developmental stage of the tomato fruit. At the mature green stage, only the pb-*Crt*I2 double homozygous line had significant increases in some isoprenoids (lutein, neoxanthin and violaxanthin; 1.1-fold) compared to the azygous line. Both pb-*Crt*I2 and pb-*Crt*B+I3 homozygous lines had decreased carotenoids levels and in the pb-*Crt*B+I3 hemizygous line there was no significant change. At breaker stage, the pb-*Crt*I2 lines had significantly increased levels of most carotenoids levels (lycopene, β-carotene, lutein, total carotenoids, by 1.1- to 1.3-fold). In the pb-*Crt*B+I3 lines, β-carotene and total carotenoids levels were significantly increased in both lines (1.1-fold increase). At breaker + 3 days stage, the phytoene and phytofluene levels significantly decreased in all the lines studied, as well as lycopene levels except in the pb-*Crt*I2 homozygous, where the lycopene level remained unchanged. The β-carotene and α-tocopherol levels were significantly increased in the homozygous lines (1.1-fold increase). The pb-*Crt*I2 line also had significant increase of γ-carotene and lutein levels, but no change in the total carotenoids. At breaker + 7 days stage, levels of phytoene and phytofluene in pb-*Crt*I2 homozygous and pb-*Crt*B+I3 hemizygous lines were similar to the ones in the azygous line. In the other studied lines, the levels were significantly decreased. All the other isoprenoids measured in pb-*Crt*I2 homozygous were significantly increased (1.1- to 1.3-fold). The levels of β-carotene and γ-carotene were also significantly increased in pb-*Crt*B+I3 homozygous line compared to azygous. The pb-*Crt*B+I3 hemizygous showed no change in any of the isoprenoids studied. At breaker + 14 days stage, levels of phytoene and phytofluene were still unchanged in the pb-*Crt*I2 homozygous and pb-*Crt*B+I3 hemizygous lines and decreased in the pb-*Crt*B+I3 homozygous line. Moreover, as in the breaker + 7d stage, the other isoprenoids studied in pb-*Crt*I2 homozygous lines were all significantly increased (1.1- to 1.4-fold), except for the total carotenoids content

176

which did not vary compared to azygous. The pb-*Crt*B+I3 lines had an increased content of β-carotene (1.2-fold). Changes through fruit development and ripening in all the pb-*Crt*I2 and pb-*Crt*B+I3 lines are shown in Figure 5-5.

Changes in pb-*Crt*I2 homozygous

	MG	Breaker	Br+3	Br+7	Br+14
Phytoene					
Phytofluene					
Lycopene					
β-Carotene					
γ-Carotene					
Lutein					
Neo / viola					
Total CAR					
α-Tocopherol					

Changes in pb-*Crt*I2 double homozygous

	MG	Breaker	Br+3	Br+7	Br+14
Phytoene					-
Phytofluene					-
Lycopene					-
β-Carotene					-
γ-Carotene					-
Lutein					-
Neo / viola					-
Total CAR					-
α-Tocopherol					-

Changes in pb-*Crt*B+I3 hemizygous

	MG	Breaker	Br+3	Br+7	Br+14
Phytoene					
Phytofluene					
Lycopene					
β-Carotene					
γ-Carotene					
Lutein					
Neo / viola					
Total CAR					
α-Tocopherol					

Changes in pb-*Crt*B+I3 homozygous

	MG	Breaker	Br+3	Br+7	Br+14
Phytoene					
Phytofluene					
Lycopene					
β-Carotene					
γ-Carotene					
Lutein					
Neo / viola					
Total CAR					
α-Tocopherol					

Compared to azygous:

- No change
- Increased level
- Decreased level
- Not detected
- Not determined

Figure 5-5 Schematic representations of changes of isoprenoid contents in pb-*Crt*I2 and B+I3 T$_1$ lines during fruit developmental and ripening stages

Changes of isoprenoids content in the pb-*Crt* lines were calculated compared to the azygous control from the values showed in Figure 5-4. Significant changes (detailed in Table 5-4) are represented by the colour code described in this figure. CAR, carotenoid; Neo / viola, neoxanthin and violaxanthin; MG, mature green; Br; breaker; Br+3d; breaker + 3 days; Br+7d; breaker + 7 days; Br+14d; breaker + 14 days.

The pb-*Crt*I2 homozygous lines showed changes in all the different stages compared to the azygous. Increased levels of carotenoids were found from the breaker stage onwards for γ-carotene and lutein. For β-carotene and α-tocopherol, increased levels only occurred from the breaker + 3 days stage, and they too remained constant. For the pb-*Crt*I2 double homozygous, increased level of isoprenoids were mainly

observed at the mature green and breaker stages. Afterwards, isoprenoid levels (i.e. phytoene, phytofluene and lycopene) were either unchanged or decreased. The hemizygous pb-*Crt*B+I3 showed fewer changes and it was mainly at breaker and breaker + 3 days stages. In the homozygous pb-*Crt*B+I3 line, like in pb-*Crt*I2 double homozygous line, phytoene and phytofluene levels started to decrease from breaker + 3 days stage. The β-carotene levels did increase, compared to azygous, but only from breaker + 7 days stage.

5.2.3.2.2 Comparison of pb-*Crt* lines and other *Crt*B and *Crt*I containing lines

In this section, the lines containing *Crt*B or/and *Crt*I genes harbouring other promoters, instead of the pb promoter, are called comparator lines (such as PG-*Crt*B, PG-*Crt*I, 35S-*Crt*I, etc.).

Levels of isoprenoids in the pb-*Crt*B7 hemizygous and homozygous lines were only analysed at breaker + 7 days stage in a concurrent manner with the comparator lines, due to the small number of fruits obtained during cultivation. Some other pb-*Crt* lines (pb-*Crt*I6; pb-*Crt*B+I6 and pb-*Crt*B+I7), showing interesting increases of carotenoids in the T_0 generation, but with a high number of inserts, were also studied at the breaker + 7 days stage. Levels of isoprenoids of all the pb-*Crt* lines and their comparators at breaker + 7 days stage are shown in Figure 5-6.

The pb-*Crt*B7 hemizygous and homozygous lines had an increased level of lycopene and total carotenoid contents (1.3-fold) compared to the azygous line (Figure 5-6, A). The pb-*Crt*B7 homozygous line also showed a significant increase in β-carotene content (1.1-fold). No changes in phytoene and α-tocopherol levels were observed. Although significant changes were observed in the pb-*Crt*B7 line compared to its azygous control, they were not as great as the changes in carotenoids levels in the PG-*Crt*B homozygous line (described in Chapter III, Table 3-1). For instance, the level of lycopene was two times greater in PG-*Crt*B compared to the hemizygous pb-*Crt*B7

.

178

A.

pb-*Crt*B and comparators

B.

pb-*Crt*I and comparators

C.

pb-*Crt*B+I and comparators
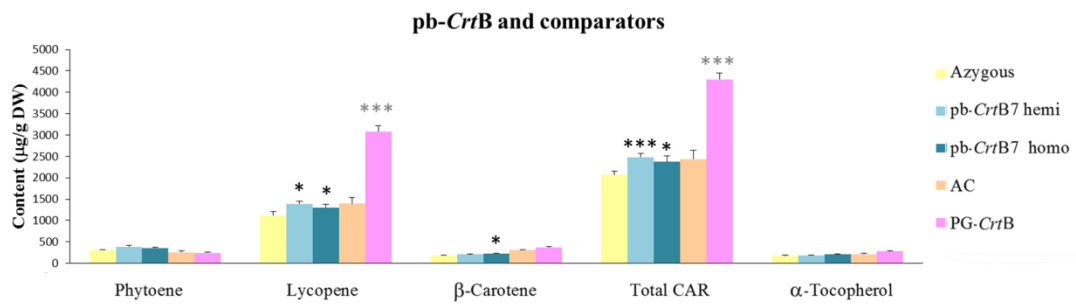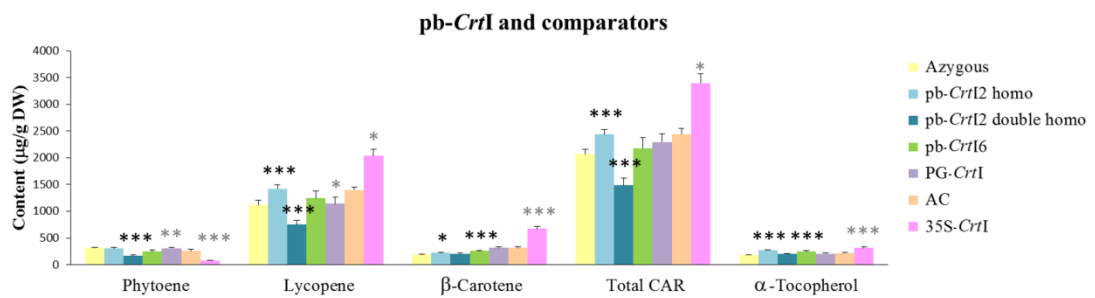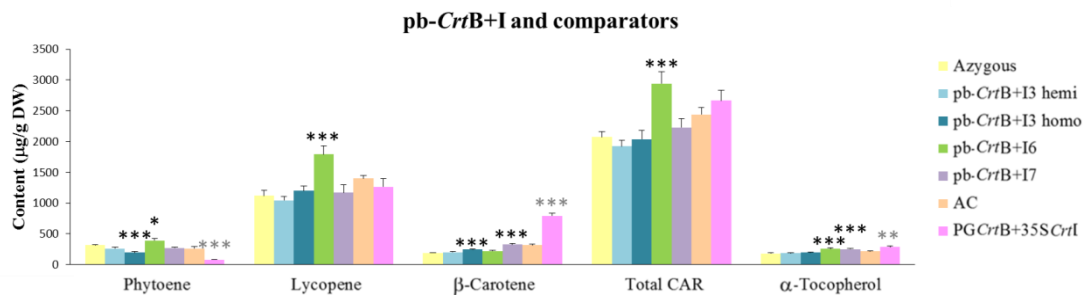
Figure 5-6 Carotenoid and α-tocopherol contents in pb-*Crt*B, pb-*Crt*I and pb-*Crt*B+I lines of T_1 generation and their comparators at breaker +7 days ripening stage

Comparators are lines containing *Crt*B or/and *Crt*I genes harbouring a promoter, other than pb. Isoprenoid contents are presented as μg/g DW. Methods used for this determination are described in the section 2.5. Determinations were made from at least three biological replicates and three technical replicates. The bars correspond to the mean data and the error bars represent the standard deviation. The pink bars correspond to data obtained in a different experiment, which were normalized to AC to be comparable. Dunnett's or student's t-tests were used to determine significant differences between the wild type background (AC or azygous) and the transgenic varieties for each compound. P<0.05, P<0.01 and P<0.001 are designated by *****, ****,** and *******, respectively. The black stars indicate a

179

significant difference compared to the azygous line. The grey stars indicate a significant difference compared to the AC control. Hemi, hemizygous line; homo, homozygous line.

Pb-*Crt*I2 homozygous was a better line compared to the double homozygous, in the terms of isoprenoid content at breaker + 7 days stage (Figure 5-6, B). The pb-*Crt*I6 line, which showed the greatest increase of β-carotene in the T_0 generation, still had the greatest β-carotene level in the T_1 generation, compared to pb-*Crt*I2 lines, but the levels of the other isoprenoids studied were unchanged compared to azygous. The PG-*Crt*I line, which had not been previously described in this thesis, had a similar level of isoprenoids compared to the pb-*Crt*I lines. The 35S-*Crt*I homozygous line, which was reported in Chapter III (Table 3-1), showed the greatest content of all isoprenoids studied except for phytoene levels, which were extremely low. The pb-*Crt*I2 homozygous line had 8-times more phytoene than the 35S-*Crt*I line.

The pb-*Crt*B+I3 lines were very similar to the azygous line at breaker + 7 days tomato stage (Figure 5-6). The pb-*Crt*B+I6 and 7 lines with high numbers of inserts, were characterised in the T_0 generation by a high level of phytoene/lycopene and β-carotene, respectively. At the T_1 generation, pb-*Crt*B+I6 had the greatest levels of phytoene and lycopene compared to all the lines studied, even compared to the PG-*Crt*B+35S-*Crt*I homozygous line, which was discussed in Chapter III (Table 3-1). The pb-*Crt*B+I7 line also had the greatest content of β-carotene compared to all the pb-*Crt*B+I lines. These two lines did not lose their characteristics from the T_0 to T_1 generation. However, the best line in terms of β-carotene content was the PG-*Crt*B+35S-*Crt*I homozygous line.

5.2.3.2.3 Pb-*Cr*t seeds

Surprisingly, the seeds of pb-*Crt*B and pb-*Crt*B+I tomato plants (T_0 and T_1 generations) had an orange-pink tinge (Figure 5-7). In order to understand the identity of the colour, isoprenoid analyses were performed on the seeds of breaker + 7 days pb-*Crt* tomato fruits (Figure 5-7). Substantial amounts of β-carotene (ca. 175 μg/g DW) were found in the pb-*Crt*B line and pb-*Crt*B+I, but not in the control and pb-*Crt*I. Lycopene was also detected in pb-*Crt*B+I (ca. 50 μg/g DW). The presence

of these two carotenoids could explain the coloured seeds. It is interesting to notice that it only occurred in the seeds of the line overexpressing the *Crt*B gene.
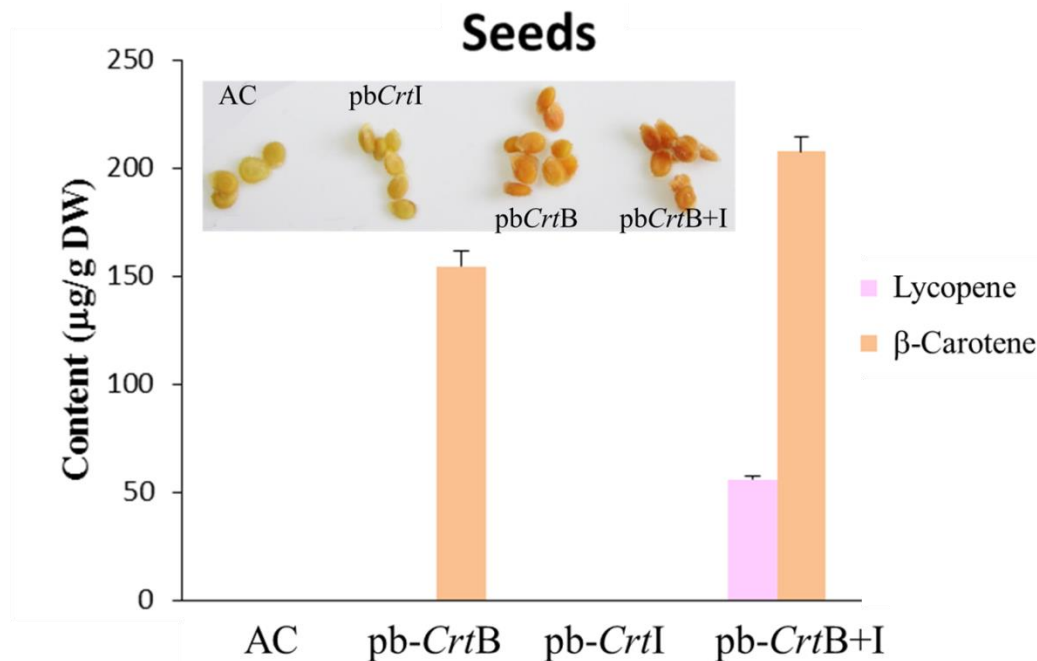
Figure 5-7 Carotenoid contents of pb-*Crt* seeds of the T_1 tomato fruits at breaker + 7 days

Carotenoid contents are presented as μg/g DW. Methods used for this determination are described in the section 2.5. Determinations were made from at least three biological replicates and three technical replicates. The bars correspond to the mean data and the errors bars represent the standard deviation. The different colours of the pb-*Crt* seeds are shown.

5.2.4 Characterisation of the pb promoter in the pb-*Crt*B+I hemizygous line

Although the pb promoter was thought to be chromoplast specific, according to studies of the promoter in other *Solanum* species (Ronen et al., 2000; Dalal et al., 2010), the coloured seeds proved that this does not seem to be the case. In order to elucidate the tissue specificity of the pb promoter, further characterisation was undertaken. The pb-*Crt*B+I hemizygous line was chosen and its levels of *Crt*I transcripts, of CRTI proteins and the contents of carotenoids (only β-carotene is shown here) were analysed in different plant organs (leaf, pericarp from different tomato stages, flower and seeds). The results are grouped in Figure 5-8. The levels of

transcript were determined by real-time RT-qPCR (method described in section 2.3.9). The *Crt*I transcripts were found in all the plant organs (Figure 5-8, 1). The seeds from mature green fruits contained the greatest level of transcripts (3- to 120-fold increase compared to the other organs). In the fruits, the highest levels of expression are at breaker and breaker + 3 days stages, thus showing that the pb promoter is active in early ripening stages. Levels in the leaves and the seeds from ripe tomatoes are extremely low compared to levels in the other organs. Proteins from the seeds, fruits and flowers of pb-*Crt*B+I hemizygous were extracted and quantified with a Bradford assay. Then the same amount of proteins for each organ was separated on SDS-PAGE (Figure 5-8, 2a; method described in section 2.6). CRTI proteins were visualised by immuno detection (Figure 5-8, 2b; method described in section 2.6.5). The greatest amount of CRTI was found in the seeds from ripe tomatoes. The level of CRTI in the seeds of mature green fruit could not be tested due to the lack of material. According to the thickness of the stained bands, the greatest levels of proteins in the fruits were at breaker + 3 days and mature green stages. Almost no CRTI proteins were detected in breaker + 14 days fruits and in the leaves. The greatest levels of β-carotene were found in the leaves of the azygous and pb-*Crt*B+I lines. All the other organs had a similar content of β-carotene in pb-*Crt*B+I. However, there was no β-carotene in the seeds of the azygous line. Consequently, the seeds had the greatest fold change increase of β-carotene when comparing the azygous and the pb-*Crt*B+I line levels (from 0 to 225 μg/g DW; Figure 5-8, 3).

1. *Crt*I expression

2. CRTI level
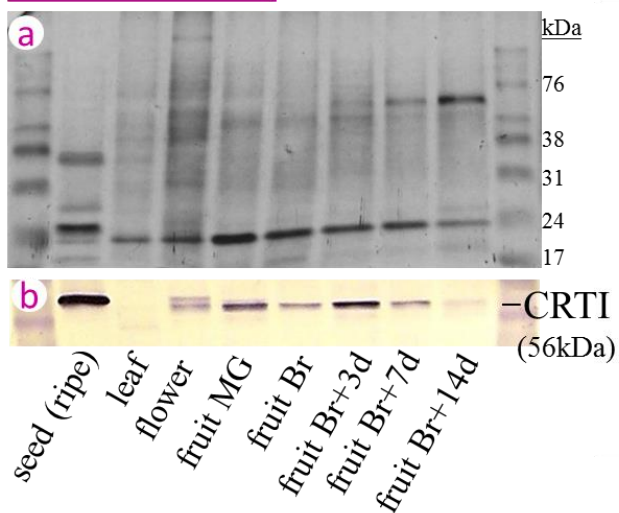
3. β-carotene content
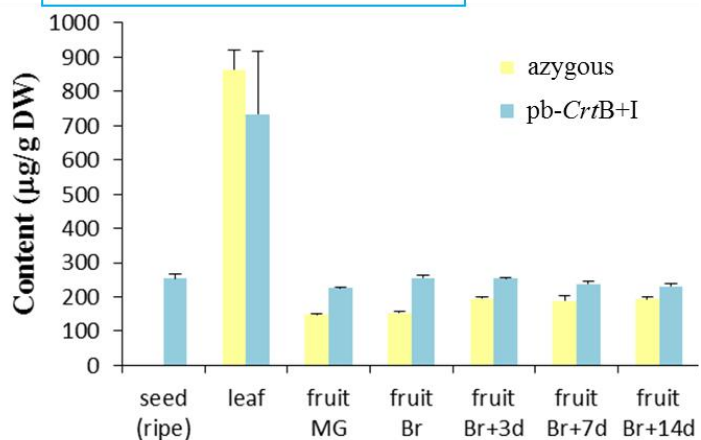
Figure 5-8 Characterisation of the pb promoter in the pb-*Crt*B+I hemizygous line

1. Levels of *Crt*I transcripts in different tomato plant organs determined by RT-qPCR. Levels are shown as relative to the leaf transcripts level. 2. Levels of CRTI protein in different tomato tissues. a, Proteins, extracted from the organs, were separated and visualised using an SDS-PAGE followed by silver staining. b, Western blot. Immuno-localisation of the CRTI proteins. 3. β-carotene contents are presented as μg/g DW. Determinations were made from at least three biological replicates and three technical replicates. The bars correspond to the mean data and the errors bars represent the standard deviation. Methods used for these determinations are described in sections 2.3.9, 2.6.5 and 2.5.3. Br, breaker; d, days.

5.3 Discussion

5.3.1 Evaluation of the pb-*Crt* transgenic lines

A surprisingly high number of *Crt* inserts were found in the pb-*Crt*B, pb*Crt*I and pb-*Crt*B+I T_0 plants (Table 5-1). Usually, when performing an *Agrobacterium*-mediated transformation, it is excepted to obtain a large proportion (> 1/3) of plants with one unique insert and then plants with 2 to 4 inserts (Cheng et al., 1997; Kohli et al., 2003). That was not the case with these three lines, where sometimes more than ten inserts were visualised (Figure 5-3). This is unusual for plants transformed by the UC Davis transformation service. So, it could indicate that an amended transformation process may have been used this time. It also could be explained by the duplication of T-DNA loci during the integration process, or ligation of separate T-DNAs prior to integration (Kohli et al., 2003). In the pb-*Crt*B and pb-*Crt*I T_0 plants, the high number of inserts did not have a particular effect (positive or negative) on isoprenoid production (Table 5-2). However, there was a positive correlation between the level of β-carotene and the number of inserts in the pb-*Crt*B+I T_0 plants (Table 5-2). The coordinated expression of *Crt*B+I usually leads to an increase of β-carotene and sometimes lycopene levels (Table 5-2; Chapter III, Table 3-1). Moreover, the isoprenoid profile of *Crt*B+I appeared to be dependent on the dose of gene. In chapter III, the *Crt*B+I hemizygous line was discussed regarding an increase of β-carotene and lycopene, while in the homozygous line, there was only an increase in β-carotene. It seems that the same phenomenon happened with the pb-*Crt*B+I T_0 lines, but that the dose of gene required to drive the unique increase of β-carotene was greater with the pb promoters than the combination of PG + 35S promoters used previously (Chapter III). It is only when more than 9 inserts were present in the plant (pb-*Crt*B+I lines 7 and 10, Table 5-2) that the level of β-carotene increased substantially (2-fold), associated with no change in lycopene level. Therefore, the same β-carotene/lycopene pattern, which is dependent on the number of gene copies, was found in the *Crt*B+I and pb-*Crt*B+I plants. Moreover, it is not the first time that multiple copies of transgenes have been shown to have a cumulative effect on carotenoid accumulation (Rai et al., 2007).

It is interesting to see the stable inheritance of isoprenoid profiles from the T_0 to T_1 generation of the pb-*Crt* plants. Only the lines with the same number of gene copies

184

can be compared. The profiles of carotenoids in pb-$CrtB7$ hemizygous (T_1) compared to pb-$CrtB7$ T_0, pb-$CrtI2$ homozygous (T_1) compared to pb-$CrtI2$ T_0, and pb-$CrtB+I3$ hemizygous (T_1) compared to pb-$CrtB+I3$ T_0 were different. One of the consistant differences was the level of phytoene and phytofluene, which both increased (1.4- to 2.5-fold) in pb-Crt T_0 plants compared to the control levels, while in the T_1 generation (Table 5-2, Table 5-4 and Figure 5-6) they were unchanged. Qualitative changes of the other isoprenoids studied were similar between T_0 and T_1. The only exception was the hemizygous pb-$CrtB+I3$, which showed no differences in isoprenoid levels compared to the control in the T_1 generation. When the changes in isoprenoid levels were qualitatively the same between T_0 and T_1 (for instance, an increase of lycopene level in pb-$CrtB$ compared to the control in T_0 and T_1), they were usually quantitatively smaller in the T_1 generation, compared to T_0 (i.e. the fold change increase of lycopene level compared to the control, was greater in T_0 than in T_1). The same conclusions can be attributed to pb-$CrtI6$, pb-$CrtB+I6$ and pb-$CrtB+I7$ lines, which had the greatest level of β-carotene, phytoene/lycopene and β-carotene, respectively, compared to the other pb-Crt lines in T_0 and T_1 generations. It will certainly take more generations to have a stabilised isoprenoid phenotype in the pb-Crt lines. Moreover, the T_0 and T_1 plants were grown at different periods of the year, spring and autumn, respectively, which could explain why the isoprenoid content of T_1 plants was not as high, compared to the T_0 plants. Additionally, different controls were used. The AC control, which represents the tomato background, was used for the T_0 analysis. The azygous line, which has been through the transformation process but lost its transgene, was used for the T_1 studies. The azygous control is a better choice, as it had also been transformed. Other studies have used the azygous line as the control of choice for carotenoid studies (Fraser et al., 2001; D'Ambrosio et al., 2004; Lee et al., 2012). Usually, the azygous lines and the AC control are not different. However, in this study, most of the isoprenoids levels are significantly different in AC compared to azygous (Figure 5-9). This may indicate that the transformation process had been quite stressful for the plants. It is plausible that in further generations the differences between AC and azygous lines will reduce. It is important to notice that for the T_1 generation studies, fewer biological replicates were available due to the study of the ripening series and poor

weather conditions during the growth period. Consequently, the same studies need to be repeated on a T_2 generation in order to confirm the T_1 results.

Changes in isoprenoid levels due to the expression of the *Crt*I and *Crt*B+I genes under the control of the pb promoter were reported during all the developmental and ripening stages studied in the fruit (Figure 5-5). That correlates with the pattern of pb expression in fruit (Figure 5-8). Although the hemizygous and homozygous lines of pb-*Crt*I lines were under the control of the same promoter, and consequently had the same timing of expression, their isoprenoid patterns were different during ripening (Figure 5-5). It shows again that different doses of gene(s) and thus presumably protein, can trigger different responses within the carotenoid pathway. The pb-*Crt*I2 double homozygous line might have been silenced from breaker + 3 days stage, as no increase in β- and γ-carotene levels were found, whereas there were still increased levels in the pb-*Crt*I2 homozygous until the breaker + 14 days stage. It is plausible that silencing of the genes in the double homozygous lines was due to DNA methylation (Finnegan and McElroy, 1994; Li et al., 2001)
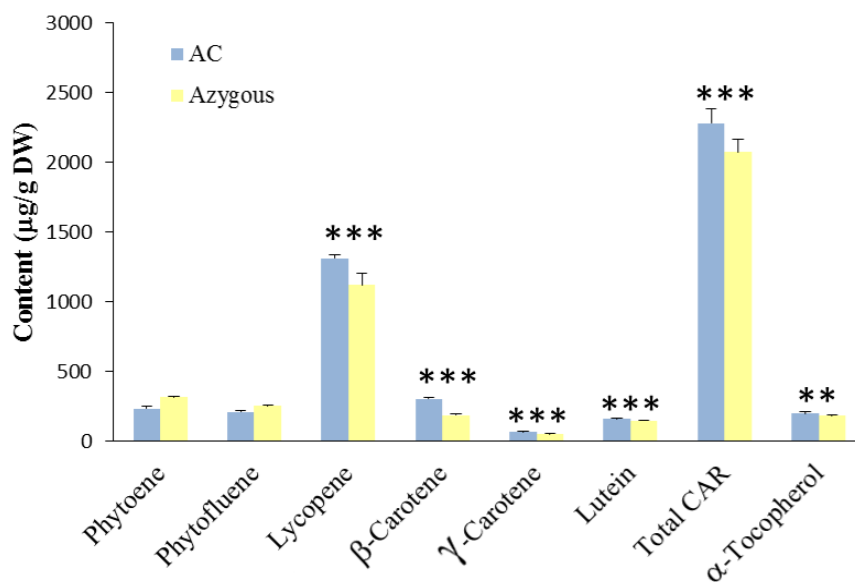
Figure 5-9 Isoprenoid contents in AC and azygous lines at breaker + 7 days

Carotenoid contents are presented as μg/g DW. Methods used for this determination are described in the section 2.5. Determinations were made from at least six biological replicates and three technical replicates. The bars correspond to the mean data and the errors bars represent the standard deviation. Student's t-test was used to determine significant differences between AC and azygous for each

compound. P<0.05, P<0.01 and P<0.001 are designated by *****, ******, and *******, respectively. AC, Ailsa Craig.

5.3.2 Effect of different promoters on carotenoid production

There is a broad spectrum of promoters available which differ in their ability to regulate the temporal and spatial expression patterns of the genes. Fine-tuning the control of the most suitable promoter for the appropriate transgene can dramatically increase the successful application of transgenic technology (Potenza et al., 2004). Consequently, the strategy chosen to optimise isoprenoid production in this study was to test a different promoter (pb) which was an earlier ripening promoter compared to the PG promoter. The hypothesis was that, by expressing the gene(s) earlier during the ripening process, more carotenoids of interest could be produced in the tomato fruit, since the CRTB enzyme would be available for a longer period, when the cells are still metabolically active. Moreover, the pb promoter had proved to deliver high expression in the *S. galapagense* (Enfissi et al., unpublished), so it was a good candidate. Other carotenoid engineering studies have tested several promoters in order to find the best one for their transgenes of interest (Davuluri et al., 2005; Enfissi et al., 2010). In this case, the promoters used to down-regulate DET-1 (2A11, TFM7 and P119) would be problematic because the presence of phytoene synthase early in fruit ripening has pleiotrophic effects (Enfissi and Fraser, unpublished). The choice of the suitable promoter is complicated since the best anticipated time for its expression is within a tight period of fruit ripening.

In order to assess the effect of the pb promoter, it was necessary to compare the isoprenoid levels in pb-*Crt* plants with the levels in the previous *Crt* plants (under the control of PG or/and 35S promoters), described in Chapter III. It is clear that the PG-*Crt*B, 35S-*Crt*I and PG-*Crt*B+35S-*Crt*I lines are better in terms of carotenoid production compared to the pb-*Crt* lines, with ca. twice as much of the carotenoids of interest in each line (Figure 5-6, pink bars). This was not the result predicted. Moreover, it was surprising to find the pb promoter expressed not only in the fruit and flower, but also in the seed (Figures 5-7 and 5-8). The expression in the fruit and flower was expected as the *Cyc-B* promoter (pb) has been described as a chromoplast specific promoter in *S. pennelli* (Ronen et al., 2000) and in *S. habrochaites* (Dalal et al., 2010). However, no experiment on pb expression in the seed were shown in these

latter papers. Consequently, it seems that the pb promoter was not functioning to the same extent, in terms of level of expression, in the Ailsa Craig variety of *S. lycopersicum* compared to the *S. galapagense*.

The control of gene expression by the promoter relies on a multitude of factors. The initiation of the transcription depends on the core sequence and upstream region of the promoter. Much of the gene expression control is realised by transcription factors and enhancer binding proteins, which bind to *cis*-elements called enhancer elements. These elements can be located hundreds or thousands of base pairs away from the gene that they control, and they are associated with tissue-specificity, expression, regulation by light or by a specific cellular substrate (Potenza et al., 2004). Consequently, when a promoter from one tomato species (such as *S. galapagense*) is introduced in another one (such as *S. lycopersicum*), unforeseen difficulties can occur: (i), the more distant 5′ *cis*-acting enhancer elements can be removed during the promoter isolation; (ii), the random integration of the pb-*Crt* gene into *S. lycopersicum* genome can eliminate potential *trans*-interactions that occur based on the chromatin structure or location within the genome; (iii), interaction between the *trans*-acting factors and *cis*-elements from the different genome may not be possible (Potenza et al., 2004). A similar situation to the one occurring with the pb promoter in AC was observed when the pectin methyl esterase gene and its promoter were transferred from *S. pennelli* into AC (Seymour et al., unpublished). The promoter seemed to not be fully functional in AC, compared to *S. pennelli.* Then, it was previously shown that the upstream region of the *Cyc-B* promoter (pb) in *S. pennelli* and *S. lycopersicum* contained different *cis*-elements (Figure 5-10) and that could be the reason for different expression patterns (Ronen et al., 2000). It is plausible that the same differences occur between *S. lycopersicum* and *S. galapagense*, explaining why the pb-*Crt* plants were not producing high levels of isoprenoids.

1. *S. lycopersicum*

GTCTAATACTCTAACTA

ATG

AATTTTCAAA

2. *S. pennelli*

TTTAAAAAATTGACTAGAAA

AGAGTCTGGGTTC   CTAAATAT

ATTT   TGACTTCACCCTTCTTTCTTGTCTTG   CTAGTATCG

ATG

AATTTCAAA

500 bp
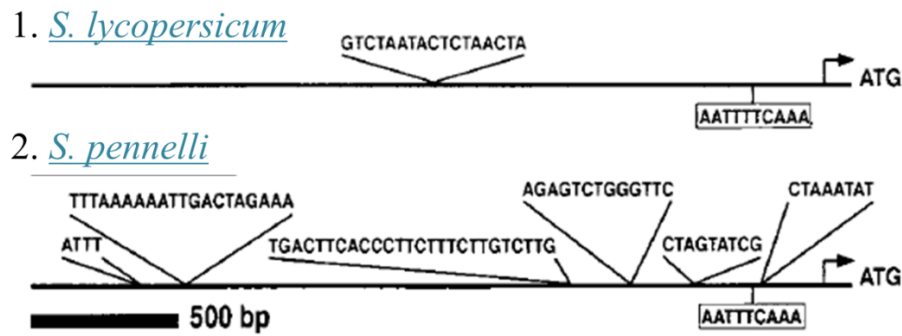
Figure 5-10 *Cis*-elements in the upstream sequences of the promoters of *Cyc-B* in *S. lycopersicum* (1) and *S. pennelli* (2) adapted from Ronen et al. (2000)

They are six additional sequence elements that exist in (2) but are absent from (1), and one sequence element that exists in (1) but not in (2).

5.3.3 Insight into the carotenoid pathway in the tomato seeds

The seeds from the pb-*Crt*B and pb-*Crt*B+I (T_0 and T_1) had an orange/pink colour (Figure 5-7). This phenotype has not been reported in other studies on the *Cyc-B* gene. Investigations on carotenoid contents in the seeds of the AC control and the pb-*Crt* lines showed that pb-*Crt*B and pb-*Crt*B+I contained high level of β-carotene, similar to the ones in the fruits (Figure 5-9). Therefore, this indicates that *Crt*B and *Crt*B+I were expressed in the seeds, leading to the production of carotenoids. It is plausible that the tissue-specificity of the pb promoter was lost by elimination of one or several enhancer elements of the pb promoter during the isolation of the pb promoter from *S. galapagense*. This hypothesis correlates with the ones described in section 5.3.2. It is interesting to note that only the *Crt*B containing lines were able to produce β-carotene. This observation gives an insight into the carotenoid pathway in the tomato seeds. It appears that phytoene synthase is not present in the wild type seeds but some of the other carotenoid enzymes potentially are (phytoene desaturase, ζ-carotene desaturase, carotene isomerase and β-lycopene cyclase enzymes). When the *Crt*B gene is expressed in the seed, phytoene is synthesised and can be utilised as a precursor by either β-lycopene cyclase enzymes or CR*T*I (if it is in pb-*Crt*B+I). In pb-*Crt*B+I, CRTI catalyses the synthesis of lycopene which may be converted to β-carotene by the β-lycopene cyclase enzymes or accumulated in the seed, which

189

seems plausible since lycopene was detected in pb-*Crt*B+I seeds (Figure 5-7). A schematic representation is displayed in Figure 5-11.
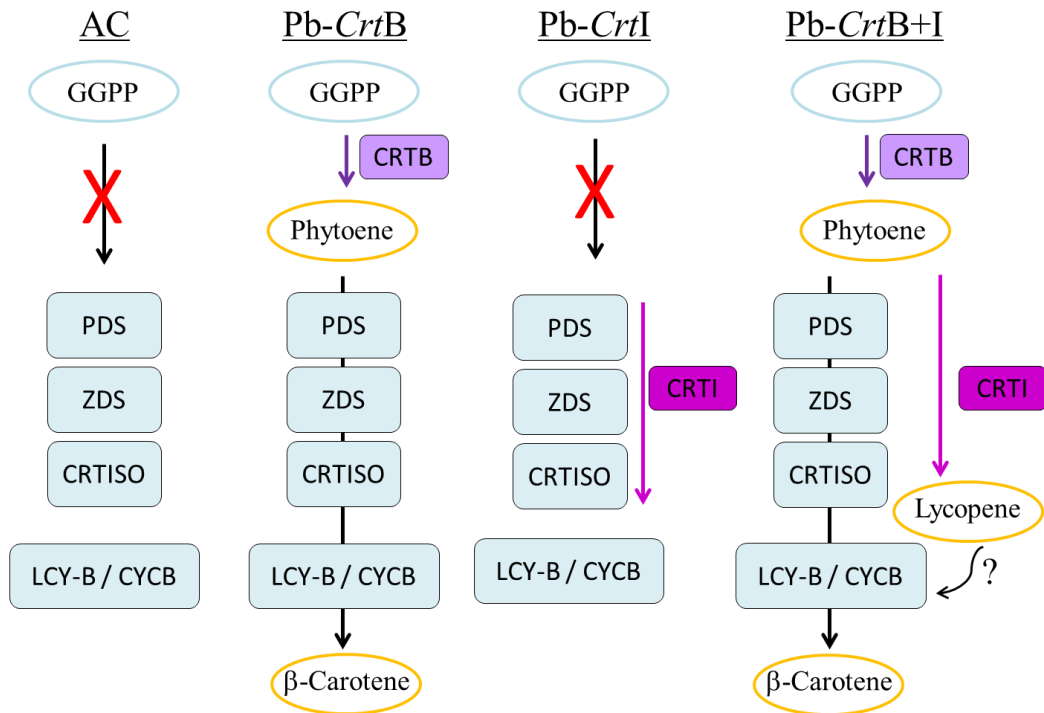
Figure 5-11 Schematic representation of carotenoid pathway in the seeds of the pb-*Crt* lines and the AC control

Blue colour represents endogenous compounds. Purple indicates the heterologous enzymes. Orange displays carotenoids only found in the *Crt*B containing lines. Enzymes are in a rectangular shape, while metabolites have an oval shape. The red cross indicates a biosynthetic step which does not exist in the particular line. GGPP, geranylgeranyl diphosphate; PDS, phytoene desaturase; ZDS, ζ-carotene desaturase, CRTISO, carotene isomerase; LCY-B, β-lycopene cyclase; CYC-B, fruit specific β-lycopene cyclase; CRTB, phytoene synthase; CRTI, phytoene desaturase.

Chapter VI: Combining ketocarotenoid synthesis with putative transcriptional regulators

6.1 Introduction

Manipulating transcription factors is of great interest in metabolic engineering, since they are regulatory proteins that can control an entire pathway (Broun and Somerville, 2001) and, consequently, have a large scale impact (Martin, 1996). Overexpressing transcription factors has been a successful strategy to increase carotenoid (Pan et al., 2013) and flavonoid (Butelli et al., 2008) contents in tomato fruit. Some of the transcription factors, which regulate specific pathways, have been found by correlation network analysis (Rohrmann et al., 2011). The transcription factors described in this chapter, Phytochrome-Interacting Factor 5 (PIF5) and Arabidopsis Response Regulator 14 (ARR14), have been identified as being linked with carotenoid pathways in a similar manner. PIF5 acts on ethylene biosynthesis and phytochrome signalling (Khanna et al., 2007), but also has been shown to take part in the regulation of phytoene synthase gene expression (Toledo-Ortiz et al., 2010). ARR14 is known to play a role in modulating the cellular response to cytokinin (Mason et al., 2005) and potentially in light signalling (D'Agostino and Kieber, 1999). The transcription factors were chosen as a strategy to improve the production of ketocarotenoids in plants. Ketocarotenoids are formed from a common substrate, β-carotene, by the carotene hydroxylase (CRTZ) and carotene ketolase (CRTW) enzymes (Figures 1-14 and 1-20). They are high value products, as they serve as colourants for animal feeding (Breithaupt, 2007) and have health-promoting effects (Yuan et al., 2011). In this study, transient expression of the transcription factors associated with *Crt*Z and *Crt*W genes was undertaken in order to evaluate the potential of expressing PIF5 or ARR14 to optimise ketocarotenoid production.

6.2 Results

Vectors used in this study were kindly provided by Dr N. Misawa (Ishikawa Prefectural University, Japan). They are represented in Figure 6-1. The *Crt*Z and *Crt*W genes originated from the marine bacterium *Brevundimonas* sp strain SD212 (Hasunuma et al., 2008), and were chemically synthesised with altered codons designed for plants (appendix Figure A6-1).
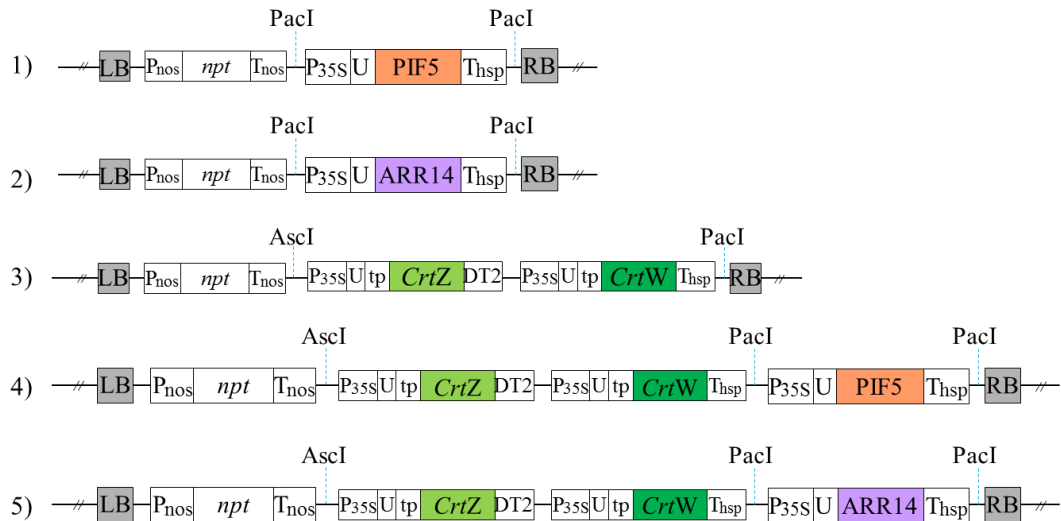
Figure 6-1 Structure of the vectors harbouring the transcription factors

1, PIF5 vector; 2, ARR14 vector; 3, ZW vector; 4, ZW-PIF5 vector; 5, ZW-ARR14 vector. Locations of the restriction sites are shown by the blue dashed lines. LB, left border; P_{nos}, promoter of nopaline synthase gene from *Agrobacterium tumefaciens*; *npt*, gene conferring the kanamycin resistance; T_{nos}, terminator of nopaline synthase gene from *Agrobacterium tumefaciens*; P_{35S}, 35S promoter from the cauliflower mosaic virus; U, untranslated region of *Nicotiana tabacum* alcohol dehydrogenase; tp, transit peptide of the *Pisum sativum* L. RuBisCO small subunit; *Crt*Z, carotene hydroxylase from *Brevundimonas* sp stain SD212; *Crt*W; carotene ketolase from *Brevundimonas* sp stain SD212 T_{hsp}, terminator of the *Arabidospsis thaliana* heat shock protein 18.2 gene; DT2, succession of T_{hsp} and T_{nos} terminators; PIF5, phytochrome-interacting factor 5 transcription factor from *Arabidopsis thaliania*; ARR14, *Arabidopsis thaliana* response regulator 14 transcription factor from *Arabidopsis thaliania*; RB, right border.

6.2.1 Selection of an appropriate platform for transient expression experiments

One of the advantages of plant transient agro-infiltration transformations is the rapidity with which transformed biomass can be produced. When the plants are ready for transformation, it only takes approximately two weeks to agro-infiltrate the plants, collect plant tissues and analyse ketocarotenoid contents. However, it was necessary to first ascertain whether ketocarotenoids could be produced in a transient expression experiment and which plant platform would be the more suitable for this approach. Three platforms were tested. Moneymaker tomatoes were chosen since stable ZW (Figure 6-1) transformed tomatoes lines were already available with this tomato background and could be used for comparison. Micro-Tom tomatoes were selected for their small size, which is a benefit in terms of agro-infiltration
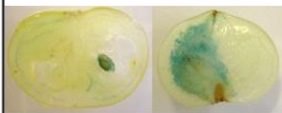
efficiency. *Nicotiana benthamiana* was also chosen for its amenability to transient transformation. Methods of agro-infiltration are described in section 2.4.1.1. For all the agro-infiltration experiments described in this chapter, *Agrobacterium* cultures of each vector infiltrated were mixed with the *Agrobacterium* culture of p19 vector prior to infiltration. This vector, harbouring the p19 gene from the tomato bushy stunt virus, was used to maximise protein production by suppression of gene silencing (Voinnet et al., 2003). For the sake of clarity, the p19 vector will not be mentioned independently for each transient experiment in the following sections; its use should be assumed unless stated. In order to test the different platforms for ketocarotenoid production, the three types of plants were agro-infiltrated with an empty vector (control), a GUS vector (containing the β-glucuronidase gene under 35S promoter) and the ZW vector. After 4 days, leaf tissues from the control and ZW plants were collected and flash-frozen in liquid nitrogen. Ketocarotenoids were then extracted and analysed by UPLC (methods are described in sections 2.5.1 and 2.5.3). Chromatographic profiles of the ketocarotenoids found and their spectral characteristics are shown in Figure 6-2. The tissues freshly collected from the GUS plants, at the same time as the others, were tested with a histochemical GUS assay in order to evaluate the efficiency of the transformation. The tissues were put in contact with the 5-bromo-4-chloro-3-indolyl glucuronide (X-Gluc) compound, which is the substrate of the β-glucuronidase enzyme. If the enzyme was present in the tissue, its product was synthesised and then dimerised through its reaction with the oxygen present in the air, which results in a blue dye being produced. The results are summarised in Figure 6-3. The Moneymaker tomato fruits were poorly transformed (20 to 50%) and no ketocarotenoids were detected in the fruits. The efficiency of transformation of Micro-Tom tomato fruits was much better, with 70 to 100% of the fruit transformed and echineone was produced. However, the *Nicotiana benthamiana* leaves had the best rate of transformation (90 to 100%) and three ketocarotenoids were synthesised (pheonicaxanthin, canthaxanthin and echineone) at high levels (25 to 275 µg/g of DW). Consequently, *Nicotiana benthamiana* leaves represent the best platform tested in this study for the production of ketocarotenoids, with the best variety and highest contents of ketocarotenoids produced and the best efficiency of agro-infiltration.
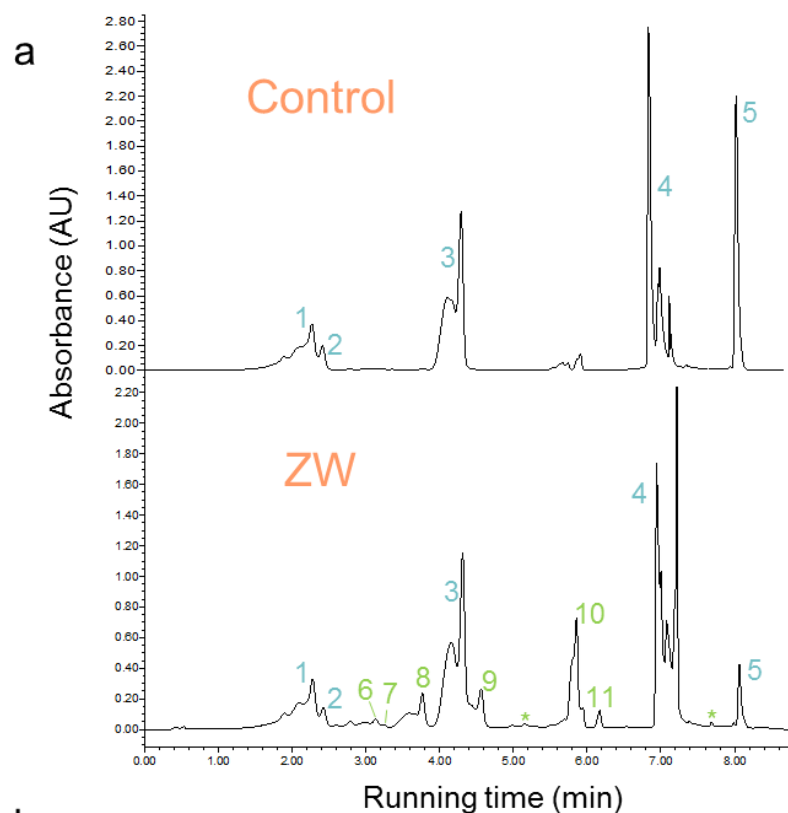
NAMES	Peak number	Retention time (min)	Spectra λ_{max} (nm)
Neoxanthin	1	2.28	(414.1), 438.3, 467.4
Violaxanthin	2	2.43	(416.5), 440.7, 471.1
Lutein	3	4.31	(421.3), 446.8, 477.2
Chlorophylls	4	6.94 to 7.22	431.9 (a) / 469.3 (b)
β-Carotene	5	7.22	- , 450.4, 480.4
Astaxanthin	6	3.20	474.7
Antheraxanthin	7	3.25	-, 448.0, 477.2
Adonixanthin	8	3.78	469.9
Pheonicaxanthin	9	4.56	479.6
Unknown	*	5.16	460.2
Canthaxanthin	10	5.86	473.5
Echineone	11	6.17	466.2
Unknown	*	7.68	473.5

Figure 6-2 UPLC Chromatographic profiles of carotenoids, chlorophylls and ketocarotenoids found in control and ZW transformed tobacco leaves (a), the chromatographic annotations and spectral characteristics (recorded from 250 to 600 nm) are shown in (b)

The chromatographic profile was recorded at 470 nm. Blue numbers correspond to carotenoids and green to ketocarotenoids. Control designates tobacco plants transformed with an empty vector.

	Moneymaker	Micro-Tom	*Nicotiana benthamina*
Tissue transformed	Mature green tomato fruit (ca. 6 cm diameter)	Mature green tomato fruit (ca. 2 cm diameter)	Tobacco leaves (ca. 9 cm x 6 cm)
Transformation efficiency (GUS)	C ZW 20 to 50% transformed	C ZW 70 to 100% transformed	C ZW 90 to 100% transformed
Ketocarotenoid produced	none	- Echineone (ca. 5µg/g DW)	- Pheonicaxanthin (ca. 25µg/g DW) - Canthaxanthin (ca. 275µg/g DW) - Echineone (ca. 40µg/g DW)

Figure 6-3 Comparison of three platforms for transient production of ketocarotenoids

Mature green Moneymaker and Micro-Tom tomatoes and *Nicotiana benthamiana* leaves were agro-infiltrated with ZW (illustrated in Figure 6-1) and GUS constructs as described in section 2.4.1.1. C, control, which correspond to a plant infiltrated with an empty vector. A minimum of 9 to 12 biological replicates and three technical replicates were analysed. Methods for histochemical detection of GUS activity and quantification of ketocarotenoids are explained in sections 2.4.1.2 and 2.5.3. An average quantity of ketocarotenoids is shown as µg/g of DW.

6.2.2 Ketocarotenoid analysis in transgenic tobacco plants

Six week old *Nicotiana benthamiana* leaves were independently agro-infiltrated with an empty vector, GUS, PIF5, ARR14, ZW, ZW-PIF5 and ZW-ARR14 vectors (Figure 6-1). Histochemical GUS assay was performed to verify the efficiency of the transformation. The efficiency of the tobacco leaf transformations were always high (90 to 100%, such as in Figure 6-3). The phenotypes of the control, GUS, PIF5 and ARR14 transformed leaves remained the same post infiltration. However, the ZW containing leaves showed a difference in their colour compared to the control, from 3 or 4 days post infiltration onwards. In the ZW, ZW-PIF5 and ZW-ARR14 transformed leaves a brown colour intensified with each day post infiltration. The

representative phenotypes of all the transformed leaves and the control at 8 days post infiltration are shown in Figure 6-4.
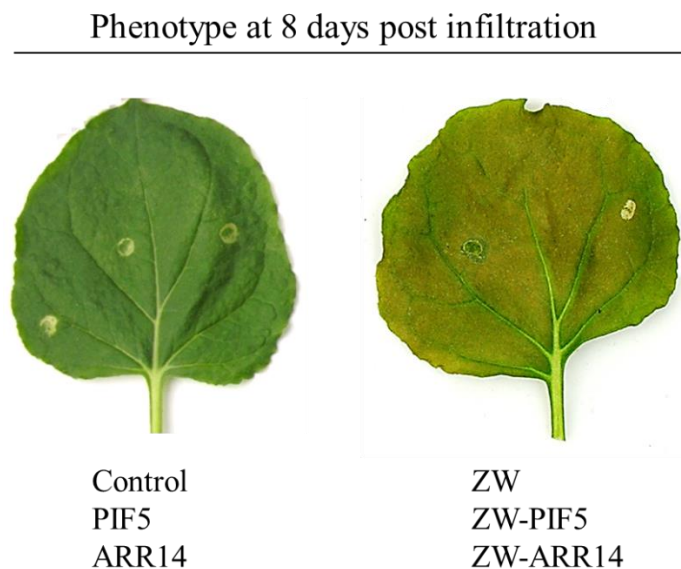
Figure 6-4 Leaf phenotypes 8 days post agro-infiltration

Control represents a leaf, which has been agro-infiltrated with an empty vector. The control, PIF5 and ARR14 leaves have the same phenotype. The ZW containing leaves have similar phenotypes.

Leaves were collected either at 4 or 8 days post infiltration. Usually, carotenoids and ketocarotenoids were extracted and analysed by UPLC (methods are described in sections 2.5.1 and 2.5.3). A parallel experiment was performed with saponified samples, in order to see the colours of the transformed leaf extracts, otherwise masked by the green colour of the chlorophylls. The extracted samples from the control, and other non- ZW containing leaves were yellow, while the samples from all the ZW containing leaves were orange (Figure 6-5). That indicated the production of ketocarotenoids in the ZW containing leaves.
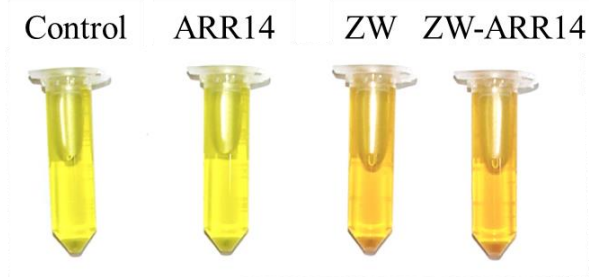
Figure 6-5 Microcentrifuge tubes containing saponified metabolites extracted from tobacco leaves

Control, ARR14, ZW and ZW-ARR14 correspond to the plants agro-infiltrated with an empty vector, ARR14, ZW and ZW-ARR14 vectors, respectively. Methods used to extract the carotenoids and ketocarotenoids are described in the section 2.5.1.

Carotenoid and ketocarotenoid contents of all transformed leaves (control, PIF5, ARR14, ZW, ZW-PIF5 and ZW-ARR14) were analysed at 4 days post infiltration (Figure 6-6). The control, PIF5 and ARR14 had similar carotenoid profiles. PIF5 and ARR14 were not significantly different to the control. The ketocarotenoids, pheonicaxanthin, canthaxanthin and echineone, were only detected in ZW, ZW-PIF5 and ZW-ARR14 plants. These plants were also characterised by significant decreases of endogenous carotenoid contents. The β-carotene level in the ZW containing leaves was 2.6-fold lower, compared to the control. Smaller decreases of neoxanthin and violaxanthin levels were found (1.3-fold decrease) in ZW, ZW-PIF5 and ZW-ARR14 plants compared to the control. The ZW-ARR14 transformed leaves had a greater level of canthaxanthin compared to ZW (1.3-fold increase). The ZW-PIF5 leaves did not contain more ketocarotenoids compared to ZW. Consequently, ZW-ARR14 was the best construct tested for production of ketocarotenoid in tobacco leaves. These experiments were repeated to generate data from three independent experiments that confirmed the formation of ketocarotenoids.
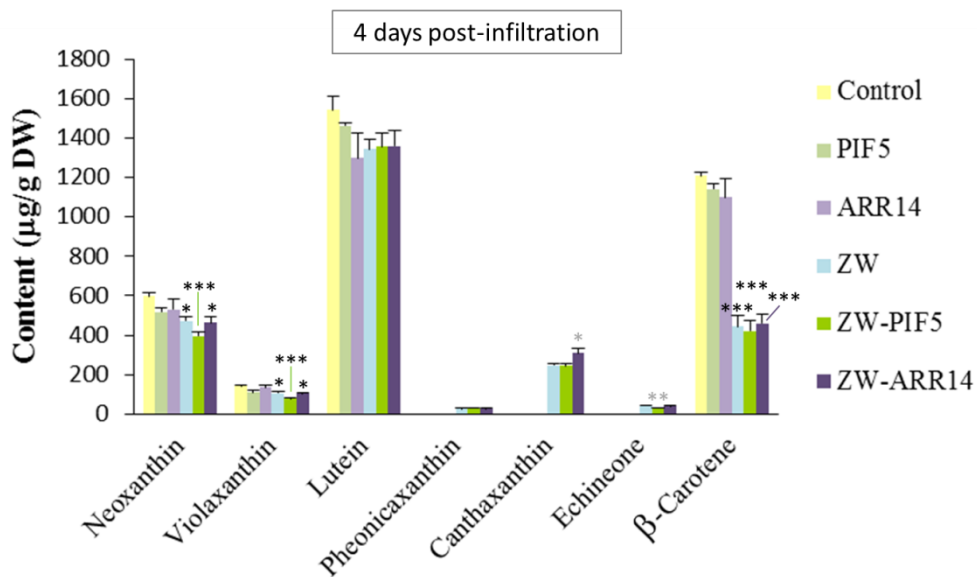
Figure 6-6 Carotenoid and ketocarotenoid contents of transgenic tobacco leaves 4 days post-infiltration

Carotenoid and ketocarotenoid contents are presented as µg/g DW. Methods used for this determination are described in the section 2.5.3. Determinations were made from at least twelve biological replicates (which were collected from three different plants) and three technical replicates. The bars correspond to the mean data and the error bars represent the standard deviation. Control, PIF5, ARR14, ZW, ZW-PIF5 and ZW-ARR14 correspond to the plants agro-infiltrated with an empty vector, PIF5, ARR14, ZW, ZW-PIF5 and ZW-ARR14 vectors, respectively. Dunnett's test was used to determine significant differences between the control and the transgenic leaves and between ZW and ZW-transcription factor. $P<0.05$, $P<0.01$ and $P<0.001$ are designated by *****, ******, and *******, respectively. The black stars indicate a significant difference compared to the control. The grey stars demonstrate a significant difference compared to ZW.

Nicotiana benthamiana leaves were also agro-infiltrated with the empty vector, GUS, ARR14, ZW and ZW-ARR14 vectors (Figure 6-7). In this experiment, the leaves were collected at 8 days post infiltration, instead of 4 days post infiltration. The purpose was to verify if a longer period of transformation could have an effect on the quantity of ketocarotenoids produced. New ketocarotenoids, astaxanthin, antheraxanthin and adonixanthin, were detected in ZW and ZW-ARR14 (10 to 40 µg/g DW), which were not present at 4 days post infiltration. The other ketocarotenoids, found at 4 days post infiltration, were detected in similar amounts at 8 days post infiltration. The ZW-ARR14 transformed leaves contained significantly more adonixanthin, pheonicaxanthin, canthaxanthin and echineone compared to ZW

leaves (1.3 to 1.5-fold increase). Consequently, ZW-ARR14 was again considered the best construct for ketocarotenoid production. The effects on the endogenous carotenoids were qualitatively similar at 4 and 8 days post infiltration, with a significant decrease of neoxanthin, violaxanthin and β-carotene levels in the ZW containing leaves compared to the control. However, in comparison with the control, there was a 4.4-fold decrease in β-carotene content in ZW-ARR14 at 8 days post infiltration, while it was a 2.6-fold decrease at 4 days post infiltration.
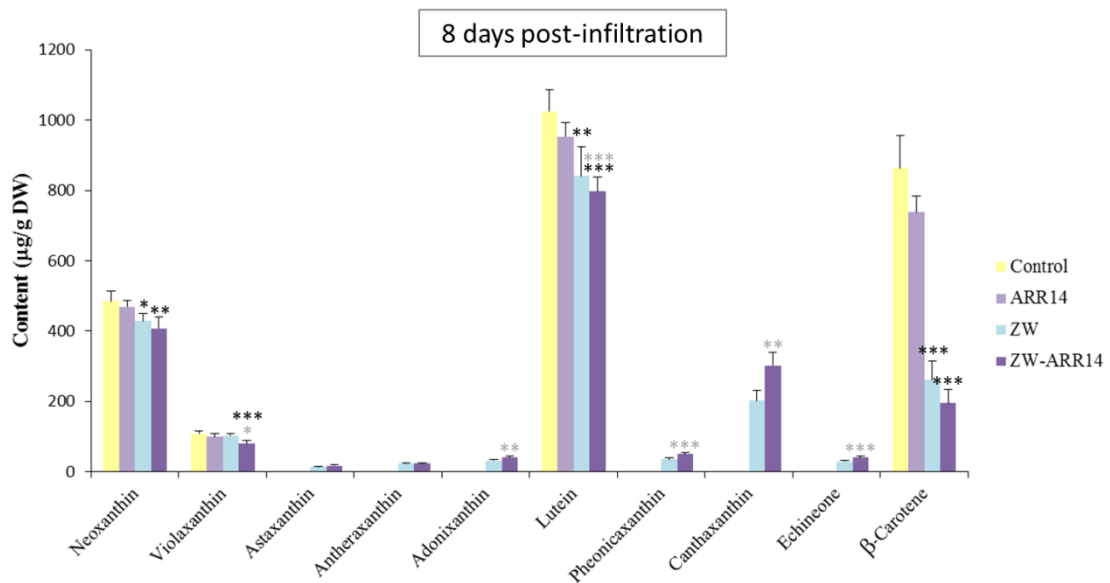
Figure 6-7 Carotenoid and ketocarotenoid contents of transgenic tobacco leaves 8 days post-infiltration

Carotenoid and ketocarotenoid contents are presented as μg/g DW. Methods used for this determination are described in section 2.5.3. Determinations were made from at least twelve biological replicates (which were collected from three different plants) and three technical replicates per sample. The bars correspond to the mean data and the error bars represent the standard deviation. Control, ARR14, ZW and ZWARR14 correspond to the plants agro-infiltrated with an empty vector, ARR14, ZW and ZWARR14 vectors, respectively. Dunnett's test and student's t-test were used to determine significant differences between the control and the transgenic leaves and between ZW and ZW-ARR14, respectively. P<0.05, P<0.01 and P<0.001 are designated by *, **, and ***, respectively. The black stars indicate a significant difference compared to the control. The grey stars demonstrate a significant difference compared to ZW.

6.2.3 Generation of stable ZW-ARR14 transgenic *glauca* plants

Nicotiana glauca has been previously used as an engineering model for the production of ketocarotenoids (Gerjets et al., 2007; Zhu et al., 2007). It is an attractive system for the production of ketocarotenoids, due to its carotenoid accumulating flowers. Moreover, it is a potential advanced renewable biofuel source (Mortimer et al., 2012). Therefore, it could be used as a multipurpose system. Several attempts were performed to transform *Nicotiana glauca* plants in a stable manner with the ZW-ARR14 (method is described in section 2.4.1.3). However, despite modifications to the concentration of the *Agrobacterium* inoculum as well to the media, no plantlet was successfully regenerated from the transformed ZW-ARR14 *N. glauca* calli. The positive controls, which were not transformed calli, successfully produced plantlets. One possible reason might be that the ZW-ARR14 vectors with the constitutive 35S promoter are lethal and cannot be used to stably transform *N. glauca* plants.

6.3 Discussion

6.3.1. Transient production of ketocarotenoids

The production of high-value ketocarotenoids and especially astaxanthin has been the focus of many studies over the years. Plants from different genera (*Nicotiana*, *Arabidopsis*, *Lotus*, *Solanum*, *Daucus*, *Brassica*, *Zea*) have been transformed in a stable manner with β-carotene ketolase and/or hydroxylase genes from different origins (Mann et al., 2000; Stalberg et al., 2003; Ralley et al., 2004; Gerjets and Sandmann, 2006; Morris et al., 2006; Gerjets et al., 2007; Suzuki et al., 2007; Zhu et al., 2007; Cho et al., 2008; Hasunuma et al., 2008; Zhu et al., 2008; Fujisawa et al., 2009; Ahn et al., 2012; Huang et al., 2013). In this study, the optimised vector harbouring the chemically synthesised *Crt*Z and *Crt*W genes with plant codon usage, which encode the same amino acid sequences of CRTZ and CRTW of *Brevundimonas* sp, was agro-infiltrated in a transient manner. The expression of heterologous genes in plants can be limited by differences in codon usage. Optimised codon use has been successfully utilised to enhance protein content (Perlak et al., 1991; Rouwendal et al., 1997; Batard et al., 2000; Vervoort et al., 2000; Wang and Roossinck, 2006). The 5´UTR region from *N. tabacum* alcohol dehydrogenase

(*NtADH*) has also been included in this vector to enhance the stability of the *Crt*Z and *Crt*W mRNAs and therefore, translation (Van Der Velden and Thomas, 1999; Satoh et al., 2004). To date, the highest level of ketocarotenoid accumulation achieved in plants, was obtained through the stable expression of this optimised *Crt*Z/*Crt*W vector. Ketocarotenoid levels up to 8,000-14,000 μg/g DW have been reported (Hasunuma et al., 2008; Mortimer et al., unpublished).

In this study, transient production of ketocarotenoids was successfully achieved in tomato (Micro-Tom) and *N. benthamiana* using the optimised *Crt*Z/*Crt*W vector. It is the first time that transient production of ketocarotenoids in plants has been reported. Large contents of ketocarotenoids (ca. 500 μg/g DW) were quantified in *N. benthamiana* leaves. The levels achieved, at just 8 days post agro-infiltration, are greater or of similar range compared to the ketocarotenoid levels obtained in the studies previously cited, which did not use the optimised *Crt*Z/*Crt*W vector. Contrary to the majority of studies reporting the production of ketocarotenoids in plants, the main ketocarotenoid synthesised in the transiently transformed *N. benthamiana* leaves was not astaxanthin but canthaxanthin (Figure 6-6; Figure 6-7). Astaxanthin was not detected in the tobacco leaves at 4 days post infiltration and represented only 4% of the total ketocarotenoids at 8 days post infiltration. Therefore, it seems that the last steps of the ketocarotenoid pathway are not efficiently catalysed in this transient system, which causes an accumulation of the intermediate ketocarotenoid canthaxanthin (Figure 1-14). It may be possible that a longer period of agro-infiltration will provide greater quantities of astaxanthin. The fact that there is no increase of canthaxanthin levels at 8 days compared to 4 days post-infiltration whereas all the ketocarotenoids, which are synthesised post canthaxanthin have increased levels at 8 days compared to 4 days, encourages this hypothesis. The presence of canthaxanthin suggests that hydroxylation of ketolated β-ionone rings does not occur readily following transient expression. Perhaps this approach restricts the concurrent participation of the heterologous and/or the endogenous hydroxylases. In addition, the spatial organization of the enzymes and precursors could be more affected by transient expression.

The production of ketocarotenoids was always associated with a decrease of the β-carotene content in *N. benthamiana* leaves (Figure 6-6; Figure 6-7). This was expected as β-carotene is the first precursor of the ketocarotenoid pathway (Figure 1-

14). However, the decrease of β-carotene level in the ZW containing lines was not equivalent to the content of ketocarotenoid produced in the respective lines. There was a reduction of 9 to 37% of β-carotene content depending on the experiments (4 or 8 days post infiltration) and on the lines (ZW or ZW-ARR14). The loss of β-carotene corresponds to the percentage of β-carotene content, which was not transformed into ketocarotenoids. Some unidentified ketocarotenoids (represented by a star in Figure 6-2) were detected but not quantified. Therefore, the total amount of ketocarotenoid is under-estimated and this could explain the lack of stoichiometry. Another cause may be the action of carotenoid cleavage dioxygenase enzymes (CCD), which could degrade the newly formed ketocarotenoids in the plants or β-carotene. This hypothesis is strengthened by the fact that no ketocarotenoids are endogenously synthesised in plants and consequently, they might be targeted preferentially for degradation as non-endogenous compounds, with presumably no defined sequestration mechanisms. The production of ketocarotenoids in the ZW containing lines was also connected to decreased levels of neoxanthin, violaxanthin and sometimes lutein (Figure 6-6; Figure 6-7). A decrease of β-carotene level could have a negative impact on violaxanthin and neoxanthin levels, since β-carotene is upstream in the carotenoid pathway (Figure 1-20). Moreover, according to Misawa (2009), β-carotene is not the only endogenous carotenoid precursor of the ketocarotenoid pathway in tobacco leaves but zeaxanthin and lutein can also be directly transformed into ketocarotenoids (Figure 6-8). Thus, it could explain the reduction of the lutein levels in the ZW containing lines.
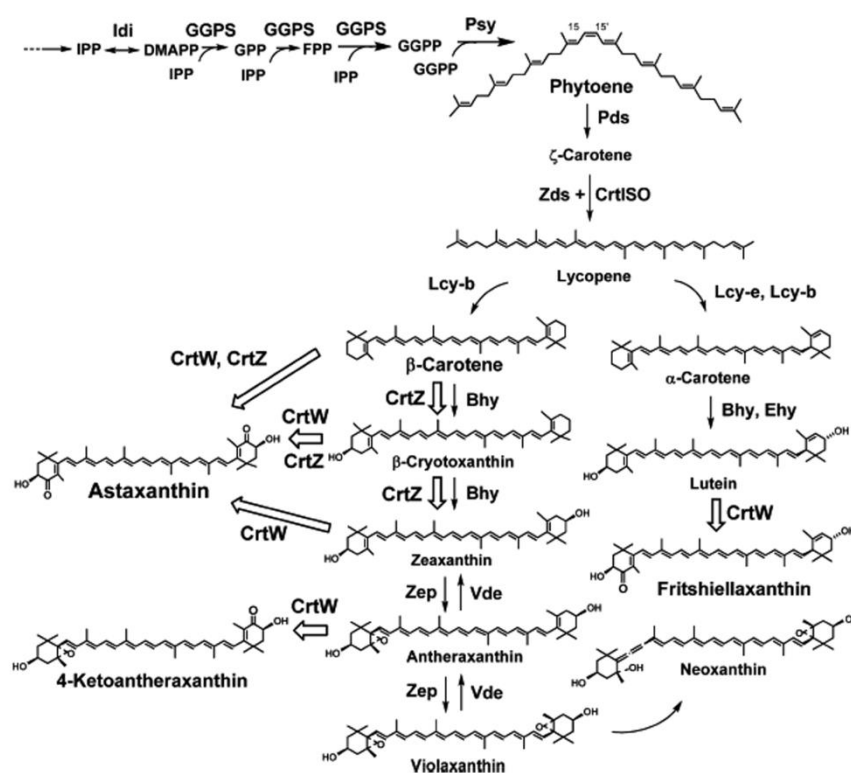
Figure 6-8 Carotenoid biosynthetic pathway in plants and the catalytic functions of *Crt*W and *Crt*Z introduced and expressed in tobacco leaves (Misawa, 2009)

Fritshiellaxanthin corresponds to 4-ketolutein. IPP, isopentenyl diphosphate (pyrophosphate); DMAPP, dimethylallyl diphosphate; GPP; geranyl diphosphate; FPP, farnesyl diphosphate; GGPP, geranylgeranyl diphosphate; Idi, IPP isomerase; GGPS, GGPP synthase; Psy, phytoene synthase; Pds, phytoene desaturase; Zds, zcarotene desaturase; CrtISO, carotene isomerase; Lcy-b, lycopene β-cyclase; Lcy-e, lycopene ε-cyclase; Bhy, β-carotene hydroxylase; Zep, zeaxanthin epoxidase; Vde, violaxanthin de-epoxidase; Ehy, ε–carotene hydroxylase.

6.3.2. *N. benthamiana* as an evaluation platform of transcription factors

In this study, *N.benthamiana* was the best system tested to transiently produce large quantities of diverse ketocarotenoids (Figure 6-3). Therefore, it was the platform of choice to test the potential effect of transcription factors on carotenoid levels. Transient gene expression systems have multiple advantages. A transient system is rapid, flexible and straightforward (Kapila et al., 1997; Fischer and Emans, 2000). Numerous genes present in different population of *Agrobacterium* can be simultaneously expressed. It can be used to produce substantial quantities of proteins

in a matter of weeks (Twyman et al., 2003). The expression level of proteins can be enhanced by co-expressing the p19 gene from the tomato bushy stunt virus, which helps the suppression of gene silencing (Voinnet et al., 2003). Transient expression systems have been previously used for a broad range of purposes, such as characterising a novel gene expression (Zhao et al., 2013), studying gene silencing (Bhagwat et al., 2013; Kumar et al., 2013), and producing high-value compounds, such as artemisinin precursors (Van Herpen et al., 2010). In this study, *N. benthamiana* transient system was used to evaluate the potential of transcription factors for ketocarotenoid production. Overexpressing select transcription factors coordinately with *Crt*W and *Crt*Z genes in plants was the strategy of choice to optimise the production of ketocarotenoids, as similar strategies were successfully exploited previously. For instance, the overexpression of the ARABIDOPSIS PSEUDO RESPONSE REGULATOR2-LIKE gene (APRR2-Like), which was identified by artificial neural network inference analysis, increased plastid number, area, and pigment content, enhancing the levels of chlorophyll in immature fruits and carotenoids in red ripe fruits (Pan et al., 2013). The expression of the two transcription factors Delila and Rosea1 genes from snapdragon in tomato, which induce anthocyanin biosynthesis in snapdragon flower, led to higher content of anthocyanins in the transgenic tomatoes (Butelli et al., 2008). Silencing of the ethylene response factor SIERF6, which was identified by correlation network analysis, enhanced both carotenoid and ethylene levels in tomato (Lee et al., 2012).

However, in general, most of the transcription factors are poorly characterised. Therefore, selecting and testing in a stable manner the appropriate transcription factors, which positively regulate the pathway of interest, is time-consuming. The option of transient transformation of plants to test transcription factors is therefore suitable. In the knowledge that the levels of proteins and metabolites produced depend on the number of days post infiltration, as it was shown in Figure 6-6 and Figure 6-7, it is necessary to verify which period of incubation is optimal. In this study, two periods were tested (i.e. 4 and 8 days post infiltration); the longer period was the more appropriate for this work, since greater amounts of ketocarotenoids were produced. Nevertheless, other time periods could be tested to ensure the selection of the best conditions for ketocarotenoid production. The *N. benthamiana* platform is ideal to evaluate transcription factors when the final aim is to stably transform *N. benthamiana* plants with the transcription factors. However, if the final

target is tomato plants or other plant species, the results transiently obtained in *N. benthamiana* may vary in the stably transformed plants. Results from the *N. benthamiana* platform should then be only used as indications.

Futhermore, the *N. benthamiana* evaluation platform could be translated into a ketocarotenoid production platform by scaling up the system as it is done at the Fraunhofer institute, (http://www.fhcmb.org/technology/overview; www.fhcmb .org/our-story-video; Figure 6-9).
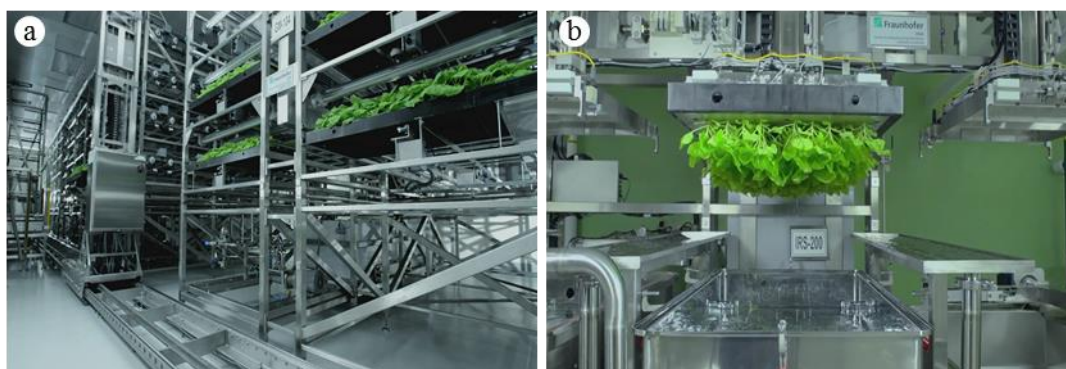
Figure 6-9 Innovative protein production platform at Fraunhofer, USA

Large scale production of *N. benthamiana* plants (a), which are transiently transformed by submersion in a tank containing *Agrobacterium* culture harbouring the vector of interest and under vacuum (b). The vaccines and therapeutics are then purified from the transformed tobacco plants.

6.3.3. Evaluation of PIF5 and ARR14 in optimising ketocarotenoid production

In order to adapt to the environment, plants continuously monitor and respond to changes in red and far-red lights via phytochromes, which are plant photoreceptors. Phytochrome Interacting Factor 5 (PIF5), a basic helix-loop-helix transcription factor, belongs to the PIFs family. The Phytochrome Interacting Factors directly bind to photoactivated phytochrome and control light-regulated gene expression (Castillon et al., 2007). They play negative roles in light responses as light activated phytochromes are responsible for post-translational inhibitions of PIFs via promoting their degradation and directly or indirectly preventing their binding to DNA (Jeong and Choi, 2013). Red light induces rapid phosphorylation and subsequent degradation of PIF5 through the proteasome system (Shen et al., 2007). PIF5 was shown to act on ethylene biosynthesis (Khanna et al., 2007) and on the regulation of

the phytoene synthase gene and therefore carotenoid biosynthesis (Toledo-Ortiz et al., 2010). A model of PSY regulation via the PIFs has been proposed (Figure 6-10). Manipulating levels of PIF transcription factors is therefore a potential strategy to act on carotenoid levels. Moreover, if the expression of PIF5 is synchronized with the expression of *Crt*Z and *Crt*W, then a modification of ketocarotenoid levels could be anticipated.
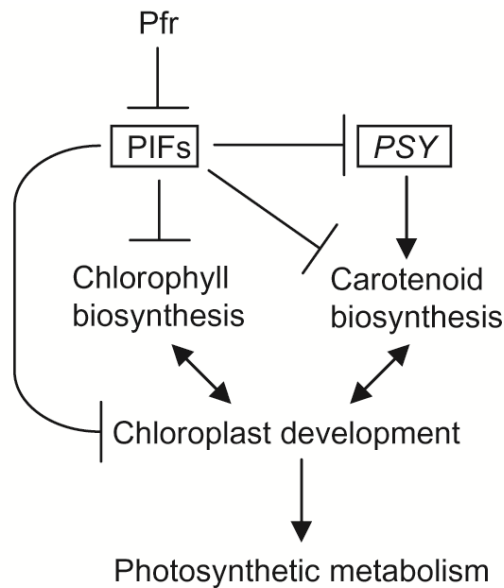
Figure 6-10 Model for the role of PIFs in regulating photosynthetic metabolism during seedling development (Toledo-Ortiz et al., 2010)

In dark-grown seedlings, high PIF1 levels repress PSY gene expression by direct binding to its promoter. PIFs also repress other genes involved in carotenoid biosynthesis (likely by indirect pathways), as well as genes required for the biosynthesis of chlorophylls and the differentiation of etioplasts into chloroplasts (such as those encoding components of the photosynthetic apparatus). All of these genes are rapidly and coordinately derepressed when PIFs levels drop on illumination, when photoactivated phytochromes (Pfr form) migrate to the nucleus and interact with PIFs to promote their degradation. This leads to a rapid production of carotenoids and chlorophylls together with components of the photosynthetic machinery in an interdependent fashion, eventually resulting in the development of functional chloroplasts and the transition to photosynthetic metabolism.

In this study, the transient overexpression of ZW-PIF5 combination of genes in *N.benthamiana* did not increase the levels of ketocarotenoids compared to ZW expression alone (Figure 6-6). This result does not seem very surprising as PIF5 has, in the dark, a negative effect on carotenoid biosynthesis (Figure 6-10). Only if the

overexpression of PIF5 led to silencing, carotenoid and therefore ketocarotenoid contents could have been increased. Consequently, an antisense strategy seems more appropriate, although it could have detrimental effects on the plants, since PIFs have essential and far reaching roles.

Little is known about the Arabidopsis Response Regulator 14 (ARR14), except that it plays a role in modulating the cellular response to cytokinin (Mason et al., 2005) and potentially in light signalling (D'Agostino and Kieber, 1999). This transcription factor was selected through correlation network analysis for its potential effects on carotenoid biosynthesis (Misawa et al., unpublished). Indeed, the overexpression of this transcription factor in coordination with the *Crt*Z and *Crt*W genes had a positive effect on the levels of ketocarotenoids (Figure 6-7). Levels of ketocarotenoids (i.e. adonixanthin, pheonicaxanthin, canthaxanthin and echineone) were significantly increased (1.3- to 1.5-fold) in ZW-ARR14 compared to ZW. Consequently, the coordinated expression of ZW-ARR14 was a successful strategy to transiently increase levels of ketocarotenoids in *N. benthamiana.* Additional analyses need to be performed in order to further our understanding of the regulation mechanisms of the carotenoid pathway by ARR14 transcription factor.

6.3.4 *Nicotiana glauca* as a multipurpose plant

The interesting properties of *Nicotiana glauca* make it an attractive plant to be used as a multipurpose system, as it was described in section 6.2.3. Previously, *N. glauca* was successfully transformed with ZW in a stable manner. The transformed plants had pink/orange coloured flower and leaves but no detrimental effects were observed (Mortimer et al., unpublished).

Figure 6-10 Phenotypes of the wild type and ZW *Nicotiana glauca* (Mortimer et al., unpublished)

Scale bars are 3cm for flower images and 8cm for images of aerial parts.

Transiently overexpressing *Crt*Z, *Crt*W and ARR14 genes proved to be a valuable strategy to optimise the production of ketocarotenoids in plants (as described in section 6.3.3). Therefore, stable transformation of ZW-ARR14 was undertaken in *N. glauca,* but all attempts failed. Consequently, it suggests that the expression of ARR14 under the control of the 35S constitutive promoter was detrimental resulting in no regeneration of the calli. A tissue specific or an inducible promoter may overcome this lethal effect, facilitating controlled expression of the ARR14 transcription factor when the vigour of the plant is vulnerable (i.e. an early developmental stage).

Chapter VII: General discussion

7.1 Summary and general conclusions

7.1.1 Summary

The overarching aim of this PhD study was to optimise the production of high-value carotenoids and ketocarotenoids in higher plants, especially tomato and tobacco. Several metabolic engineering strategies were used and assessed.

The first objective was to evaluate the potential benefits of simultaneously overexpressing two bacterial carotenoid genes in plants compared to single independent expression (Chapter III). Three genes (*Crt*E, *Crt*B and *Crt*I) and their combinations (*Crt*E+B, *Crt*E+I and *Crt*B+I) were studied. *Crt*I and *Crt*B genes had the greatest impact on fruit carotenoid levels. Moreover, in the hemizygous state, the expression of *Crt*B+I genes in combination had a synergistic effect on the formation of high value carotenoids (i.e. lycopene, β-carotene) compared to the expression of *Crt*B and *Crt*I independently. This direction of research also highlighted the positive correlation between gene dosage, the level of carotenoids and regulation mechanisms operating in response to altered carotenoid contents.

The second objective was to further our understanding of the plants adaption mechanisms to perturbed carotenoid contents at the level of fruit and in the chromoplast (Chapter III), but also at a sub-chromoplast level (Chapter IV). These studies focused on the *Crt*B+I tomato lines, the best *Crt* combination line in terms of carotenoid levels. Changes in transcription, plastid ultrastructure and levels of primary and secondary metabolites were observed in *Crt*B+I. Special attention was given to the sequestration of the carotenoids and related regulatory mechanisms were revealed and proposed within the different tomato tissues and sub-chromoplast compartments.

The third objective was to optimise the production of carotenoids by using a promoter, whose timing and strength of expression was thought to be more appropriate for the carotenoid pathway compared to the ones utilised previously (Chapter V). The chromoplast specific lycopene β-cyclase promoter from the orange fruited *Solanum galapagense* was chosen to control the expression of the *Crt*B and *Crt*I genes. Results were unexpected, as carotenoid production was only slightly increased in fruits, whereas accumulation of β-carotene was observed in the seeds.

211

The reasoning underlying these findings is discussed in section 5.3.2 of chapter V. Moreover, the unexpected expression of the *Crt*B and *Crt*I genes in the seeds gave insights into the carotenoid pathway in tomato seeds (Figure 5-11).

The fourth objective was to optimise the production of high-value ketocarotenoids via combining the expression of ketocarotenoid genes (*Crt*Z and *Crt*W), with transcription factors potentially related to carotenoid regulation (PIF5 and ARR14). A transient transformation platform of *N.benthamiana* was developed and the ARR14 transcription factor was found to positively upregulate the formation of ketocarotenoids (Chapter VI).

Carotenoid and ketocarotenoid formation in higher plants occurs in complex branched pathways (Figures 1-9 to 1-14). Multiple enzymes, which sometimes catalyse more than one enzymatic step, are involved. Consequently, optimising high-value compound production is not straightforward. However, it was shown in this study that overexpressing several genes, the corresponding enzymes of which can work synergistically, is a good option to increase high-value isoprenoids. The choice of the gene overexpressed is essential as well as the timing and strength of expression of the heterologous genes. It was noticed that the identity and quantity of the carotenoids produced could trigger different regulatory mechanisms of carotenoid formation and sequestration within the pathway. It is important to understand these regulation mechanisms, especially for the future rational design of isoprenoid metabolic engineering. The following sections focus on carotenoid regulation mechanisms, which were revealed by the study of the transgenic *Crt* lines.

7.1.2 Discussion on carotenoid regulation mechanisms

The comparison of the isoprenoid levels in the tomato fruits of *Crt*B, *Crt*I and *Crt*B+I hemizygous and homozygous lines gave insights into carotenoid pathway regulatory mechanisms in the transgenic plants (Table 3-1, Figure 7-1). The carotenoid patterns of the six lines were different, even between the same *Crt* lines with different zygosity states. The level of the product of the CRTB enzyme, phytoene, increased in the *Crt*B hemizygous line. However, in the homozygous line, it was not phytoene, which increased, but lycopene levels (Figure 7-1). The effect of the two copies of *Crt*B gene was the activation of the synthesis of lycopene. It seems that the phytoene synthesised by CRTB was not accumulated, but utilised by the

enzymes of the downstream pathway. If the assumption that two copies of *Crt*B gene lead to more phytoene content than a single copy is correct, it could mean that a greater quantity of phytoene induced the formation of an enzyme complex (possibly, a metabolon of PDS, ZDS, ZISO and CRTISO). Thus, this could explain the unchanged levels of phytoene with the increased levels of lycopene in *Crt*B homozygous. Formation of transient enzyme complexes is a metabolic system, which provides a rapid and efficient regulation of metabolism (Jorgensen et al., 2005). Other examples of metabolite-induced metabolons are described in the literature (Norris et al., 1999; McKenna et al., 2006; McKenna, 2011). Metabolite-induced metabolons are fast and adaptable systems, which can react to changes in the environment (for instance, the level of a specific metabolite in the plastid) and provide rapid adaptation. Metabolite-induced metabolons are a faster regulatory system than transcriptional regulation (Norris et al., 1999). Another possibility is that the metabolon is stable and already present but maybe not working at its fastest pace in hemizygous *Crt*B. The higher content of phytoene, in homozygous *Crt*B, may have induced a change in the metabolon's catalytic activity. In the *Crt*I containing lines, although the pattern of carotenoid changed, three aspects remained the same. There was always an increase of β-carotene and α-tocopherol levels and a decrease of phytoene levels. It appears that the presence of the *Crt*I gene, and therefore an increase of lycopene level, always induced the formation of β-carotene. Moreover, the level of *Ggpps-2* mRNA was increased and that of *Psy* was decreased (Figure 7-1). Consequently, these combined data suggest that there was a negative feedback mechanism on phytoene content, which was previously described (Al-Babili et al., 1999; Romer et al., 2000), but also a positive feedback mechanism on α-tocopherol content. They both seem to be induced by the level of β-carotene or a molecule resulting from its transformation/degradation. The homozygous *Crt*I and hemizygous *Crt*B+I plants both had greater levels of both lycopene and β-carotene, compared to the control AC. It may be that the level of lycopene induced by two copies of *Crt*I or one copy of *Crt*B, plus one copy of *Crt*I, are equivalent and consequently, the effects on the carotenoid pathway were similar. However, when two copies of *Crt*B and two copies of *Crt*I were present, there was only an increase of β-carotene level. This suggests that the regulation was different in this case. Moreover, in the homozygous *Crt*B+I, β-carotene cyclase enzyme (LCY-B) seemed to be up-regulated as its

mRNA level was increased (Figure 7-1). It is plausible that LCY-B was recruited to regulate the high content of lycopene, as the CYC-B fruit-specific enzyme was saturated. The formation of a lycopene-induced metabolon formed with CRTI and LCY-B could also be proposed to explain the homozygous *Crt*B+I lines. It is also interesting to note that the increase in total carotenoid levels was always linked to the increase in lycopene level. This means that it is only when levels of lycopene were changed that the flux of the carotenoid pathway was improved. In the other cases, only the concentration control was modified and not the flux control of the pathway (Morandini, 2013).
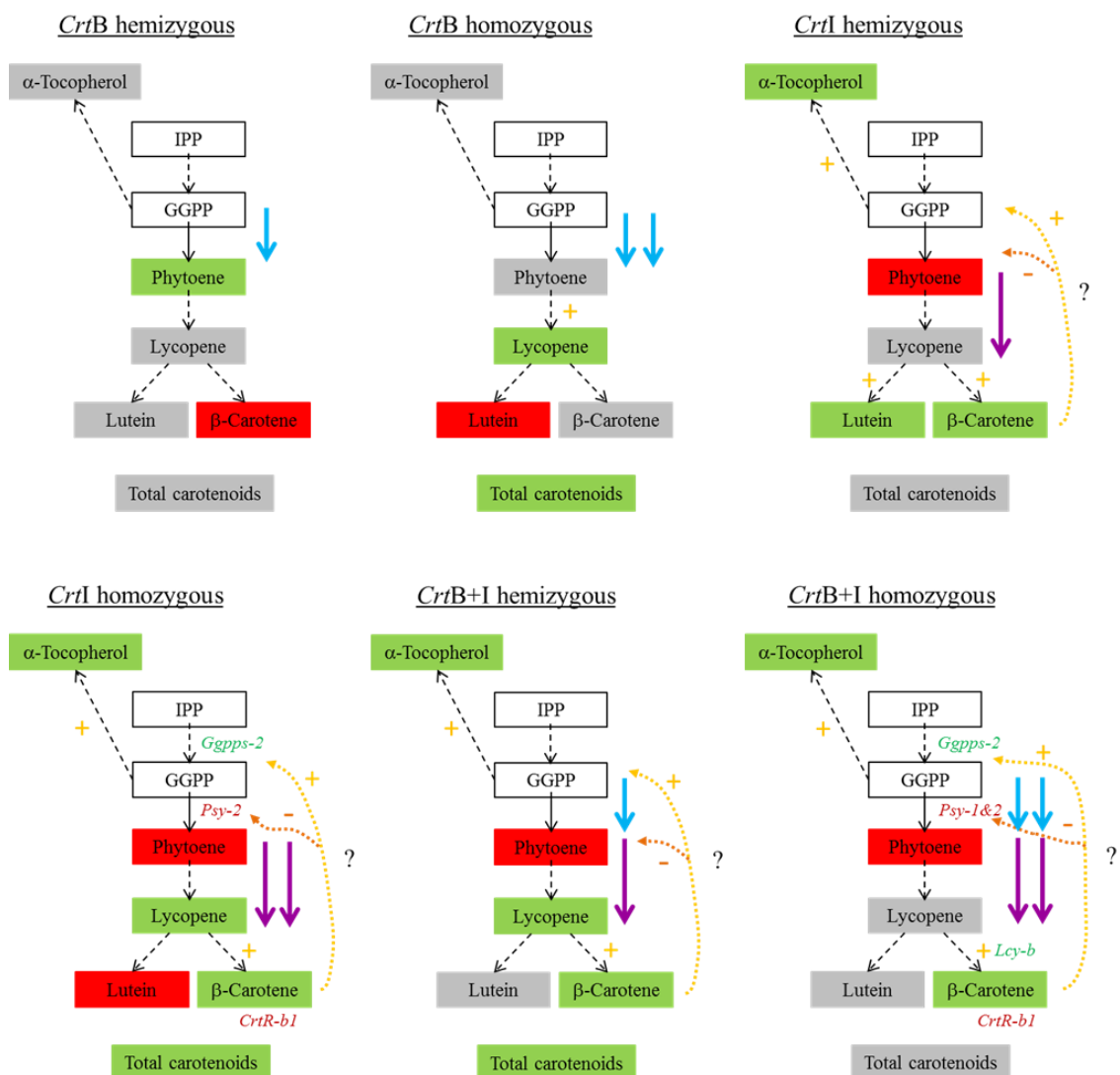
Figure 7-1 Carotenoid metabolite and transcript changes in *Crt* lines

This figure combines data from Table 3-1 and Figure 3-5. Carotenoid metabolites are represented as squares. The mRNAs are represented by their name of corresponding gene in italics. Green indicates a significant increase compared to the control AC. Red shows a significant decrease, grey corresponds

to no significant changes and white, not determined. Statistical tests (Dunnett's) were used to determine the significance (p-value < 0.05). Arrows indicate a catalytic step. Solid arrows represent a single step; dashed arrows, several steps. Blue arrow indicates CRTB enzyme; purple, CRTI enzyme. +, positive activation. -, negative activation. IPP, isopentenyl diphosphate; GGPP, geranylgeranyl diphosphate; *Ggpps-2*, geranyl diphosphate synthase 2; *Psy1&2,* phytoene synthase-2; *Lcy-b*, β-lycopene cyclase; *CrtR-b1,* carotene β-hydroxylase 1.

The same pattern of carotenoid regulation, which is associated with the dose of gene, was observed in the study of the pb-*Crt* lines (Chapter V), but only in pb-*Crt*B+I and with at least 9 inserts. The pb promoter was not very efficient, presumably explaining why 9 inserts (9 x B+I) are necessary to equal the effect in the *Crt*B+I homozygous line (2 x B+I). The lack of correlation between the dose of gene and the levels of carotenoids in pb-*Crt*B and pb-*Crt*I may be due to the fact that levels of expression are too low to really be influential and trigger regulatory mechanisms.

As discussed in the previous section, the regulation of the carotenoid pathway appears to be a fine-tuned mechanism, which could be induced by carotenoid levels. The transcriptomic data (Figure 3-5, Figure 7-2) brings a second aspect to carotenoid regulation. In the homozygous *Crt*B+I transgenic leaves, only fruit specific and flower specific mRNA levels, corresponding to enzymes downstream of CRTI, were increased. Moreover, as described in the previous section, in the transgenic fruit, it seems that the LCY-B enzyme activity was induced. This suggests that carotenoid levels in the transgenic plants are not able to be regulated only by the enzymes, which are already highly active in this specific tissue. Therefore, ectopically expressed enzymes, whose activity is negligible in this particular tissue, are utilised to take part in the regulation of the additional carotenoids as it is shown in Figure 7-2.
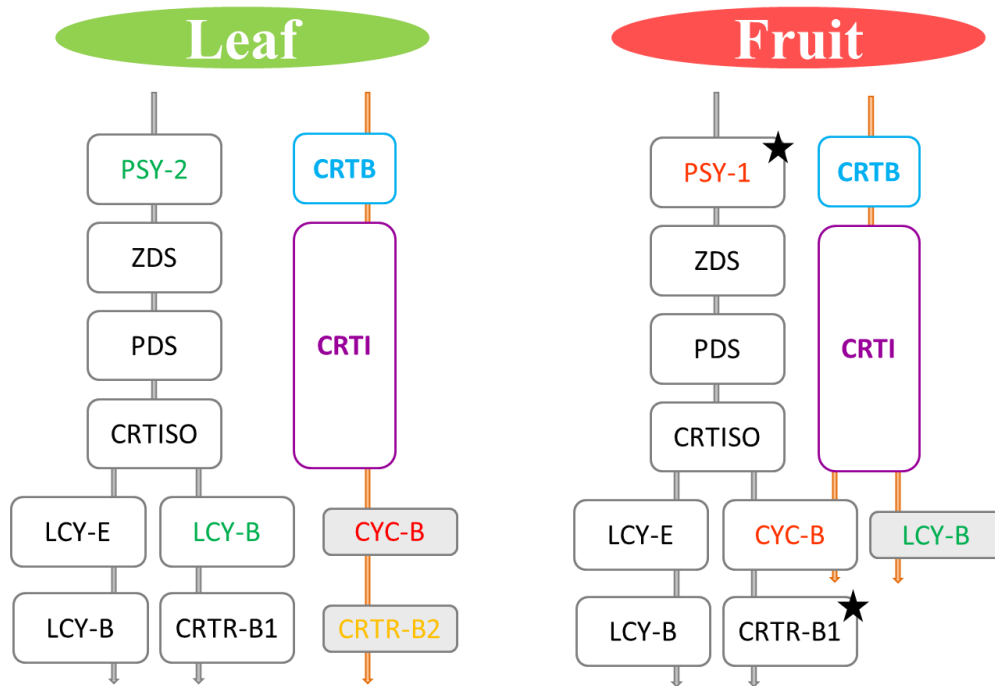
Figure 7-2 Putative induction of the endogenous carotenoid enzymes in *Crt*B+I leaves and fruits

Data are based on carotenoid transcript and metabolite levels. Pathway of the AC control is indicated in grey. Enzymes are represented as rectangles. Endogenous enzymes correspond to the grey rectangles. The CRTB and CRTI heterologous enzymes are shown in blue and purple, respectively. The grey rectangles filled in grey represent enzymes which are almost not active in the specific tissue of the control AC. Green, red and orange indicate tissue specificity of the enzymes, leaf, fruit and flower, respectively. The black star shows a decrease of mRNA levels in *Crt*B+I. PSY-1, fruit specific phytoene synthase-1, PSY-2, phytoene synthase-2; PDS, phytoene desaturase; ZDS, ζ-carotene desaturase, CRTISO, carotene isomerase; LCY-E, ε–lycopene cyclase; LCY-B, β-lycopene cyclase; CYC-B, fruit specific β-lycopene cyclase; CRTR-B1, carotene β-hydroxylase 1; CRTR-B2, carotene β-hydroxylase 2 (flower specific); ZEP, zeaxanthin epoxidase; NXS, neoxanthin synthase; VDE, violaxanthin de-epoxidase; CRTB, phytoene synthase; CRTI, phytoene desaturase.

The carotenoid levels also appear to have an effect on the distribution of carotenoids through the tomato tissues. Levels of carotenoids were measured in the pericarp, jelly and columella tissues of AC, *Crt*B, *Crt*I and *Crt*B+I tomatoes (Table 3-2). A representation of the hypothetical regulation of the carotenoid distribution in the transgenic tomato lines is shown Figure 7-3. The following hypothesis is based on two facts. The first is that, although the pericarp is the tissue most amenable to sequestrate carotenoid (greatest levels), the increase of lycopene and β-carotene

levels are greater in the columella (when changes do occur in the columella). This implies that the cell area left in the pericarp to store extra carotenoids is limited; otherwise it would be expected that the greatest increase of carotenoids would be in the pericarp. The second fact is that when there is an increase of carotenoids, it is at least always in the pericarp or in the pericarp plus the columella or in the three tissues, but never only in the columella or only in the jelly (Figure7-3). Therefore, the hypothesis is that there is a saturation limit for carotenoid storage in each tissue of the tomato. Carotenoids will be preferentially stored in the pericarp. If this is saturated then the carotenoids will be sequestrated in the columella and, lastly, in the jelly. Moreover, the saturation in carotenoids seems to be specific to each carotenoid. For instance, in *Crt*I, the pericarp is saturated with β-carotene but not lycopene (Figure 7-3). It is another aspect of the carotenoid regulation which appears to be dependent on the quantity and identity of the carotenoid.
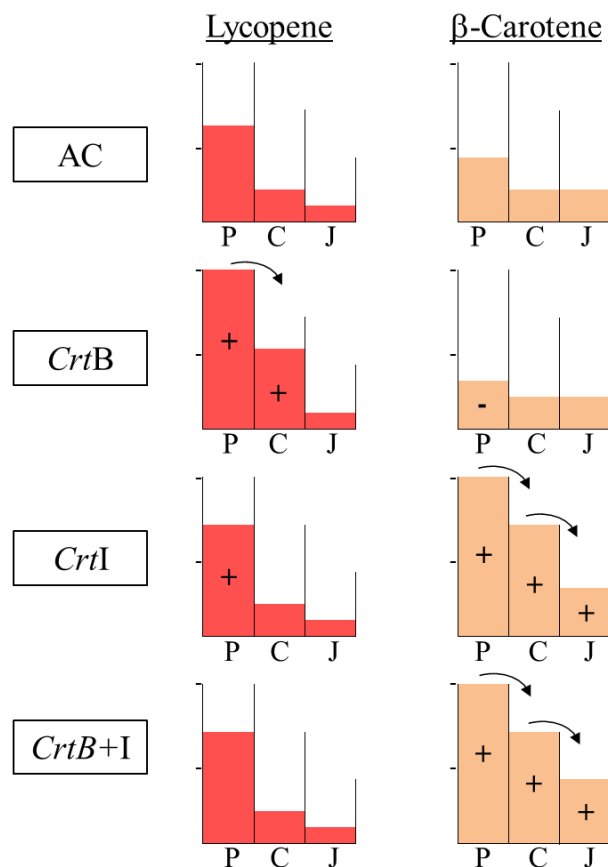
Figure 7-3 Interpretation of lycopene and β-carotene level changes in the different tissues of *Crt* lines tomato fruits

Scale is arbitrary. +, indicates a significant increase of carotenoid compared to the control AC; -, shows a significant decreased compared to AC. Statistical tests (Dunnett's) were used to determine significant changes. P, pericarp; C, columella; J, jelly.

Carotenoid regulation also occurs at the sub-chromoplast level. The localisation of the carotenoids within the chromoplast compartments (Figure 4-3) of *Crt*B+I and the control AC gave insight into the regulation of carotenoids, especially phytoene within the membranes of the chromoplasts. A hypothetical regulation mechanism is proposed (Figure 7-4). This is based upon the following findings: (i), phytoene was found in higher quantity in the plastoglobules of the control than in the plastoglobules of *Crt*B+I (Figure 4-3); (ii), the CRTB and CRTI enzymes were localised in the thylakoid membranes of *Crt*B+I (Figure 4-6); (iii) carotenoids were stored as crystals in the membrane (Figure 4-7) and this mechanism of sequestration was enhanced in *Crt*B+I (Figure 4-1); (iv) MGDG lipids appeared to take part in the regulation of the carotenoid sequestration via augmenting the flexibility of the chromoplasts membranes (Table 3-4, Figure 3-14). Combined, these data lead to the hypothesis that in AC all the phytoene is not utilised in the carotenoid pathway, and consequently, part of it is stored in the plastoglobules. However, in the transgenic line, the CRTB and CRTI enzymes, which may act as a complex with or without β-carotene cyclase enzymes (CYC-B and in the case of the homozygous line, LCY-B), recruit most of the phytoene into the carotenoid pathway and eventually formation of lycopene and β-carotene crystals is induced.
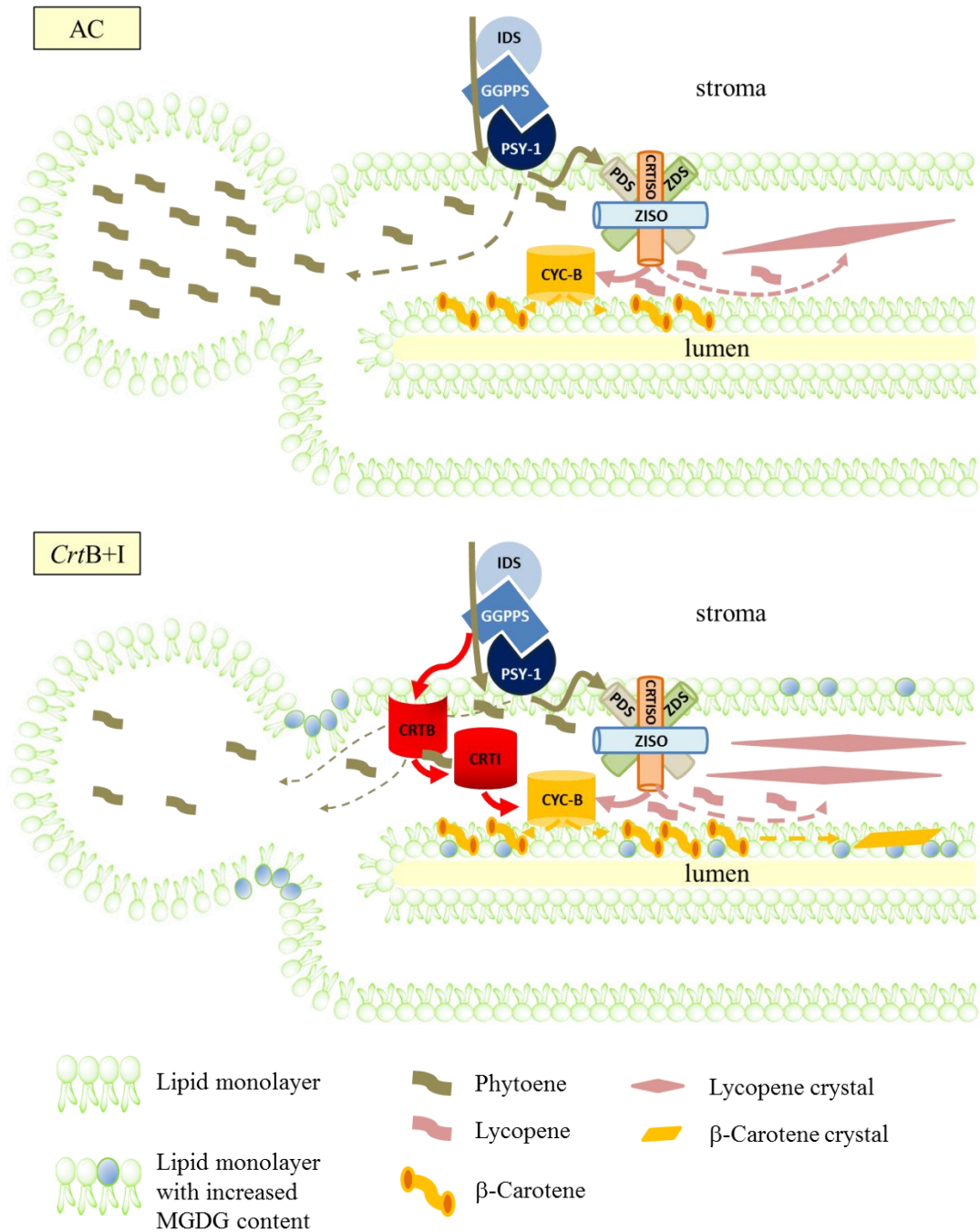
Figure 7-4 Schematic representation of the regulation of carotenoid production within the thylakoid-like membranes of AC and *Crt*B+I chromoplasts

In AC, the pool of phytoene, synthesised by PSY-1, can be used by PDS. However, at saturated levels, the excess phytoene appears to be sequestrated in the plastoglobules. Some lycopene and β-carotene are sequestrated in the thylakoid-like membranes and lycopene crystals are formed subsequently. In *Crt*B+I, although the pool of phytoene is greater due to the catalytic activity of CRTB, it is utilised by PDS and the excess by CRTI. Consequently, less phytoene is stored in the plastoglobules. A greater quantity of β-carotene and lycopene are formed, leading to the formation of carotenoid crystals. Solid arrows represent a catalytic step; dashed arrows indicate a movement of

carotenoid. The significant changes in the galactolipid content of the membranes are also illustrated. IDS, IPP/DMAPP; synthase; GGPPS, 1-geranylgeranyl pyrophosphate synthase; PSY-1, phytoene synthase-1; PDS, phytoene desaturase; ZDS, ζ-carotene desaturase; Z-ISO, 15-*cis*-ζ-carotene isomerase; CRTISO, carotene isomerase; CYC-B, β-lycopene cyclase; CRTB, phytoene synthase; CRTI, phytoene desaturase; MGDG, monogalactodiacylglycerol.

Regulation of the sequestration of carotenoids was also controlled via structural changes to the chromoplast structure (Figure 3-6, Figure 4-4). A schematic representation of the structural changes in the transgenic chromoplast is shown in Figure 7-5. It seems that in order to sequestrate more carotenoids, thylakoid membranes are maintained for a longer period, via the formation of thylakoid plexus. This allows the formation of more plastoglobules from thylakoid membranes. Moreover, the transgenic chromoplasts appear to create more internal envelope membranes, via the formation of membranous sacs. Carotenoids are stored in all these different types of membranous sub-compartments and especially as crystal-like structures. Therefore, plastoglobules, membranous sacs and thylakoid plexus are three subcompartments, which play an important role in carotenoid sequestration. Plastoglobules, as well as membranous sacs are created via a blistering mechanism from the thylakoid and inner envelope membranes, respectively (Austin et al., 2006). The plastoglobules are exclusively formed at areas of high curvature. Moreover, the lipid class MGDG has a high propensity for interfacial curvature (Figure 3-14) and the content of MGDG was 3.6-fold greater in *Crt*B+I chromoplasts compared to AC (Table 3-6). Altogether, this seems to indicate that MGDG could play an important role by allowing the membranes to curve, which could trigger the formation of plastoglobules and membranous sacs (Figure 7-4, Figure 7-5). Evidence that increase in MGDG content is due to an activation of its formation from the prokaryote pool was discussed in section 3.3.2. The prokaryote pool represents the lipid classes which are synthesised within the plastids (18:1 and 16:0). The eukaryote pool (18:2) is imported from the endoplasmic reticulum (Ohlrogge and Browse, 1995). It is coherent that activation of MGDG formation was done at a plastidial level, thus the regulation can be quicker compared to importing lipids from outside of the chromoplast. Moreover, the latter option may not even be possible at that stage of fruit development. Long lycopene crystals were found in AC and *Crt*B+I chromoplasts, but they appeared with different aspects. In AC, the lycopene crystals

were seen as multiple wavy lines, whereas in *Crt*B+I, only remnants of crystals were found. This may indicate a fundamental difference, but the reasons behind this alteration are unclear.
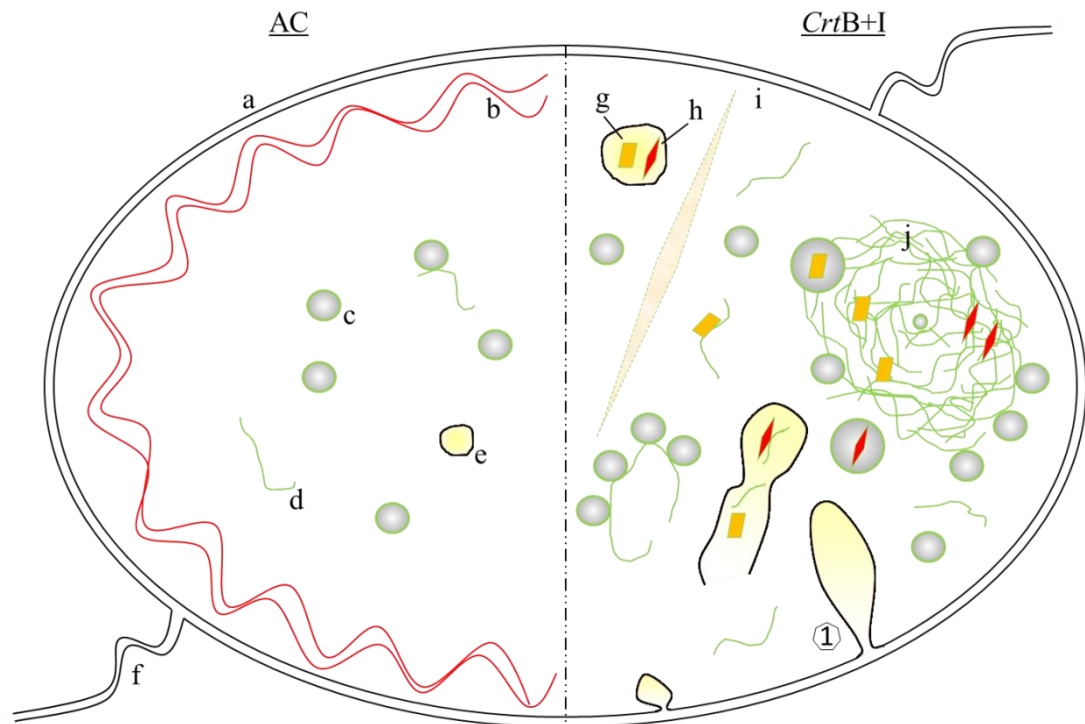
Figure 7-5 Schematic representation and interpretation of AC and *Crt*B+I sub-chromoplast structures observed by electron microscopy

The initial chromoplasts were stained with osmium tetroxide. a; envelope membranes, b; lycopene crystals in AC; c, plastoglobule; d, thylakoid membrane remnant; e, membranous sac; f, stromule; g, β-carotene crystal-like structure; h, lycopene crystal-like structure; i, remnant of lycopene crystals in *Crt*B+I; j, thylakoid plexus-like structure. The scheme shows the formation of the membranous sacs from the inner envelope of the chromoplast (1). This scheme is based on Figure 3-6 and 4-7.

Regulation of carotenoids is complex, dynamic and precise. An abundance of mechanisms are involved around their biosynthesis and sequestration. Therefore, it is difficult to predict the level of success of a genetic engineering strategy. Additionally, as it was observed in this study, the heterologous enzymes were not found in the same sub-chromoplast compartment as the endogenous homologues (Figure 4-6). They did not seem to interact with the same endogenous enzymes (recruitment of ectopic enzymes) and in the case of transient transformation, the heterologous enzymes seemed to be poorly functional (for instance *Crt*Z) or the

participation of the endogenous carotene hydroxylases had been restricted (Chapter VI). These are other aspects that can influence the success of the strategy. Furthermore, in Chapters III and V, the notion of timing and strength of gene expression was addressed. It was discussed that the timing of carotenoid gene expression must be extremely precise within a tight period of the fruit development in order to have the best impact on carotenoid levels without having detrimental effects. In Chapter VI, lethal effects due to the association of a constitutive promoter with ZW-ARR14 during stable transformation were observed (section 6.2.3). In consequence, the choice of the promoter is another aspect, which must be approached carefully. Plant codon use and a potent 5′ UTR are two features used in the constructs of Chapters V and VI. They enhance the expression and translation of the heterologous genes. The advantages of these strategies were discussed in section 6.3.1. All the aspects described in this section are important and should be addressed in order to optimise the production of high-value carotenoids and ketocarotenoids in plants.

Although more and more parameters of genetic engineering are tested and improved in order to optimise the production of metabolites in plants, this study reveals that knowledge on the regulation mechanisms of the carotenoid pathway achieved by the plant in order to adapt to elevated contents is key to pursuing this challenge.

7.2 Relevance to current understanding

7.2.1 Production of carotenoids and ketocarotenoids in plants

Tomato lines producing up to 3500 μg/g DW of total carotenoid, 2700 μg/g DW of lycopene and 800 μg/g DW of β-carotene were engineered (Table 3-1). These levels are comparable with the highest levels of carotenoids previously reported in tomato fruit metabolic engineering studies (Fraser et al., 2002; Enfissi et al., 2005; Apel and Bock, 2009, Table 1-2). Moreover, knowing that the rate conversion of β-carotene to vitamin A is 12:1, only 75 to 150 g FW of *Crt*B+I tomato (i.e. ca. one tomato) fruit provides the daily recommended dietary allowance for vitamin A, which is 500 μg for a children, 800 μg for a female and 1000 μg for a male. It is 4 to 20 times less than the amount recommended for engineered maize (Naqvi et al., 2009), potato

222

(Diretto et al., 2007b), cassava (Welsch et al., 2010) and carrot (Maass et al., 2009) plants (Table 1-2). Additionally, the *Crt*B+I tomato fruits contain high levels of lycopene, which was shown to also have health-promoting antioxidant activities (Fraser and Bramley, 2004; Zhu et al., 2013). Therefore, biofortified tomato plants with enhanced antioxidant content (β-carotene and lycopene) have been created.

In a period of 8 days, 500 μg/g DW of ketocarotenoids were transiently produced in *N. benthamiana.* This level could be further enhanced by extending the period of agro-infiltration. Transient production of ketocarotenoids has not been reported previously. The highest levels of ketocarotenoids have been achieved via stable transformation of tobacco plants (leaves and nectary; Hasunuma et al., 2008, Mortimer et al., unpublished; Hernandez-Marin et al., 2013, Table 1-2). Astaxanthin and canthaxanthin are valuable ketocarotenoids due to their natural colour and their health-promoting antioxidant activities (Hernandez-Marin et al., 2013). In section 6.3.2, a possible *N.benthamina* transient transformation platform, which could be used for industrial production of these high-value ketocarotenoids, was discussed.

Different strategies are used to genetically engineer plants with higher contents of carotenoids (section 1.3, Table 1-2). The carotenoid pathway itself can be targeted or the formation of its precursors or the storage capacity of the carotenoids can be modified. However, the results of this study showed that the regulation of the carotenoid pathway is a very complex and sensitive system, and that could impact on the strategy chosen in unpredictable ways. This study reveals that carotenoid regulation and signalling systems are important factors that must be taken into account when considering which engineering strategy to choose.

7.2.2 Isoprenoid/carotenoid pathways regulation and signalling system

Contrary to other organisms, the biosynthesis of isoprenoid in plants takes place within two distinct compartmentalised pathways, the mevalonate (MVA) and the 2-C-methyl-D-erythritol 4-phosphate (MEP) pathways (Figure 1-2). The co-existence of these pathways in the cytosol and in the plastids, respectively, allows the synthesis of a multitude of isoprenoid molecules with a wide range of physiological processes. This unusual dynamic is presumably an essential process for the interaction of plants with their environment (Hemmerlin et al., 2012). Moreover, since isoprenoids are part of such a diverse range of plant processes, their biosynthesis needs to be

specifically coordinated with these mechanisms. For instance, the roles of carotenoids in photosynthesis, photomorphogenesis and plant development suggest that their biosynthesis is regulated with processes such as plastid biogenesis, flowering and fruit development (Bramley, 2002; Fraser and Bramley, 2004; Lu and Li, 2008). Consequently, regulation of isoprenoids is complex, multifaceted and acts at multiple levels in the plants.

The state of the art of isoprenoid, and more precisely carotenoid, pathway regulation in plants is presented in the next section. However, isoprenoid regulation mechanisms can differ between plant species as it was discussed in section 3.3.1. Therefore, the regulation mechanisms described here are general and may not be present in all plants.

Pathway regulatory nodes correspond to rate limiting enzymes, whose activities are slow and therefore represent steps with great influence over the pathway. It was common assumption to think that there was a unique rate limiting enzyme within each pathway, which had the control of the entire metabolic flux. However, it seems that it is a rare case and that most often control of the flux is shared between many enzymes (Morandini, 2013; Vranova et al., 2013). Several regulatory nodes have been identified within the upstream isoprenoid pathway and carotenoid pathway, such as 3-hydroxy-3-methylglutaryl-CoA reductase (HMGR), 1-deoxy-D-xylulose 5-phosphate synthase *(*DXS*)*, 4-hydroxy-3-methylbut-2-enyl diphosphate reductase (HDR) and phytoene synthase (PSY) enzymes (Botella-Pavia et al., 2004; Cazzonelli and Pogson, 2010; Hemmerlin, 2013; Vranova et al., 2013). To date, there is only one example where flux control coefficients have been obtained to illustrate unequivocally that phytoene synthase is the most influential step in the formation of fruit carotenoids (Fraser et al., 2001). Due to their importance in controlling the metabolic flux of the pathway, these enzymes are under tight regulation. However, they are not the only ones to be controlled. For instance, the carotenoid isomerase CRTISO is regulated through an epigenetic process (Cazzonelli et al., 2009). Some of the regulation mechanisms occurring in the MEP pathway are represented in Figure 7-6. The following lists enumerate all the factors and processes involved in the regulation of carotenoids and isoprenoids.

Factors:

- o Light[1]
- o Circadian oscillations[2]
- o Other abiotic factors[3] (i.e. salt, drought, temperature)
- o Environmental biotic factors[4] (interaction with microbes and fungi)
- o Developmental cues[5] (conversion from protoplast to chloroplast; chloroplast to chromoplast; flower development; fruit ripening)

[1]Von Lintig et al., 1997; Park et al., 2002); [2]Thompson et al., 2000; Facella et al., 2008; [3]Welsch et al., 2008; [4]Vogeli and Chappell, 1988; Akiyama et al., 2005; [5]Bramley, 2002; Sandmann et al., 2006.

Processes:

- o Modulation of transcription

Pattern of carotenoid genes expression varies along with physiological processes, for instance the ripening of the tomato fruit (Bramley, 2002; Fraser and Bramley, 2004). Carotenoid transcription can also be regulated by transcription factors, such as phytochrome interacting factor (PIF; Toledo-Ortiz et al., 2010), SIER6 (Lee et al., 2012), APETALA2 (Chung et al., 2010; Karlova et al., 2011), RAP2.2 (Welsch et al., 2007), APRR2 (Pan et al., 2013). Most of them act on *Psy* expression.

- o Post translational regulation

Post translation regulation can act as a rapid response to environmental and physiological challenges. There are several regulatory mechanisms possible (Hemmerlin, 2013).

(i) Metabolite-enzyme interaction: Some metabolites can act as activators or inhibitors of gene expression, by interacting directly with the enzyme, through non-covalent binding, which modifies the enzymes' catalytical properties. This can occur during feedback modulations of enzyme activities by substrate/product accumulation (for instance, free CoA and HMG-CoA are described as the potential metabolites, which act on HMGR-CoA) or during the modulation of enzyme activities by the

isoprenoid intermediates (for example, the mevalonate kinase enzyme is found inhibited by downstream metabolites, principally FPP, but also IPP, DMAPP or GPP).
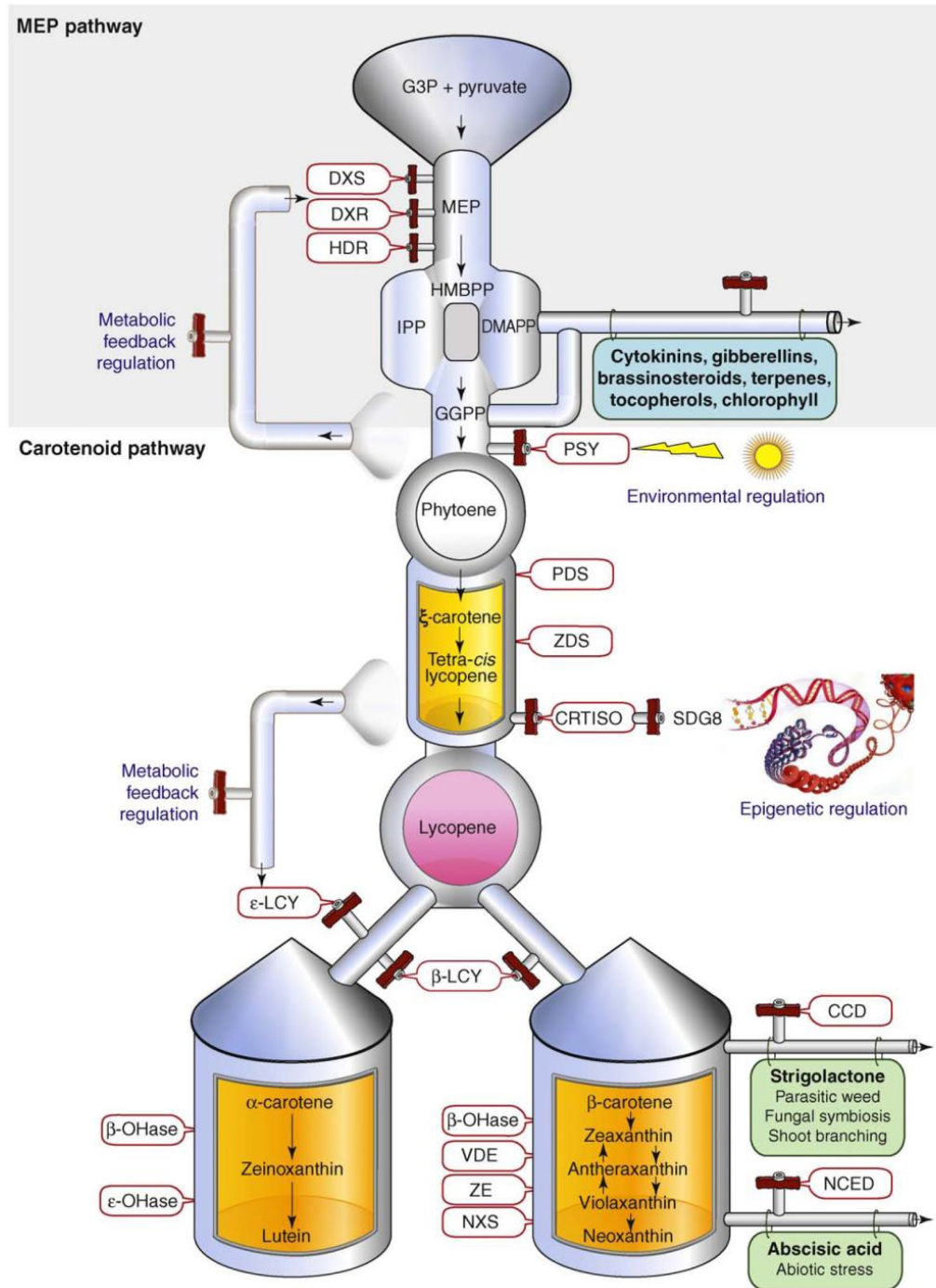
Figure 7-6 Major reactions in the higher plant carotenoid biosynthetic pathway (Cazzonelli and Pogson, 2010)

Enzymes (encircled in red), carotenoids and their precursors (pipes), carotenoid sinks (barrels), carotenoid-derived signalling hormones (green signs) and other MEP isoprenoid-derived metabolites

(blue sign). The windows displayed within the chrome pipes indicate abundant carotenoid pigments found in photosynthetic tissues and also represent key nodes for regulation in the pathway. Carotenoid biosynthesis is modulated by environmental factors (light), chromatin modification and metabolic feedback regulation. The side funnels represent examples of metabolic feedback control mechanisms acting upon biosynthetic gene expression as a result of altered PSY and CRTISO enzymatic activity, respectively. First, the bottleneck in phytoene biosynthesis is regulated by PSY and its overexpression increased DXS and DXR mRNA levels post-transcriptionally in etiolated tissues. Second, loss-of-function CRTISO mutants show reduced ε-LCY transcript levels in etiolated tissues. Abbreviations: β-LCY, β-cyclase; β-OHase, β-hydroxylase; CCD, carotenoid cleavage dioxygenase; CRTISO, carotenoid isomerase; DXR, 1-deoxy-D-xylulose 5-phosphate reductoisomerase; DXS, 1-deoxy-xylulose-5-phosphate synthase; ε-LCY, ε-cyclase; ε-OHase, ε-hydroxylase; GGPP, geranylgeranyl diphosphate; HDR, 1-hydroxy-2-methyl-2-(E)-butenyl 4-diphosphate reductase; NCED, 9-*cis*-epoxycarotenoid dioxygenase; NXS, neoxanthin synthase; PDS, phytoene desaturase; PSY, phytoene synthase; SDG8, histone methyltransferase; VDE, violaxanthin de-epoxidase; ZDS, ζ-carotene desaturase; and ZE, zeaxanthin epoxidase.

(ii) <u>Structural regulation</u>: The allosteric regulation of the enzyme can be done via modification of the enzyme structure, which causes variation of the enzyme activity. It can happen via changes in the primary structure of the enzyme or the organisation of the enzymes in multiprotein complexes (metabolon).

(iii) <u>Redox regulation</u>: Several enzymes in the isoprenoid pathway are thought to be redox regulated, such as HMGR-CoA and DXR.

Post translational modifications can be chemical, via modification of the amino acids (phosphorylation, glycosylation or ubiquitination), or linked with a proteolysis regulatory mechanism. Consequences of post translational regulation are the modification of enzyme activities, or their subcellular location, or the initiation of their degradation (Hemmerlin, 2013).

o   Modification of carotenoid sequestration

Organelle biogenesis, especially chromoplast biogenesis, has a great impact on the accumulation of carotenoids. There is a positive correlation between the area of storage available and the carotenoid content. Plant mutants with increased plastid area (number or size), such as the tomato hp-1 (*ddb1*), hp-2 (*det1*), and hp-3 (*zep*) mutants have shown a concurrent increase in carotenoid content (Liu et al., 2004; Kolotilin et al., 2007; Galpaz et al., 2008). The *Or* gene of the cauliflower mutant,

induces the differentiation of proplastids or other non-colored plastids into chromoplast. Therefore, it creates a metabolic sink for carotenoid biosynthesis and accumulation (Lu et al., 2006; Li and van Eck, 2007). Moreover, other proteins have been found to be part of the regulation of plastid biogenesis and to promote carotenoid accumulation. For instance, the HSP21 protein chaperone from tomato not only protects photosystem II from oxidative stress, but also induces the conversion of chloroplasts to chromoplasts and consequently the accumulation of carotenoids (Neta-Sharir et al., 2005; Carvalho et al., 2012). Several carotenoid-associated proteins such as CHRC, CHRD and fibrillin, which participate in the biogenesis of carotenoid-lipoprotein structures in chromoplast, have been characterised (Vishnevetsky et al., 1999). Expression of these genes is associated with chromoplast development and increased carotenoid content (Leitner-Dagan et al., 2006; Simkin et al., 2007; Kilambi et al., 2013). The acetyl-CoA carboxylase gene (ACCD), which is the only plastid-encoded gene involved in fatty acid biosynthesis (Kahlau and Bock, 2008), could also play an important part in chromoplast biogenesis (Barsan et al., 2010) and therefore, represents another potential regulatory gene.

o Control of carotenoid degradation and turnover

Degradation of carotenoids is performed by the carotenoid cleavage dioxygenase enzymes (CCDs). Therefore, the activity of the CCDs controls the rate of carotenoid turnover. Some of the apocarotenoids (end products) are linked with the abscisic acid (ABA) pathway. This phytohormone is involved in complex plant signalling mechanisms (Hirayama and Shinozaki, 2007; Golldack et al., 2013). Therefore, regulation of the degradation of carotenoids is another important node of control.

o Epigenetic regulation (Cazzonelli et al., 2009)
o Phytochrome-mediated pathway (Alba et al., 2000; Welsch et al., 2000)

In this study, heterologous genes were introduced in plants. Their expression led to increased content of carotenoids (Chapter III, IV and V) and to the production of ketocarotenoids, unknown metabolites in the plants (Chapter VI). Consequently, perturbation was created within the plant homeostatic system. When a plant system

faces disruption, it tends to regulate it and adapt to the perturbation if necessary. Several regulatory mechanisms were highlighted in this work: (i), transcription adjustment of carotenoid genes (ectopic or not; Chapter IV); (ii), structural adaptation of the chromoplasts and its sub-compartments (Chapter IV); (iii), modification of carotenoid storage location at different levels (tomato tissues and chromoplast sub-compartments; Chapter III and IV) and (iv) potential post translational regulation with the formation of metabolite induced transient metabolon (Chapter III).

The questions that remain are: How do these regulatory mechanisms work? What is the signal? In Chapter III, evidence that the increased carotenoid content induced changes in primary metabolite levels was presented (Table 3-4). It is likely that changes of carotenoid levels led to modified levels of ABA or/and even gibberellin (GA) and strigalactone (Figure 7-6). Previous studies reported the existence of feedback mechanisms from ABA to PSY (Welsch et al., 2000) and from ABA and GA to CHRD proteins (Vishnevetsky et al., 1999). Therefore, it strengthens the hypothesis that these phytohormones play an important role in the signalling system of the regulatory mechanisms described previously. It was also reported in the current study, how the levels of specific carotenoids could affect the accumulation and the storage of other carotenoids. Metabolite feedback mechanisms have been extensively reported; however, the molecular nature of the process remains unknown (Cazzonelli and Pogson, 2010). *Cis*-carotenes or *cis*-apocarotenoids have been proposed to act as signalling molecules of the carotenoid pathway (Kachanovsky et al., 2012). In human studies, the role of carotenoids and apocarotenoids as signalling molecules related to cancer and their modes of action have been described (Sharoni et al., 2012). There are two types of regulation and both involve transcription factors. In the first one, the carotenoid or apocarotenoid acts as a ligand and binds to a nuclear receptor, which activates its transcription factor function. For instance, in the case of the retinoid receptors, they are composed of two families of nuclear receptors (RAR and RXR). When the carotenoid or apocarotenoid binds to a RAR receptor, it hetero-dimerises with a RXR receptor and attaches to the promoter of a tumor suppressor gene to induce its expression. In the second system, such as in the case of the EpRE/ARE system, the transcription factors are bound to their cysteine rich inhibitory proteins and it is the interaction of carotenoids or apocarotenoids with the

inhibitory protein that activates the transcription factor. Additionally, the methylerythritol cyclodiphophshate (MEcPP) produced by the plastidial MEP pathway has been shown to regulate the expression of nuclear stress-response genes by retrograde signalling (Xiao et al., 2012), so it could also be a good candidate. Transposon elements are also believed to provide *cis*-acting regulatory elements that lead to changes in expression patterns (Kidwell and Lisch, 1997). They could be part of the carotenoid regulation and signalling mechanisms.

In order to have a complete vision of the isoprenoid metabolic network and its regulation systems, it is important to determine the sub-cellular and sub-plastidial location of the pathway enzymes. The compilation of recent proteomics studies have resulted in a hypothetical topology of the carotenoid biosynthetic pathway in maize chloroplasts (Figure 7-7, Shumskaya and Wurtzela, 2013). However, it is plausible that the topology of the carotenoid pathway differs from one plant species to another. Moreover, it is necessary to confirm these data using, for instance, immuno-detection techniques and yeast hybrid systems to verify the protein-protein interactions. The results from proteomics alone could be sometimes misleading, for example, when the protein of interest has not yet been identified in a particular subcompartment but in another one, or if there is no sequence available for the species studied and the comparison is done with another species that may have different sub-plastidial location for the protein of interest. Special care needs to be brought to the enzyme sub-plastidial localisations, since this knowledge is crucial to advance our understanding of the interaction within the carotenoid pathway and therefore facilitate the improvement of metabolic engineering strategies.
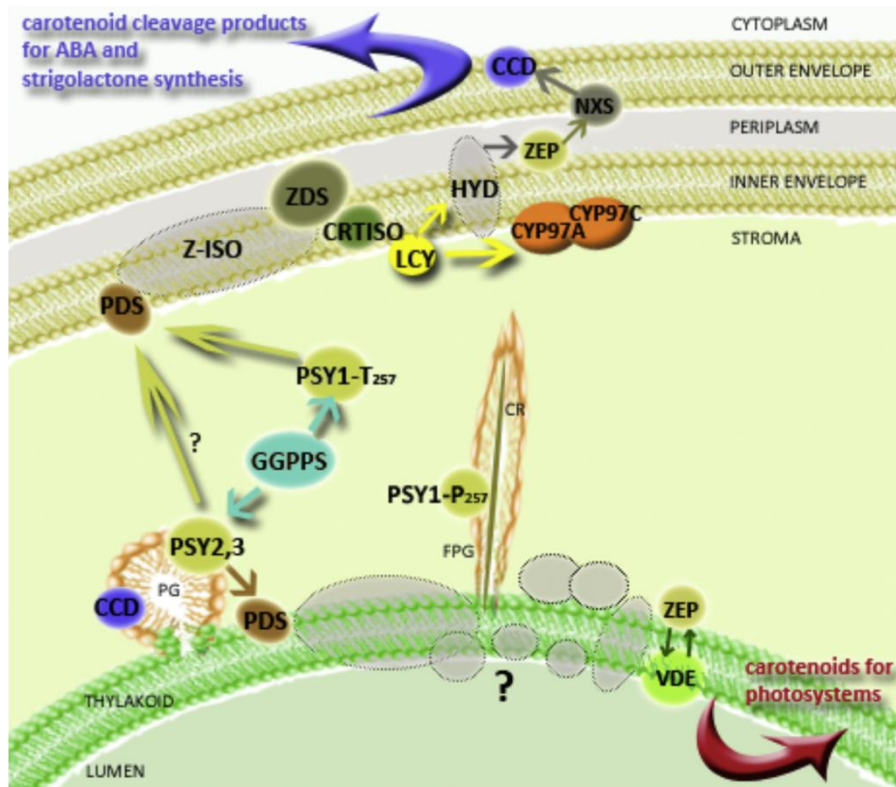
Figure 7-7 Hypothetical topology of carotenoid biosynthetic pathway in maize chloroplast (Shumskaya and Wurtzela, 2013)

Grey shadows: proteins were not localized experimentally. PG, globular plastoglobules; FPG, fibrillar plastoglobules; CR, hypothetical carotenoid crystals. GGPPS, geranylgeranyl pyrophosphate synthase; PSY, phytoene synthase; PDS, phytoene desaturase; ZISO, 15-*cis*-ζ-carotene isomerase; ZDS, ζ-carotene desaturase; CRTISO, carotenoids isomerase; LCYE, lycopene ε-cyclase; LCYB, lycopene β-cyclase; HYD, nonheme diiron carotene hydroxylase; CYP97A, P450 carotene hydroxylase 97A; CYP97C, P450 carotene hydroxylase 97C; ZEP, zeaxanthin epoxidase; VDE, violaxanthin de-epoxidase; NXS, neoxanthin synthase; CCD/NCED, carotenoid cleavage enzymes.

7.3 Future directions and recommendations

Further experiments could be performed to advance our understanding of how the plants respond and adapt to elevated carotenoid or ketocarotenoid content.

*Crt*B+I tomato lines (Chapter III and IV)

It would be interesting to look at the transcript levels of genes involved in the regulatory nodes of both the plastid localised MEP pathway and extra-plastidial mevalonate isoprenoid pathway, such as *hmgr* and *dxs*, to see whether changes in the carotenoid pathway induce a modification in the control points of the upstream isoprenoid pathway at a transcriptional level. The levels of the MEP pathway metabolites in response to carotenoid perturbation would also be interesting given their recent association with plastid to nuclear retrograde signalling (Xiao et al., 2012).

Knowledge of carotenoid enzyme activities and the determination of flux control coefficients, possibly at different time points during tomato ripening, would also be a very valuable addition to the work presented, to ascertain how enzymes respond to additional heterologous enzymes in the pathway and how the overall flux is controlled through the pathway. *In vitro* assays would give information about the enzyme activities and the flux control. The metabolite-induced transient metabolon theory needs to be investigated further. Blue native gels (Reisinger and Eichacker, 2006) could be used to isolate protein complexes and identification of protein components performed using modern proteomic (MS/MS) approaches. This could shed light on the existence and nature of a metabolon for CRTB+I as well as the endogenous enzymes. This knowledge could be utilised in the design of new engineering strategies such as using synthetic protein scaffolding technique or similar approaches to force the creation of enzyme complexes of interest in the plants (Conrado et al., 2008; Dueber et al., 2009; Whitaker and Dueber, 2011).

Electron micrographs of the chromoplasts within the different tomato tissues (pericarp, jelly and columella), may partially explain the differences of carotenoid accumulation within these tissues. The work done at a sub-chromoplast level could be improved by adding more sucrose steps (around the 38% sucrose step) in the discontinuous sucrose gradient. Thus, the envelope membrane may be easier to separate from the thylakoid membrane. Moreover, as it was highlighted before

(section 7.2.2), localisation of the enzymes is crucial to improve the conception of the carotenoid network. Consequently, it would be interesting to synthesise more polyclonal antibodies to localise a greater number of carotenoid enzymes. Then, as a comparison, it would also be informative to perform the same work that was done on *Crt*B+I, on carotenoid tomato mutants. Information on the specific level of carotenoid saturation, which triggers the regulation mechanisms, would also be valuable. Therefore, *in vitro* approaches to the process of carotenoid formation could be performed. Associated with this approach would be further studies to understand how the carotenoid crystals are attached to the thylakoid membranes. Protein-protein interaction or protein-membrane interaction studies will further our understanding on enzyme complex formation and maybe the crystal's relation with the membranes. Tandem affinity purification (TAP) of protein complexes, fluorescence recovery after photobleaching (FRAP), fluorescence lifetime imaging microscopy (FLIM) and fluorescence resonance energy transfer (FRET) experiments could be utilised as it was recently done to understand the protein and lipid association in the lignin pathway (Bassard et al., 2012). However, in these cases, it is important to not lose sight of the fact that the protein stoichiometry is altered through overexpression. One way around this would be to use deletion mutants and express the endogenous tagged gene products under the control of their endogenous promoters.

In order to verify the importance of the MGDG lipid class in the formation of membranous sacs and plastoglobules, experiments of overexpression or down expression (RNAi) of enzymes involved in the MGDG synthesis could be performed. Finally, levels of phytohormones (abscisic acid, gibberellins, cytokinins and strigalactones) could be analysed in order to reveal a possible signalling mechanism of the carotenoid pathway.

Pb*Crt* tomato lines (Chapter V)

Firstly, the experiment needs to be repeated at T2 generation during spring/summer time and with a greater number of replicates to ensure the robustness of the results. Then, it would be crucial to understand why and how the pb promoter is not optimal in the Ailsa Craig (AC) tomato variety. Sequencing of the upstream promoter sequences (up to 2,500 bp) in AC and *S. galapagense* would give an indication of *cis*-element differences. Finally, tomato seeds containing high levels of β-carotene

were created (Figure 5-7). They could potentially be exploited to produce biofortified tomato oil a since market for tomato oil is already present.

ZW-PIF5 and ZW-ARR14 constructs (Chapter VI)

ZW-ARR14 tobacco transient experiments could further be improved by testing different times of agro-infiltration periods. Consequently, it would be an even more advantageous technique to be transferred to an industrial scale, as discussed in section 6.3.2. Concerning the tobacco stable transformation with the ZW-ARR14 construct, it is necessary to change the constitutive promoter to an inducible one, for instance ethanol-inducible promoter (Caddick et al., 1998). Work on ZW-PIF5 should be continued, as PIF is a transcription factor directly linked to phytoene synthase and consequently with the carotenoid pathway. However, as mentioned previously (section 6.3.3), it would probably be more efficient and advantageous to achieve a phenotype by down-regulation using a TILLING approach, since from a nutritional perspective and consumer perception, it would be more acceptable than a genetic modification. From a more fundamental point of view, increased knowledge of the carotenoid and ketocarotenoid pathway at a transcriptional and translational level would facilitate understanding of the regulation mechanisms in the transgenic tobacco.

In conclusion, the transgenic tomato and tobacco lines studied highlighted regulatory mechanisms that operate across multiple levels of cellular regulation, including transcription, protein localisation, metabolite cell/tissue type, and organelle/sub-organelle structure/organisation. Previous descriptions of regulatory mechanisms operating in the pathway have focussed on transcription, protein levels and protein interactions. It is clear now that pathway regulation, including secondary metabolite formation, is a more complex process and intrinsically connected to global metabolic and cellular processes. In the present study, we have demonstrated how changes to cellular structures, such as crystal formation, plastoglobule and membrane composition/structures can arise in response to changes in metabolites. The partitioning of phytoene in plastoglobules as a regulatory mechanism was revealed for the first time. Synthesis and sequestration are two processes which are important for engineering carotenoids in plants, with the latter requiring further investigation.

All these adaptive mechanisms of the plant influence the accumulation of carotenoids or ketocarotenoids. It is therefore crucial to understand them in order to rationally manipulate levels in future engineering strategies. The control of the flux is an important factor that needs to be considered in the design of the engineering strategy (Moreno-Sanchez et al., 2008; Morandini, 2013). Acting on multiple enzymes, especially the ones in the regulatory nodes of the isoprenoid/carotenoid pathway, seems a good approach. Nevertheless, the enzymes synthesising the products of interest and those involved in the carotenoid sequestration must not be ignored. Therefore, according to the results obtained in this study, the best combination of genes to be used in an overexpression approach is: (i), genes controlling the level of precursors plus (ii), genes of the intermediate pathway and (iii), genes controlling the accumulation of carotenoids. A potential construct would be *dxs*/*Crt*B/*Crt*I/*fibrillin.* Moreover, further transcription factors remain good candidates, due to their widespread effect on the pathway. As a consequence, they may also be associated within the construct previously described. Gene regulatory network can be identified using a systems biology approach. For example, correlation networks have identified the APRR2-like transcription factor gene, which is linked to pigment accumulation in tomato and pepper fruits (Pan et al., 2013). Systems biology integrates various experimental datasets from high-throughput biochemical and bioanalytical platforms, into models, which can functionally describe the physiological and biochemical processes within an organism. Consequently, this approach can go beyond the targeted pathway to be engineered and identify complex regulators of cellular metabolism, which can also be exploited to produce valuable products.

Appendices

Appendix 1 **Table A1-1** Carotenogenic genes cloned from bacteria, fungi and plants

Gene (protein)	Species	Function	References
Crt E (GGPP synthase)	Bacteria: *Pantoea ananatis* , *Erwinia herbicola, Paracoccus* sp., *Rhodobacter capsulatus*	Converts IPP to GGPP	Misawa et al., 1990; Lee et al., 2006; Sandmann and Misawa, 1992; Math et al., 1992; Armstrong et al., 1989
Crt B (phytoene synthase)	Bacteria: *P. ananatis, E. herbicola, Paracoccus* sp., *Bradyrhizobium* sp. strain ORS278, *R. capsulatus*	Converts GGPP to phytoene	Misawa et al., 1990; Lee et al., 2006; Sandmann and Misawa, 1992; Armstrong et al., 1989; Hannibal et al., 2000; Misawa et al., 1995b
Crt I (phytoene desaturase)	Bacteria: *P. ananatis, E. herbicola, Paracoccus* sp., *Deinococcus radiodurans* , *Bradyrhizobium* sp. Strain ORS278	Converts phytoene to lycopene	Misawa et al., 1990; Lee et al., 2006; Misawa et al., 1995b; Hannibal et al., 2000; Fraser at al., 1992; Xu et al., 2007
	Cyanobacteria: *Gloeobacter violaceus*	Converts phytoene to lycopene	Tsuchiya et al., 2005; Steiger et al., 2005
	Fungi: *Xanthophyllomyces dendrorhous* (*Phaffia rhodozyma*)	Converts phytoene to lycopene	Verdoes et al., 1999 and 2003
	Bacteria: *Rhodobacter sphaeroides*	Converts phytoene to neurosporene (three desaturation steps)	Lang et al., 1994
Crt Y (lycopene β-cyclase)	Bacteria: *P. ananatis, E. herbicola, Paracoccus* sp., *Bradyrhizobium* sp. strain ORS278	Converts lycopene to β-carotene	Misawa et al., 1990; Lee et al., 2006; Sandmann and Misawa, 1992; Hundle et al., 1993; Hannibal et al., 2000; Misawa et al., 1995b
Crt YB	Fungi: *X. dendrorhous* (*P. rhodozyma*)	Bifunctional enzyme, equivalent to bacterial CrtB and CrtY	Verdoes et al., 1999 and 2003
Crt Z (β-carotene hydroxylase)	Bacteria: *P. ananatis, E. herbicola, Paracoccus* sp. (incl N81106 and PC1) *Brevundimonas* sp. SD212	Converts β-carotene to zeaxanthin and can accept canthaxanthin as a substrate. Hydroxylates at C-3 on the β-ring of γ-carotene	Misawa et al., 1990 and 1995b; Lee et al., 2006; Fraser et al., 1997; Choi et al., 2006
	Cyanobacteria: *Haematococcus pluvialis*	Converts β-carotene to zeaxanthin. Diketolation at position 4 and 4′ to canthaxanthin; unable to convert zeaxanthin to astaxanthin	Linden et al., 1999
Crt R (β-carotene hydroxylase)	Cyanobacteria: *Synechocysti* s sp. PCC 6803, *Anabaena* sp. PCC 7120	Converts β-carotene to zeaxanthin but is unable to accept canthaxanthin as a substrate. Anabaena enzyme is poor in accepting either β-carotene or canthaxanthin as substrates. Substrate for Synechocystis sp. PCC 6803: Deoxymyxol 2' -dimethylfucoside Substrate for Anabaena sp. PCC 7120: Deoxymyxol 2' -fucoside	Makino et al., 2008
Crt X (zeaxanthin glucosylase)	Bacteria: *P. ananatis* , *E. herbicola*	Converts zeaxanthin to zeaxanthin β-D-diglucoside	Misawa et al., 1990; Hundle et al., 1992

Table A1-1 (continued)

Gene (protein)	Species	Function	References
Crt W (β-carotene ketolase)	Cyanobacteria: *G. violaceus*	Converts β-carotene to echinenone and a small amount of canthaxanthin	Tsuchiya et al., 2005
	Bacteria: *Paracoccus* sp.,*Bradyrhizobium* sp. strain ORS278, *Brevundimonas* sp. SD212	Converts β-carotene to canthaxanthin. Introduction of keto group at the 4,4′ position	Lee et al., 2006; Misawa et al., 1995b; Hannibal et al., 2000; Fraser et al., 1997; Choi et al., 2007
	Cyanobacteria: *Nostoc punctiforme* PCC 73102; *Anabaena* sp. PCC 7120		Makino et al., 2008; Steiger et al., 2004
Crt O (β-carotene ketolase)	Bacteria: *Rhodococcus erythropolis* strain PR4; *D. radiodurans*	Converts β-carotene to canthaxanthin. Unable to accept 3-hydroxy β-ionone ring as a substrate. Substrate: β-carotene	Tao et al., 2006; Choi et al., 2007
	Cyanobacteria: *Synechocystis* sp. PCC 6803		Choi et al., 2006; Fernandez-Gonzalez et al., 1997
Crt O (β-carotene ketolase)	Cyanobacteria: *H. pluvialis*	Bifunctional enzyme: synthesises canthaxanthin via echinenone from β-carotene and 4-ketozeaxanthin (adonixanthin) with trace amounts of astaxanthin from zeaxanthin	Fraser et al., 1997; Breitenbach et al., 1996
	Cyanobacteria: *Chlorella zofingiensis*	Bifunctional enzyme: Converts β-carotene to canthaxanthin, and converts zeaxanthin to astaxanthin via adonixanthin	Huang et al., 2006
Crt YE	Cyanobacteria: *Prochlorococcus marinus*	Bifunctional enzyme catalyzing the formation of ε and β-ionone end groups	Stickforth et al., 2003
Crt YF and *Crt* YE (decaprenoxanthin synthase)	Bacteria: *Corynebacterium glutamicum*	Converts flavuxanthin to decaprenoxanthin	Krubasik et al., 2001
Crt EB (lycopene elongase)	Bacteria: *C. glutamicum*	Converts lycopene to cyclic C50 carotenoids	Krubasik et al., 2001
Crt D (methochineurosporene desaturase)	Bacteria: *R. capsulatus*	Desaturase 1-hydroxy-neurosporene. Synthesises demethylspheroidene	Albercht et al., 1997
Crt C (1-hydroxyneurosporene synthase)	Bacteria: *R. capsulatus*	Hydratase which adds water to the double bond at position 1,2 of the end group yielding a 1-hydroxy derivative. Synthesizes neurosporene and its isomers. Catalyses the conversion of lycopene to 1-HO- and 1,1'-(HO)(2)-lycopene	Albrecht et al., 1997
	Bacteria: *Rubrivivax gelatinosus* and *Thiocapsa roseopersicina*		Hiseni et al., 2011
Astaxanthin synthase gene (cytochrome P450 monooxygenase)	Fungi: *X. dendrorhous* (*P. rhodozyma*)	Multifunctional enzyme catalyzing all steps from β-carotene to astaxanthin formation by oxygenation of C-3 and C-4	Ojima et al., 2006
Crt S (cytochrome-P450 hydroxylase)	Fungi: *X. dendrorhous* (*P. rhodozyma*)	Can hydroxylate canthaxanthin to phoenicoxanthin and finally astaxanthin	Alvarez et al., 2006
P450 monooxygenase (CYP175A1)	Bacteria: *Thermus thermophilus*	β-carotene hydroxylase. β-carotene-specific enzyme and does not accept canthaxanthin as a substrate	Blasco et al., 2004
Gene s110033	Cyanobacteria: *Synechocystis* 6803	Carotene isomerase	Breitenbach et al., 2001

Table A1-1 (continued)

Gene (protein)	Species	Function	References
ggpps (GGPP synthase)	Arabidopsis (*Arabidopsis thaliana*), rubber tree (*Hevea brasiliensis)* , pepper (*Capsicum annuum*), yellow gentian (*Gentiana lutea*)	Converts IPP to GGPP	Zhu et al., 1997a, b and 2002; Kuntz et al., 1992; Takaya et al., 2003
	Jatropha curcas	Converts IPP to GGPP	Lin et al., 2010
	Salvia miltiorrhiza	Converts IPP to GGPP	Kai et al., 2010
	Catharanthus roseus	Converts IPP to GGPP	Thabet et al., 2012
psy (phytoene synthase)	Tomato (*Solanum esculentum*), yellow gentian	Converts GGPP to phytoene	Zhu et al., 2002; Misawa et al., 1994
	Corn (*Zea mays* ; *psy-* 1, *psy-* 2), rice (*Oryza sativa* ; *psy* -2)	Two tissue-specific genes cloned from corn (from three present in the genome). Expression of *psy-* 1 is in endosperm and is predominantly responsible for carotenoids in seed.	Gallagher et al., 2004
	Corn (*Zea mays* ; *psy-* 3) and sorghum (*Sorghum bicolor* ; *psy* -1 and *psy* -3 cDNAs)	*Psy-3* expression plays a role in controlling flux to carotenoids in roots in response to drought stress. Maize *psy-3* is mainly expressed in root and embryo tissue	Li et al., 2008a and b
	babana (cv. *Asupina* and cv. *Cavendish* ; *psy-1* and *psy-2*)	Converts GGPP to phytoene	Mlalazi et al., 2012
	Osmanthus fragrans	Converts GGPP to phytoene	Han et al., 2013
pds (phytoene desaturase)	Tomato, corn, pepper, yellow gentian, soybean (*Glycine max*)	Converts phytoene to ζ-carotene	Bartley et al., 1991; Zhu et al., 2002; Li et al., 1996; Pecker et al., 1992; Hugueney et al., 1992
	Chlorella prototothecoides CS-41		Li et al., 2011
zds (ζ-carotene desaturase)	Corn, yellow gentian	Converts ζ-carotene to pro-lycopene	Matthews et al., 2003; Zhu et al., 2003
lyc-b (lycopene β-cyclase)	Tomato, tobacco (*Nicotiana tabacum*), Arabidopsis, yellow gentian	Converts lycopene to β-carotene	Zhu et al., 2002; Pecker et al., 1996; Cunningham et al., 1996
	Papaya (*Carica papaya*)	Two papaya *lyc-b* genes: *lyc-b1* is downregulated during fruit ripening, and *lyc-b2* is chomoplast specific	Skelton et al., 2006; Devitt et al., 2010
lyc-e (lycopene ε-cyclase)	Arabidopsis, yellow gentian	Adds one ε-ionone ring to lycopene to δ-carotene	Zhu et al., 2003; Cunningham et al., 1996
bch (β-carotene hydroxylase)	Arabidopsis, yellow gentian	Converts β-carotene to zeaxanthin	Sun et al., 1996; Zhu et al., 2003
zep (zeaxanthin epoxidase)	Yellow gentian	Converts zeaxanthin to antheraxanthin	Zhu et al., 2003
HYD4 (nonheme diiron β-carotene hydroxylases)	Yellow gentian	Encode carotene β-ring hydroxylases	Zhu et al., 2003
cDNA encoding the enzyme β-carotene hydroxylase	Arabidopsis (*Arabidopsis thaliana*)	Adds hydroxyl groups to both β rings of the symmetrical β-carotene (β-β-carotene) to form zeaxanthin and converts the monocyclic β-zeacarotene to hydroxy-β-zeacarotene	Sun et al., 1996
P450 CYP97C2 (Clan C enzyme)	Rice (*Oryza sativa*)	ε-Ring hydroxylase activity	Quinlan et al., 2007
P450 CYP97A4 (Clan A enzyme)	Rice (*Oryza sativa*)	β-Ring hydroxylase activity with some minor activity towards ε-rings	Quinlan et al., 2007
P450 CYP97C11	Tomato (*Solanum esculentum*)	ε-Ring hydroxylase activity	Stigliani et al., 2011
P450 CYP97A29	Tomato (*Solanum esculentum*)	β-Ring hydroxylase activity	Stigliani et al., 2011

Table A1-1 (continued)

Gene (protein)	Species	Function	References
CCD4 (carotenoid cleavage dioxygenase protein)	Apple (*Malus ×domestica*) Chrysanthemum (Chrysanthemum×morifolium) Rose (Rosa×damascena) Osmanthus (Osmanthus fragans) Arabidopsis	Degrades β-carotene to yield β-ionone	Huang et al., 2009
	bitter melon (*Momordica charantia*)	McCCD4, not determined	Pham Anh and Park., 2013
CCD1 (carotenoid cleavage dioxygenase)	Strawberry (*Fragaria × ananassa*)	Degradation of β-carotene *in vivo*	Garcia-Limones et al., 2008
	Corn (*Zea mays*)	Cleaves carotenoids at the 9, 10 position	Sun et al., 2008
	bitter melon (*Momordica charantia*)	McCCD1, not determined	Pham Anh and Park., 2013
	Artemisis annua	AaCCD1, cleaves carotenoids	Liu et al., 2012
	Vitis vinifera	Cleaves zeaxanthin symmetrically yielding 3-hydroxy-β-ionone, a C13-norisoprenoidic compound, and a C14-dialdehyde	Mathieu et al., 2005
Z-ISO	maize (*Zea mays*) and *Arabidopsis* (*Arabidopsis thaliana*)	Isomerization of the 15-*cis* double bond in 9,15,9'-tri-*cis*-zeta-carotene	Chen et al., 2010
CRTISO (crtiso1)	*Zea Mays*	Converts tetra-cis prolycopene to all-trans lycopene but could not isomerize the 15-cis double bond of 9,15,9 -tri-cis-ζ-carotene.	Li et al., 2010
bch1 (β-carotene hydroxylase1)	*Zea Mays*	Convert β-carotene into β-cryptoxanthin and zeaxanthin	Li et al., 2010
bch2 (β-carotene hydroxylase2)	*Zea Mays*	Convert β-carotene into β-cryptoxanthin and had a lower overall activity than ZmBCH1	Li et al., 2010
CCS (capsanthin-capsorubin synthase)	*Lolium lancifolium* 'Splendens	Catalyses the conversion of antheraxanthin and violaxanthin into capsanthin and capsorubin, respectively	Jeknic et al., 2012

Table A1-1 Carotenogenic genes cloned from bacteria, fungi and plants (adapted from Farre et al., 2010)

Figure A2-1 Description of vectors used in this work
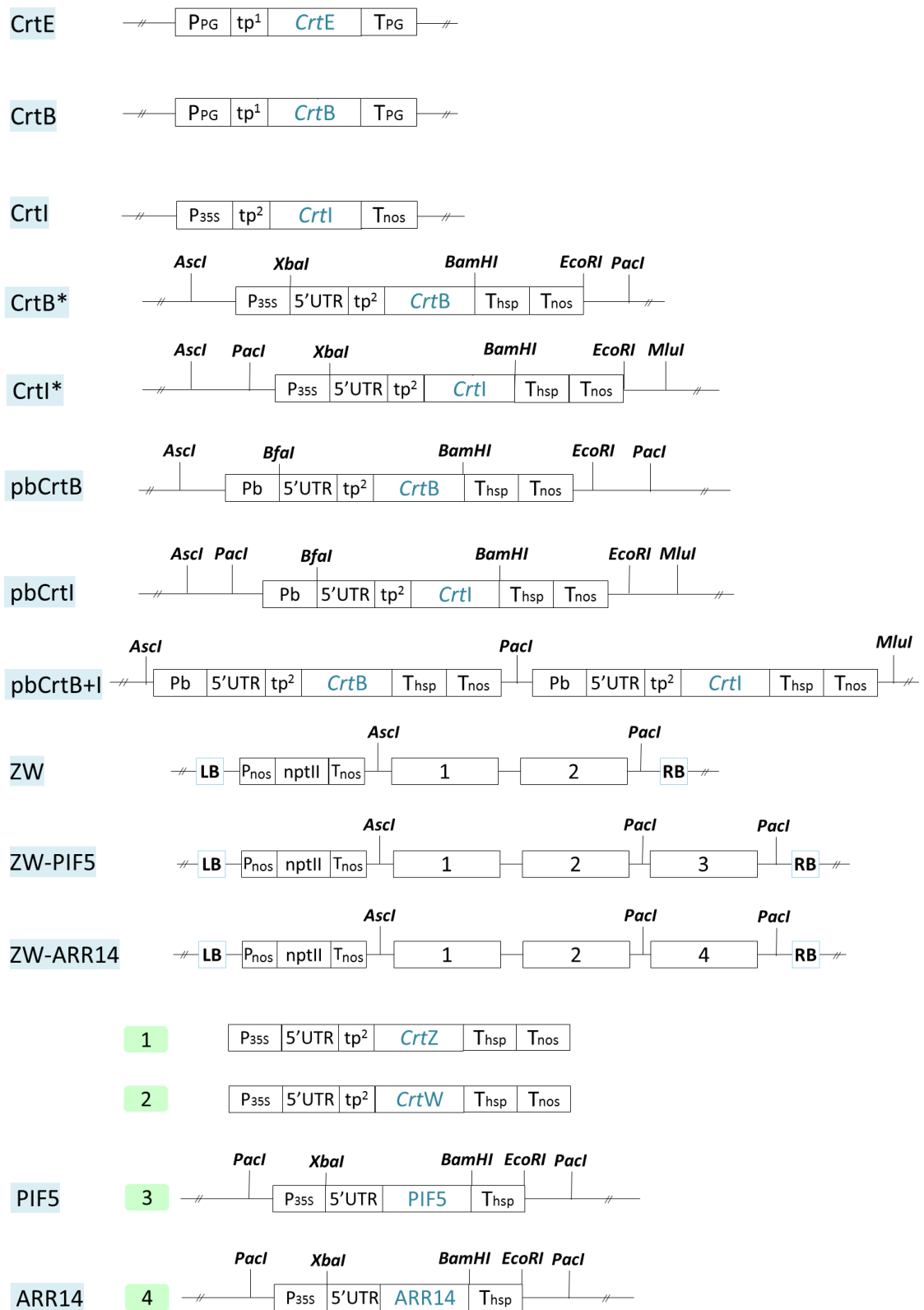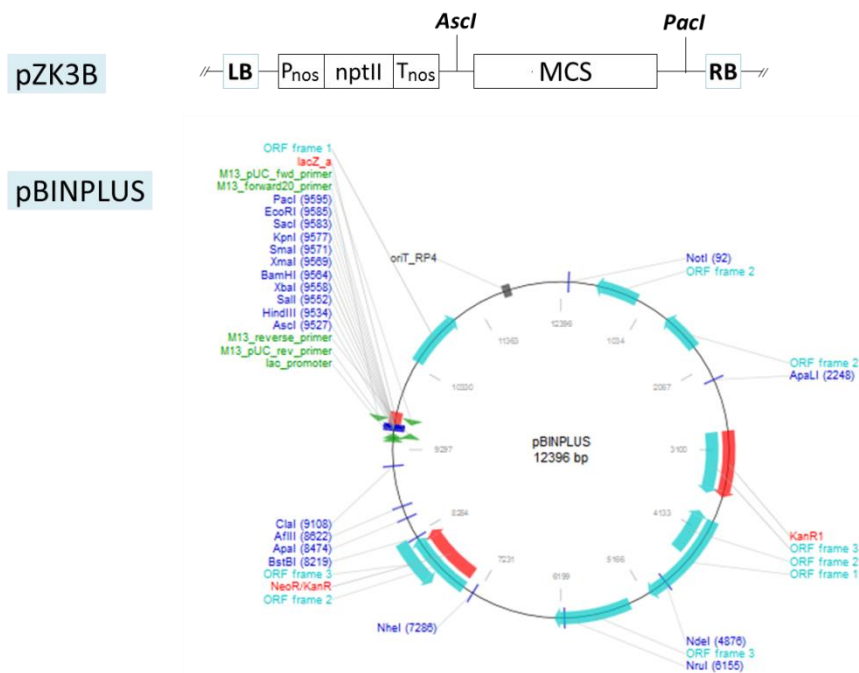
Figure A2-1 Description of vectors used in this work

P, promoter; T, terminator; *Crt*E, geranylgeranyl diphosphate synthase gene from *Pantoea ananatis*; *Crt*B, phytoene synthase gene from *Pantoea ananatis*; *Crt*I, lycopene desaturase gene from *Pantoea ananatis*; *Crt*Z, carotene hydroxylase gene from *Brevundimonas sp. SD212*; *Crt*W, carotene ketolase gene from *Brevundimonas sp. SD212*; PIF5, phytochrome interacting factor 5 transcription factor from *Arabidopsis thaliana*; ARR14, arabidopsis response regulator 14 transcription factor from *Arabidopsis thaliana*; MCS, multiple cloning site; *npt*II, kanamycin resistance gene; PG, polygalacturonase from *Solanum lycopersicum*; *Nos*, nopaline synthase from *Agrobacterium tumefaciens*; 35S, 35S RNA reverse transcriptase from the cauliflower mosaic virus (*Caulimovirus*); *Hsp*, heat shock protein 18.2 from *Arabidopsis thaliana*; 5UTR, untranslated region of alcohol dehydrogenase gene from *Nicotiana tabacum*; tp^1, transit peptide of the phytoene synthase-1 gene from *Solanum lycopersicum*; tp^2, transit peptide of the RuBisCO small subunit from *Pisum sativum L.*; LB, left border of the T-DNA; RB, right border of the T-DNA; Restriction enzyme sites are represented.

Appendix 3 **Table A2-2** Sequences of primers used in (RT) real-time qPCR and PCR

Gene ID	Accession number	Primers sequences	
		Forward	Reverse
Primers used for real-time qPCR* and RT real-time qPCR			
GGPPS-1	DQ267902	GACAGCATCTGAGTCCGTCA	CTTGGCCAGGACAGAGTAGC
GGPPS-2	SGNU223568	GGGATTGGAAAAGGCTAAGG	AGCAATCAATGGAGCAGCTT
PSY-1	Y00521	TGGCCCAAACGCATCATATA	CACCATCGAGCATGTCAAATG
PSY-2	L23424	GTTGATGGCCCTAATGCATCA	TCAAGCATATCAAATGGCCG
PDS	X59948 AC	GTGCATTTTGATCATCGCATTGA	GCAAAGTCTCTCAGGATTACC
ZDS	AF195507	TTGGAGCGTTCGAGGCAAT	AGAAATCTGCATCTGGCGTATAGA
CRTISO	AF416727	TTTTGGCGGAATCAACTACC	GAAAGCTTCACTCCCACAGC
LCY-E	Y14387	AACACTTGCATTTGGTGCTG	AGTACAGAGGCGCATTTTGG
LCY-B	AF254793	TCGTTGGAATCGGTGGTACAG	AGCTAGTGT CCTTGCCACCAT
CYC-B	Y18297 T	GTTATTGAGGAAGAGAAATGTGTGAT	TCCCACCAATAGCCATAACATTTT
CRTR-B1	Y14809	CTCGAGGATGAGAAGCTGAAACCTC	GCCAAGCGAGTAGCTAAGATCTGTT
CRTR-B2	DQ864755	TTTCTCAGTCCAAAATCCGCCTCAA	TCATTCTCCAGCACAAAACAAACCG
ZEP-1	Z83835.1	TTGGGTTTTAGGAGGCAATG	CCCGCAGGTAAAAGTAACCA
CRTB	D90087.2	CGCCTGTGACCTTGGGCTGG	GGCTCAGCGCCTGACGGTTT
CRTI	D90087.2	AGCCATATGGAAACGACAGG	TCTGCAGTTTGTTGGACTGC
CRTB*	D90087.2	CGCCTGTGACCTTGGGCTGG	GGCTCAGCGCCTGACGGTTT
CRTI*	D90087.2	AGCCATATGGAAACGACAGG	TCTGCAGTTTGTTGGACTGC
PDS*	X59948 AC	CTAGGTTCTTGCTGCCTTGG	CCAACTTTTTGGCAATGCTT
ACTIN#	BT012695.1	GGTATTGTGTTGGACTCTGGTGA	ACGGAGAATGGCATGTGGAA
Primers used for PCR			
CRTE	D90087.2	AACTGCTGGACGATTTGACC	TCACTGGCAAGCTGAAGA
CRTB	D90087.2	TATTGCTCGCGATATTGTGG	TTTTCAGGTGCCGCATAAT
CRTI	D90087.2	AGCCATATGGAAACGACAGG	TCTGCAGTTTGTTGGACTGC
CRTZ	AB181388.1	ATGCATGGTTTCCTTTGGTC	CCAAGGCCAAAGATGAAGTC
CRTW	AB181388.1	TGGCTTCCTCACAGACACAC	GTCTCCACCAAGGTCTCCAA
pb promoter	-	CACCTGCCCGTTTTATTGGTCTGAG	TATAGAGAATGTATAAGATTGATAATGG

Table A2-2 Sequences of primers used in (RT) real-time qPCR and PCR

GGPPS-1, 1-geranylgeranyl pyrophosphate synthase-1; GGPPS-2, 1-geranylgeranyl pyrophosphate synthase-2; PSY-1, phytoene synthase-1; PSY-2, phytoene synthase 2; PDS, phytoene desaturase; ZDS. ζ-carotene desaturase; CRTISO, carotene isomerase; LCY-E, ε-lycopene cyclase; LCY-B, β-lycopene cyclase; CYC-B, β-lycopene cyclase; CRTR-B1, carotene β-hydroxylase 1; CRTR-B2, carotene β-hydroxylase 2; ZEP-1, zeaxanthin epoxidase-1; CRTE, geranylgeranyl diphosphate synthase; CRTB, phytoene synthase; CRTI, phytoene desaturase; CRTZ, carotene hydroxylase, CRTW, carotene ketolase; pb promoter, lycopene β-cyclase promoter from the orange fruited *Solanum galapagense*; #, predicted actin-97-like.

Figure A2-2 Spectra of metabolites of interest

Astaxanthin

476.0

Pheonicaxanthin

486.9

Echineone

465.0

Adonixanthin

468.7

Chlorophyll b

458.9

Chlorophyll a

431.1

α-Tocopherol

292.2
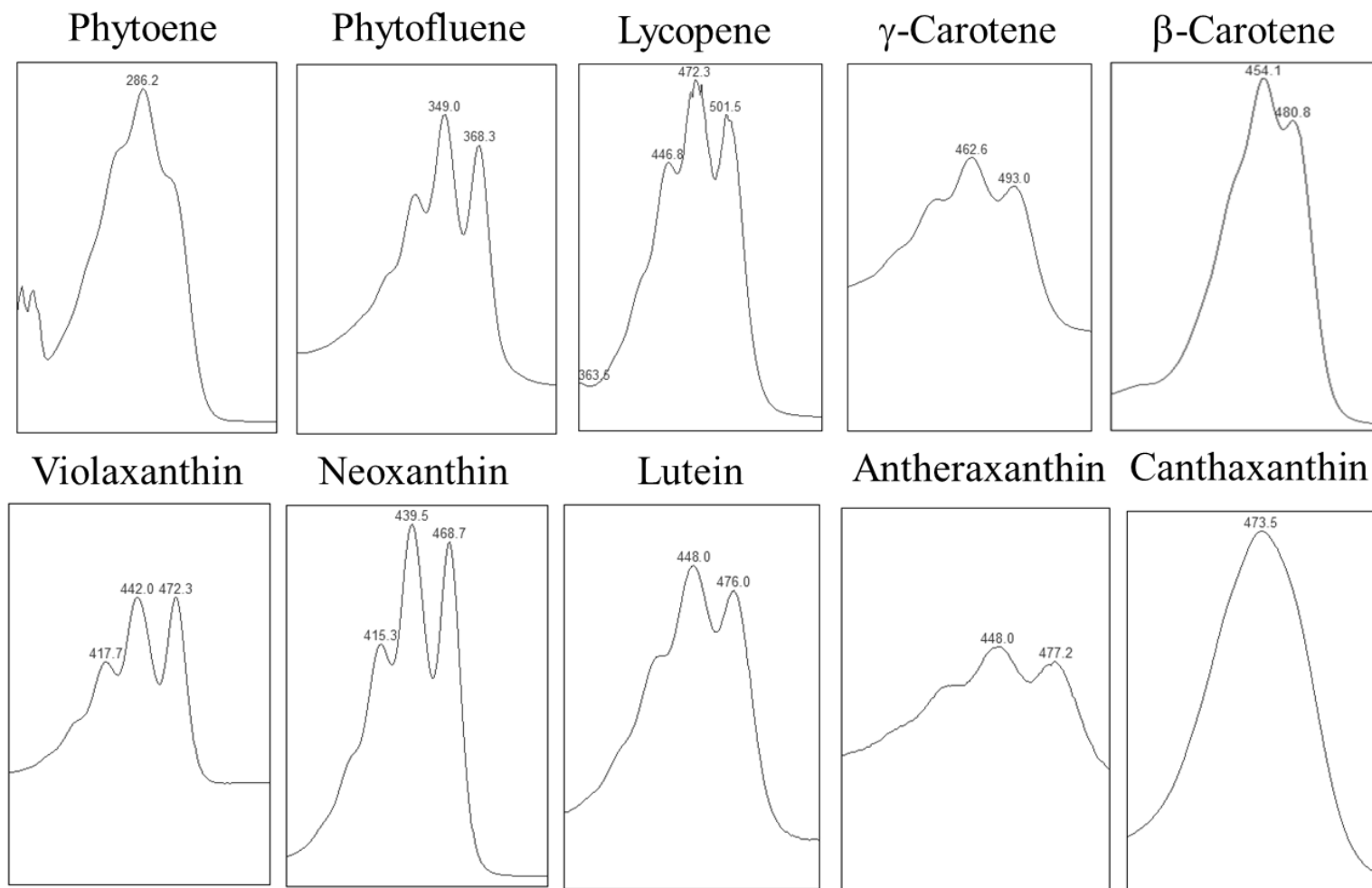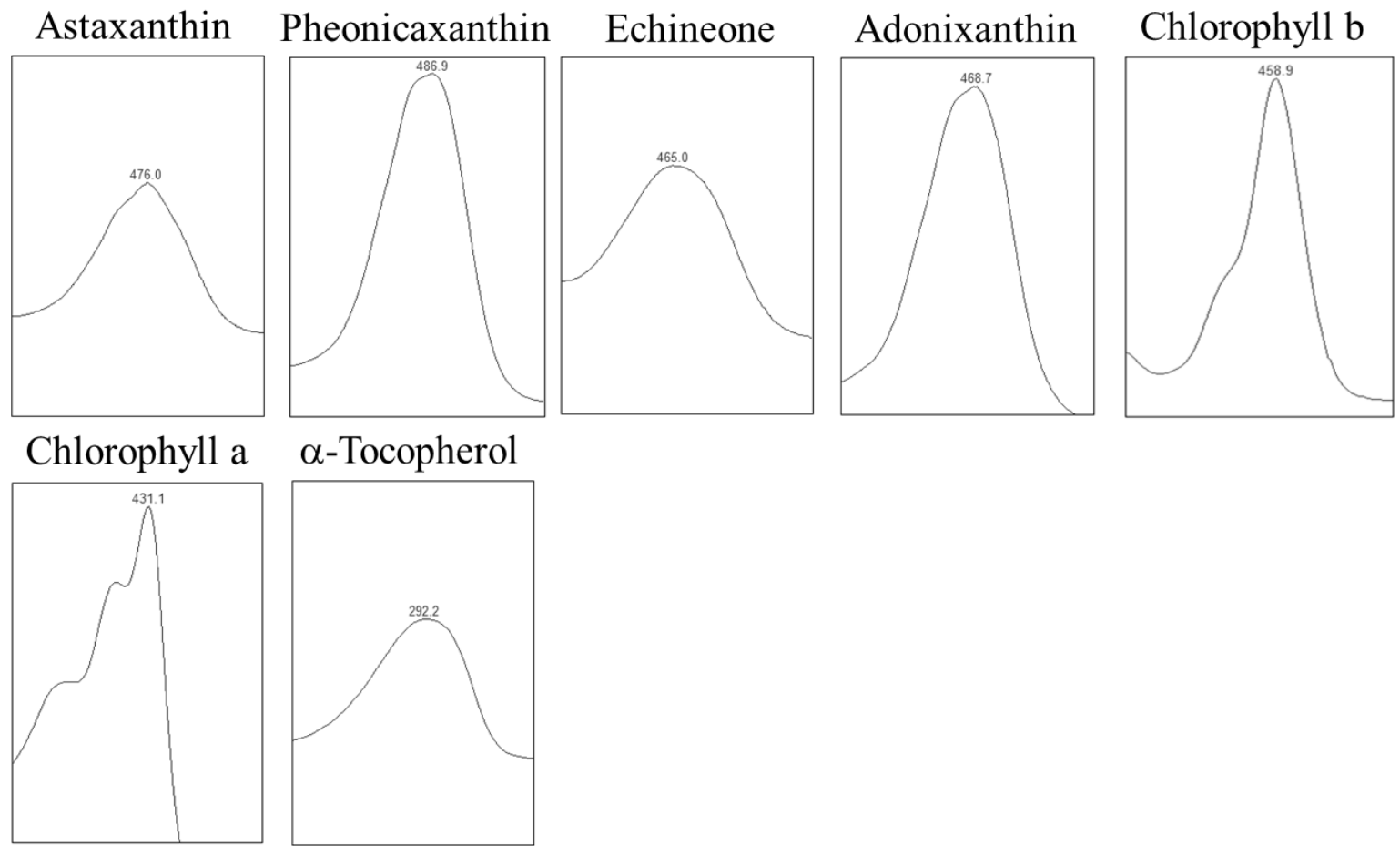
Appendix 5 **Figure A2-3** Carotenoid and α-tocopherol dose response curves

Phytoene dose response curve
y = 4E+06x - 24989
R² = 0.9842
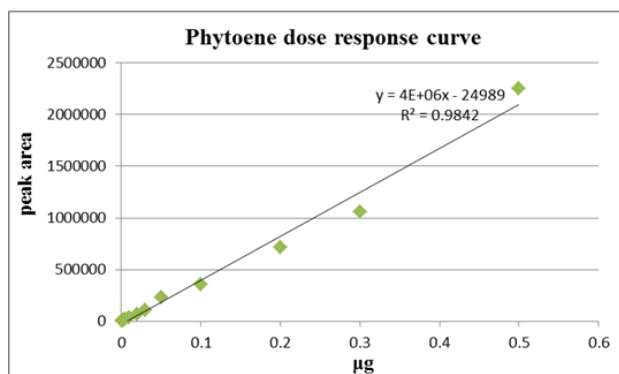
Equations of dose response curves:

Phytoene	y=4000000x-24989
Phytofluene	y=3000000x- 68968
Lycopene	y=6000000x-101170
γ-Carotene	y=4000000x-72737
β-Carotene	y=7000000x-408108
Violaxanthin	y=8000000x-205083
Neoxanthin	y=7000000x-182335
Lutein	y=9000000x-462175
Antheraxanthin	y=7000000x-202392
Canthaxanthin	y=9000000x-116270
Astaxanthin	y=7000000x-58748
Pheonicoxanthin	y=30000000x-299896
Echinenone	y=90000000x-195582
α-Tocopherol	y=261388x-4244.7

Appendix 6 **Figure A2-4** Schematic representation of the systems (1 and 2) used to fractionate chromoplasts and isolate their respective sub-membrane compartments

Figure A2-4 Schematic representation of the systems (1 and 2) used to fractionate chromoplasts and isolate their respective sub-membrane compartments

The scheme shows the different chromoplasts fractionation systems used. System 1 isolates intact chromoplasts, which are subsequently lysed and their sub-membrane compartments separated over the sucrose density gradient described. System 2 isolates initially intact
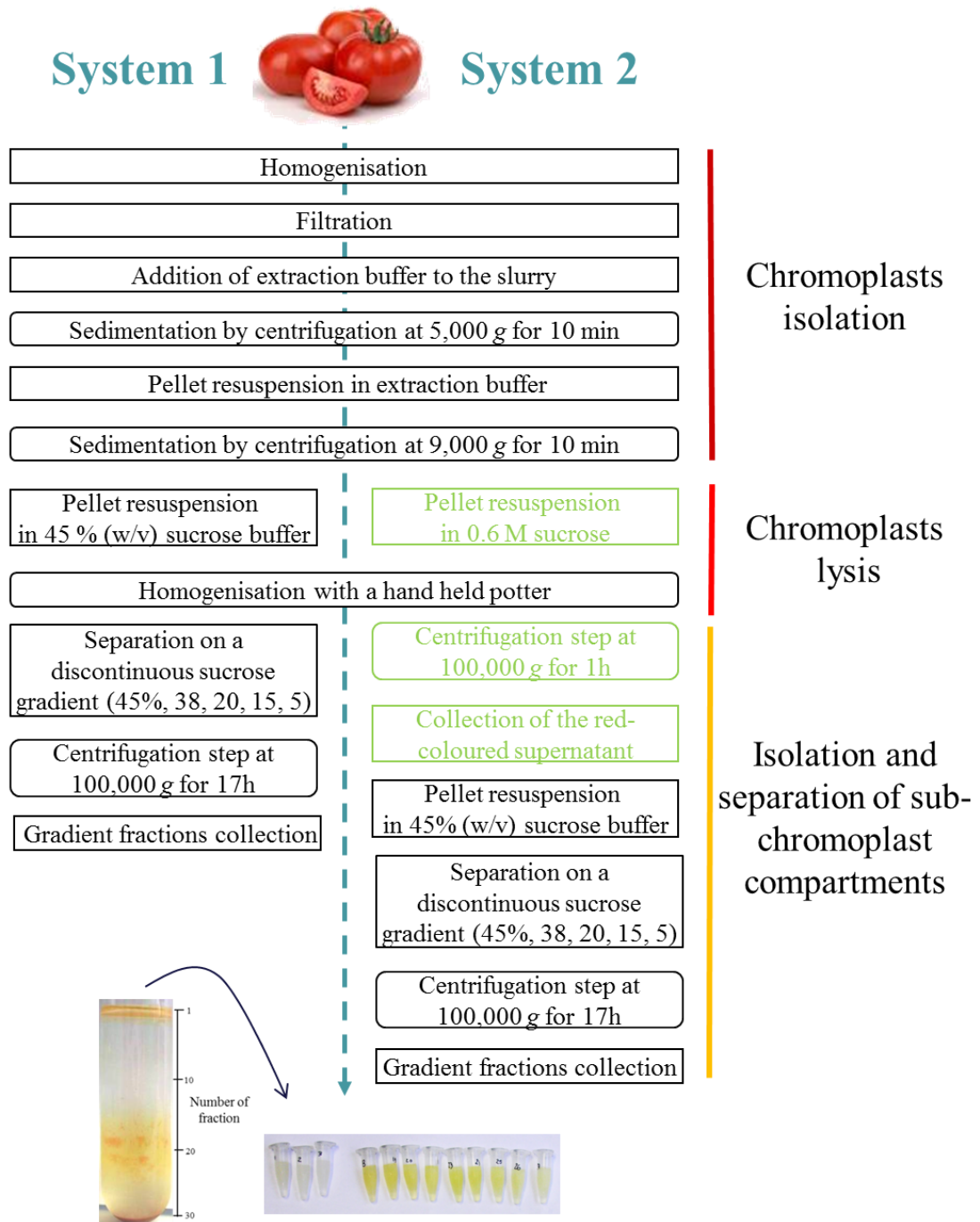
chromoplasts and subsequently, the chromoplast membranes (pellet) and the majority of the chromoplasts plastoglobules and crystals (supernatant). The sub-membrane compartments of the chromoplast membranes are then separated over the sucrose density gradient described. Green rectangles correspond to the steps, which are unique to system 2. Details of the respective methods are provided in sections 2.7.1 and 2.7.2.

Appendix 7 **Figure A4-1** Comparison of phytoene synthase amino acid sequence in *P. ananatis* (*Crt*B; D90087.2) and *S. lycopersicum* (*Psy*-1; EF157835.1)

```
CrtB           1 -------------------------------------------------    0

Psy-1          1 MSVALLWVVSPCDVSNGTSFMESVREGNRFFDSSRHRNLVSNERINRGGG   50

CrtB           1 -------------------------------------------------    0

Psy-1         51 KQTNNGRKFSVRSAILATPSGERTMTSEQMVYDVVLRQAALVKRQLRSTN  100

CrtB           1 ----------MNNPSLLNHAV----ETMAVGSKSFATASKLFDAKTRRSV   36
                           ..|..||:.|.    |..|..:|:|...:.|...:.||::
Psy-1        101 ELEVKPDIPIPGNLGLLSEAYDRCGEVCAEYAKTFNLGTMLMTPERRRAI  150

CrtB          37 LMLYAWCRHCDDVIDDQTLGFQARQPALQTPEQRLMQLEMKTRQAYAGSQ   86
                 ..:|.|||..|:::|.....:  ....|.||.|.||        ...:.|..
Psy-1        151 WAIYVWCRRTDELVDGPNASY-ITPAALDRWENRL-------EDVFNGRP  192

CrtB          87 MHEPAFAAFQEVA-MAHDIAPAYAFDHLEGFAMDVREAQYSQLDDTLRYC  135
                 ......|....|: ...||.|..  |.:||..||:|:::|...|:...||
Psy-1        193 FDMLDGALSDTVSNFPVDIQPFR--DMIEGMRMDLRKSRYKNFDELYLYC  240

CrtB         136 YHVAGVVGLMMAQIMGV--RDNATLD----RACDLGLAFQLTNIARDIVD  179
                 |:|||.|||||...|||:  ...||.:   .|..||:|.|||||.||:.:
Psy-1        241 YYVAGTVGLMSVPIMGIAPESKATTESVYNAALALGIANQLTNILRDVGE  290

CrtB         180 DAHAGRCYLPASWLEHEGLNKENYAAPENRQALSRIARRLVQEAEPYYLS  229
                 ||..||.|||...|...||:.|:..|...............:::..|..:.
Psy-1        291 DARRGRVYLPQDELAQAGLSDEDIFAGRVTDKWRIFMKKQIHRARKFFDE  340

CrtB         230 ATAGLAGLPLRSAWAIATAKQVYRKIGVKVEQAGQQAWDQRQSTTTPEKL  279
                 |..|:..|...|.:.:.:..:||||..:|......::|...:...::||
Psy-1        341 AEKGVTELSSASRFPVWASLVLYRKILDEIEANDYNNFTKRAYVSKSKKL  390

CrtB         280 TLLLAASGQALTSRMRAHPPRPAHLWQRPL     309
                 ..|..|..::|.      ||......||
Psy-1        391 IALPIAYAKSLV------PPTKTASLQR--     412
```

Identity: 94/430 (21.9%)

Appendix 8 **Figure A5-1** Sequence of the pb promoter

```
TGCCCGTTTTATTGGTCTGAGAACGGCGTGATGCCAAATTCTGCCGCTCCACAGTG
AGCATTTCGATCTACTGGAAATTGACCAACTTATTTTATCACTTGATAACTAGAGT
TTGGGTTCAACAAAATCCTATTAACTTTAATCATACATTGTATTTATACCGAAAAA
GTTATGCATAACTCAGTAAATTACCTTTTTTAGCAGTCAAATTCTAGATGAGTTTC
CAATTTATCAAAATGGCTTTTATAGGGTCTCAGTTCCACTAATATACCTGCCGTCC
ATGCACTGACTACAAGACAAATACCTCACTATGTTTGTTAGTGCTTGGTAATATAA
AACCTTTTCTTTTATGAGAAAGTTCACCGAAAATAATTTTCTATTTGTGGCATAAC
```

```
TAGTATATAGTGCAGATTGACAAGAATTTAATTTTGCAGTTGGGCACATGAACAAT
TTTCCTCAAAGTTGTAGAAAGTATTTTTCATTTTCTTGTCACCGAAAATTATTTAT
AATTGAAATTAAAACCGAATGAGCTGCAAGATTCAAGTCGAATTTCAAAAGATTGA
CCAAGAAAAAATTCAAAAATATCCCCCACCCCCTACCAAACACATCCTAAAGTGAG
GTATAGACTGGGACTGGGATTGGGAAAAGGGTAAAATGCTTTCACTAGCTTTGCAA
AGATTCCACTTTGTTAGCTATCTTTCTTTCTCATTTCCTTTTTTTCTTTTTCTTTTT
TTTGTTATATAAGCCAAAGTAGGTACCCAAAAGCATCAATATTTTGTATTGCTTGG
TGATTCCTCTTTAGTCCAGTATTTCATTTTCTACAAGTTCCACCTCCCTCCATAAT
TAACCATTATCAATCTTATA
```

Appendix 9 **Figure A6-1** Sequences comparison of *Crt*Z and *Crt*W of *Brevundimonas* before and after plant codon optimisation

```
CrtZ         1 ------------------------------TCAGGCGCCGCTGCT----   15
                                            |.|        |||||
CrtZopt      1 ATGGCTTGGCTTACTTGGATCGCTCTTTTCCTTA-------CTGCTTTTT   43

CrtZ        16 --GGAA--GAGCC--CCGCTT--------CTGAG----------------   35
                 ||||   |||.|  .|||||          |..||
CrtZopt     44 TGGGAATGGAGGCTTTCGCTTGGATCATGCATAGATATGTTATGCATGGT   93

CrtZ        36 --CCAGTTCGGCCT--------------TCAGCGCCCGCGCCGACCGCAC   69
                 ||  ||.||.||              |||....||.| .|||  .|||
CrtZopt     94 TTCC--TTTGGTCTTGGCATAGAAGTCATCATGAACCTC-ACGA--TCAC  138

CrtZ        70 CCAC---AGAAAGCCGAAGGA----GACGCAG---CCTTCGCGCGTGCGC  109
                 ||.|    ||||    |||.||    ..|||.|   .|||||||  |||.|
CrtZopt    139 CCTCTTGAGAA----GAACGATCTCTTCGCTGTTATCTTCGC---TGCTC  181

CrtZ       110 ACGG----CGTGATGCAGACGGTGC------------------GCCTGGA  137
                 |.|    |||.|||     |.|||                  ||||.|
CrtZopt    182 -CTGCTATCGTTATG-----GTTGCTGTTGGACTTCATCTTTGGCCTTG-  224

CrtZ       138 TGCGCCGCGTCC----------AGAAGCCGGACCGC--CCGGAAAAGCCC  175
                  |.|.|.|||          .|||.|  ||||| .|||||
CrtZopt    225 ---GGCTCTTCCTGTTGGACTTGGAATC---ACCGCTTACGGAA------  262

CrtZ       176 GTCGGGAAC--------CGCCGGTGCACCAGGCCGTCGTGGA-AGAAGAA  216
                 |.|.|.||        |..||.||.|| ||||..| |||||
CrtZopt    263 -TGGTGTACTTCTTCTTCCACGATGGAC-------TCGTTCATAGAAG--  302

CrtZ       217 ATAGACCATCCCATAGGCCGTGATCCCCAGGCCGACCGGCAGGGCCCAGG  266
                      ||.||.||  ||| |||.|.|.||..||  .|.||...|.||
CrtZopt    303 -------ATTCCCTA--CCG-GATTCTCTGGAAGA---TCTGGATTCTGG  339

CrtZ       267 GCCACAGG--TGCAGACCCACGGCCACCATGACGATGGCCGGGGCGGCGA  314
                  .|||.|.|  |.|||.|.||..|.|..|||.|||.||             ..
CrtZopt    340 ACCAGAAGAATCCAGGCTCATAGACTTCATCACGCTG-----------TT  378

CrtZ       315 AGACCACGGCGAACAGG--------TCGTTC---TTCTCCAGGG---GGT  350
                 |||.|..|     |.|||        ||.|||   |||..|.|||   |||
CrtZopt    379 AGAACTAG----AGAGGGATGCGTTTCTTTCGGATTCCTCTGGGTTAGGT  424

CrtZ       351 ------GATCGT--GCGGCTCATGATGGCT-----GCGGTGCCAGGACCA  387
                       ||.|.|  |.|||||.| |.|||||      |.||       |||.|
CrtZopt    425 CTGCTAGAGCTTTGGAGGCTGA-GTTGGCTCAAAAGAGG-----GGATC-  467

CrtZ       388 CAGGAAACCGTGCATCACATAGCGGTGC---ATGATCCAGGCGAACGCCT  434
                           |.|.||  ||||||.|| |.|||||
CrtZopt    468 ----------TTCTTC---TAGCGGAGCTTGAGGATCC------------  492

CrtZ       435 CCATGCCCAAAAAGGCGGTCAGGAACAGCGCGATCCACGTCAGCCAGGCC  484
CrtZopt    493 --------------------------------------------------  492
```

250

```
CrtZ        485 AT     486

CrtZopt     493 --     492
```
Identity: 239/652 (36.7%)

```
Crtw           1 AAGTGGAAGCAGGTGAGCAGGGAAAGAACGGGGCCGTAGCCGCTGCTGCG    50

CrtWopt        1 --------------------------------------------------     0

Crtw          51 GGCGTGGTGGGCGTCGGCGAACGGCTGGTCGGTGTGGCGGTGCGGCAGCC   100
                                 |.|.|||.| |.|||.||.|       ||||
CrtWopt        1 -------------------ATGACTGCT-GCTGTTGCTG------AGCC     23

Crtw         101 -AG----GTGCCGAAGGTGA-AGAGCTGAAGC-----------GCTGAA   132
                  ||     ||.||.|    || |||..||.|.|           ||||
CrtWopt       24 TAGAATCGTTCCTA----GACAGACTTGGATCGGACTTACTCTTGCTG--    67

Crtw         133 AGCAGGGCCGGCGCGGCCCCAGAAGG--------TCA-------GGAGATT   167
                  |.|.|..||..||.|    ||.||        |||       ||||.||
CrtWopt       68 -GAATGATCGTTGCTG----GATGGGGATCTCTTCACGTTTACGGAGTTT   112

Crtw         168 GGCCGGCCGCGCCCCCAGGCCGAAGAGGGCGATCAGGACCAGGGCGGTCA   217
                              .|..|||     .|||.||
CrtWopt      113 ----------ACTTCCA-----CAGATGG--------------------   126

Crtw         218 GGACCGCCATC-------TCGCGCCAGCCGAAATAGGTGCGAAAGAAGT   259
                  |||.|..|.||       |||..||.||   .||.|.|||      .||
CrtWopt      127 GGAACTTCTTCTCTTGTTATCGTTCCTGC---TATCGTTGC------TGT   167

Crtw         260 TCAGGAACCAGG-----------------------------GAAGGAAG   279
                  ||||  ||..||                               ||.|..|.
CrtWopt      168 TCAG--ACTTGGCTTTCTGTTGGACTTTTCATCGTTGCTCATGATGCTAT   215

Crtw         280 GCGCGG------GGCGCCGGGGCGTAAAAGTCCGGGTCGTCGGCCGTGCC   323
                  ||.|||       .||.||.||     |||.||..|.|.|
CrtWopt      216 GCACGGATCTCTTGCTCCTGG------AAGACCTAGACTT----------   249

Crtw         324 GGGCGCGGCGTGGTGG---------GCGTGG----TGCGCCGTCTTCAG-   359
                  ..|||.|| ||.|||         .|.|||    |.|||.|..||||||
CrtWopt      250 -AACGCTGC-TGTTGGAAGACTTACTCTTGGACTTTACGCTGGATTCAGA   297

Crtw         360 -CCGATCGAAGCGGAAGCCCGCATAGAGCCCCAGGGTCAGCCGGCCG---   405
                  .|||||.|| |..|||.|.||     .|.||||.|.||||..||.|
CrtWopt      298 TTCGATAGA--CTTAAGACTGC-----TCACCACGCTCACCACGCTGCTC   340

Crtw         406 -----ACTGCGG----------------CGTTCAGCCGCGGCCGTCCCGG   434
                       |||||.|                ||.|| |.|| |||..|
CrtWopt      341 CTGGAACTGCTGATGATCCTGATTTCTACGCTC--CTGC-----TCCTAG   383

Crtw         435 CGC------------------------CAG----------GGA----   443
                  .||                        |||          |||
CrtWopt      384 AGCTTTCCTTCCTTGGTTCCTTAACTTCTTCAGAACTTACTTCGGATGGA   433

Crtw         444 --------GCCGTGC----------------ATGGC--------GTCAT   460
                          ||.||.|                ||.||        |.|.|
CrtWopt      434 GAGAGATGGCTGTTCTTACTGCTCTTGTTCTTATCGCTCTTTTCGGACTT   483

Crtw         461 GG-GCGACGATGAAAAGGCCGACC-GACAACC------AGGTCTGGACCG   502
                  || ||.|     |||| |..||||       ...|||||.|.|
CrtWopt      484 GGAGCTA-------------GACCTGCTAACCTTCTTACTTTCTGGGCTG   520

Crtw         503 CTAC-GATC--------GC------------------CGGGAC-------   518
                  ||.| |.||        ||                  |||.||
CrtWopt      521 CTCCTGCTCTTCTTTCTGCTCTTCAGCTTTTCACTTTCGGAACTTGGCTT   570

Crtw         519 GATCAC---CAGACTG--------------GAGGTGCCCCAGCGGTGAAA   551
                  ..|||||   ||.||||              ||.|...|.||| ||.|  |.
CrtWopt      571 CCTCACAGACACACTGATCAGCCTTTCGCTGATGCTCACCA-CGCT--AG   617

Crtw         552 AT-------AGACGCCGTAGACGTG--------------CAGGCTCCCC   579
                  ||        |.|||     |||.||              |..|||.||.
CrtWopt      618 ATCTTCTGGATACG-----GACCTGTTCTTTCTCTTCTTACTTGCTTCCA   662
```

251

```
Crtw        580 CATC-----CCGCCACGATCATTCC------CGCCAGGGTCAGACCGATC       618
                |.||      .|.||||||.|| ||      |.||..||  |||||
CrtWopt     663 CTTCGGAAGACACCACGAGCA--CCACCTTACTCCTTGG--AGACC----       704

Crtw        619 CAGGTCTGGCGCGGGACGATGCGGGGCTCGGCGACGGCGGCG-GTCAT--       665
                 .|||.| |.|||..||            ||  |.||.| |||.|
CrtWopt     705 -----TTGGTG-GAGACTTTG-----------GA--GAGGAGAGTCTTGA       735

Crtw        666 -      665

CrtWopt     736 G      736
```

Identity: 322/951 (33.9%)

References

Abdel-Aal, E.-S.M., Akhtar, H., Zaheer, K., and Ali, R. (2013). Dietary sources of lutein and zeaxanthin carotenoids and their role in eye health. Nutrients **5,** 1169-1185.

Aharoni, A., Jongsma, M., and Bouwmeester, H. (2005). Volatile science? Metabolic engineering of terpenoids in plants. Trends in Plant Science **10,** 594-602

Ahn, M.-J., Noh, S.A., Ha, S.-H., Back, K., Lee, S.W., and Bae, J.M. (2012). Production of ketocarotenoids in transgenic carrot plants with an enhanced level of beta-carotene. Plant Biotechnology Reports **6,** 133-140.

Akiyama, K., Matsuzaki, K., and Hayashi, H. (2005). Plant sesquiterpenes induce hyphal branching in arbuscular mycorrhizal fungi. Nature **435,** 824-827.

Alba, R., Cordonnier-Pratt, M.M., and Pratt, L.H. (2000). Fruit-localized phytochromes regulate lycopene accumulation independently of ethylene production in tomato. Plant Physiology **123,** 363-370.

Al-Babili, S., Hartung, W., Kleinig, H., and Beyer, P. (1999). CPTA modulates levels of carotenogenic proteins and their mRNAs and affects carotenoid and ABA content as well as chromoplast structure in *Narcissus pseudonarcissus* flowers. Plant Biology **1,** 607-612.

Albrecht, M., Takaichi, S., Misawa, N., Schnurr, G., Boger, P., and Sandmann, G. (1997). Synthesis of atypical cyclic and acyclic hydroxy carotenoids in Escherichia coli transformants. Journal of Biotechnology **58,** 177-185.

Aluru, M., Xu, Y., Guo, R., Wang, Z., Li, S., White, W., Wang, K., and Rodermel, S. (2008). Generation of transgenic maize with enhanced provitamin A content. Journal of Experimental Botany **59,** 3551-3562.

Alvarez, V., Rodriguez-Saiz, M., de la Fuente, J.L., Gudina, E.J., Godio, R.P., Martin, J.F., and Barredo, J.L. (2006). The crtS gene of *Xanthophyllomyces dendrorhous* encodes a novel cytochrome-P450 hydroxylase involved in the conversion of beta-carotene into astaxanthin and other xanthophylls. Fungal Genetics and Biology **43,** 261-272.

Angaman, D.M., Petrizzo, R., Hernandez-Gras, F., Romero-Segura, C., Pateraki, I., Busquets, M., and Boronat, A. (2012). Precursor uptake assays and metabolic analyses in isolated tomato fruit chromoplasts. Plant Methods **8:1**.

Apel, W., and Bock, R. (2009). Enhancement of carotenoid biosynthesis in transplastomic tomatoes by induced lycopene-to-provitamin A conversion. Plant Physiology **151,** 59-66.

Armstrong, G.A., Alberti, M., Leach, F., and Hearst, J.E. (1989). Nucleotide sequence, organization, and nature of the protein products of the carotenoid biosynthesis gene cluster of *Rhodobacter capsulatus*. Molecular & General Genetics **216,** 254-268.

Atkinson, R.G., Bolitho, K.M., Wright, M.A., Iturriagagoitia-Bueno, T., Reid, S.J., and Ross, G.S. (1998). Apple ACC-oxidase and polygalacturonase: ripening-specific gene expression and promoter analysis in transgenic tomato. Plant Molecular Biology **38,** 449-460.

Austin, J.R., Frost, E., Vidi, P.A., Kessler, F., and Staehelin, L.A. (2006). Plastoglobules are lipoprotein subcompartments of the chloroplast that are permanently coupled to thylakoid membranes and contain biosynthetic enzymes. Plant Cell **18,** 1693-1703.

Azadi, P., Otang, N.V., Chin, D.P., Nakamura, I., Fujisawa, M., Harada, H., Misawa, N., and Mii, M. (2010). Metabolic engineering of Lilium x formolongi using multiple genes of the carotenoid biosynthesis pathway. Plant Biotechnology Reports **4,** 269-280.

Barsan, C., Sanchez-Bel, P., Rombaldi, C., Egea, I., Rossignol, M., Kuntz, M., Zouine, M., Latche, A., Bouzayen, M., and Pech, J.C. (2010). Characteristics of the tomato chromoplast revealed by proteomic analysis. Journal of Experimental Botany **61,** 2413-2431.

Barsan, C., Zouine, M., Maza, E., Bian, W.P., Egea, I., Rossignol, M., Bouyssie, D., Pichereaux, C., Purgatto, E., Bouzayen, M., Latche, A., and Pech, J.C. (2012). Proteomic analysis of chloroplast-to-chromoplast transition in tomato reveals metabolic shifts coupled with disrupted thylakoid biogenesis machinery and elevated energy-production components. Plant Physiology **160,** 708-725.

Bartley, G.E., Viitanen, P.V., Pecker, I., Chamovitz, D., Hirschberg, J., and Scolnik, P.A. (1991). Molecular cloning and expression in photosynthetic bacteria of a soybean cDNA coding for phytoene desaturase, an enzyme of the carotenoid bisynthesis pathway. Proceedings of the National Academy of Sciences USA **88,** 6532-6536.

Bassard, J.-E., Richert, L., Geerinck, J., Renault, H., Duval, F., Ullmann, P., Schmitt, M., Meyer, E., Mutterer, J., Boerjan, W., De Jaeger, G., Mely, Y., Goossens, A., and Werck-Reichhart, D. (2012). Protein-protein and protein-membrane associations in the lignin pathway. Plant Cell **24,** 4465-4482.

Batard, Y., Hehn, A., Nedelkina, S., Schalk, M., Pallett, K., Schaller, H., and Werck-Reichhart, D. (2000). Increasing expression of P450 and P450-reductase proteins from monocots in heterologous systems. Archives of Biochemistry and Biophysics **379,** 161-169.

Beyer, P., Al-Babili, S., Ye, X.D., Lucca, P., Schaub, P., Welsch, R., and Potrykus, I. (2002). Golden rice: Introducing the beta-carotene biosynthesis pathway into rice endosperm by genetic engineering to defeat vitamin A deficiency. Journal of Nutrition **132,** 506S-510S.

Bhagwat, B., Chi, M., Su, L., Tang, H., Tang, G., and Xiang, Y. (2013). An invivo transient expression system can be applied for rapid and effective selection of artificial microrna constructs for plant stable genetic transformation. Journal of genetics and genomics **40,** 261-270.

Blasco, F., Kauffmann, I., and Schmid, R.D. (2004). CYP175A1 from *Thermus thermophilus* HB27, the first beta-carotene hydroxylase of the P450 superfamily. Applied Microbiology and Biotechnology **64,** 671-674.

Block, M.A., Dorne, A.J., Joyard, J., and Douce, R. (1983). Preparation and characterization of membrane fractions enriched in outer and inner envelope membranes from spinach chloroplasts. II Biochemical characterization. Journal of Biological Chemistry **258,** 3281-3286.

Bojorquez, R.M.C., Gallego, J.G., and Collado, P.S. (2013). Functional properties and health benefits of lycopene. Nutricion Hospitalaria **28,** 6-15.

Botella-Pavia, P., Besumbes, O., Phillips, M.A., Carretero-Paulet, L., Boronat, A., and Rodriguez-Concepcion, M. (2004). Regulation of carotenoid biosynthesis in plants: evidence for a key role of hydroxymethylbutenyl diphosphate reductase in controlling the supply of plastidial isoprenoid precursors. Plant Journal **40,** 188-199.

Bourgaud, F., Gravot, A., Milesi, S., and Gontier, E. (2001). Production of plant secondary metabolites: a historical perspective. Plant Science **161,** 839-851.

Bouvier, F., Rahier, A., and Camara, B. (2005). Biogenesis, molecular regulation and function of plant isoprenoids. Progress in Lipid Research **44,** 357–429.

Bramley, P.M. (1985). The in vitro biosynthesis of carotenoids. Advances in Lipid Research **21,** 243-279.

Bramley, P.M. (2002). Regulation of carotenoid formation during tomato fruit ripening and development. Journal of Experimental Botany **53,** 2107-2113.

Bramley, P.M. (2013). Carotenoid biosynthesis and chlorophyll degradation. In The molecular biology and biochemistry of fruit ripening, G.B. Seymour, M. Poole, J.J. Giovannoni, and G.A. Tucker, eds (Oxford, UK: John Wiley & sons, Inc), pp. 75-102.

Breitenbach, J., Misawa, N., Kajiwara, S., and Sandmann, G. (1996). Expression in *Escherichia coli* and properties of the carotene ketolase from Haematococcus pluvialis. Fems Microbiology Letters **140,** 241-246.

Breitenbach, J., Vioque, A., and Sandmann, G. (2001). Gene sll0033 from *Synechocystis* 6803 encodes a carotene isomerase involved in the biosynthesis of all-E lycopene. Zeitschrift Fur Naturforschung C-a Journal of Biosciences **56,** 915-917.

Breithaupt, D.E. (2007). Modern application of xanthophylls in animal feeding - a review. Trends in Food Science & Technology **18,** 501-506.

Britton, G. (1995). Structure and properties of carotenoids in relation to function. FASEB Journal **9,** 1551-1558.

Britton, G. (2009). Vitamin A and vitamin A deficiency. In Carotenoids, G. Britton, S. Liaaen-Jensen, and H. Pfander, eds (Basal: Birkhasuer Verlag), pp. 173-190.

Britton, G., Liaaen-Jensen, S. and Pfander, H. (1995b). UV/Visible Spectroscopy in Carotenoids. In Spectroscopy, R. gemgemgem A, ed (Basel), pp. 13-62.

Britton, G., Liaaen-Jensen, S. and Pfander, H. (2004). Carotenoids Handbook.

Broun, P., and Somerville, C. (2001). Progress in plant metabolic engineering. Proceedings of the National Academy of Sciences USA **98,** 8925-8927.

Buckner, B., Miguel, P.S., JanickBuckner, D., and Bennetzen, J.L. (1996). The Y1 gene of maize codes for phytoene synthase. Genetics **143,** 479-488.

Burkhardt, P.K., Beyer, P., Wunn, J., Kloti, A., Armstrong, G.A., Schledz, M., vonLintig, J., and Potrykus, I. (1997). Transgenic rice (*Oryza sativa*) endosperm expressing daffodil (*Narcissus pseudonarcissus*) phytoene

synthase accumulates phytoene, a key intermediate of provitamin A biosynthesis. Plant Journal **11,** 1071-1078.

Busch, M., Seuter, A., and Hain, R. (2002). Functional analysis of the early steps of carotenoid biosynthesis in tobacco. Plant Physiology **128,** 439-453.

Butelli, E., Titta, L., Giorgio, M., Mock, H.-P., Matros, A., Peterek, S., Schijlen, E.G.W.M., Hall, R.D., Bovy, A.G., Luo, J., and Martin, C. (2008). Enrichment of tomato fruit with health-promoting anthocyanins by expression of select transcription factors. Nature Biotechnology **26,** 1301-1308.

Caddick, M.X., Greenland, A.J., Jepson, I., Krause, K.P., Qu, N., Riddell, K.V., Salter, M.G., Schuch, W., Sonnewald, U., and Tomsett, A.B. (1998). An ethanol inducible gene switch for plants used to manipulate carbon metabolism. Nature Biotechnology **16,** 177-180.

Camara, B., Bardat, F., Dogbo, O., Brangeon, J., and Moneger, R. (1983). Terpenoid metabolism in plastids- Isolation and biochemical characteristics of *Capsicum annuun* chromoplasts. Plant Physiology **73,** 94-99.

Cao, H., Zhang, J., Xu, J., Ye, J., Yun, Z., Xu, Q., Xu, J., and Deng, X. (2012). Comprehending crystalline beta-carotene accumulation by comparing engineered cell models and the natural carotenoid-rich system of citrus. Journal of Experimental Botany **63,** 4403-4417.

Carvalho, L.J., Lippolis, J., Chen, S., Batista de Souza, C.R., Vieira, E.A., and Anderson, J.V. (2012). Characterization of carotenoid-protein complexes and gene expression analysis associated with carotenoid sequestration in pigmented cassava (*manihot esculenta* crantz) storage root. The open biochemistry journal **6,** 116-130.

Castillon, A., Shen, H., and Huq, E. (2007). Phytochrome Interacting Factors: central players in phytochrome-mediated light signaling networks. Trends Plant Science **12,** 514-521.

Cazzonelli, C.I. (2011). Carotenoids in nature: insights from plants and beyond. Functional Plant Biology **38,** 833-847.

Cazzonelli, C.I., and Pogson, B.J. (2010). Source to sink: regulation of carotenoid biosynthesis in plants. Trends Plant Science **15,** 266-274.

Cazzonelli, C.I., Cuttriss, A.J., Cossetto, S.B., Pye, W., Crisp, P., Whelan, J., Finnegan, E.J., Turnbull, C., and Pogson, B.J. (2009). Regulation of

Carotenoid composition and shoot branching in *arabidopsis* by a chromatin modifying histone methyltransferase, SDG8. Plant Cell **21,** 39-53.

Chen, F.Q., Foolad, M.R., Hyman, J., St Clair, D.A., and Beelaman, R.B. (1999). Mapping of QTLs for lycopene and other fruit traits in a *Lycopersicon esculentum* x *L. pimpinellifolium* cross and comparison of QTLs across tomato species. Molecular Breeding **5,** 283-299.

Chen, Y., Li, F., and Wurtzel, E.T. (2010). Isolation and characterization of the Z-ISO gene encoding a missing component of carotenoid biosynthesis in plants. Plant Physiology **153,** 66-79.

Cheng, M., Fry, J.E., Pang, S.Z., Zhou, H.P., Hironaka, C.M., Duncan, D.R., Conner, T.W., and Wan, Y.C. (1997). Genetic transformation of wheat mediated by *Agrobacterium tumefaciens*. Plant Physiology **115,** 971-980.

Cheung, A.Y., Mcnellis, T., and Piekos, B. (1993). Maintenance of chloroplast components during chromoplast differentiation in the tomato mutant green flesh. Plant Physiology **101,** 1223-1229.

Chilton, M.D. (1979). Agrobacterium Ti plasmids as a tool for genetic engineering in plants. Basic Life Science **14,** 23-31.

Cho, D.H., Jung, Y.J., Choi, C.-S., Lee, H.-J., Park, J.-H., Dane, F., and Kang, K.-K. (2008). Astaxanthin production in transgenic *Arabidopsis* with chyB gene encoding beta-carotene hydroxylase. Journal of Plant Biology **51,** 58-63.

Choi, S.-K., Harada, H., Matsuda, S., and Misawa, N. (2007). Characterization of two beta-carotene ketolases, CrtO and CrtW, by complementation analysis in *Escherichia coli*. Applied Microbiology and Biotechnology **75,** 1335-1341.

Choi, S.-K., Matsuda, S., Hoshino, T., Peng, X., and Misawa, N. (2006). Characterization of bacterial beta-carotene 3,3'-hydroxylases, CrtZ, and P450 in astaxanthin biosynthetic pathway and adonirubin production by gene combination in *Escherichia coli*. Applied Microbiology and Biotechnology **72,** 1238-1246.

Choi, S.K., Nishida, Y., Matsuda, S., Adachi, K., Kasai, H., Peng, X., Komemushi, S., Miki, W., and Misawa, N. (2005). Characterization of beta-carotene ketolases, CrtW, from marine bacteria by complementation analysis in *Escherichia coli*. Marine Biotechnology **7,** 515-522.

Chung, M.Y., Vrebalov, J., Alba, R., Lee, J., McQuinn, R., Chung, J.D., Klein, P., and Giovannoni, J. (2010). A tomato (*Solanum lycopersicum*) APETALA2/ERF gene, SlAP2a, is a negative regulator of fruit ripening. Plant Journal **64,** 936-947.

Clarke, J.L., and Daniell, H. (2011). Plastid biotechnology for crop production: present status and future perspectives. Plant Molecular Biology **76,** 211-220.

Cong, L., Wang, C., Chen, L., Liu, H., Yang, G., and He, G. (2009). Expression of phytoene synthase1 and carotene desaturase crtl genes result in an increase in the total carotenoids content in transgenic elite wheat (*Triticum aestivum* L.). Journal of Agricultural and Food Chemistry **57,** 8652-8660.

Conrado, R.J., Varner, J.D., and DeLisa, M.P. (2008). Engineering the spatial organization of metabolic enzymes: mimicking nature's synergy. Current Opinion in Biotechnology **19,** 492-499.

Cookson, P.J., Kiano, J.W., Shipton, C.A., Fraser, P.D., Romer, S., Schuch, W., Bramley, P.M., and Pyke, K.A. (2003). Increases in cell elongation, plastid compartment size and phytoene synthase activity underlie the phenotype of the high pigment-1 mutant of tomato. Planta **217,** 896-903

Cunningham, F.X., Jr., Pogson, B., Sun, Z., McDonald, K.A., DellaPenna, D., and Gantt, E. (1996). Functional analysis of the beta and epsilon lycopene cyclase enzymes of *Arabidopsis* reveals a mechanism for control of cyclic carotenoid formation. Plant Cell **8,** 1613-1626.

D'Agostino, I.B., and Kieber, J.J. (1999). Phosphorelay signal transduction: the emerging family of plant response regulators. Trends in Biochemical Science **24,** 452-456.

Dalal, M., Chinnusamy, V., and Bansal, K.C. (2010). Isolation and functional characterization of lycopene beta-cyclase (CYC-B) promoter from Solanum habrochaites. BMC Plant Biology **10,** 61.

D'Ambrosio, C., Giorio, G., Marino, I., Merendino, A., Petrozza, A., Salfi, L., Stigliani, A.L., and Cellini, F. (2004). Virtually complete conversion of lycopene into beta-carotene in fruits of tomato plants transformed with the tomato lycopene beta-cyclase (tlcy-b) cDNA. Plant Science **166,** 207-214.

Davison, P.A., Hunter, C.N., and Horton, P. (2002). Overexpression of beta-carotene hydroxylase enhances stress tolerance in *Arabidopsis*. Nature **418,** 203-206.

Davuluri, G.R., Tuinen, A.v., Fraser, P.D., Manfredonia, A., Newman, R., Burgess, D., Brummell, D.A., King, S.R., Palys, J., Uhlig, J., Bramley, P.M., Pennings, H.M.J., and Bowler, C. (2005). Fruit-specific RNAi-mediated suppression of DET1 enhances carotenoid and flavoinoid content in tomatoes. Nature biotechnology letters **23,** 890-895.

De Camilli, P., Harris, S.M., Huttner, W.B., and Greengard, P. (1983). Synapsin-I (ProteinI), anerve terminal-specific phosphoprotein.2. Its specfific association with synaptic vesicles demontrated by immunocytochemistry in agarose-embeeded synaptosomes. Journal of Cell Biology **96,** 1355-1373.

DellaPenna, D. (2001). Plant metabolic engineering. Plant Physiology **125,** 160-163.

DemmigAdams, B., and Adams, W.W. (1996). The role of xanthophyll cycle carotenoids in the protection of photosynthesis. Trends in Plant Science **1,** 21-26.

Deruere, J., Romer, S., Dharlingue, A., Backhaus, R.A., Kuntz, M., and Camara, B. (1994). Fibril assembly and carotenoid overaccumulation in chromoplasts - A model for supramolecular lipoprotein structures. Plant Cell **6,** 119-133.

Devitt, L.C., Fanning, K., Dietzgen, R.G., and Holton, T.A. (2010). Isolation and functional characterization of a lycopene beta-cyclase gene that controls fruit colour of papaya (*Carica papaya* L.). Journal of Experimental Botany **61,** 33-39.

Dharmapuri, S., Rosati, C., Pallara, P., Aquilani, R., Bouvier, F., Camara, B., and Giuliano, G. (2002). Metabolic engineering of xanthophyll content in tomato fruits. FEBS Letters **519,** 30-34.

Diretto, G., Al-Babili, S., Tavazza, R., Papacchioli, V., Beyer, P., and Giuliano, G. (2007a). Metabolic engineering of potato carotenoid content through tuber-specific overexpression of a bacterial mini-pathway. PLoS ONE **2**.

Diretto, G., Tavazza, R., Welsch, R., Pizzichini, D., Mourgues, F., Papacchioli, V., Beyer, P., and Giuliano, G. (2006). Metabolic engineering of potato tuber carotenoids through tuber-specific silencing of lycopene epsilon cyclase. BMC Plant Biology **6**.

Diretto, G., Welsch, R., Tavazza, R., Mourgues, F., Pizzichini, D., Beyer, P., and Giuliano, G. (2007b). Silencing of beta-carotene hydroxylase increases total carotenoid and beta-carotene levels in potato tubers. BMC Plant Biology **7**.

Ducreux, L.J., Morris, W.L., Hedley, P.E., Shepherd, T., Davies, H.V., Millam, S., and Taylor, M.A. (2005). Metabolic engineering of high carotenoid potato tubers containing enhanced levels of beta-carotene and lutein. Journal of Experimental Botany **56,** 81-89.

Dudareva, N., Klempien, A., Muhlemann, J.K., and Kaplan, I. (2013). Biosynthesis, function and metabolic engineering of plant volatile organic compounds. New Phytologist **198,** 16-32.

Dudareva, N., Pichersky, E., and Gershenzon, J. (2004). Biochemistry of plant volatiles. Plant Physiology **135,** 1893-1902.

Dueber, J.E., Wu, G.C., Malmirchegini, G.R., Moon, T.S., Petzold, C.J., Ullal, A.V., Prather, K.L.J., and Keasling, J.D. (2009). Synthetic protein scaffolds provide modular control over metabolic flux. Nature Biotechnology **27,** 753-759.

Egea, I., Barsan, C., Bian, W.P., Purgatto, E., Latche, A., Chervin, C., Bouzayen, M., and Pech, J.C. (2010). Chromoplast Differentiation: Current Status and Perspectives. Plant Cell Physiology **51,** 1601-1611.

Enfissi, E.M., Fraser, P.D., Lois, L.M., Boronat, A., Schuch, W., and Bramley, P.M. (2005). Metabolic engineering of the mevalonate and non-mevalonate isopentenyl diphosphate-forming pathways for the production of health-promoting isoprenoids in tomato. Plant Biotechnology J **3,** 17-27.

Enfissi, E.M.A., Barneche, F., Ahmed, I., Lichtle, C., Gerrish, C., McQuinn, R.P., Giovannoni, J.J., Lopez-Juez, E., Bowler, C., Bramley, P.M., and Fraser, P.D. (2010). Integrative transcript and metabolite analysis of nutritionally enhanced DE-ETIOLATED1 downregulated tomato fruit. Plant Cell **22,** 1190-1215.

Facella, P., Lopez, L., Carbone, F., Galbraith, D.W., Giuliano, G., and Perrotta, G. (2008). Diurnal and circadian rhythms in the tomato transcriptome and their modulation by cryptochrome photoreceptors. Plos One **3**.

Farre, G., Sanahuja, G., Naqvi, S., Bai, C., Capell, T., Zhu, C.F., and Christou, P. (2010). Travel advice on the road to carotenoids in plants. Plant Science **179,** 28-48.

Fernandez-Gonzalez, B., Sandmann, G., and Vioque, A. (1997). A new type of asymmetrically acting beta-carotene ketolase is required for the synthesis of

echinenone in the cyanobacterium *Synechocystis* sp. PCC 6803. Journal of Biological Chemistry **272,** 9728-9733.

Finnegan, J., and McElroy, D. (1994). Transgene inactivation: Plants fight back. Bio-Technology **12,** 883-888.

Fischer, R., and Emans, N. (2000). Molecular farming of pharmaceutical proteins. Transgenic Research. **9,** 279-299.

Frank, H.A., and Cogdell, R.J. (1993). The photochemistry and function of carotenoids in photosynthesis. In Carotenoids in photosynthesis, A.J. Young and G. Britton, eds (London: Chapman & Hall), pp. 253-315.

Fraser, P., and Bramley, P. (2004). The biosynthesis and nutritional uses of carotenoids. Progress in Lipid Research **43,** 228-265.

Fraser, P.D., Enfissi, E., and Bramley, P.M. (2009). Genetic engineering of carotenoid formation in tomato fruit and the potential application of systems and synthetic biology approaches. Archives of Biochemistry and Biophysics **483,** 196–204.

Fraser, P.D., Kiano, J.W., Truesdale, M.R., Schuch, W., and Bramley, P.M. (1999). Phytoene synthase-2 enzyme activity in tomato does not contribute to carotenoid synthesis in ripening fruit. Plant Molecular Biology **40,** 687-698.

Fraser, P.D., Misawa, N., Linden, H., Yamano, S., Kobayashi, K., and Sandmann, G. (1992). Expression in Escherichia-coli, purification, and reactivation of the recombinant *Erwinia uredovora* phytoene desaturase. Journal of Biological Chemistry **267,** 19891-19895.

Fraser, P.D., Miura, Y., and Misawa, N. (1997). In vitro characterization of astaxanthin biosynthetic enzymes. Journal of Biological Chemistry **272,** 6128-6135.

Fraser, P.D., Pinto, M.E.S., Holloway, D.E., and Bramley, P.M. (2000b). Application of high-performance liquid chromatography with photodiode array detection to the metabolic profiling of plant isoprenoids. The Plant Journal **24,** 551–558.

Fraser, P.D., Romer, S., Kiano, J.W., Shipton, C.A., Mills, P.B., Drake, R., Schuch, W., and Bramley, P.M. (2001). Elevation of carotenoids in tomato by genetic manipulation. Journal of the Science of Food and Agriculture **81,** 822-827.

Fraser, P.D., Romer, S., Shipton, C.A., Mills, P.B., Kiano, J.W., Misawa, N., Drake, R.G., Schuch, W., and Bramley, P.M. (2002). Evaluation of transgenic tomato plants expressing an additional phytoene synthase in a fruit-specific manner. Proceedings of the National Academy of Sciences USA **99,** 1092-1097.

Fraser, P.D., Schuch, W., and Bramley, P.M. (2000a). Phytoene synthase from tomato (*Lycopersicon esculentum*) chloroplasts - partial purification and biochemical properties. Planta **211,** 361-369.

Fraser, P.D., Shimada, H., and Misawa, N. (1998). Enzymic confirmation of reactions involved in routes to astaxanthin formation, elucidated using a direct substrate in vitro assay. European Journal of Biochemistry **252,** 229-236.

Fraser, P.D., Truesdale, M.R., Bird, C.R., Schuch, W., and Bramley, P.M. (1994). Carotenoid biosynthesis during tomato fruit development (evidence for tissue-specific gene expression). Plant Physiology **105,** 405.

Fray, R.G., and Grierson, D. (1993). Identification and genetic analysis of normal and mutant phytoene synthase genes of tomato by sequencing, complementation and co-suppression. Plant Molecular Biology **22,** 589-602.

Fray, R.G., Wallace, A., Fraser, P.D., Valero, D., Hedden, P., Bramley, P.M., and Grierson, D. (1995). Constitutive expression of a fruit phytoene synthase gene in transgenic tomatoes causes dwarfism by redirecting metabolites from the gibberellin pathway. Plant Journal **8,** 693-701.

Fujisawa, M., Takita, E., Harada, H., Sakurai, N., Suzuki, H., Ohyama, K., Shibata, D., and Misawa, N. (2009). Pathway engineering of *Brassica napus* seeds using multiple key enzyme genes involved in ketocarotenoid formation. Journal of Experimental Botany **60,** 1319-1332.

Gabrielska, J., and Gruszecki, W.I. (1996). Zeaxanthin (dihydroxy-beta-carotene but not beta-carotene rigidifies lipid membranes: A H-1-NMR study of carotenoid-egg phosphatidylcholine liposomes. BBA-Biomembranes **1285,** 167-174.

Galili, G., Galili, S., Lewinsohn, E., and Tadmor, Y. (2002). Genetic, molecular, and genomic approaches to improve the value of plant foods and feeds. Critical Reviews in Plant Sciences **21,** 167-204.

Gallagher, C.E., Matthews, P.D., Li, F.Q., and Wurtzel, E.T. (2004). Gene duplication in the carotenoid biosynthetic pathway preceded evolution of the grasses. Plant Physiology **135,** 1776-1783.

Galpaz, N., Ronen, G., Khalfa, Z., Zamir, D., and Hirschberg, J. (2006). A chromoplast-specific carotenoid biosynthesis pathway is revealed by cloning of the tomato white-flower locus. Plant Cell **18,** 1947-1960.

Galpaz, N., Wang, Q., Menda, N., Zamir, D., and Hirschberg, J. (2008). Abscisic acid deficiency in the tomato mutant high-pigment 3 leading to increased plastid number and higher fruit lycopene content. Plant Journal **53,** 717-730.

Garcia-Limones, C., Schnaebele, K., Blanco-Portales, R., Luz Bellido, M., Luis Caballero, J., Schwab, W., and Munoz-Blanco, J. (2008). Functional characterization of FaCCD1: A carotenoid cleavage dioxygenase from strawberry involved in lutein degradation during fruit ripening. Journal of Agricultural and Food Chemistry **56,** 9277-9285.

Gerjets, T., and Sandmann, G. (2006). Ketocarotenoid formation in transgenic potato. Journal of Experimental Botany **57,** 3639-3645.

Gerjets, T., Sandmann, M., Zhu, C., and Sandmann, G. (2007). Metabolic engineering of ketocarotenoid biosynthesis in leaves and flowers of tobacco species. Biotechnology Journal **2,** 1263-1269.

Giliberto, L., Perrotta, G., Pallara, P., Weller, J.L., Fraser, P.D., Bramley, P.M., Fiore, A., Tavazza, M., and Giuliano, G. (2005). Manipulation of the blue light photoreceptor cryptochrome 2 in tomato affects vegetative development, flowering time, and fruit antioxidant content. Plant physiology **137,** 199.

Giorio, P., Giorio, G., Guadagno, C.R., Cellini, F, Stigliani, L.A., and D'Ambrosio, C. (2012). Carotenoid content, leaf gas-exchange, and non-photochemical quenching in transgenic tomato overexpressing the beta-carotene hydroxylase 2 gene (CrtR-b2). Environmental and Experimental Botany **75,** 1-8.

Golldack, D., Li, C., Mohan, H., and Probst, N. (2013). Gibberellins and abscisic acid signal crosstalk: living and developing under unfavorable conditions. Plant cell reports **32**.

Goodwin, T.W. (1955). Carotenoids. Annual Review of Biochemistry **24,** 497-522.

Goodwin, T.W. (1980). Nature and distribution of carotenoids. Food Chemistry **5,** 3-13.

Gray, J., Picton, S., Shabbeer, J., Schuch, W., and Grierson, D. (1992). Molecular biology of fruit ripening and its manipulation with antisense genes. In Monographs in Systematic Botany; 10 Years plant molecular biology, R.A. Schilperoort and L. Dure, eds, pp. 69-87.

Gruszecki, W.I., and Strzalka, K. (2005). Carotenoids as modulators of lipid membrane physical properties. Biochimica Et Biophysica Acta-Molecular Basis of Disease **1740,** 108-115.

Gulcin, I. (2012). Antioxidant activity of food constituents: an overview. Archives of Toxicology **86,** 345-391.

Guo, F., Zhou, W.J., Zhang, J.C., Xu, Q., and Deng, X.X. (2012). Effect of the Citrus Lycopene beta-Cyclase Transgene on Carotenoid Metabolism in Transgenic Tomato Fruits. Plos One **7**.

Han, Y., Li, L., Dong, M., Yuan, W., and Shang, F. (2013). cDNA cloning of the phytoene synthase (PSY) and expression analysis of PSY and carotenoid cleavage dioxygenase genes in *Osmanthus fragrans*. Biologia **68,** 258-263.

Hannibal, L., Lorquin, J., D'Ortoli, N.A., Garcia, N., Chaintreuil, C., Masson-Boivin, C., Dreyfus, B., and Giraud, E. (2000). Isolation and characterization of canthaxanthin biosynthesis genes from the photosynthetic bacterium *Bradyrhizobium* sp strain ORS278. Journal of Bacteriology **182,** 3850-3853.

Harris, W.M., and Spurr, A.R. (1969a). Chromoplasts of tomato-d fruits ii the red tomato-d lycopene thylakoids carotenoids pigments. American Journal of Botany **56,** 380-389.

Harris, W.M., and Spurr, A.R. (1969b). Chromoplasts of tomato-d fruits i ultrastructure of low pigment and high beta mutants carotene analyses lycopene beta carotene chloroplasts chlorophyll grana thylakoids phyto ferritin. American Journal of Botany **56,** 369-379.

Hasunuma, T., Kondo, A., and Miyake, C. (2009). Metabolic pathway engineering by plastid transformation is a powerful tool for production of compounds in higher plants. Plant Biotechnology **26,** 39-46.

Hasunuma, T., Miyazawa, S.I., Yoshimura, S., Shinzaki, Y., Tomizawa, K.I., Shindo, K., Choi, S.K., Misawa, N., and Miyake, C. (2008). Biosynthesis

of astaxanthin in tobacco leaves by transplastomic engineering. The Plant Journal **55,** 857–868.

Havaux, M. (1998). Carotenoids as membrane stabilizers in chloroplasts. Trends in Plant Science **3,** 147-151.

Havaux, M., and Niyogi, K.K. (1999). The violaxanthin cycle protects plants from photooxidative damage by more than one mechanism. Proceedings of the National Academy of Sciences USA **96,** 8762-8767.

Hemmerlin, A. (2013). Post-translational events and modifications regulating plant enzymes involved in isoprenoid precursor biosynthesis. Plant Science **203,** 41-54.

Hemmerlin, A., Harwood, J.L., and Bach, T.J. (2012). A raison d'etre for two distinct pathways in the early steps of plant isoprenoid biosynthesis? Progress in Lipid Research **51,** 95-148.

Hernandez-Marin, E., Galano, A., and Martinez, A. (2013). Cis Carotenoids: Colorful Molecules and Free Radical Quenchers. Journal of Physical Chemistry B **117,** 4050-4061.

Hirayama, T., and Shinozaki, K. (2007). Perception and transduction of abscisic acid signals: keys to the function of the versatile plant hormone ABA. Trends in Plant Science **12,** 343-351.

Hirschberg, J. (2001). Carotenoid biosynthesis in flowering plants. Current Opinion in Plant Biology **4,** 210–218.

Hiseni, A., Arends, I.W.C.E., and Otten, L.G. (2011). Biochemical characterization of the carotenoid 1,2-hydratases (CrtC) from *Rubrivivax gelatinosus* and *Thiocapsa roseopersicina*. Applied Microbiology and Biotechnology **91,** 1029-1036.

Horsch, R.B., Fry, J.E., Hoffmann, N.L., Eichholtz, D., Rogers, S.G., and Fraley, R.T. (1985). A simple and general-method for transferring genes into plants. Science **227,** 1229-1231.

Howitt, C.A., and Pogson, B.J. (2006). Carotenoid accumulation and function in seeds and non-green tissues. Plant Cell and Environment **29,** 435-445.

Huang, F.-C., Molnar, P., and Schwab, W. (2009). Cloning and functional characterization of carotenoid cleavage dioxygenase 4 genes. Journal of Experimental Botany **60,** 3011-3022.

Huang, J.-C., Wang, Y., Sandmann, G., and Chen, F. (2006). Isolation and characterization of a carotenoid oxygenase gene from *Chlorella zofingiensis* (Chlorophyta). Applied Microbiology and Biotechnology **71,** 473-479.

Huang, J.-C., Zhong, Y.-J., Liu, J., Sandmann, G., and Chen, F. (2013). Metabolic engineering of tomato for high-yield production of astaxanthin. Metabolic Engineering **17,** 59-67.

Hugueney, P., Romer, S., Kuntz, M., and Camara, B. (1992). Characterization and molecular cloning of a flavoprotein catalyzing the synthesis of phytofluene and zetacarotene in *Capsicum* chromoplasts. European Journal of Biochemistry **209,** 399-407.

Hundle, B.S., Obrien, D.A., Alberti, M., Beyer, P., and Hearst, J.E. (1992). Functional expression of zeaxanthin glucosyltransferase from Erwinia herbicola and a proposed uridine diphosphate binding site. Proceedings of the National Academy of Sciences USA **89,** 9321-9325.

Hundle, B.S., Obrien, D.A., Beyer, P., Kleinig, H., and Hearst, J.E. (1993). In vitro expression and activity of lycopene cyclase and beta-carotene hydroxylase from *Erwinia herbicola*. FEBS Letters **315,** 329-334.

Hussain, M.S., Fareed, S., Ansari, S., Rahman, M.A., Ahmad, I.Z., and Saeed, M. (2012). Current approaches toward production of secondary plant metabolites. Journal of pharmacy & bioallied sciences **4,** 10-20.

Hussein, G., Sankawa, U., Goto, H., Matsumoto, K., and Watanabe, H. (2006). Astaxanthin, a carotenoid with potential in human health and nutrition. Journal of Natural Products **69,** 443-449.

Isaacson, T. (2002). Cloning of tangerine from tomato reveals a carotenoid isomerase essential for the production of beta-carotene and xanthophylls in plants. The Plant Cell Online **14,** 333-342.

Isaacson, T., Ohad, I., Beyer, P., and Hirschberg, J. (2004). Analysis in vitro of the enzyme CRTISO establishes a poly-cis-carotenoid biosynthesis pathway in plants. Plant Physiology **136,** 4246-4255.

Jahns, P., Latowski, D., and Strzalka, K. (2009). Mechanism and regulation of the violaxanthin cycle: The role of antenna proteins and membrane lipids. BBA-Bioenergetics **1787,** 3-14.

Jayaraj, J., Devlin, R., and Punja, Z. (2008). Metabolic engineering of novel ketocarotenoid production in carrot plants. Transgenic Res. **17,** 489-501.

Jeknic, Z., Morre, J.T., Jeknic, S., Jevremovic, S., Subotic, A., and Chen, T.H.H. (2012). Cloning and Functional Characterization of a Gene for Capsanthin-Capsorubin Synthase from Tiger Lily (*Lilium lancifolium* Thunb. 'Splendens'). Plant Cell Physiology **53,** 1899-1912.

Jeong, J., and Choi, G. (2013). Phytochrome-interacting factors have both shared and distinct biological roles. Molecules and cells **35,** 371-380.

Johnson, E.J. (2002). The role of carotenoids in human health. Nutrition in clinical care : an official publication of Tufts University **5,** 56-65.

Johnson, E.J. (2010a). The impact of carotenoids on cognitive function in the elderly. Agro Food Industry Hi-Tech **21,** 41-43.

Johnson, E.J. (2010b). Age-related macular degeneration and antioxidant vitamins: recent findings. Current Opinion in Clinical Nutrition and Metabolic Care **13,** 28-33.

Johnson, E.J., Suter, P.M., Sahyoun, N., Ribayamercado, J.D., and Russell, R.M. (1995). Relation between beta-carotene intake and plasma and adipose-tissue concentrations of carotenoids and retinoids. American Journal of Clinical Nutrition **62,** 598-603.

Jones, M.O., Piron-Prunier, F., Marcel, F., Piednoir-Barbeau, E., Alsadon, A.A., Wahb-Allah, M.A., Al-Doss, A.A., Bowler, C., Bramley, P.M., Fraser, P.D., and Bendahmane, A. (2012). Characterisation of alleles of tomato light signalling genes generated by TILLING. Phytochemistry **79,** 78-86.

Jorgensen, K., Rasmussen, A.V., Morant, M., Nielsen, A.H., Bjarnholt, N., Zagrobelny, M., Bak, S., and Moller, B.L. (2005). Metabolon formation and metabolic channeling in the biosynthesis of plant natural products. Current Opinion in Plant Biology **8,** 280-291.

Josse, E.M., Simkin, A.J., Gaffe, J., Laboure, A.M., Kuntz, M., and Carol, P. (2000). A plastid terminal oxidase associated with carotenoid desaturation during chromoplast differentiation. Plant Physiology **123,** 1427-1436.

Joyard, J., Ferro, M., Masselon, C., Seigneurin-Berny, D., Salvi, D., Garin, J., and Rolland, N. (2009). Chloroplast proteomics and the compartmentation of plastidial isoprenoid biosynthetic pathways. Molecular Plant **2,** 1154-1180.

Kachanovsky, D.E., Filler, S., Isaacson, T., and Hirschberg, J. (2012). Epistasis in tomato color mutations involves regulation of phytoene synthase 1

expression by cis-carotenoids. Proceedings of the National Academy of Sciences USA **109,** 19021-19026.

Kahlau, S., and Bock, R. (2008). Plastid transcriptomics and translatomics of tomato fruit development and chloroplast-to-chromoplast differentiation: chromoplast gene expression largely serves the production of a single protein. Plant Cell **20,** 856-874.

Kai, G., Liao, P., Zhang, T., Zhou, W., Wang, J., Xu, H., Liu, Y., and Zhang, L. (2010). Characterization, expression profiling, and functional identification of a gene encoding geranylgeranyl diphosphate synthase from *Salvia miltiorrhiza*. Biotechnology and Bioprocess Engineering **15,** 236-245.

Kapila, J., DeRycke, R., VanMontagu, M., and Angenon, G. (1997). An Agrobacterium-mediated transient gene expression system for intact leaves. Plant Science **122,** 101-108.

Karlova, R., Rosin, F.M., Busscher-Lange, J., Parapunova, V., Do, P.T., Fernie, A.R., Fraser, P.D., Baxter, C., Angenent, G.C., and de Maagd, R.A. (2011). Transcriptome and metabolite profiling show that APETALA2A is a major regulator of tomato fruit ripening. Plant Cell **23,** 923-941.

Kessler, F., and Vidi, P.-A. (2007). Plastoglobule lipid bodies: Their functions in chloroplasts and their potential for applications. In Green Gene Technology: Research in an Area of Social Conflict, A. Fiechter and C. Sautter, eds, pp. 153-172.

Kessler, F., Schnell, D., and Blobel, G. (1999). Identification of proteins associated with plastoglobules isolated from pea (*Pisum sativum* L.) chloroplasts. Planta **208,** 107-113.

Khanna, R., Shen, Y., Marion, C.M., Tsuchisaka, A., Theologis, A., Eberhard, S., and Quail, P.H. (2007). The Basic helix-loop-helix transcription factor PIF5 acts on ethylene biosynthesis and phytochrome signaling by distinct mechanisms. The Plant Cell **19,** 3915-3929.

Kidwell, M.G., and Lisch, D. (1997). Transposable elements as sources of variation in animals and plants. Proceedings of the National Academy of Sciences USA **94,** 7704-7711.

Kilambi, H.V., Kumar, R., Sharma, R., and Sreelakshmi, Y. (2013). Chromoplast-specific carotenoid-associated protein appears to be important

for enhanced accumulation of carotenoids in *hp1* tomato fruits. Plant Physiology **161,** 2085-2101.

Kim, J., and DellaPenna, D. (2006). Defining the primary route for lutein synthesis in plants: The role of Arabidopsis carotenoid beta-ring hydroxylase CYP97A3. Proceedings of the National Academy of Sciences USA **103,** 3474-3479.

Kim, J.-E., Cheng, K.M., Craft, N.E., Hamberger, B., and Douglas, C.J. (2010). Over-expression of *Arabidopsis thaliana* carotenoid hydroxylases individually and in combination with a beta-carotene ketolase provides insight into in vivo functions. Phytochemistry **71,** 168-178.

Kim, S.H., Ahn, Y.O., Ahn, M.-J., Jeong, J.C., Lee, H.-S., and Kwak, S.-S. (2013a). Cloning and characterization of an Orange gene that increases carotenoid accumulation and salt stress tolerance in transgenic sweetpotato cultures. Plant physiology and biochemistry **70,** 445-454.

Kim, S.H., Ahn, Y.O., Ahn, M.J., Lee, H.S., and Kwak, S.S. (2012). Down-regulation of beta-carotene hydroxylase increases beta-carotene and total carotenoids enhancing salt stress tolerance in transgenic cultured cells of sweetpotato. Phytochemistry **74,** 69-78.

Kim, S.H., Kim, Y.-H., Ahn, Y.O., Ahn, M.-J., Jeong, J.C., Lee, H.-S., and Kwak, S.-S. (2013b). Downregulation of the lycopene epsilon-cyclase gene increases carotenoid synthesis via the beta-branch-specific pathway andenhances salt-stress tolerance in sweetpotato transgenic calli. Physiology Plantarum **147,** 432-442.

Kimura, M., Kobori, C.N., Rodriguez-Amaya, D.B., and Nestel, P. (2007). Screening and HPLC methods for carotenoids in sweetpotato, cassava and maize for plant breeding trials. Food Chemistry **100,** 1734-1746.

Ko, K., Bornemisza, O., Kourtz, L., Ko, Z.W., Plaxton, W.C., and Cashmore, A.R. (1992). Isolation and characterization of a cDNA clone encoding a cognate 70-kDa heat shock protein of the chloroplast envelope. The Journal of Biological Chemistry **267,** 2986-2993.

Kohli, A., Twyman, R.M., Abranches, R., Wegel, E., Stoger, E., and Christou, P. (2003). Transgene integration, organization and interaction in plants. Plant Molecular Biology **52,** 247-258.

Kolotilin, I., Koltai, H., Tadmor, Y., Bar-Or, C., Reuveni, M., Meir, A., Nahon, S., Shlomo, H., Chen, L., and Levin, I. (2007). Transcriptional profiling of high pigment-2(dg) tomato mutant links early fruit plastid biogenesis with its overproduction of phytonutrients. Plant Physiology **145,** 389-401.

Krinsky, N.I. (1989). Antioxidant functions of carotenoids. Free Radical Biology and Medicine **7**, 617-635.

Krinsky, N.I., and Johnson, E.J. (2005). Carotenoid actions and their relation to health and disease. Molecular Aspects of Medicine **26,** 459-516.

Krinsky, N.I., and Yeum, K.J. (2003). Carotenoid-radical interactions. Biochemical and Biophysical Research Communications **305,** 754-760.

Krubasik, P., Kobayashi, M., and Sandmann, G. (2001). Expression and functional analysis of a gene cluster involved in the synthesis of decaprenoxanthin reveals the mechanisms for C-50 carotenoid formation. European Journal of Biochemistry **268,** 3702-3708.

Kumar, S., Dubey, A.K., Karmakar, R., Kini, K.R., Mathew, M.K., and Prakash, H.S. (2013). Inhibition of virus infection by transient expression of short hairpin RNA targeting the methyltransferase domain of Tobacco mosaic virus replicase. Phytoparasitica **41,** 9-15.

Kuntz, M., Romer, S., Suire, C., Hugueney, P., Weil, J.H., Schantz, R., and Camara, B. (1992). Identification of cDNA for the plastid-located geranylgeranyl pyrophosphate synthase from *Capsicum annuum*: Correlative increase in enzyme activity and trasncript level during fruit ripening. Plant Journal **2,** 25-34.

Laferriere, A., and Beyer, P. (1991). Purification of geranylgeranyl diphosphate synthase from *Sinapis-alba* etioplasts. Biochimica et Biophysica Acta **1077,** 167-172.

Lang, H.P., Cogdell, R.J., Gardiner, A.T., and Hunter, C.N. (1994). Early steps in carotenoid biosynthesis: sequences and transcriptional analysis of the crtI and CrtB genes of *Rhodobacter sphaeroides* and overexpression and reactivation of crtI in *Escherichia coli* and *R. sphaeroides*. Journal of Bacteriology **176,** 3859-3869.

Lange, B.M., and Ghassemian, M. (2003). Genome organization in Arabidopsis thaliana: a survey for genes involved in isoprenoid and chlorophyll metabolism. Plant Molecular Biology **51,** 925-948.

Lee, J.H., and Kim, Y.T. (2006). Functional expression of the astaxanthin biosynthesis genes from a marine bacterium, *Paracoccus haeundaensis*. Biotechnology Letters **28,** 1167-1173.

Lee, J.M., Joung, J.-G., McQuinn, R., Chung, M.-Y., Fei, Z., Tieman, D., Klee, H., and Giovannoni, J. (2012). Combined transcriptome, genetic diversity and metabolite profiling in tomato fruit reveals that the ethylene response factor SlERF6 plays an important role in ripening and carotenoid accumulation. Plant Journal **70,** 191-204.

Leitner-Dagan, Y., Ovadis, M., Zuker, A., Shklarman, E., Ohad, I., Tzfira, T., and Vainstein, A. (2006). CHRD, a plant member of the evolutionarily conserved YjgF family, influences photosynthesis and chromoplastogenesis. Planta **225,** 89-102.

Lemaux, P.G. (2008). Genetically engineered plants and foods: A scientist's analysis of the issues (Part I). In Annual Review of Plant Biology, pp. 771-812.

Lemaux, P.G. (2009). Genetically Engineered Plants and Foods: A Scientist's Analysis of the Issues (Part II). In Annual Review of Plant Biology, pp. 511-559.

Lewinsohn, E., Schalechet, F., Wilkinson, J., Matsui, K., Tadmor, Y., Kyoung-Hee, N., Amar, O., Lastochkin, E., Larkov, O., Ravid, U., Hiatt, W., Gepstein, S., and Pichersky, E. (2001). enhanced levels of the aroma and flavor compound S-linalool by metabolic engineering of the terpenoid pathway in tomato fruits. Plant Physiology **127,** 1256-1265.

Li, F., Vallabhaneni, R., and Wurtzel, E.T. (2008a). PSY3, a new member of the phytoene synthase gene family conserved in the poaceae and regulator of abiotic stress-induced root carotenogenesis. Plant Physiology **146,** 1333-1345.

Li, F., Vallabhaneni, R., Yu, J., Rocheford, T., and Wurtzel, E.T. (2008b). The maize phytoene synthase gene family: Overlapping roles for carotenogenesis in endosperm, photomorphogenesis, and thermal stress tolerance. Plant Physiology **147,** 1334-1346.

Li, L., and van Eck, J. (2007). Metabolic engineering of carotenoid accumulation by creating a metabolic sink. Transgenic Research **16,** 581-585.

Li, M., Gan, Z., Cui, Y., Shi, C., and Shi, X. (2011). Cloning and characterization of the zeta-carotene desaturase gene from *Chlorella protothecoides* CS-41. Journal of biomedicine & biotechnology **2011,** 731542-731542.

Li, Q., Farre, G., Naqvi, S., Breitenbach, J., Sanahuja, G., Bai, C., Sandmann, G., Capell, T., Christou, P., and Zhu, C. (2010). Cloning and functional characterization of the maize carotenoid isomerase and beta-carotene hydroxylase genes and their regulation during endosperm maturation. Transgenic Research **19,** 1053-1068.

Li, X.G., Zhu, Z., Feng, D.J., Chang, T.J., and Liu, X. (2001). Influence of DNA methylation on transgene expression. Chinese Science Bulletin **46,** 1300-1304.

Li, Z.H., Matthews, P.D., Burr, B., and Wurtzel, E.T. (1996). Cloning and characterization of a maize cDNA encoding phytoene desaturase, an enzyme of the carotenoid biosynthetic pathway. Plant Molecular Biology **30,** 269-279.

Lieberman, M., Segev, O., Gilboa, N., Lalazar, A., and Levin, I. (2004). The tomato homolog of the gene encoding UV-damaged DNA binding protein 1 (DDB1) underlined as the gene that causes the high pigment-1 mutant phenotype. Theoretical and Applied Genetics **108,** 1574-1581.

Lin, J., Jin, Y., Zhou, X., and Wang, J. (2010). Molecular cloning and functional analysis of the gene encoding geranylgeranyl diphosphate synthase from *Jatropha curcas*. African Journal Biotechnology **9,** 3342-3351.

Linden, H. (1999). Carotenoid hydroxylase from *Haematococcus pluvialis*: cDNA sequence, regulation and functional complementation. Biochimica Et Biophysica Acta-Gene Structure and Expression **1446,** 203-212.

Lindgren, L.O., Stalberg, K.G., and Hoglund, A.S. (2003). Seed-specific overexpression of an endogenous *Arabidopsis* phytoene synthase gene results in delayed germination and increased levels of carotenoids, chlorophyll, and abscisic acid. Plant Physiology **132,** 779-785.

Liu, S., Tian, N., Liu, Z., Huang, J., and Li, J. (2012). Cloning and characterization of a carotenoid cleavage dioxygenase from *Artemisia Annua* L. In Mechanical Engineering and Materials Science, B. Tan, ed, pp. 274-281.

Liu, Y., Roof, S., Ye, Z., Barry, C., Tuinen, A.v., Vrebalov, J., Bowler, C., and Giovannoni, J. (2004). Manipulation of light signal transduction as a means of modifying fruit nutritional quality in tomato. Proceedings of the National Academy of Sciences **101,** 9897-9902.

Liu, Y.S., Gur, A., Ronen, G., Causse, M., Damidaux, R., Buret, M., Hirschberg, J., and Zamir, D. (2003). There is more to tomato fruit colour than candidate carotenoid genes. Plant Biotechnology Journal **1,** 195-207.

Lopez, A.B., Van Eck, J., Conlin, B.J., Paolillo, D.J., O'Neill, J., and Li, L. (2008). Effect of the cauliflower Or transgene on carotenoid accumulation and chromoplast formation in transgenic potato tubers. Journal of Experimental Botany **59,** 213-223.

Lu, S., and Li, L. (2008). Carotenoid metabolism: Biosynthesis, regulation, and beyond. Journal of Integrative Plant Biology **50,** 778-785.

Lu, S., Van Eck, J., Zhou, X., Lopez, A.B., O'Halloran, D.M., Cosman, K.M., Conlin, B.J., Paolillo, D.J., Garvin, D.F., Vrebalov, J., Kochian, L.V., Kupper, H., Earle, E.D., Cao, J., and Li, L. (2006). The cauliflower Or gene encodes a DnaJ cysteine-rich domain-containing protein that mediates high levels of beta-carotene accumulation. Plant Cell **18,** 3594-3605.

Lundquist, P.K., Poliakov, A., Giacomelli, L., Friso, G., Appel, M., McQuinn, R.P., Krasnoff, S.B., Rowland, E., Ponnala, L., Sun, Q., and van Wijka, K.J. (2013). Loss of Plastoglobule Kinases ABC1K1 and ABC1K3 Causes Conditional Degreening, Modified Prenyl-Lipids, and Recruitment of the Jasmonic acid Pathway. The Plant Cell **25,** 1818-1839.

Maass, D., Arango, J., Wust, F., Beyer, P., and Welsch, R. (2009). Carotenoid Crystal Formation in Arabidopsis and Carrot Roots Caused by Increased Phytoene Synthase Protein Levels. PLoS One **4**.

Makino, T., Harada, H., Ikenaga, H., Matsuda, S., Takaichi, S., Shindo, K., Sandmann, G., Ogata, T., and Misawa, N. (2008). Characterization of cyanobacterial carotenoid ketolase crtw and hydroxylase crtr by complementation analysis in *Escherichia coli*. Plant Cell Physiology **49,** 1867-1878.

Mann, V., Harker, M., Pecker, I., and Hirschberg, J. (2000). Metabolic engineering of astaxanthin production in tobacco flowers. Nature Biotechnology **18,** 888-892.

Manshardt, R. (2004). Crop improvement by conventional breeding or genetic engineering: how different are they? (The College of Tropical Agriculture and Human Resources).

Marechal, E., Block, M.A., Dorne, A.J., Douce, R., and Joyard, J. (1997). Lipid synthesis and metabolism in the plastid envelope. Physiology Plantarum **100,** 65-77.

Martin, C. (1996). Transcription factors and the manipulation of plant traits. Current Opinion Biotechnology **7,** 130-138.

Marz, U. (2011). The global market of carotenoids. BCC Research Report FOD025D.

Masamoto, K., Misawa, N., Kaneko, T., Kikuno, R., and Toh, H. (1998). beta-carotene hydroxylase gene from the cyanobacterium *Synechocystis* sp. PCC6803. Plant Cell Physiology **39,** 560-564.

Mason, M.G., Mathews, D.E., Argyros, D.A., Maxwell, B.B., Kieber, J.J., Alonso, J.M., Ecker, J.R., and Schaller, G.E. (2005). Multiple type-B response regulators mediate cytokinin signal transduction in *Arabidopsis*. Plant Cell **17,** 3007-3018.

Math, S.K., Hearst, J.E., and Poulter, C.D. (1992). The CrtE gene in *Erwinia Herbicola* encodes geranylgeranyl diphosphate synthase. Proceedings of the National Academy of Sciences USA **89,** 6761-6764.

Mathieu, S., Terrier, N., Procureur, J., Bigey, F., and Gunata, Z. (2005). A Carotenoid Cleavage Dioxygenase from *Vitis vinifera* L.: functional characterization and expression during grape berry development in relation to C-13-norisoprenoid accumulation. Journal of Experimental Botany **56,** 2721-2731.

Matthews, P.D., Luo, R.B., and Wurtzel, E.T. (2003). Maize phytene desaturase and zeta-carotene desaturase catalyse a poly-Z desaturation pathway: implications for genetic engineering of carotenoid content among cereal crops. Journal of Experimental Botany **54,** 2215-2230.

McCallum, C.M., Comai, L., Greene, E.A., and Henikoff, S. (2000a). Targeted screening for induced mutations. Nature Biotechnology **18,** 455-457.

McCallum, C.M., Comai, L., Greene, E.A., and Henikoff, S. (2000b). Targeting induced local lesions in genomes (TILLING) for plant functional genomics. Plant Physiology **123,** 439-442.

McGraw, K.J. (2006). Dietary carotenoids mediate a trade-off between egg quantity and quality in Japanese quail. Ethology Ecology & Evolution **18,** 247-256.

McGraw, K.J., and Klasing, K.C. (2006). Carotenoids, immunity, and integumentary coloration in red junglefowl (*Gallus gallus*). Auk **123,** 1161-1171.

McKenna, M.C. (2011). Glutamate dehydrogenase in brain mitochondria: Do lipid modifications and transient metabolon formation influence enzyme activity? Neurochemistry International **58,** 525-533.

McKenna, M.C., Hopkins, I.B., Lindauer, S.L., and Bamford, P. (2006). Aspartate aminotransferase in synaptic and nonsynaptic mitochondria: Differential effect of compounds that influence transient hetero-enzyme complex (metabolon) formation. Neurochemistry International **48,** 629-636.

Minoia, S., Petrozza, A., D'Onofrio, O., Piron, F., Mosca, G., Sozio, G., Cellini, F., Bendahmane, A., and Carriero, F. (2010). A new mutant genetic resource for tomato crop improvement by TILLING technology. BMC research notes **3,** 69-69.

Misawa, N. (2009). Pathway engineering of plants toward astaxanthin production. Plant Biotechnology **26,** 93-99.

Misawa, N., Kajiwara, S., Kondo, K., Yokoyama, A., Satomi, Y., Saito, T., Miki, W., and Ohtani, T. (1995a). Canthaxanthin biosynthesis by the conversion of methylene toketo groups in a hydrocarbon beta-carotene by a single gene. Biochemical Biophysics Research Co **209,** 867-876.

Misawa, N., Nakagawa, M., Kobayashi, K., Yamano, S., Izawa, Y., Nakamura, K., and Harashima, K. (1990). Elucidation of the *Erwinia uredovora* carotenoid biosynthetic pathway by functional analysis of gene products expressed in *Escherichia coli*. Journal of Bacteriology **172,** 6704-6712.

Misawa, N., Satomi, Y., Kondo, K., Yokoyama, A., Kajiwara, S., Saito, T., Ohtani, T., and Miki, W. (1995b). Structure and functional analysis of a marine bacetrial carotenoid biosynthesis gene cluster and astaxanthin biosynthetic pathway proposed at the gene level. Journal of Bacteriology **177,** 6575-6584.

Misawa, N., Truesdale, M.R., Sandmann, G., Fraser, P.D., Bird, C., Schuch, W., and Bramley, P.M. (1994). Expression of a tomato cDNA coding for phytoene synthase in *Escherichia coli*, phytoene formation in-vivo and in-

vitro, and functional analysis of the various truncated gene-products. Journal of Biochemistry **116,** 980-985.

Misawa, N., Yamano, S., and Ikenaga, H. (1991). Production of beta-carotene in Zymomonas mobilis and Agrobacterium tumefaciens by introduction of the biosynthesis genes from *Erwinia uredovora*. Applied and Environmental Microbiology **57,** 1847-1849.

Mlalazi, B., Welsch, R., Namanya, P., Khanna, H., Geijskes, R.J., Harrison, M.D., Harding, R., Dale, J.L., and Bateson, M. (2012). Isolation and functional characterisation of banana phytoene synthase genes as potential cisgenes. Planta **236,** 1585-1598.

Moco, S., Capanoglu, E., Tikunov, Y., Bino, R.J., Boyacioglu, D., Hall, R.D., Vervoort, J., and De Vos, R.C. (2007). Tissue specialization at the metabolite level is perceived during the development of tomato fruit. Journal of Experimental Botany **58,** 4131-4146.

Moeller, S.M., Voland, R., Tinker, L., Blodi, B.A., Klein, M.L., Gehrs, K.M., Johnson, E.J., Snodderly, M., Wallace, R.B., Chappell, R.J., Parekh, N., Ritenbaugh, C., Mares, J.A., and Grp, C.S. (2008). Associations between age-related nuclear cataract and lutein and zeaxanthin in the diet and serum in the Carotenoids in the Age-Related Eye Disease Study (CAREDS), an ancillary study of the women's health initiative. Archives of Ophthalmology **126,** 354-364.

Montero, O., Sanchez-Guijo, A., Lubian, L.M., and Martinez-Rodriguez, G. (2012). Changes in membrane lipids and carotenoids during light acclimation in a marine cyanobacterium S*ynechococcus* sp. Journal Biosciences **37,** 635-645.

Morandini, P. (2013). Control limits for accumulation of plant metabolites: brute force is no substitute for understanding. Plant Biotechnology J **11,** 253-267.

Moreno, J.C., Pizarro, L., Fuentes, P., Handford, M., Cifuentes, V., and Stange, C. (2013). Levels of lycopene beta-cyclase 1 modulate carotenoid gene expression and accumulation in *Daucus carota*. Plos One **8**.

Moreno-Sanchez, R., Saavedra, E., Rodriguez-Enriquez, S., and Olin-Sandoval, V. (2008). Metabolic control analysis: A tool for designing strategies to manipulate metabolic pathways. Journal of Biomedicine and Biotechnology.

Morris, W.L., Ducreux, L.J.M., Fraser, P.D., Millam, S., and Taylor, M.A. (2006b). Engineering ketocarotenoid biosynthesis in potato tubers. Metabolic Engineering **8,** 253-263.

Morris, W.L., Ducreux, L.J.M., Hedden, P., Millam, S., and Taylor, M.A. (2006a). Overexpression of a bacterial 1-deoxy-D-xylulose 5-phosphate synthase gene in potato tubers perturbs the isoprenoid metabolic network: implications for the control of the tuber life cycle. Journal of Experimental Botany **57,** 3007-3018.

Mortimer, C.L., Bramley, P.M., and Fraser, P.D. (2012). The identification and rapid extraction of hydrocarbons from *Nicotiana glauca*: A potential advanced renewable biofuel source. Phytochemistry Letters **5,** 455-458.

Muller, P., Li, X.P., and Niyogi, K.K. (2001). Non-photochemical quenching. A response to excess light energy. Plant Physiology **125,** 1558-1566.

Mustilli, A.C., Fenzi, F., Ciliento, R., Alfano, F., and Bowler, C. (1999). Phenotype of the tomato high pigment-2 mutant is caused by a mutation in the tomato homolog of DEETIOLATED1. Plant Cell **11,** 145-157.

Naito, Y. (2011). Recent advances in the disease prevention and health promotion of astaxanthin. Vitamins (Kyoto) **85,** 587-594.

Naqvi, S., Zhu, C., Farre, G., Ramessar, K., Bassie, L., Breitenbach, J., Perez Conesa, D., Ros, G., Sandmann, G., Capell, T., and Christou, P. (2009). Transgenic multivitamin corn through biofortification of endosperm with three vitamins representing three distinct metabolic pathways. Proceedings of the National Academy of Sciences USA **106,** 7762-7767.

Neta-Sharir, I., Isaacson, T., Lurie, S., and Weiss, D. (2005). Dual role for tomato heat shock protein 21: Protecting photosystem II from oxidative stress and promoting color changes during fruit maturation. Plant Cell **17,** 1829-1838.

Nicholass, F.J., Smith, C.J.S., Schuch, W., Bird, C.R., and Grierson, D. (1995). High levels of ripening-specific reporter gene expression directed by tomato fruit polygalacturonase gene-flanking regions. Plant molecular biology **28,** 423–435.

Niyogi, K.K. (1999). Photoprotection revisited: Genetic and molecular approaches. Annual Review of Plant Physiology and Plant Molecular Biology **50,** 333-359.

Norris, V., Gascuel, P., Guespin-Michel, J., Ripoll, C., and Saier, M.H. (1999). Metabolite-induced metabolons: the activation of transporter-enzyme complexes by substrate binding. Molecular Microbiology **31,** 1592-1595.

Ohlrogge, J., and Browse, J. (1995). Lipid biosynthesis. Plant Cell **7,** 957-970.

Ojima, K., Breitenbach, J., Visser, H., Setoguchi, Y., Tabata, K., Hoshino, T., van den Berg, J., and Sandmann, G. (2006). Cloning of the astaxanthin synthase gene from *Xanthophyllomyces dendrorhous* (*Phaffia rhodozyma*) and its assignment as a beta-carotene 3-hydroxylase/4-ketolase. Molecular Genetics and Genomics **275,** 148-158.

Ortiz-Monasterio, J.I., Palacios-Rojas, N., Meng, E., Pixley, K., Trethowan, R., and Pena, R.J. (2007). Enhancing the mineral and vitamin content of wheat and maize through plant breeding. Journal of Cereal Science **46,** 293-307.

Orzaez, D., Mirabel, S., Wieland, W.H., and Granell, A. (2006). Agroinjection of tomato fruits. A tool for rapid functional analysis of transgenes directly in fruit. Plant Physiology **140,** 3-11.

Paine, J.A., Shipton, C.A., Chaggar, S., Howells, R.M., Kennedy, M.J., Vernon, G., Wright, S.Y., Hinchliffe, E., Adams, J.L., Silverstone, A.L., and Drake, R. (2005). Improving the nutritional value of Golden Rice through increased pro-vitamin A content. Nature Biotechnology **23,** 482-487.

Pan, Y., Bradley, G., Pyke, K., Ball, G., Lu, C., Fray, R., Marshall, A., Jayasuta, S., Baxter, C., van Wijk, R., Boyden, L., Cade, R., Chapman, N.H., Fraser, P.D., Hodgman, C., and Seymour, G.B. (2013). Network Inference Analysis identifies an APRR2-like gene linked to pigment accumulation in tomato and pepper fruits. Plant Physiology **161,** 1476-1485.

Park, H., Kreunen, S.S., Cuttriss, A.J., DellaPenna, D., and Pogson, B.J. (2002). Identification of the carotenoid isomerase provides insight into carotenoid biosynthesis, prolamellar body formation, and photomorphogenesis. Plant Cell **14,** 321-332.

Pecker, I., Chamovitz, D., Linden, H., Sandmann, G., and Hirschberg, J. (1992). A single polypeptide catalyzing the conversion of phytoene to zeta-carotene is transcriptionally regulated during tomato fruit ripening. Proceedings of the National Academy of Sciences USA **89,** 4962.

Pecker, I., Gabbay, R., Cunningham, F.X., and Hirschberg, J. (1996). Cloning and characterization of the cDNA for lycopene beta-cyclase from tomato

reveals decrease in its expression during fruit ripening. Plant Molecular Biology **30,** 807-819.

Peñuelas, J., and Munné-Bosch, S. (2005). Isoprenoids: an evolutionary pool for photoprotection. Trends in Plant Science **10,** 166-169.

Perlak, F.J., Fuchs, R.L., Dean, D.A., McPherson, S.L., and Fischhoff, D.A. (1991). Modification of the coding sequence enhances plant expression of insect control protein genes. Proceedings of the National Academy of Sciences USA **88,** 3324-3328.

Pham Anh, T., and Park, S.U. (2013). Molecular cloning and characterization of cDNAs encoding carotenoid cleavage dioxygenase in bitter melon (*Momordica charantia*). Journal of Plant Physiology **170,** 115-120.

Pichersky, E., and Gang, D.R. (2000). Genetics and biochemistry of secondary metabolites in plants: an evolutionary perspective. Trends in Plant Science **5,** 439-445.

Polivka, T., and Frank, H.A. (2010). Molecular factors controlling photosynthetic light harvesting by carotenoids. Accounts of Chemical Research **43,** 1125-1134.

Porter, J.W., and Lincoln, R.E. (1950). Lycopersicon selections containing a high content of carotenes and colorless polyenes; the mechanism of carotene biosynthesis. Archives of biochemistry **27,** 390-403.

Potenza, C., Aleman, L., and Sengupta-Gopalan, C. (2004). Targeting transgene expression in research, agricultural, and environmental applications: Promoters used in plant transformation. In Vitro Cellular & Developmental Biology-Plant **40,** 1-22.

Potrykus, I. (2010). Regulation must be revolutionized. Nature **466,** 561-561.

Quinlan, R.F., Jaradat, T.T., and Wurtzel, E.T. (2007). *Escherichia coli* as a platform for functional expression of plant P450 carotene hydroxylases. Archives of Biochemistry and Biophysics**458,** 146-157.

Quinlan, R.F., Shumskaya, M., Bradbury, L.M.T., Beltran, J., Ma, C., Kennelly, E.J., and Wurtzel, E.T. (2012). Synergistic interactions between carotene ring hydroxylases drive lutein formation in plant carotenoid biosynthesis. Plant Physiology **160,** 204-214.

Rabbani, S., Beyer, P., Von Lintig, J., Hugueney, P., and Kleinig, H. (1998). Induced beta-carotene synthesis driven by triacylglycerol deposition in the unicellular alga *Dunaliella bardawil*. Plant Physiology **116,** 1239-1248.

Rai, M., Datta, K., Parkhi, V., Tan, J., Oliva, N., Chawla, H.S., and Datta, S.K. (2007). Variable T-DNA linkage configuration affects inheritance of carotenogenic transgenes and carotenoid accumulation in transgenic indica rice. Plant Cell Reports **26,** 1221-1231.

Ralley, L., Enfissi, E., Misawa, N., Schuch, W., Bramley, P.M., and Fraser, P.D. (2004). Metabolic engineering of ketocarotenoid formation in higher plants. The Plant Journal **39,** 477–486.

Rao, A.Q., Bakhsh, A., Kiani, S., Shahzad, K., Shahid, A.A., Husnain, T., and Riazuddin, S. (2009). The myth of plant transformation. Biotechnology Advances **27,** 753-763.

Ravanello, M.P., Ke, D., Alvarez, J., Huang, B., and Shewmaker, C.K. (2003). Coordinate expression of multiple bacterial carotenoid genes in canola leading to altered carotenoid production. Metabolic Engineering **5,** 255-263.

Reisinger, V., and Eichacker, L.A. (2006). Analysis of membrane protein complexes by blue native PAGE. Proteomics **6 Suppl 2,** 6-15.

Rodriguez-Concepion, M. (2004). The MEP pathway: A new target for the development of herbicides, antibiotics and antimalarial drugs. Current Pharmaceutical Design **10,** 2391-2400.

Rohrmann, J., Tohge, T., Alba, R., Osorio, S., Caldana, C., McQuinn, R., Arvidsson, S., van der Merwe, M.J., Riano-Pachon, D.M., Mueller-Roeber, B., Fei, Z., Nesi, A.N., Giovannoni, J.J., and Fernie, A.R. (2011). Combined transcription factor profiling, microarray analysis and metabolite profiling reveals the transcriptional control of metabolic shifts occurring during tomato fruit development. Plant Journal **68,** 999-1013.

Romer, S., Fraser, P.D., Kiano, J.W., Shipton, C.A., Misawa, N., Schuch, W., and Bramley, P.M. (2000). Elevation of the provitamin A content of transgenic tomato plants. Nature Biotechnology **18,** 666-669.

Romer, S., Lubeck, J., Kauder, F., Steiger, S., Adomat, C., and Sandmann, G. (2002). Genetic engineering of a zeaxanthin-rich potato by antisense inactivation and co-suppression of carotenoid epoxidation. Metabolic Engineering **4,** 263-272.

Ronen, G., Carmel-Goren, L., Zamir, D., and Hirschberg, J. (2000). An alternative pathway to beta-carotene formation in plant chromoplasts discovered by map-based cloning of beta and old-gold color mutations in tomato. Proceedings of the National Academy of Sciences USA **97,** 11102-11107.

Ronen, G., Cohen, M., Zamir, D., and Hirschberg, J. (1999). Regulation of carotenoid biosynthesis during tomato fruit development: Expression of the gene for lycopene epsilon-cyclase is down-regulated during ripening and is elevated in the mutant Delta. Plant Journal **17,** 341-351.

Rosati, C., Aquilani, R., Dharmapuri, S., Pallara, P., Marusic, C., Tavazza, R., Bouvier, F., Camara, B., and Giuliano, G. (2000). Metabolic engineering of beta-carotene and lycopene content in tomato fruit. Plant Journal **24,** 413-419.

Rosso, S.W. (1967). An ultrastructural study of the mature chromoplasts of the tangerine tomato (*Lycopersicon esculentum* var. "golden jubilee"). Journal of ultrastructure research **20,** 179-189.

Rosso, S.W. (1968). The ultrastructure of chromoplast development in red tomatoes. Journal of ultrastructure research **25,** 307-322.

Rouwendal, G.J.A., Mendes, O., Wolbert, E.J.H., and deBoer, A.D. (1997). Enhanced expression in tobacco of the gene encoding green fluorescent protein by modification of its codon usage. Plant Molecular Biology **33,** 989-999.

Rozin, P., Fischler, C., and Shields-Argeles, C. (2012). European and American perspectives on the meaning of natural. Appetite **59,** 448-455.

Sandmann, G., and Misawa, N. (1992). New functional assignment of the carotenogenic genes crtB and crtE with constructs of these genes from Erwinia species. FEMS Microbiol Letters **69,** 253-257.

Sandmann, G., Römer, S., and Fraser, P.D. (2006). Understanding carotenoid metabolism as a necessity for genetic engineering of crop plants. Metabolic engineering **8,** 291–302.

Sanford, J.C. (2000). The development of the biolistic process. In Vitro Cellular & Developmental Biology-Plant **36,** 303-308.

Satoh, J., Kato, K., and Shinmyo, A. (2004). The 5'-untranslated region of the tobacco alcohol dehydrogenase gene functions as an effective translational enhancer in plant. Journal of bioscience and bioengineering **98,** 1–8.

Schaub, P., Al-Babili, S., Drake, R., and Beyer, P. (2005). Why is Golden Rice golden (yellow) instead of red? Plant Physiology **138,** 441-450.

Schaub, P., Yu, Q.J., Gemmecker, S., Poussin-Courmontagne, P., Mailliot, J., McEwen, A.G., Ghisla, S., Al-Babili, S., Cavarelli, J., and Beyer, P. (2012). On the Structure and Function of the Phytoene Desaturase CRTI from Pantoea ananatis, a Membrane-Peripheral and FAD-Dependent Oxidase/Isomerase. Plos One **7**.

Schweiggert, R.M., Steingass, C.B., Heller, A., Esquivel, P., and Carle, R. (2011). Characterization of chromoplasts and carotenoids of red- and yellow-fleshed papaya (Carica papaya L.). Planta **234,** 1031-1044.

Sharoni, Y., Linnewiel-Hermoni, K., Khanin, M., Salman, H., Veprik, A., Danilenko, M., and Levy, J. (2012). Carotenoids and apocarotenoids in cellular signaling related to cancer: A review. Molecular nutrition & food research **56,** 259-269.

Sheludko, Y.V. (2010). Recent advances in plant biotechnology and genetic engineering for production of secondary metabolites. Cytology and Genetics **44,** 52-60.

Shen, Y., Khanna, R., Carle, C.M., and Quail, P.H. (2007). Phytochrome induces rapid PIF5 phosphorylation and degradation in response to red-light activation. Plant Physiology **145,** 1043-1051.

Shewmaker, C.K., Sheehy, J.A., Daley, M., Colburn, S., and Ke, D.Y. (1999). Seed-specific overexpression of phytoene synthase: increase in carotenoids and other metabolic effects. Plant Journal **20,** 401-412.

Shimada, H., Kondo, K., Fraser, P.D., Miura, Y., Saito, T., and Misawa, N. (1998). Increased carotenoid production by the food yeast Candida utilis through metabolic engineering of the isoprenoid pathway. Applied and Environmental Microbiology **64,** 2676-2680.

Shumskaya, M., and Wurtzela, E.T. (2013). The carotenoid biosynthetic pathway: Thinking in all dimensions. Plant Science **208,** 58-63.

Shumskaya, M., Bradbury, L.M.T., Monaco, R.R., and Wurtzel, E.T. (2012). Plastid localization of the key carotenoid enzyme phytoene synthase is altered by isozyme, allelic variation, and activity. Plant Cell **24,** 3725-3741.

Silletti, M.F., Petrozza, A., Stigliani, A.L., Giorio, G., Cellini, F., D'Ambrosio, C., and Carriero, F. (2013). An increase of lycopene content in tomato fruit is associated with a novel Cyc-B allele isolated through TILLING technology. Molecular Breeding **31,** 665-674.

Simkin, A.J., Gaffe, J., Alcaraz, J.P., Carde, J.P., Bramley, P.M., Fraser, P.D., and Kuntz, M. (2007). Fibrillin influence on plastid ultrastructure and pigment content in tomato fruit. Phytochemistry **68,** 1545-1556.

Sinensky, M. (2000). Recent advances in the study of prenylated proteins. Biochimica Et Biophysica Acta-Molecular and Cell Biology of Lipids **1484,** 93-106.

Skelton, R.L., Yu, Q., Srinivasan, R., Manshardt, R., Moore, P.H., and Ming, R. (2006). Tissue differential expression of lycopene beta-cyclase gene in papaya. Cell Research **16,** 731-739.

Sparkes, I.A., Runions, J., Kearns, A., and Hawes, C. (2006). Rapid, transient expression of fluorescent fusion proteins in tobacco plants and generation of stably transformed plants. Nature Protocols **1,** 2019-2025.

Spurr, A.R., and Harris, M. (1968). Ultrastructure of chloroplasts and chromoplasts in capsicum annum.l. Thylakoid Membrane changes during fruit ripening. American Journal of Botany **55,** 1210-1224.

Stalberg, K., Lindgren, O., Ek, B., and Hoglund, A.S. (2003). Synthesis of ketocarotenoids in the seed of *Arabidopsis thaliana*. Plant Journal **36,** 771-779.

Steiger, S., and Sandmann, G. (2004). Cloning of two carotenoid ketolase genes from *Nostoc punctiforme* for the heterologous production of canthaxanthin and astaxanthin. Biotechnol Letters **26,** 813-817.

Steiger, S., Jackisch, Y., and Sandmann, G. (2005). Carotenoid biosynthesis in *Gloeobacter violaceus* PCC4721 involves a single crtI-type phytoene desaturase instead of typical cyanobacterial enzymes. Archives of Microbiology **184,** 207-214.

Stickforth, P., Steiger, S., Hess, W.R., and Sandmann, G. (2003). A novel type of lycopene epsilon-cyclase in the marine cyanobacterium *Prochlorococcus marinus* MED4. Archives of Microbiology **179,** 409-415.

Stigliani, A.L., Giorio, G., and D'Ambrosio, C. (2011). Characterization of P450 carotenoid beta- and epsilon-hydroxylases of tomato and transcriptional regulation of xanthophyll biosynthesis in root, leaf, petal and fruit. Plant Cell Physiology **52,** 851-865.

Subczynski, W.K., Markowska, E., Gruszecki, W.I., and Sielewiesiuk, J. (1992). Effects of polar carotenoids on dimyristoylphosphatidylcholine menbranes: A spin-label study. Biochimica et Biophysica Acta **1105,** 97-108.

Sun, L., Yuan, B., Zhang, M., Wang, L., Cui, M., Wang, Q., and Leng, P. (2012). Fruit-specific RNAi-mediated suppression of SlNCED1 increases both lycopene and beta-carotene contents in tomato fruit. Journal of Experimental Botany **63,** 3097-3108.

Sun, Z., Hans, J., Walter, M.H., Matusova, R., Beekwilder, J., Verstappen, F.W.A., Ming, Z., van Echtelt, E., Strack, D., Bisseling, T., and Bouwmeester, H.J. (2008). Cloning and characterisation of a maize carotenoid cleavage dioxygenase (ZmCCD1) and its involvement in the biosynthesis of apocarotenoids with various roles in mutualistic and parasitic interactions. Planta **228,** 789-801.

Sun, Z.R., Gantt, E., and Cunningham, F.X. (1996). Cloning and functional analysis of the beta-carotene hydroxylase of *Arabidopsis thaliana*. Journal of Biological Chemistry **271,** 24349-24352.

Sun-Waterhouse, D. (2011). The development of fruit-based functional foods targeting the health and wellness market: a review. International Journal of Food Science and Technology **46,** 899-920.

Suzuki, S., Nishihara, M., Nakatsuka, T., Misawa, N., Ogiwara, I., and Yamamura, S. (2007). Flower color alteration in *Lotus japonicus* by modification of the carotenoid biosynthetic pathway. Plant Cell Reports **26,** 951-959.

Szilagyi, A., Sommarin, M., and Akerlund, H.E. (2007). Membrane curvature stress controls the maximal conversion of violaxanthin to zeaxanthin in the violaxanthin cycle - influence of alpha-tocopherol, cetylethers, linolenic acid, and temperature. BBA-Biomembranes **1768,** 2310-2318.

Takaya, A., Zhanga, Y.W., Asawatreratanakul, K., Wititsuwannakul, D., Wititsuwannakul, R., Takahashi, S., and Koyama, T. (2003). Cloning, expression and characterization of a functional cDNA clone encoding geranylgeranyl diphosphate synthase of *Hevea brasiliensis*. Biochimica Et Biophysica Acta-Gene Structure and Expression **1625,** 214-220.

Tang, G., and Russell, R. (2009). Carotenoids as provitamin A. In Carotenoids, G. Britton, S. Liaaen-Jensen, and H. Pfander, eds (Basal: Birkhasuer Verlag), pp. 149-172.

Tao, L., Wilczek, J., Odom, J.M., and Cheng, Q. (2006). Engineering a beta-carotene ketolase for astaxanthin production. Metabolic Engineering **8,** 523-531.

Thabet, I., Guirimand, G., Guihur, A., Lanoue, A., Courdavault, V., Papon, N., Bouzid, S., Giglioli-Guivarc'h, N., Simkin, A.J., and Clastre, M. (2012). Characterization and subcellular localization of geranylgeranyl diphosphate synthase from *Catharanthus roseus*. Molecular Biology Reports **39,** 3235-3243.

Theis, N., and Lerdau, M. (2003). The evolution of function in plant secondary metabolites. International Journal of Plant Sciences **164,** S93-S102.

Thompson, A.J., Jackson, A.C., Parker, R.A., Morpeth, D.R., Burbidge, A., and Taylor, I.B. (2000). Abscisic acid biosynthesis in tomato: regulation of zeaxanthin epoxidase and 9-cis-epoxycarotenoid dioxygenase mRNAs by light/dark cycles, water stress and abscisic acid. Plant Molecular Biology **42,** 833-845.

Tian, L., and DellaPenna, D. (2001). Characterization of a second carotenoid beta-hydroxylase gene from *Arabidopsis* and its relationship to the LUT1 locus. Plant Molecular Biology **47,** 379-388.

Tian, L., Magallanes-Lundback, M., Musetti, V., and DellaPenna, D. (2003). Functional analysis of beta- and epsilon-ring carotenoid hydroxylases in *Arabidopsis*. Plant Cell **15,** 1320-1332.

Tian, L., Musetti, V., Kim, J., Magallanes-Lundback, M., and DellaPenna, D. (2004). The *Arabidopsis* LUT1 locus encodes a member of the cytochrome P450 family that is required for carotenoid epsilon-ring hydroxylation activity. Proceedings of the National Academy of Sciences USA **101,** 402-407.

Toledo-Ortiz, G., Huq, E., and Rodriguez-Concepcion, M. (2010). Direct regulation of phytoene synthase gene expression and carotenoid biosynthesis by phytochrome-interacting factors. Proceedings of the National Academy of Sciences USA **107,** 11626-11631.

Tsuchiya, T., Takaichi, S., Misawa, N., Maoka, T., Miyashita, H., and Mimuro, M. (2005). The cyanobacterium *Gloeobacter violaceus* PCC 7421 uses bacterial-type phytoene desaturase in carotenoid biosynthesis. FEBS Letters **579,** 2125-2129.

Tucker, G.A., and Grierson, D. (1982). Synthesis of polygalacturonase during tomato fruit ripening. Planta **155,** 64-67.

Twyman, R.M., Stoger, E., Schillberg, S., Christou, P., and Fischer, R. (2003). Molecular farming in plants: host systems and expression technology. Trends in Biotechnology **21,** 570-578.

Ushiyama, K., and Hibino, K. (1997). Commercial production of ginseng by plant cell culture. Abstracts of Papers of the American Chemical Society **213,** 57-AGFD.

Vallabhaneni, R., Gallagher, C.E., Licciardello, N., Cuttriss, A.J., Quinlan, R.F., and Wurtzel, E.T. (2009). Metabolite Sorting of a Germplasm Collection Reveals the Hydroxylase3 Locus as a New Target for Maize Provitamin A Biofortification. Plant Physiology **151,** 1635-1645.

Van Der Velden, A.W., and Thomas, A.A.M. (1999). The role of the 5'untranslated region of an mRNA in translation regulation during development. The international journal of biochemistry & cell biology **31,** 87–106.

Van Eck, J., Conlin, B., Garvin, D.F., Mason, H., Navarre, D.A., and Brown, C.R. (2007). Enhancing beta-carotene content in potato by RNAi-mediated silencing of the beta-carotene hydroxylase gene. American Journal of Potato Research **84,** 331-342.

Van Herpen, T.W.J.M., Cankar, K., Nogueira, M., Bosch, D., Bouwmeester, H.J., and Beekwilder, J. (2010). *Nicotiana benthamiana* as a production platform for artemisinin precursors. Plos One **5**.

Vanengelen, F.A., Molthoff, J.W., Conner, A.J., Nap, J.P., Pereira, A., and Stiekema, W.J. (1995). pBINPLUS: An improved plant transformation vector based on pBIN19. Transgenic Research. **4,** 288-290.

Vasquez-Caicedo, A.L., Heller, A., Neidhart, S., and Carle, R. (2006). Chromoplast morphology and beta-carotene accumulation during postharvest ripening of mango cv. 'Tommy Atkins'. Journal of Agricultural and Food Chemistry **54,** 5769-5776.

Verdoes, J.C., Krubasik, P., Sandmann, G., and van Ooyen, A.J.J. (1999). Isolation and functional characterisation of a novel type of carotenoid biosynthetic gene from *Xanthophyllomyces dendrorhous*. Molecular and General Genetics **262,** 453-461.

Verdoes, J.C., Sandmann, G., Visser, H., Diaz, M., van Mossel, M., and van Ooyen, A.J.J. (2003). Metabolic engineering of the carotenoid biosynthetic pathway in the yeast *Xanthophyllomyces dendrorhous* (*Phaffia rhodozyma*). Applied and Environmental Microbiology **69,** 3728-3738.

Vervoort, E.B., van Ravestein, A., van Peij, N., Heikoop, J.C., van Haastert, O.J.M., Verheijden, G.F., and Linskens, M.H.K. (2000). Optimizing heterologous expression in Dictyostelium: importance of 5' codon adaptation. Nucleic Acids Research **28,** 2069-2074.

Villoutreix, J. (1960). Carotenoids of Rhodotorula mucilaginosa. Study of their biosynthesis with the aid of analysis of mutants and the use of an inhibitor of carotenogenesis. Biochimica et Biophysica Acta **40,** 442-457.

Vishnevetsky, M., Ovadis, M., and Vainstein, A. (1999). Carotenoid sequestration in plants: the role of carotenoid-associated proteins. Trends in Plant Science **4,** 232-235.

Vogeli, U., and Chappell, J. (1988). Induction of sesquiterpene cyclase and suppression of squalene synhtetase activities in plant-cell cultures treated with fungal ellicitor. Plant Physiology **88,** 1291-1296.

Voinnet, O., Rivas, S., Mestre, P., and Baulcombe, D. (2003). An enhanced transient expression system in plants based on suppression of gene silencing by the p19 protein of tomato bushy stunt virus. Plant Journal **33,** 949-956.

Von Lintig, J., Welsch, R., Bonk, M., Giuliano, G., Batschauer, A., and Kleinig, H. (1997). Light-dependent regulation of carotenoid biosynthesis occurs at the level of phytoene synthase expression and is mediated by phytochrome in *Sinapis alba* and *Arabidopsis thaliana* seedlings. Plant Journal **12,** 625-634.

Voutilainen, S., Nurmi, T., Mursu, J., and Rissanen, T.H. (2006). Carotenoids and cardiovascular health. American Journal of Clinical Nutrition **83,** 1265-1271.

Vranova, E., Coman, D., and Gruissem, W. (2012). Structure and dynamics of the isoprenoid pathway network. Molecular Plant **5,** 318-333.

Vranova, E., Coman, D., and Gruissem, W. (2013). Network Analysis of the MVA and MEP Pathways for Isoprenoid Synthesis. Annual review of plant biology **64,** 665-700.

Walter, M.H., Floss, D.S., and Strack, D. (2010). Apocarotenoids: hormones, mycorrhizal metabolites and aroma volatiles. Planta **232,** 1-17.

Wang, L., and Roossinck, M.J. (2006). Comparative analysis of expressed sequences reveals a conserved pattern of optimal codon usage in plants. Plant Molecular Biology **61,** 699-710.

Wang, S., Liu, J., Feng, Y., Niu, X., Giovannoni, J., and Liu, Y. (2008). Altered plastid levels and potential for improved fruit nutrient content by downregulation of the tomato DDB1-interacting protein CUL4. Plant Journal **55,** 89-103.

Wang, Y.-Q., Yang, Y., Fei, Z., Yuan, H., Fish, T., Thannhauser, T.W., Mazourek, M., Kochian, L.V., Wang, X., and Li, L. (2013). Proteomic analysis of chromoplasts from six crop species reveals insights into chromoplast function and development. Journal of Experimental Botany **64,** 949-961.

Weedon, B.C.L., and Moss, G.P. (1995). Nomenclature of Carotenoids: IUPAC-IUB Rules, In Carotenoids, Vol 1A: isolation and analysis, G. Britton, Liaaen-Jensen, S., Pfander,H., ed, pp. 54-69.

Wellburn, A. (1994). The spectral determination of chlorophylls a and b, as well as total carotenoids, using various solvents with spectrophotometers of different resolution. Plant Physiology **144,** 307-313.

Welsch, R., Arango, J., Baer, C., Salazar, B., Al-Babili, S., Beltran, J., Chavarriaga, P., Ceballos, H., Tohme, J., and Beyer, P. (2010). Provitamin A accumulation in cassava (*Manihot esculenta*) roots driven by a single nucleotide polymorphism in a phytoene synthase gene. Plant Cell **22,** 3348-3356.

Welsch, R., Beyer, P., Hugueney, P., Kleinig, H., and von Lintig, J. (2000). Regulation and activation of phytoene synthase, a key enzyme in carotenoid biosynthesis, during photomorphogenesis. Planta **211,** 846-854.

Welsch, R., Maass, D., Voegel, T., DellaPenna, D., and Beyer, P. (2007). Transcription factor RAP2.2 and its interacting partner SINAT2: Stable elements in the carotenogenesis of *Arabidopsis* leaves. Plant Physiology **145,** 1073-1085.

Welsch, R., Wuest, F., Baer, C., Al-Babili, S., and Beyer, P. (2008). A third phytoene synthase is devoted to abiotic stress-induced abscisic acid formation in rice and defines functional diversification of phytoene synthase genes. Plant Physiology **147,** 367-380.

Whitaker, W.R., and Dueber, J.E. (2011). Metabolic pathway flux enhancement by synthetic protein scaffolding In Methods in Enzymology, Vol 497: Synthetic Biology, Methods for Part/Device Characterization and Chassis Engineering, Pt A, C. Voigt, ed, pp. 447-468.

Williams, R.J., Britton, G., and Goodwin, T.W. (1967). The biosynthesis of cyclic carotenes. The Biochemical journal **105,** 99-105.

Wrischer, M., Prebeg, T., Magnus, V., and Ljubesic, N. (2007). Crystals and fibrils in chromoplast plastoglobules of *Solanum capsicastrum* fruit. Acta Botanica Croatica **66,** 81-87.

Wurbs, D., Ruf, S., and Bock, R. (2007). Contained metabolic engineering in tomatoes by expression of carotenoid biosynthesis genes from the plastid genome. Plant Journal **49,** 276-288.

Xiao, Y.M., Savchenko, T., Baidoo, E.E.K., Chehab, W.E., Hayden, D.M., Tolstikov, V., Corwin, J.A., Kliebenstein, D.J., Keasling, J.D., and Dehesh, K. (2012). Retrograde signaling by the plastidial metabolite MEcPP regulates expression of nuclear stress-response genes. Cell **149,** 1525-1535.

Xu, Z., Tian, B., Sun, Z., Lin, J., and Hua, Y. (2007). Identification and functional analysis of a phytoene desaturase gene from the extremely radioresistant bacterium *Deinococcus radiodurans*. Society for General Microbiology **153,** 1642-1652.

Ye, X.D., Al-Babili, S., Kloti, A., Zhang, J., Lucca, P., Beyer, P., and Potrykus, I. (2000). Engineering the provitamin A (beta-carotene) biosynthetic pathway into (carotenoid-free) rice endosperm. Science **287,** 303-305.

Yonekura-Sakakibara, K., and Saito, K. (2006). Genetically modified plants for the promotion of human health. Biotechnology Letters **28,** 1983-1991.

Young, A.J. (1993). Occurrence and distribution of carotenoids in photosynthetic systems. In Carotenoids in photosynthesis, A.J. Young and G. Britton, eds (London: Chapman & Hall), pp. 16-65.

Ytterberg, A.J., Peltier, J.B., and van Wijk, K.J. (2006). Protein profiling of plastoglobules in chloroplasts and chromoplasts. A surprising site for differential accumulation of metabolic enzymes. Plant Physiology **140,** 984-997.

Yuan, J.P., Peng, J.A., Yin, K., and Wang, J.H. (2011). Potential health-promoting effects of astaxanthin: A high-value carotenoid mostly from microalgae. Molecular nutrition & food research **55,** 150-165.

Zhao, H., Guan, X., Xu, Y., and Wang, Y. (2013). Characterization of novel gene expression related to glyoxal oxidase by agro-infiltration of the leaves of accession Baihe-35-1 of *Vitis pseudoreticulata* involved in production of H2O2 for resistance to Erysiphe necator. Protoplasma **250,** 765-777.

Zhou, B., Deng, Y.-S., Kong, F.-Y., Li, B., and Meng, Q.-W. (2013). Overexpression of a tomato carotenoid ε-hydroxylase gene alleviates sensitivity to chilling stress in transgenic tobacco. Plant physiology and biochemistry : PPB / Societe francaise de physiologie vegetale **70**.

Zhu, C., Gerjets, T., and Sandmann, G. (2007). *Nicotiana glauca* engineered for the production of ketocarotenoids in flowers and leaves by expressing the cyanobacterial crtO ketolase gene. Transgenic Research. **16,** 813-821.

Zhu, C., Naqvi, S., Breitenbach, J., Sandmann, G., Christou, P., and Capell, T. (2008). Combinatorial genetic transformation generates a library of metabolic phenotypes for the carotenoid pathway in maize. Proceedings of the National Academy of Sciences USA **105,** 18232-18237.

Zhu, C., Naqvi, S., Capell, T., and Christou, P. (2009). Metabolic engineering of ketocarotenoid biosynthesis in higher plants. Archives of Biochemistry and Biophysics**483,** 182-190.

Zhu, C., Yamamura, S., Nishihara, M., Koiwa, H., and Sandmann, G. (2003). cDNAs for the synthesis of cyclic carotenoids in petals of *Gentiana lutea* and their regulation during flower development. Biochimica et Biophysica Acta **1625,** 305-308.

Zhu, C.F., Sanahuja, G., Yuan, D.W., Farre, G., Arjo, G., Berman, J., Zorrilla-Lopez, U., Banakar, R., Bai, C., Perez-Massot, E., Bassie, L., Capell, T., and Christou, P. (2013). Biofortification of plants with altered antioxidant content and composition: genetic engineering strategies. Plant Biotechnology Journal **11,** 129-141.

Zhu, C.F., Yamamura, S., Koiwa, H., Nishihara, M., and Sandmann, G. (2002). CDNA cloning and expression of carotenogenic genes during flower development in *Gentiana lutea*. Plant Molecular Biology **48,** 277-285.

Zhu, X.F., Suzuki, K., Okada, K., Tanaka, K., Nakagawa, T., Kawamukai, M., and Matsuda, H. (1997a). Cloning and functional expression of a novel geranylgeranyl pyrophosphate synthase gene from *Arabidopsis thaliana* in *Escherichia coli*. Plant Cell Physiology **38,** 357-361.

Zhu, X.F., Suzuki, K., Saito, T., Okada, K., Tanaka, K., Nakagawa, T., Matsuda, H., and Kawamukai, M. (1997b). Geranylgeranyl pyrophosphate synthase encoded by the newly isolated gene GGPS6 from *Arabidopsis thaliana* is localized in mitochondria. Plant Molecular Biology **35,** 331-341.

Zouine, M., Latché, A., Rousseau, C., Regad, F., Pech, J.-C., Philippot, M., Bouzayen, M., Delalande, C., Frasse, P., Schiex, T., Noirot, C., Bellec, A., Klopp, C., Berges, H., Mariette, J., Vautrin, S., Causse, M., and Rothan, C. (2012). The tomato genome sequence provides insights into fleshy fruit evolution. Nature **485,** 635-641.

Publication

Nogueira, M., Mora, L., Enfissi, M. A., Bramley, P. M., Fraser, P. D. (2013). Subchromoplast sequestration of carotenoids affects regulatory mechanisms in tomato lines expressing different carotenoid gene combinations. The Plant Cell, DOI 10.1105/tpc.113.116210.

Subchromoplast Sequestration of Carotenoids Affects Regulatory Mechanisms in Tomato Lines Expressing Different Carotenoid Gene Combinations[C][W]

Marilise Nogueira, Leticia Mora,[1] Eugenia M.A. Enfissi, Peter M. Bramley, and Paul D. Fraser[2]

School of Biological Sciences, Royal Holloway University of London, Egham, Surrey TW20 0EX, United Kingdom

ORCID IDs: 0000-0001-6088-474X (M.N.); 000-0003-1571-5781 (L.M.); 0000-0001-9612-6393 (E.M.A.E.); 0000-0001-8204-1073 (P.M.B.); 0000-0002-5953-8900 (P.D.F.).

Metabolic engineering of the carotenoid pathway in recent years has successfully enhanced the carotenoid contents of crop plants. It is now clear that only increasing biosynthesis is restrictive, as mechanisms to sequestrate these increased levels in the cell or organelle should be exploited. In this study, biosynthetic pathway genes were overexpressed in tomato (*Solanum lycopersicum*) lines and the effects on carotenoid formation and sequestration revealed. The bacterial *Crt* carotenogenic genes, independently or in combination, and their zygosity affect the production of carotenoids. Transcription of the pathway genes was perturbed, whereby the tissue specificity of transcripts was altered. Changes in the steady state levels of metabolites in unrelated sectors of metabolism were found. Of particular interest was a concurrent increase of the plastid-localized lipid monogalactodiacylglycerol with carotenoids along with membranous subcellular structures. The carotenoids, proteins, and lipids in the subchromoplast fractions of the transgenic tomato fruit with increased carotenoid content suggest that cellular structures can adapt to facilitate the sequestration of the newly formed products. Moreover, phytoene, the precursor of the pathway, was identified in the plastoglobule, whereas the biosynthetic enzymes were in the membranes. The implications of these findings with respect to novel pathway regulation mechanisms are discussed.

INTRODUCTION

Carotenoids are a large class of natural yellow, orange, and red pigments, which color fruits, flowers, birds, and crustacea (Hirschberg, 2001; Fraser and Bramley, 2004). Moreover, in higher plants, carotenoids act as free-radical scavengers (Demmig-Adams and Adams, 2002), ancillary photosynthetic pigments (Dall'Osto et al., 2007), and precursors of phytohormones (Auldridge et al., 2006). Dietary carotenoids with biological antioxidant properties have been intensively studied with respect to their potential in alleviating age-related diseases in humans (Fraser and Bramley, 2004; Krinsky and Johnson, 2005). These health-promoting properties, along with their ability to act as natural colorants, have created intense biotechnological interest to increase or alter their contents in foodstuffs and to develop new, renewable sources that are capable of competing with chemical synthesis, which for many carotenoids is the present production method of choice.

Biosynthetically, carotenoids are isoprenoids synthesized in the plastid, using isopentenyl diphosphate (C_5) derived from the methylerythritol-4-phosphate pathway (Pulido et al., 2012). The conversion of two geranylgeranyl diphosphate (C_{20}) molecules into phytoene (C_{40}) represents the first committed step in the carotenoid pathway and is catalyzed by the enzyme phytoene synthase. Phytoene is a colorless carotene with three conjugated double bonds that can then undergo a sequential series of desaturations and isomerizations to form all-*trans* lycopene, which has a characteristic red coloration as a result of the 11 conjugated double bonds. In plants and algae, the optimal desaturation and isomerization of phytoene to lycopene requires four proteins, a phytoene and ζ-carotene desaturase, and two isomerases acting on ζ-carotene and *poly cis*-lycopene (Sandmann, 2009). Depending on the action and specificity of the cyclase enzymes, lycopene can then undergo cyclization to form β- or ε-ionone rings, yielding β-carotene and/or α-carotene. These cyclic carotenoids can then be decorated by hydroxylation and epoxidation reactions (Fraser and Bramley, 2004; Figure 1). Transcriptional regulation of the carotenoid pathway has been well documented (Fraser and Bramley, 2004; Fraser et al., 2009).

The heterologous expression of the *Pantoea ananatis* carotenoid biosynthetic genes (*Crt*E, *Crt*B, and *Crt*I; Misawa et al., 1990, 1991; Shimada et al., 1998; Ravanello et al., 2003) has proven to be a useful tool in the engineering of the pathway, as their low homology with respective plant genes alleviates potential silencing/cosuppression, the potential effects of endogenous allosteric regulators is reduced, and the phytoene desaturase (CRTI) from this organism is a single enzyme that will convert 15-*cis* phytoene to all-*trans* lycopene, thus overcoming the need for four proteins (Figure 1). To make further progress in carotenoid engineering of higher plants, knowledge of carotenoid pathway regulation and sequestration within the plastids are of considerable importance. Over recent years, correlations between carotenoid content and

Figure 1. Representative Scheme of the Carotenoid Biosynthetic Pathway in Higher Plants.

sequestration mechanisms have been highlighted (Simkin et al., 2007; Li et al., 2012; Kilambi et al., 2013). The biosynthesis and sequestration of carotenoids are two aspects that need to be considered simultaneously to optimize carotenoid accumulation through engineering of plants. Moreover, our understanding of cellular compartmentalization (Heinig et al., 2013) and plastid compartmentalization remain key in metabolic engineering.

In this article, the optimal combination of the *Crt* heterologous carotenoid biosynthetic genes has been ascertained in tomato (*Solanum lycopersicum*) fruit for increased carotenoid levels. Characterization of these events has furthered our understanding of regulation mechanisms associated with carotenoid formation, revealed subcellular adaptation to newly synthesized carotenoids, and demonstrated how perturbations to carotenoids can impact the metabolome.

RESULTS

The Combinations of *Crt* Genes and Their Zygosity Affect Carotenoid Content

Three homozygous tomato lines, containing the *P. ananatis* (1) geranylgeranyl diphosphate synthase (*Crt*E) and (2) phytoene synthase (*Crt*B), both under the control of fruit-specific promoters, and (3) phytoene desaturase (*Crt*I), under the control of a constitutive promoter, were used to perform genetic crosses (Figure 1). A minimum of six complementary crossing events were performed to establish the heterologous carotenoid gene combinations *Crt*E+B, *Crt*E+I, and *Crt*B+I. From these crosses, 10 F1 plants per cross were generated and screened by PCR for the presence of transgenes (see Supplemental Figure 1 online). Four PCR positive lines for each combination were selected for further analysis. The lines exhibiting the highest or altered carotenoid contents were then grown to maturity in the F2 generation.

To fully assess the *Crt* gene combinations and the effects of gene dosage, analyses of carotenoids, chlorophylls, and tocopherols were performed on hemizygous and homozygous lines over several growth cycles. Absolute levels of carotenoids did change with environmental conditions (growth season). However, the concurrent generation and analysis of wild types enable accurate evaluation of the transgenic plants. Leaf pigments revealed significant qualitative differences that could be attributed to the presence of *Crt*I (Table 1; see Supplemental Figure 2 online). β-carotene increased almost twofold and other β-ring–derived carotenoids, such as violaxanthin (and its isomers),

displayed similar increases (Table 1). The total carotenoid content was also increased (1.3- to 1.4-fold), which contributed to a decreased chlorophyll:carotenoid ratio (Table 1). Compared with the wild type, no significant difference in carotenoid content was found in the lines expressing *Crt*E and *Crt*B alone.

A similar situation occurred in the tomato fruit, where the presence of *Crt*I in the ripe fruit conferred the greatest changes in carotenoid and tocopherol levels compared with the other genes, *Crt*E and *Crt*B (Table 2). Indeed, compared with the wild type, the hemizygous and homozygous *Crt*E lines showed a similar carotenoid profile, and only a modest, but significant increase of phytoene (1.2-fold) was noticeable in the hemizygous *Crt*B line. However, there was a significant increase of lycopene in the *Crt*E+B line (1.4-fold), as well as in the homozygous *Crt*B line (2.2-fold). The hemizygous *Crt*I line was characterized by a higher level of β-carotene (2.4-fold increase compared with Ailsa Craig [AC]), a greater content of γ-carotene, lutein, and α-tocopherol, and a substantial decrease of phytoene and phytofluene (0.4-fold). The presence of an early step carotenoid gene (*Crt*E or *Crt*B) in the hemizygous *Crt*E+I and *Crt*B+I lines alleviates the decrease of phytoene and phytofluene contents. Moreover, an increase in lycopene (1.4-fold) was also observed in the hemizygous *Crt*B+I line. The homozygous *Crt*I line had a similar carotenoid profile to hemizygous *Crt*B+I. Surprisingly, the level of lycopene in the homozygous *Crt*B+I line was comparable with the wild type. However, the β-carotene content of this line was the highest compared with all the *Crt*I-containing lines. Analysis of ripe fruit pigments from the various *Crt* gene combinations indicated that the CRTI enzyme solely, or in combination with the CRTE and CRTB enzymes, conferred the greatest effects on lycopene and β-carotene contents compared with the wild type, either in the hemizygous or homozygous states (Table 2).

*Crt*B+I Lines Showed Changes in Transcription, Plastid Ultrastructure, and Levels of Primary and Secondary Metabolites

Since analysis of carotenoids among the lines of the different *Crt* gene combinations revealed *Crt*B+I as the best line for fruit carotenoid content and showed that this combination could exist in a stable homozygous state maintaining the high β-carotene phenotype, further characterization was performed to ascertain the underlying mechanisms associated with the effects of this gene combination.

Pigment analysis of mature green, breaker, breaker + 3 d, breaker + 7 d, and breaker + 14 d, in the *Crt*B+I line and its wild

Figure 1. (continued).

Enzymes in red are tomato fruit ripening specific or enhanced, and those in blue are flower specific. GA3P, glyceraldehyde-3-phosphate; DXP, 1-deoxy-ᴅ-xylulose 5-phosphate; MEP, 2-C-methyl-ᴅ-erythritol 4-phosphate; IPP, isopentenyl diphosphate; DMAPP, dimethylallyl diphosphate; FPP, farnesyl diphosphate; GGPP, geranylgeranyl diphosphate; GGPPS-1 and -2, geranylgeranyl diphosphate synthase; PSY-1, fruit-specific phytoene synthase-1; PSY-2, phytoene synthase-2; PDS, phytoene desaturase; ZDS, ζ-carotene desaturase; CRTISO, carotene isomerase; LCY-E, ε-lycopene cyclase; LCY-B, β-lycopene cyclase; CYC-B, fruit-specific β-lycopene cyclase; CRTR-B1, carotene β-hydroxylase 1; CRTR-B2, carotene β-hydroxylase 2 (flower specific); ZEP, zeaxanthin epoxidase; NXS, neoxanthin synthase; VDE, violaxanthin deepoxidase; CRTE, geranylgeranyl diphosphate synthase; CRTB, phytoene synthase; and CRTI, phytoene desaturase. The *cis* configurations are not shown for all molecules, but they are represented with blue numbers. The dashed arrows illustrate biochemical steps that are not represented in this scheme.
[See online article for color version of this figure.]

Table 1. Carotenoid and Chlorophyll Contents in the Leaves of the Transgenic Lines

Content	AC	Homozygous			Hemizygous		
		*Crt*E	*Crt*B	*Crt*I	*Crt*E+B	*Crt*E+I	*Crt*B+I
β-Carotene	219 ± 15	331 ± 7	217 ± 7	**298 ± 6***	228 ± 4	**361 ± 32***	**319 ± 13***
Violaxanthin#	335 ± 16	347 ± 10	322 ± 9	**535 ± 4****	344 ± 4	**552 ± 22***	**549 ± 14****
Lutein	303 ± 20	316 ± 8	311 ± 7	294 ± 9	310 ± 11	280 ± 16	253 ± 8
Total CAR	856 ± 51	894 ± 24	851 ± 23	**1,127 ± 18***	881 ± 19	**1,193 ± 69***	**1,120 ± 26***
Chlorophyll *a*	9,433 ± 2,210	10,825 ± 642	11,005 ± 448	8,107 ± 213	9,534 ± 1,264	7,501 ± 422	7,301 ± 507
Chlorophyll *b*	1,346 ± 598	1,817 ± 289	2,217.± 93	589 ± 190	1,468 ± 429	426 ± 274	519 ± 70
CHL:CAR	13 ± 3	15 ± 1	15 ± 1	8 ± 1	13 ± 2	7 ± 1	7 ± 1

Carotenoid and chlorophyll contents are presented as µg/g dry weight. Methods used for determinations are described in Methods. Four representative leaves from a minimum of three plants were used. The leaves were respectively pooled, and three determinations were made per sample, making a minimum of three biological and three technical replicates. The mean data are presented ± sd; # violaxanthin and isomers; CHL, chlorophyll; CAR, carotenoid. Dunnett's test was used to determine significant differences between the wild-type background (AC) and the transgenic varieties. Values in bold indicate where significant differences have been found. P < 0.05 is designated by *.

type (AC), revealed differences in carotenoids at the breaker stage onwards (Figure 2). With the onset of ripening at the breaker stage, the phytoene content decreased, while β-carotene content increased in the *Crt*B+I line. These significant differences remained throughout fruit ripening. A decrease in the lycopene content occurred at the breaker + 3 d stage but was not significantly different at other stages.

In ripe fruit, carotenoids and tocopherols were quantified in the pericarp, jelly, and columella tissues of the *Crt*B, *Crt*I, and *Crt*B+I lines and compared with the same material in the wild-type background (Figure 3; see Supplemental Table 1 online). Carotenoids and α-tocopherol were found in all the compartments of the fruit, but not in the same proportions. Pericarp tissue contained the most carotenoids in the control (AC), with ~50% of total carotenoids present. The columella sequestrated 30%, while the jelly tissue contained ~20%. In *Crt*B, *Crt*I, and *Crt*B+I lines, the distribution of total carotenoids within the fruit

compartments was comparable to that of the control, but small increases were evident (see Supplemental Table 1 online).

Lycopene was mainly found in the pericarp of all the lines, while β-carotene was the most abundant carotenoid in the jelly. However, the predominant carotenoid in the columella varied among the lines. Lycopene was the main carotenoid in the columella tissue of the wild type and the *Crt*B lines, whereas β-carotene predominated in *Crt*I and *Crt*B+I lines. When calculated as fold changes, although the lycopene levels increase in the pericarp and the columella of *Crt*B (homozygous) line, the greatest increase was in the columella (2.3-fold increase). The β-carotene levels increased in all the fruit compartments of *Crt*I and *Crt*B+I (homozygous), but the greatest change was in the columella (2.2- and 2.5-fold increase, respectively, for *Crt*I and *Crt*B+I).

Levels of mRNAs were studied in the leaf and tomato fruit (at breaker + 3 d) of *Crt*B, *Crt*I, and *Crt*B+I lines and the wild type (Figure 4). In the leaf, the majority of the pathway transcripts

Table 2. Carotenoid and Tocopherol Contents in the Fruits of the Transgenic Lines

Variety	Phytoene	Phytofluene	Lycopene	β-Carotene	γ-Carotone	Lutein	Total CAR	α-Tocopherol
AC	133 ± 16	134 ± 24	1,224 ± 255	321 ± 32	62 ± 7	122 ± 15	1,995 ± 327	256 ± 39
Hemizygous								
*Crt*E	136 ± 4	141 ± 4	1,434 ± 55	322 ± 10	56 ± 2	**132 ± 3****	2,220 ± 73	283 ± 10
*Crt*B	**160 ± 4***	146 ± 11	1,352 ± 108	**220 ± 19*****	**48 ± 2***	117 ± 9	2,042 ± 136	229 ± 8
*Crt*I	**52 ± 7*****	**55 ± 3*****	1,191 ± 10	**785 ± 11*****	**93 ± 14***	**155 ± 5***	2,330 ± 26	**319 ± 8****
*Crt*E+B	143 ± 8	138 ± 5	**1,681 ± 258***	296 ± 18	61 ± 3	116 ± 2	2,435 ± 251	232 ± 21
*Crt*E+I	**70 ± 7*****	**84 ± 2****	1,285 ± 168	**560 ± 39*****	71 ± 3	120 ± 2	2,190 ± 177	**336 ± 19****
*Crt*B+I	**56 ± 8*****	**81 ± 2****	**1,656 ± 6***	**665 ± 55*****	**74 ± 2***	121 ± 1	**2,649 ± 117****	**385 ± 42****
Homozygous								
*Crt*E	149 ± 15	153 ± 11	1,602 ± 21	286 ± 8	66 ± 4	120 ± 4	2,376 ± 328	**334 ± 40***
*Crt*B	124 ± 12	134 ± 8	**2,696 ± 146*****	377 ± 40	71 ± 5	**114 ± 1***	**3,517 ± 179*****	331 ± 63
*Crt*I	**41 ± 1*****	**79 ± 1****	**1,780 ± 74***	**680 ± 93*****	**81 ± 6****	**114 ± 2***	**2,775 ± 368***	**378 ± 24*****
*Crt*B+I	**42 ± 3*****	**40 ± 1*****	1,109 ± 113	**803 ± 40*****	69 ± 3	117 ± 5	2,179 ± 140	**343 ± 16****

Carotenoid and tocopherol contents are presented as µg/g dry weight. Methods used for determinations are described in Methods. Three representative fruits from a minimum of three plants were used. The fruits were respectively pooled, and three determinations were made per sample, making a minimum of three biological and three technical replicates. The mean data are presented ± sd; CAR, carotenoid. Dunnett's test was used to determine significant differences between the wild-type background (AC) and the transgenic varieties. Values in bold indicate where significant differences have been found. P < 0.05, P < 0.01, and P < 0.001 are designated by *,**, and ***, respectively.
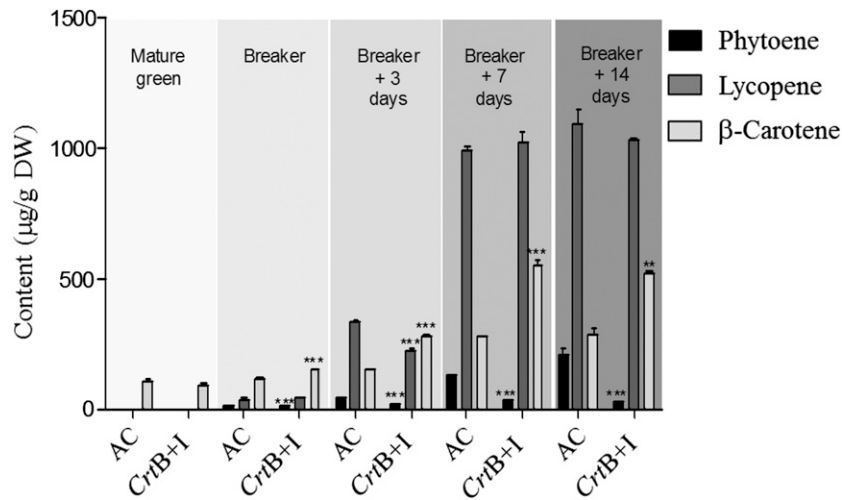
**Figure 2.** The Changes of Carotenoid Composition in the Fruit of *Crt*B+I through Ripening Compared with AC.

Lycopene, β-carotene, and phytoene contents are given as μg/g dry weight (DW). Methods used for determinations are described in Methods. Three representative fruits were used. Three determinations were made per fruit, making three biological and three technical replicates. The bars represent the mean ± SD. Student's *t* test was used to determine significant differences between the wild-type background (AC) and the *Crt*B+I line for each ripening stage indicated. Asterisks indicate significant differences. P < 0.05, P < 0.01, and P < 0.001 are designated by *, **, and ***, respectively. The *Crt*B+I homozygous line was used.

were not significantly affected compared with the control (AC). Only the levels of the fruit-specific lycopene β-cyclase (*Cyc*-b) and the flower-specific carotene β-hydroxylase (*Crt*R-b2) transcripts were significantly different in the *Crt*I lines, showing a two- to threefold increase in comparison with the wild-type levels. In the transgenic fruit, several carotenogenic genes were upregulated, including geranylgeranyl pyrophosphate synthase-2 (*Ggpps*-2), zeaxanthin epoxidase-1 (*Zep*-1), ε-lycopene cyclase (*Lcy*-E), and the lycopene β-cyclase (*Lcy*-B). By contrast, the *Crt*B and *Crt*B+I lines had reduced levels of *Psy*-1 and *Psy*-2 transcripts (~0.7-fold) compared with their control. However, *Crt*I only exhibited a significant reduction in *Psy*-2. The levels of carotene β-hydroxylase (*Crt*R-b1) transcripts were reduced in all transgenic lines, whereas the phytoene and ζ-carotene desaturase (*Pds* and *Zds*) transcripts were only reduced in the *Crt*B line (Figure 4). Several ultrastructural changes were apparent in the transgenic lines. The chromoplasts of *Crt*B+I were significantly larger in volume (9.1 ± 1.3 μm²) than those of the wild type (3.12 ± 0.5 μm²). In addition, the plastids contained significantly more plastoglobules in the *Crt*B+I line (36.3 ± 8.3) than in AC (12.9 ± 2.9). Some of these plastoglobules were larger (approximately twofold) and had different staining characteristics. Structures termed thylakoid plexus and membranous sacs were identified and were more abundant in the chromoplasts derived from this line (Figure 5). Among the different transgenic lines, similar types of chromoplasts were apparent. To verify that no heterogeneity in chromoplast structure and carotenoid content existed, separation of potential chromoplast types was performed by Suc density gradient centrifugation (see Supplemental Figure 3 online; system 3 as described in Methods). The intact chromoplasts, accumulating at different densities on the gradient, all appeared to have a similar ultrastructure and similar carotenoid profiles.

The distinct changes at the cellular level suggested perturbations beyond the isoprenoid pathway had arisen in the *Crt*B+I line. To assess the global effects across metabolism, metabolite profiling was performed. Over 50 metabolites were identified and quantified in a relative or absolute manner in the tomato leaf and fruit of the *Crt*B+I line and in the wild type. Metabolite changes relative to their control (AC) levels were determined and statistical analysis performed to assess the differences (Table 3; see Supplemental Figure 4 online). Significant changes in metabolite levels were found in all classes of compounds studied. In the fruit of *Crt*B+I, all amino acids and most of the sugar levels were significantly greater compared with their levels in AC, while the majority of organic acids significantly decreased in *Crt*B+I. Among the lipids, the level of monogalactosyldiacylglycerol (MGDG) lipids increased (3.6-fold increase) in *Crt*B+I. MGDG fatty acids of the *Crt*B+I line had increased levels of C16:0 and C16:1 *cis* 9 fatty acids (see Supplemental Table 2 online). No significant difference was observed in the total amount of fatty acids for all other lipids analyzed.

Elevated Carotenoid Levels Are Sequestered in Subplastidial Compartments

To identify the subplastidial location of carotenoids in *Crt*B+I and wild-type lines, chromoplasts were fractionated by Suc density gradient centrifugation (Figure 6A; see Supplemental Figure 5 online, system 1). Three distinct colored sectors in the gradient were observed, the first at the top of the gradient, in fractions 1 and 2. The red/orange color intensity of these fractions was greater in the *Crt*B+I preparations. In the lower part of the gradient, from fractions 16 to 24, two sectors of color intensity occurred. These two sectors were in close proximity in the gradient but separated by the less intense area arising at fractions
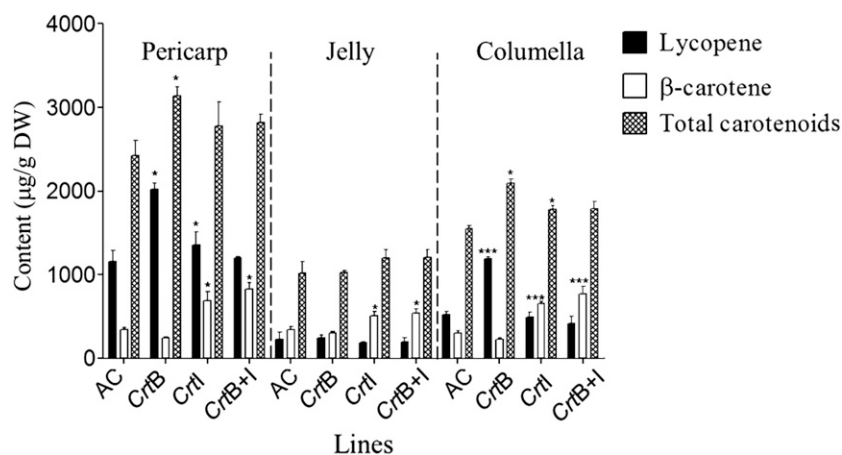
Figure 3. Lycopene and β-Carotene Content in the Pericarp, Jelly, and Columella of the Fruits of the Genetic Crosses.

Carotenoid contents are given as μg/g dry weight (DW). Methods used for determinations are described in Methods. Three representative fruits were used for a minimum of three plants. Three determinations were made per fruit, making three biological and three technical replicates. The bars represent the mean ± SD. Dunnett's test was used to determine significant differences between the wild-type background (AC) and the transgenic lines for each compartment. Asterisks indicate significant differences. $P < 0.05$, $P < 0.01$, and $P < 0.001$ are designated by *,**, and ***, respectively. The CrtB+I homozygous line was used.

20 and 21. One of the distinguishing features arose from the presence of particulates, crystal-like structures, within the two sectors. Comparison between the wild-type and CrtB+I lines indicated a greater intensity of crystal-like aggregates in the upper sector derived from the wild type, with relatively few structures in the lower phase. By contrast, the CrtB+I line exhibited a greater intensity of crystalline aggregates over both sections (Figure 6A).

Sixteen fractions (F) throughout the gradient were analyzed to identify and designate the different subcompartments of the chromoplasts (Figure 6). The protein and lipid profiles of these fractions have been determined (Figure 6B). Their ultrastructure and carotenoid profile have been investigated (Figures 6C and 6D), and the location of heterologous enzymes (CRTB and CRTI) as well as the endogenous enzyme (the fruit-specific phytoene synthase PSY-1) have been determined (Figure 6E). The protein profile of AC and CrtB+I is similar (Figure 6B, i), with F1 and F2 characterized by two major proteins. These proteins are plastoglobule-associated plastoglobulin-1 and the Chromoplast-specifc associated protein C (CHRC). The amount of proteins present in F7 to F12 was too low for detection on SDS-PAGE stained with silver reagents. F17 to F30 contained comparatively higher protein intensity than earlier fractions, with prominent bands displaying Gaussian distribution across adjacent fractions (Figure 6B). In F17 to F24, all the proteins identified were derived from the photosynthetic systems present in the thylakoid membrane; for example, ATP synthase subunit β, photosystem I reaction center subunit II, photosystem II 22-kD protein, and the oxygen evolving enhancer proteins 1 and 2. In F24 to F30, thylakoid proteins were present, but additional proteins such as the heat shock cognate 70-kD protein were detected. This protein has been attributed to the chromoplast envelope (Ko et al., 1992). The ribulose-1,5-bisphosphate carboxylase/oxygenase protein, from the chromoplast stroma, was mainly detected in F28 and F30. Further details on the proteins identified are in Supplemental Table 3 online.

To complement the proteomic approach, immunodetection of biomarker proteins of known subplastid location was used. The immunolocalization of the plastoglobulin 35, PSBA (for photosystem II protein D1), TIC40 (for translocon at the inner envelope of chloroplasts), TOC75 (for translocon at the outer envelope of chloroplasts), and the stromal RBCL (for ribulose-1,5-bisphosphate carboxylase/oxygenase large subunit) proteins was performed across the gradient (Figure 6B, ii). The plastoglobulin was detected in F1 and F2, but also in F18 to F30. Following comparative protein loading of wild-type and CrtB+I samples, a greater quantity of PGL was prevalent in the CrtB+I fractions. The PSBA was mainly detected in F17 to F26 fractions and at low level in control F1 and F2. TIC was found principally in F28 and F30 in AC and in F24 to F26 in CrtB+I, while TOC75, specific to the chloroplast envelope, was not detected in the fractions. The RBCL was mainly discovered at the bottom of the gradient in F26 to F30 in AC and F25 to F30 in CrtB+I.

The lipid profile of AC and CrtB+I fractions was comparable. All the fractions contained complex lipids. However, MGDG, digalactodiacylglycerol, phosphatidylethanolamine, phosphatidylserine, and phosphatidylcholine lipids were only found in F17 to F26/28 (Figure 6B, iii). These data show that F1 and F2 correspond to the free plastoglobules of the chromoplasts, F17 to F23 represent the subcompartment structure with thylakoid membrane, while F24 to F26/28 are a mix of thylakoid membrane and envelope membrane structures and the last fractions represent enriched stromal proteins (F25 to F31).

Electron microscopy was used to visualize the structures fractionated through the gradient (Figure 6C). Plastoglobules were found in F1 and F2 of both the wild type and the CrtB+I line. Membranous structures, with varying degrees of complexity and aggregation, were seen in F16 and F18 to F22, and F24, although, clear vesicle-like structures predominated in these fractions. The structures varied in the thickness of the membrane, as judged by
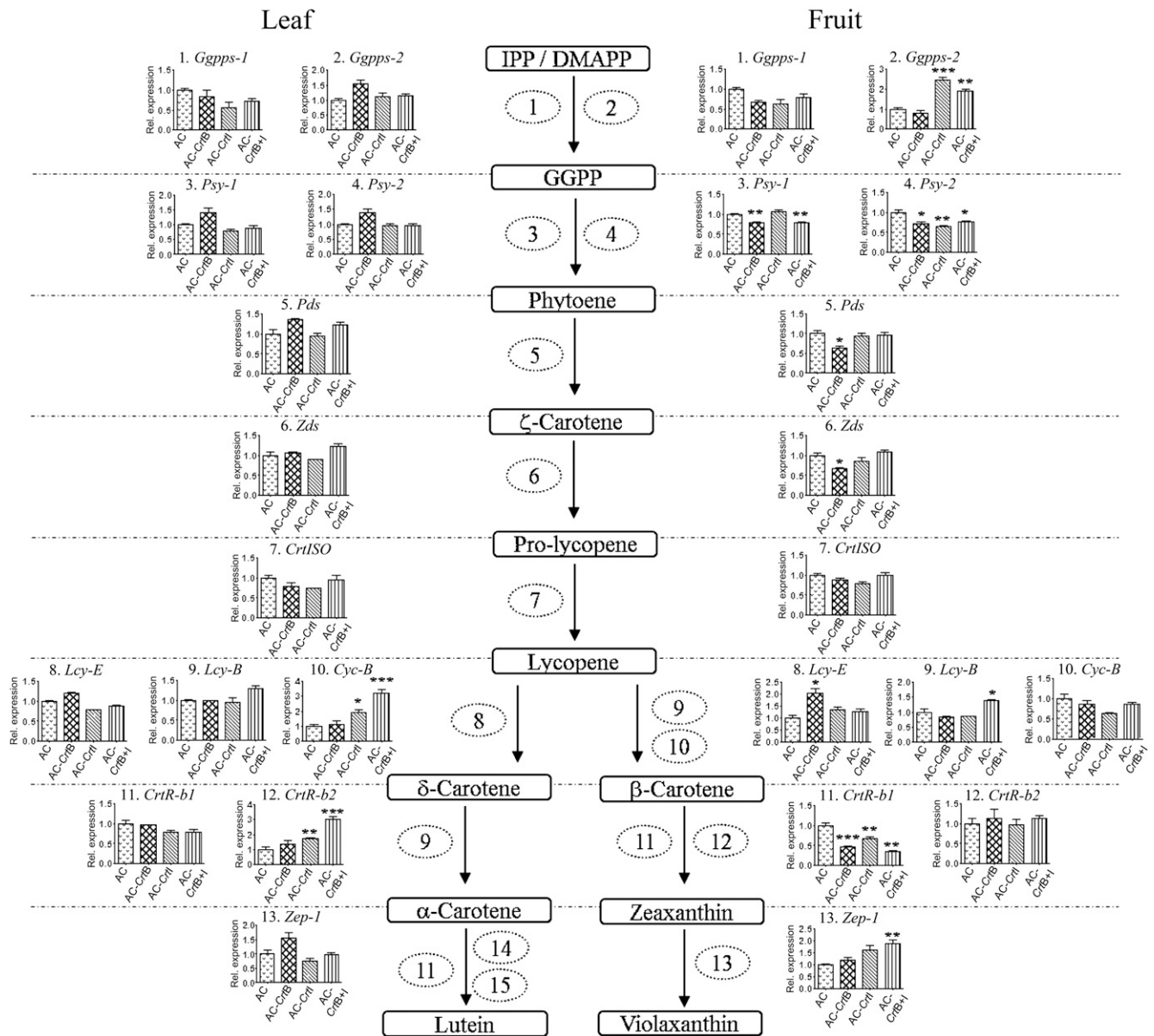
Figure 4. Changes in the Transcript Levels of Carotenoid Biosynthetic Genes in Response to Changes in Carotenoid Content Resulting from the Expression of *Crt*B, *Crt*I, and *Crt*B+I Genes in Tomato.

Pooled fruit originating from three plants per genotype (AC, AC-*Crt*B, AC-*Crt*I, and AC-*Crt*B+I; homozygous lines) were ground in liquid nitrogen to provide a homogenous powder as described in Methods. Total RNA was then extracted from an aliquot of this material. Quantitative real-time RT-PCR was performed with gene-specific primers for (1) *Ggpps-1*, (2) *Ggpps-2*, (3) *Psy*-1, (4) *Psy-2*, (5) *Pds*, (6) *Zds*, (7) *CrtISO*, (8) *Lcy-E*, (9) *Lcy-B*, (10), *Cyc-B*, (11) *CrtR-b1*, (12) *CrtR-b2*, (13) *Zep-1*, (14) CYP97A, P450 β-ring hydroxylase, and (15) CYP97C, P450 hydroxylase. The expression data shown have been normalized to the expression of actin. Data are represented as relative levels found in the three varieties compared with the wild-type AC. Statistical determinations are shown as mean ± SD values, where $n = 3$. Dunnetts's test illustrates statistically significant differences (*P < 0.05, **P < 0.01, and ***P < 0.001) from the wild-type levels. The first bars of the histogram indicate levels in the wild-type AC, the second bars in AC-*Crt*B, the third bars in AC-*Crt*I, and the fourth bars in AC-*Crt*B+I. IPP, isopentenyl pyrophosphate; DMAPP, demethylallyl diphosphate; GGPP, gerenaylgeranyl diphosphate.

the intensity of staining and size, with some vesicles embedded in larger membrane structures. In addition, some vesicles appeared to retain plastoglobules and/or dense staining amorphous material associated with these membranes. The different electron density levels throughout the membranes suggest a variability of

the carotenoid lipoprotein structure of the membrane. The contents of fractions lower in the gradient (e.g., F24) appeared to be enriched with larger vesicles containing electron dense material.

Carotenoids and α-tocopherol were profiled in all the fractions derived from the fractionated chromoplasts (Figure 6D). The
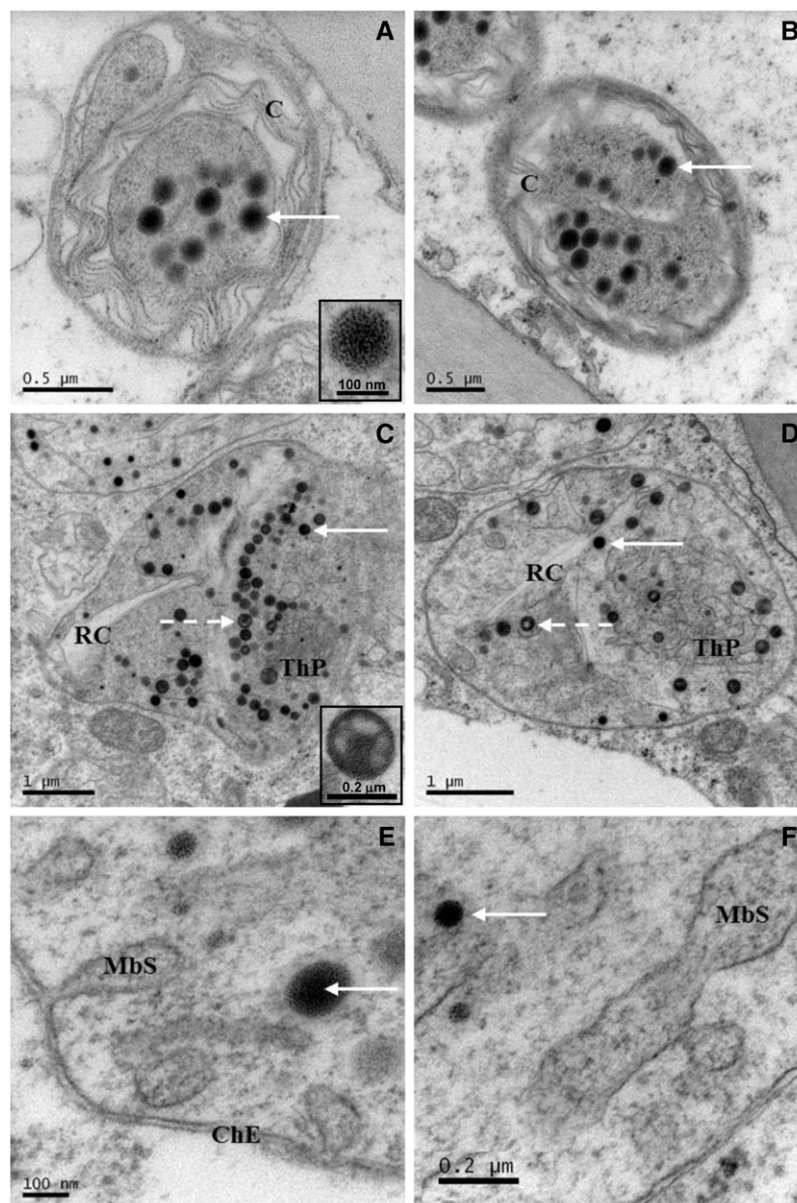
Figure 5. Electron Micrographs of Chromoplasts and Substructures of the *Crt*B+I Line and the AC Control at the Breaker + 5 d Stage.

Chromoplasts found in AC (control) (**[A]** and **[B]**), chromoplasts of the *Crt*B+I line (**[C]** and **[D]**), and substructures of the *Crt*B+I chromoplasts (**[E]** and **[F]**). Arrows show plastoglobules (close-up of **[A]**); dashed arrows show morphologically different plastoglobules (close-up of **[C]**). C, lycopene crystal; RC, remains of crystal; ThP, thylakoid plexus-like; MbS, membranous sac; ChE, chromoplast envelope. Methods used to obtain the electron micrographs are described in Methods. The *Crt*B+I homozygous line was used.

percentage of each compound studied varied through the gradient and was dependant on the line (see Supplemental Figure 6 online). Two sectors of dense pigmentation, forming peaks of metabolite intensity, were observed for lycopene, β-carotene, lutein, and α-tocopherol derived from the fractionation of the *Crt*B+I material. The first peak of pigmentation was located from F16 to F21 and designated as the submembrane compartment I. The second peak, located in F21 to F26, was termed submembrane compartment II. Lycopene, β-carotene, and lutein have similar profiles through the gradient. In AC, they mainly accumulate in submembrane I. In the *Crt*B+I line, there is an increase of lycopene, β-carotene, and lutein contents. The accumulation of these carotenoids was greater in both submembrane compartments I and II in the *Crt*B+I line compared with the control, especially in compartment II, which contained a higher ratio of β-carotene to lycopene, compared with compartment I. In the control, phytoene accumulated in the plastoglobules (15%) and then mainly in submembrane compartment

Table 3. Metabolite Changes Occurring in Tomato Leaves and Fruit in the *Crt*B+I Line Compared to the Control AC

Metabolite	Ratio *Crt*B+I to AC	
	Leaf	Fruit
Amino acid		
Ala	**1.43 ± 0.08**	–
Asp	**10***	**2.10 ± 0.53**
β-Ala	**10***	–
γ-Aminobutyric acid	1.03 ± 0.06	**2.44 ± 0.11**
Leu	**10***	–
Pro	**10***	–
Gln	**1.98 ± 0.2**	**1.41 ± 0.33**
Ser	**10***	**1.73 ± 0.29**
Thr	1.32 ± 0.39	**10***
Val	1.34 ± 0.37	–
Isoprenoid		
α-Tocopherol	–	**1.34 ± 0.12**
Violaxanthin	**1.64 ± 0.08**	–
Lutein	0.83 ± 0.06	0.97 ± 0.07
β-Carotene	**1.46 ± 0.21**	**2.50 ± 0.25**
Chlorophyll *a*	0.77 ± 0.35	–
Chlorophyll *b*	0.39 ± 0.32	–
γ-Carotene	–	1.11 ± 0.11
Lutein	–	0.96 ± 0.07
Lycopene	–	0.91 ± 0.19
Phytoene	–	**0.31 ± 0.04**
Phytofluene	–	**0.30 ± 0.02**
Non-amino acid N-containing compound		
Putrescine	**10***	–
Lipid		
DGDG	ND	1.05 ± 0.50
MGDG	ND	**3.61 ± 1.03**
PE	ND	1.09 ± 1.12
PS/PC	ND	0.75 ± 0.22
Triglycerides	ND	0.99 ± 0.10
Organic acid		
Aconitic acid	–	**0.01#**
Citric acid	**1.13 ± 0.09**	0.98 ± 0.14
Erythronic acid	**6.80 ± 1.01**	–
Fumaric acid	**0.61 ± 0.09**	**0.01#**
Glucaric acid	**8.88 ± 1.57**	1.53 ± 0.10
Gluconic acid	**0.29 ± 0.09**	**0.76 ± 0.15**
Glycerate	**0.01#**	–
Itaconic acid	–	**0.28 ± 0.04**
Isocitrate	**0.01#**	–
Lactic acid	**10***	–
Maleic acid	**0.61 ± 0.06**	**0.01#**
Malic acid	**1.49 ± 0.17**	1.05 ± 0.14
Succinic acid	0.96 ± 0.07	**0.89 ± 0.07**
Phosphate		
Glc-6-phosphate	**10***	**0.01#**
Glycerol-3-phosphate	**10***	–
Phosphate	**8.87 ± 1.91**	0.99 ± 0.06
Polyol		
Glycerol	**10***	–
Inositol	**0.74 ± 0.14**	**1.96 ± 0.20**
Sugar		
Ara	**0.58 ± 0.23**	**3.45 ± 0.88**
Fru	**0.90 ± 0.06**	1.10 ± 0.21

(Continued)

I. In the *Crt*B+I line, the level of phytoene in the plastoglobules was lower (6%). The percentage of phytoene was comparable in submembrane compartments I and II.

An additional experiment was performed to ascertain if the carotenoid crystals in submembrane compartments I and II (system 1) were attached/embedded into the membrane. Another fractionation system was used (see Supplemental Figure 5 online, system 2). At the top of the gradient, a large red area was observed, while the membranes pelleted at the bottom of the gradient. The membranes were then separated using system 1. No crystals were observed in submembrane compartments I and II of the system 2 gradients (see Supplemental Figure 6A online). However, membrane-free crystals were observed by light microscopy when analyzing the red sector obtained in the first step gradient of system 2 (see Supplemental Figure 6B online). Observation of submembrane compartments I and II with a light microscope showed carotenoid crystals wrapped in a membranous structure. Therefore, carotenoid crystals are normally attached/embedded into the membrane but can be separated during fractionation. The importance of the crystalline structures in the sequestration of carotenoids in the *Crt*B+I line is illustrated by the comparison of carotenoid content in membranes with embedded crystals (obtained from system 1) with that in crystal-free membranes (obtained from system 2), where the ratio of carotenoid content in plastoglobules to membranes with embedded crystals is decreased in *Crt*B+I compared with AC (system 1) and the ratio of plastoglobules plus crystals to crystal-free membrane is increased in *Crt*B+I compared with AC (see Supplemental Figure 6C online). The localization of CRTB, CRTI, and PSY-1 was performed using specific antibodies (Figure 6E). The heterologous enzymes CRTB and CRTI in the *Crt*B+I line appeared to be strongly associated with the thylakoid-related fractions and were mainly present in submembrane compartment II. However, PSY-1 was found mainly in the stroma of both the control and *Crt*B+I lines.

DISCUSSION

Expression of Bacterial Carotenoid Gene Combinations Can Have a Synergistic Effect on Carotenoid Formation in Tomato Fruit

The carotenoid profiles of the homozygous *Crt*B and *Crt*I tomato lines have been studied previously by Fraser et al. (2002) and Römer et al. (2000), respectively. The results shown in this study correlate with the previous description of these lines. Moreover, the expression of *Crt*I in tobacco (*Nicotiana tabacum*) leaves was studied (Misawa et al., 1994) and also shown to result in an increase in xanthophylls. The strategy to coordinate the expression of multiple bacterial carotenoid genes to improve carotenoid formation in plants has been used previously in crops with low basal levels of carotenoids, for example, in canola (*Brassica napus*) seed (Ravanello et al., 2003) and potato (*Solanum tuberosum*) tuber (Diretto et al., 2007). The decrease of phytoene and increase in lycopene/β-carotene levels in *Crt*I lines was reported in both studies and is supported by the results with tomato fruit (Table 2), which are chromoplasts-containing tissues predisposed to

Table 3. (continued).

| | Ratio *Crt*B+I to AC | |
Metabolite	Leaf	Fruit
Glc	**1.90 ± 0.18**	**1.15 ± 0.20**
Rib	**0.58 ± 0.23**	**3.45 ± 0.88**
Sedoheptulose	**0.18 ± 0.05**	0.95 ± 0.17
Xyl	**0.58 ± 0.23**	**3.45 ± 0.88**
Xylulose	–	**0.01#**

Data were compiled from multiple analytical platforms. The ratio data are presented as mean ± SD. Student's *t* test analysis was carried out. Significant changes are represented in bold (P value < 0.05). 10*, theoretical value when a metabolite is unique to *Crt*B+I at the concentration used; 0.01#, theoretical value when a metabolite is unique to AC at the sample concentration used. – indicates metabolite not detected in both *Crt*B+I and AC at the sample concentration used. ND indicates metabolite not determined; PS/PC, phosphatidylserine/phosphatidylcholine; PE, phosphatidylethanolamine; DGDG; digalactosyldiacylglycerol.

carotenoid accumulation. The coordinate expression of two bacterial hemizygous carotenoid genes in tomato highlights synergistic effects on carotenoid formation, which were not observed in the lines expressing only one gene. For instance, there is no significant increase in lycopene in the hemizygous *Crt*E, *Crt*B, and *Crt*I lines compared with the control. However, there is a significant increase in the hemizygous *Crt*E+B and *Crt*B+I lines. The production of lycopene, which was not enhanced by the expression of only one bacterial carotenoid gene, is positively affected, while two bacterial carotenoid genes are expressed. This suggests that there is a functional interaction between CRTE and CRTB plus CRTB and CRTI in the fruit. By contrast, no such synergistic effect on lycopene formation was found in the *Crt*E+I line (Table 2), indicating that CRTE and CRTI do not interact via the endogenous phytoene synthase enzyme PSY-1. Thus, only the bacterial enzymes of consecutive steps of the carotenoid pathway have a synergistic effect on carotenoid formation. This suggests that CRTE, CRTB, and CRTI need to form an aggregate complex to be able to interact or to be sequestrated into a common microenvironment within the plastid to form a functionally complete metabolon. Previous work also suggested that a complex of the bacterial phytoene synthase, phytoene desaturase, and the lycopene cyclase enzymes allowed in vivo activity of all three proteins through substrate channeling (Ravanello et al., 2003). Although the strategy of combining expression of bacterial hemizygous carotenoid genes increased carotenoid levels, the dose of the heterologous gene(s) had a similar impact. For instance, while the level of lycopene was not significantly increased in the *Crt*B hemizygous and *Crt*I hemizygous lines compared with the wild type, it was increased in the *Crt*B homozygous and *Crt*I homozygous lines, as in the *Crt*E+B and *Crt*B+I hemizygous lines. Surprisingly, no significant increase in lycopene and total carotenoids was found in the homozygous *Crt*B+I line, although it did contain the highest level of β-carotene of all the lines. Consequently, the hemizygous *Crt*B+I line appears to be a better option than the homozygous line in regard to increasing total carotenoid levels. In summary, the choice of the

heterologous carotenoid genes, their combination, and gene dosage (hemizygous or homozygous) are factors that affect carotenoid formation and that therefore need to be assessed in order to manipulate the pathway. These data also highlight why characterization of transgenic plants should not be performed solely on primary transformants. It is also feasible that the homozygous state is more prone to silencing by methylation. The involvement of epigenetic regulatory mechanisms that affect heterologous genes has not been studied intensively, but methylation has been shown to be an important mode of regulation in tomato fruit (Zhong et al., 2013). However, in this case, immunoblot analysis of CRTB and CRTI levels in the hemizygous and homozygous states indicated an increase in protein content approaching twofold in the latter. Therefore, determination of enzyme activities/flux coefficients (Fraser et al., 2002) would be an informative approach to reveal underlying mechanisms associated with the changes in carotenoid profiles between the different *Crt* gene combinations. This study demonstrated the potential beneficial effects of combining two *Crt* genes on carotenoid content. Future approaches could use the triple combination (*Crt*E+B+I) to potentially enhance carotenoid levels further.

The Effects of *Crt*B+I Go Beyond the Carotenoid Pathway

Small changes in transcription correlated, as expected, with increases in carotenoids (Tables 1and2). Interestingly, those transcripts most affected in the transgenic lines corresponded to genes associated with alternative tissue-specific expression (Figure 4). For example, in the leaf, transcripts of the fruit-specific lycopene cyclase (*CYC*-B) and the flower-specific carotene β-hydroxylase carotene (*CrtR*-b2) genes were altered. This suggests that transcription is tightly regulated for those carotenoid genes expressed in certain tissues, but genes not usually expressed in a given tissue are not under the same regulatory mechanisms.

The activity of CRTB and CRTI also affected the spatial accumulation of pigments over fruit development and ripening, as well as the partitioning of the carotenoids within the fruit tissues. For example, comparisons between the pericarp of the homozygous *Crt*B+I line with its control, at different ripening stages, showed that the timing of carotenoid formation is altered in the *Crt*B+I line. From the breaker stage, the *Crt*B+I line contained significantly more β-carotene and less phytoene compared with AC, but lycopene levels are significantly greater in the *Crt*B+I line at the breaker + 3 d ripening stage (Figure 2). These changes in carotenoids reflect the timing of expression of the different promoters that regulate the *Crt*B and *Crt*I genes, the *Crt*I gene being under constitutive control and *Crt*B under ripening-specific promoter control (Atkinson et al., 1998). The constitutive presence of CRTI influenced the levels of β-carotene and phytoene from the breaker stage, while synthesis of CRTB later in the ripening process affected the level of lycopene. Another phenotype resulting from CRTB and CRTI was the intrafruit partitioning of carotenoids in the pericarp, jelly, and columella. The pericarp was the fruit compartment with the greatest capacity to store carotenoids (i.e., the highest levels), but the largest changes of lycopene in the *Crt*B line and β-carotene level in the *Crt*I and *Crt*B+I lines, were associated with the columella (Figure 3). This suggests that the accumulation of carotenoids in the tomato fruit depends
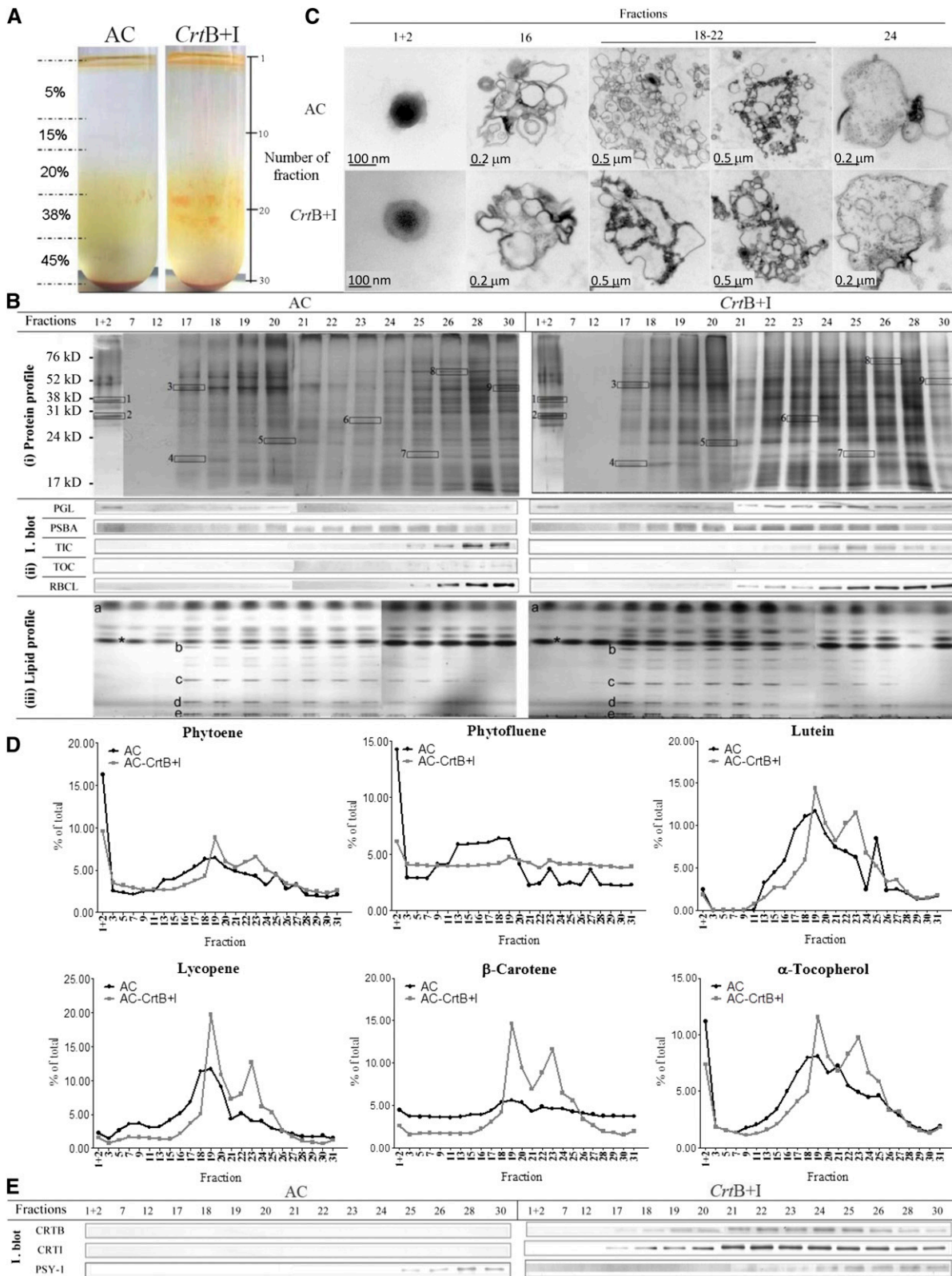
Figure 6. Subplastidial Carotenoid Sequestration in Response to Elevated Carotenoid Synthesis.

on several tissue-related factors, such as the type of cell, the composition and quantity of membranes, and the aqueous content of each tissue/cell type. Apparently, there is a saturation limit for a specific carotenoid in a given tissue and beyond that concentration, another region of the fruit must be used. In addition to the altered tissue distribution of carotenoids in the transgenic lines, structural differences of the chromoplasts were observed (Figure 5). The chromoplasts from the CrtB+I line were significantly larger (2.8-fold) and contained more membranes (previously described as thylakoid plexus in Spurr and Harris, 1968). The thylakoid plexus has also been identified in the chromoplast of ripe fruit of the high β-mutant of tomato (Harris and Spurr, 1969). The presence of the thylakoid-like membranes could allow a greater storage environment for the carotenoids. In CrtB+I, most of the plastoglobules were the same size as the control; however, some of them appeared to be larger and contained a possible crystal-like structure. Plastoglobules containing crystals have been reported in another Solanum species (Wrischer et al., 2007). Therefore, storing crystals of carotenoids in the plastoglobules of the CrtB+I chromoplasts is plausible. Membranous sacs in CrtB+I formed from the inner envelope of chromoplasts (Figure 6B). The hypothetical role of the membranous sacs is to store crystals of carotenoids (Egea et al., 2010). In conclusion, it would appear that the ultrastructure of the chromoplast adapts or responds to perturbations in carotenoid composition. This phenomenon has been observed previously (Fraser et al., 2009; Maass et al., 2009).

Metabolite profiling illustrated that, in addition to cellular changes, the expression of CrtB+I genes in the tomato fruit had effects across the metabolome (Table 3). The precise biochemical/molecular links with the increased sugars and amino acid levels, decreased organic acid levels, and altered carotenoids await further systematic analysis. However, it could be that perturbations in

fruit ripening via phytohormone imbalances have arisen. Such changes in sugars, amino acids, and organic acids have the potential to alter taste, which is an important consumer attribute. It is also feasible that the changes in leaf carotenoids affect source tissue metabolism, which then manifests itself in sink tissues. Further studies under different environmental conditions would be beneficial to clarify how the modifications can alter the plant's responses to abiotic stresses. Increased MGDG content (3.6-fold increase; Table 3) was determined in the transgenic line, especially the C16:0, C16:1 cis 9, and C18:1 fatty acid moieties of this complex lipid (see Supplemental Table 2 online). An associated increase of carotenoid and MGDG lipid (C16:0 and C18:3 fatty acids) levels was observed in a marine bacterium (Synechococcus sp) during high-light acclimation (Montero et al., 2012). It seems that the prokaryotic pool of MGDG (C16:0 plus C18:1, from plastids) is positively regulated in parallel with the carotenoid level in the CrtB+I line. MGDG is found in abundance in the inner envelope and in the thylakoid membranes of the chloroplast/chromoplast (Marechal et al., 1997). The reason for elevated MGDG in relation to carotenoid content could be explained by the fact that MGDG has a high propensity for interfacial curvature, allowing the membrane to adapt to a greater quantity of β-carotene (Szilágyi et al., 2007). In the transgenic line, it appears that this plasticity of the lipid is used to accommodate the extra carotenoid produced.

Carotenoid Sequestration Mechanisms Have Implications for Pathway Regulation

A comparison between subcompartments of the fruit chromoplasts from control and CrtB+I lines showed a number of important differences. First, an increased number of β-carotene and lycopene crystal-like structures arose in the thylakoid-like

---

Figure 6. (continued).

(A) Fractionation of subplastidial components of chromoplasts from AC (the wild type) and CrtB+I lines. Chromoplasts were extracted from 90 g of a mix of breaker + 3 to + 5 d tomatoes and then broken with a handheld potter and separated in a discontinuous gradient of 5, 15, 20, 38, and 45% Suc (weight per volume). Fractions of 1 mL were collected for further analysis. Typically, a total of 30 fractions were collected per centrifuge tube. Fractions from six replicates were used to achieve all the experiments showed in Figure 6B. Validation of subplastidial components using antibodies to biomarker proteins and analysis of lipid species.

(B) (i) Protein profile. Proteins, extracted from each fraction, were separated and visualized using SDS-PAGE followed by silver staining. Selected proteins were identified by nano-LC-MS-MS: 1, Plastoglobulin-1; 2, plastid lipid-associated protein CHRC; 3, ATP synthase subunit b; 4, photosystem I reaction center subunit II; 5, photosystem II 22-kD protein; 6, oxygen evolving enhancer protein 1; 7, oxygen evolving enhancer protein 2; 8, heat shock cognate 70-kD protein-1; 9, ribulose-1,5-bis-phosphate carboxylase/oxygenase large subunit binding protein subunit b. Details of the identification of these proteins are shown in Supplemental Figure 6 online. (ii) Immunoblot (I. blot). Immunolocalization of biomarker proteins in the fractions were determined by immunoblotting: plastoglobulin (PGL, 35 kD), photosystem II protein D1 (PSBA, 28 kD), TIC (45 kD), TOC (75 kD), and ribulose-1,5-bis-phosphate carboxylase/oxygenase large subunit (RBCL, 52 kD). (iii) Lipid profile. Lipids derived from the fractions were separated in a thin layer chromatography silica plate with a mixture of acetone:toluene:water (91:30:7). Standards for lipid species were used for identification: a, triglycerides; b, monogalactodiacylglycerol; c, digalactodiacylglycerol; d, phosphatidylethanolamine; e, phosphatidylserine/phosphatidylcholine; asterisk, contaminant.

(C) Ultrastructure component of isolated fractions. After collection, the fractions were dialyzed against PB and then fixed in osmium tetroxide.

(D) Carotenoids and α-tocopherol contents of the isolated fractions. Metabolites were extracted from each fraction and separated by liquid chromatography using a ultrahigh performance liquid chromatograph. The carotenoids and α-tocopherol were identified and quantified using calibration curves of standards. Contents are given as a percentage in a fraction compared with the total content in the tube.

(E) Localization of the heterologous phytoene synthase (CRTB, 38 kD) and phytoene desaturase (CRTI, 56 kD) enzymes and the endogenous phytoene synthase (PSY-1, 35 kD) enzyme within the subplastidial component of the AC and CrtB+I chromoplasts. Specific antibodies were used to immunodetect these enzymes in each collected fraction. Experiments were performed with the hemizygous CrtB+I line and a concurrent control.

[See online article for color version of this figure.]
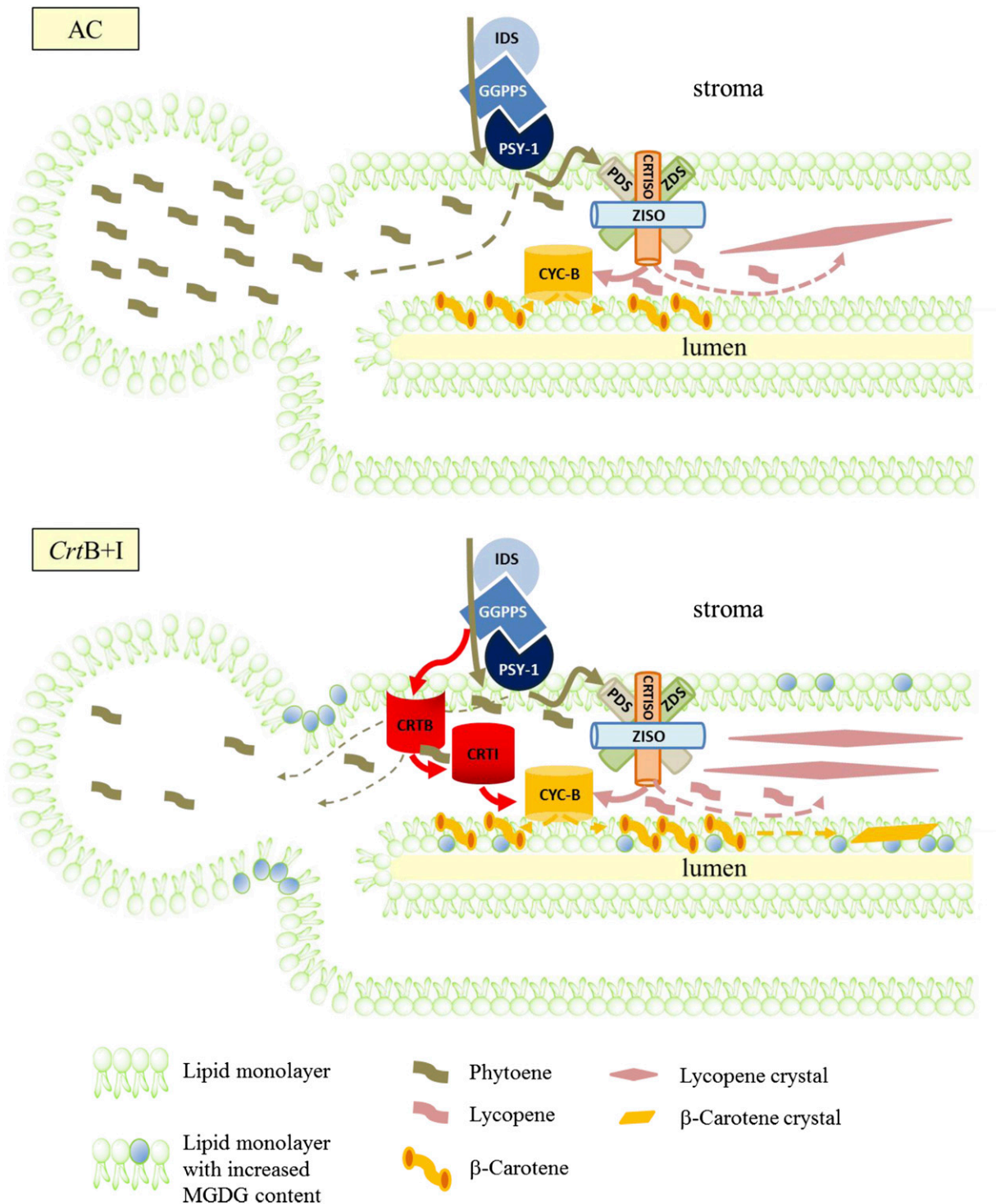
Figure 7. Schematic Representation of the Regulation of Carotenoid Production within the Thylakoid-Like Membranes of AC and *Crt*B+I Chromoplasts.

In the wild-type AC (top panel), the pool of phytoene, synthesized by PSY-1, can be used by PDS; however, at saturated levels, the excess phytoene appears to be sequestrated in the plastoglobules. Some lycopene and β-carotene are sequestrated in the thylakoid-like membranes and lycopene crystals are subsequently formed. In *Crt*B+I (bottom panel), the pool of phytoene is used by PDS and CRTI. Consequently, less phytoene is stored in the plastoglobules. A greater quantity of β-carotene and lycopene is created, leading to the formation of carotenoid crystals. Solid arrows represent a catalytic step; dashed arrows indicate movement of carotenoid. Changes in the galactolipid content of the membranes are also illustrated. IDS, isopentenyl diphosphate/dimethylallyl diphosphate isomerase; GGPPS, 1-geranylgeranyl pyrophosphate synthase; PSY-1, phytoene synthase-1; PDS,

membrane fractions of the *Crt*B+I line (Figure 6A). Storage of endogenous carotenoids in crystal-like structures has been reported in other plant species, such as mango (*Mangifera indica*) (Vasquez-Caicedo et al., 2006) and red papaya (*Carica papaya*) (Schweiggert et al., 2011) as well as in tomato (Rosso, 1967, 1968). It seems that this sequestration mechanism has been upregulated in the transgenic lines containing increased carotenoids. This phenomenon has also been observed in *Arabidopsis thaliana* and carrot (*Daucus carota*) roots (Maass et al., 2009) and embryogenic calli from citrus (Cao et al., 2012) overexpressing the phytoene synthase gene. Secondly, the membranes of the chromoplast (envelope and thylakoid-like membrane) also appeared to play an important role. The inner envelope of the *Crt*B+I chromoplasts seemed to be actively producing vesicles (membranous sacs), which were visible in the electron micrographs of the *Crt*B+I chromoplasts (Figure 5). The thylakoid-like membranes appeared in greater quantity and electron density in the *Crt*B+I chromoplasts compared with those in AC. The darker and thicker membranes could be caused by a high number of lipids, proteins, and carotenoids or complexes of these components. Harris and Spurr (1969) highlighted similar characteristics of chromoplasts of the tomato high β-mutant. They described invagination of the internal membrane of the plastid envelope and swollen grana and intergrana lamellae. CRTB and CRTI are found in the same submembrane compartment, which strengthens the hypothesis that they can interact with each other and have a synergistic effect on carotenoid production. However, PSY-1 was mainly found in the stroma, whereas its product phytoene was predominantly found in the membranes and in the plastoglobules. The location of PSY-1 within the chromoplasts confirmed results found in the literature (Fraser et al., 1994, 2002). The presence of phytoene in plastoglobules means that a significant quantity of the substrate for phytoene desaturase (and carotene formation) is partitioned away from the enzyme, possibly causing it to be metabolically inert, unless it is reincorporated into the membrane enzyme complex. Collectively, the data illustrate that synthesis and sequestration are two processes that are important for engineering carotenoids in plants, with the latter requiring further investigation. Only a few proteins have been identified with a potential link to the accumulation of carotenoids in plants, including the chromoplast-specific carotenoid-associated proteins (CHRC; Kilambi et al., 2013), the plastid-encoded acetyl CoA carboxylase D (Barsan et al., 2012), and the heat shock protein 21 (Neta-Sharir et al., 2005; Carvalho et al., 2012), while the *Or* gene in potato enhances carotenoid accumulation and stability (Li et al., 2012).

Plant Cells Adapt to Changes in Carotenoid Content at Multiple Levels

The characterization of transgenic lines with moderate increases in carotenoid levels has demonstrated the ability of the plant to adapt to changes in the homeostatic levels of carotenoid pigments.

Adaptation occurs across multiple levels of cellular regulation, including transcription, protein localization, metabolite cell/tissue type, and organelle/suborganelle structure/organization. Previous descriptions of regulatory mechanisms operating in the pathway have focused mainly on transcription and their response to developmental or environmental responses. This study also shows that the identity and level of carotenoids can trigger different regulatory mechanisms. Consequently, it implies that changes in levels of carotenoids can be sensed, causing signaling cascades that trigger adaptive mechanisms in the cell. Little is known about these sensors and signaling molecules, although *cis*-carotenes or *cis*-apocarotenoids have been proposed to act as signaling molecules (Kachanovsky et al., 2012) for the carotenoid pathway and the methylerythritol cyclodiphosphate, produced by the plastidial methylerythritol-4-phosphate pathway, has been shown to regulate the expression of nuclear stress response genes by retrograde signaling (Xiao et al., 2012). Further detailed knowledge of how the plant cell can sense, adapt, and modulate these changes is important for further exploitation of biodiversity and holistic engineering approaches.

Recently, there has been an increasing trend to create schematic representations relating to the plastid topology of carotenoid formation in the plastid. To date, these models are predominantly based on proteomic data (Barsan et al., 2012). However, valuable limitations do arise; for example, interrogating proteomic databases without implementing stringent parameters or validation procedures can lead to misleading identifications. Moreover, the expression of proteins with visualization tags, such as green fluorescent protein, could alter the protein conformation and/or the stoichiometric ratio of proteins within a complex or microenvironment of the membrane.

In this study, our perturbation of the system by transgenesis has enabled us to acquire valuable insight into the fundamental subplastidial organization of carotenoid synthesis and sequestration. From the experimental data, a model is presented in Figure 7. The wild-type state (AC) is illustrated with isopentenyl diphosphate isomerase, geranylgeranyl pyrophosphate synthase, and phytoene synthase(s) functioning as a metabolon for efficient channeling of precursors. This has been proven experimentally using biochemical approaches with the topology of the complex designated as membrane associated (Dogbo et al., 1988; Fraser et al., 2000). This study shows the presence of phytoene in the membrane and plastoglobule. Thus, the desaturase cannot completely use the phytoene synthesized or the delivery of the phytoene from the synthase to the desaturase is not a tethered process. Given that in green tissues no phytoene accumulates, it would appear that the desaturase is capable of converting phytoene efficiently. Thus, perhaps during the transition from chloroplast to chromoplast, the dismantling of the membrane structure affects the efficiency of the carotenoid biosynthetic pathway at the stroma–membrane juncture. The determination of phytoene in relatively high amounts in the

Figure 7. (continued).

phytoene desaturase; ZDS, ζ-carotene desaturase; Z-ISO, 15-*cis*-ζ-carotene isomerase; CRTISO, carotene isomerase; CYC-B, β-lycopene cyclase; CRTB, phytoene synthase; CRTI, phytoene desaturase.
[See online article for color version of this figure.]

plastoglobule suggests that the cell acts to remove excess phytoene accumulating in the membrane, presumably alleviating the potential damaging effects. In addition, the compartmentalization of enzymes is a well-documented regulatory process (Heinig et al., 2013); however, in this study, we introduce the partitioning of carotenoid precursors from their biosynthetic enzymes as another means of regulating pathway flux. The formation of β-carotene infers that the lycopene produced by the desaturase/isomerase complex can be used by the cyclase. However, the process would appear to be inefficient, with lycopene accumulating and crystalline structures arising. Concurrent analysis of the transgenic variety expressing CrtB and CrtI indicates that the bacterial phytoene synthase is membrane associated but can still synthesize and influence phytoene levels. Therefore, geranylgeranyl pyrophosphate must still be accessible. Although the procedure may not be optimal, it is still operational. The reduction in phytoene present in the membrane and plastoglobule suggests that the bacterial desaturase can act on the phytoene, providing further evidence that the phytoene is not efficiency channeled to desaturation. The interaction of the CRTI with the endogenous pathway has important fundamental implications, as it is the gene product that drives β-carotene production in Golden rice, a paradigm-changing resource of humanitarian benefit (Beyer, 2010). The increased β-carotene content in the presence of the bacterial desaturase indicates that the pool of lycopene generated by the nonendogenous enzymes is more accessible to the endogenous β-cyclase than the lycopene produced by the endogenous desaturase/isomerase complex. Adaptation of the membrane to accommodate these increases in β-carotene and-lycopene arises via the modulation of MGDG content.

Despite modification of the membrane, it would appear that, at a certain concentration, carotenoid will crystallize. Presumably, storage of carotenoids in this manner makes them metabolically and osmotically inert and probably less prone to oxidative degradation than in solution. However, in this state, it is unlikely that carotenoids can be used by carotenoid cleavage dioxygenases. Shumskaya and Wurtzel (2013) proposed that carotenoid is resolubilized and transported to the outer envelope. This seems unlikely in tomato. It is more likely that the carotenoid cleavage dioxygenases act on the carotenoid in the membrane/or plastoglobule prior to crystallization. The molar ratios between carotenoid and derived volatiles also suggest this pattern of events, as the carotenoid content is at least two orders of magnitude more than the volatiles.

In conclusion, the use of transgenesis to modulate the carotenoid pathway has revealed important regulatory mechanisms: (1) how pathway transcription can respond to perturbations in pathway metabolites, (2) how altering the partition of precursors from the biosynthetic enzymes on a subplastid level can modulate pathway flux, and (3) how metabolite composition can direct cellular structures. The latter has a generic implication to all engineering approaches across genera, as it illustrates the need for concurrent sequestration/deposition with pathway engineering.

METHODS

Plant Material and Cultivation

The control (AC) variety of tomato (*Solanum lycopersicum*) had been previously transformed with the *Crt*B construct (Fraser et al., 2002), the

*Crt*I construct (Römer et al., 2000), and the *Crt*E construct, which corresponds to the *Crt*B vector only with the *Crt*E gene from *Pantoea ananatis* (D90087.2) using the *Agrobacterium tumefaciens* strain LBA 4404. The lines were crossed by cross pollination using a small paintbrush. The plants were greenhouse grown (25°C day/15°C night) with supplementary lighting (6-h light/8-h dark). Three plants each of three to four separate cross-pollination events were grown for each transgenic line concurrently with AC.

Confirmation of Gene's Presence by PCR

The *Crt* genes in the crossed lines were detected by PCR, using the set of primers shown in the Supplemental Table 4 online. PCR reactions were performed using Illustra puReTaq Ready-to-Go PCR beads (GE Healthcare), with reagents prepared to the manufacturer's guidelines. Reactions contained 10 pmol each of the respective template's forward (5′3′) and reverse (3′5′) primers and 50 ng of genomic DNA. Tubes were incubated at 95°C for 5 min to denature the template before 30 cycles of PCR amplification (denaturation 94°C for 30 s, annealing 50°C for 30 s, and extension 72°C for 30 s). A final incubation of 5 min at 72°C completed the reaction. Reactions were performed using a Techgene thermo cycler (Techne). PCR products were analyzed by agarose gel electrophoresis.

Determination of the *Crt*B+I Homozygous Line

The *Crt*B+I homozygous line was screened by real-time PCR. The *Crt*B and *Crt*I genes in the potential *Crt*B+I homozygous lines were quantified and compared to the same genes in known hemizygous and homozygous lines and normalized to *Pds*. The Δ-Δ cycle threshold method was used to calculate the ratios. Three young leaves (±3-cm long) from three independent plants of the same line were harvested, pooled, and frozen in liquid nitrogen. Leaf material was homogenized using a Tissue Lyser LT (Qiagen) for 1 min at 50 Hz, while keeping the samples frozen. DNA was extracted from leaf powder (100 mg) using the DNeasy reagents and protocol (Qiagen). The QuantiFast SYBR Green PCR kit (Qiagen) was used to quantify the gene of interest using a 25-ng sample of DNA. Primers were added to a final concentration of 1 μM in a reaction volume of 20 μL. Reactions were performed on a Rotor-Gene 3000 thermocycler (Qiagen). Thermocycling conditions were 95°C for 15 min followed by 40 cycles of 15 s at 94°C, 30 s at 50°C, and 15 s at 72°C. Melt curve analysis verified the reactions' specificity. For quantification, calibration curves were run simultaneously, using actin as a housekeeping gene to normalize the data.

Measurement of Gene Expression by Real-Time Quantitative RT- PCR

Measurement of expression by real-time quantitative RT-PCR was performed as described by Enfissi et al. (2010) and using the primers reported in Supplemental Table 4 online.

Extraction and Analysis of Metabolites

Carotenoids, tocopherols, chlorophylls, and lipids were extracted from freeze-dried fruit and leaf tissue. Extractions were made from sample powder (15 mg) in 1.5-mL centrifuge tubes. Metabolites were extracted by the addition of chloroform and methanol (2:1). Samples were stored for 20 min on ice. Subsequently, water (1 volume) was added. Samples were centrifuged for 5 min at top speed in a Heraeus Pico21 centrifuge (Thermo Scientific). The organic phase, containing the pigment extract, was placed in a fresh centrifuge tube, and the aqueous phase was reextracted with chloroform (×2 by volume). Organic phases were pooled and dried using the Genevac EZ.27. Dried samples were stored at −20°C and resuspended in ethyl acetate prior to spectrophotometric and chromatographic analysis.

Total carotenoids and chlorophyll *a* and *b* were determined spectrophotometrically, as described by Wellburn (1994).

Chromatographic Analysis

Carotenoids were separated and identified by ultrahigh performance liquid chromatography with photodiode array detection. An Acquity ultrahigh performance liquid chromatography system (Waters) was used with an Ethylene Bridged Hybrid (BEH C18) column (2.1×100 mm, 1.7 μm) with a BEH C18 VanGuard precolumn (2.1×50 mm, 1.7 μm). The mobile phase used was A, methanol/water (50/50), and B, acetonitrile (ACN)/ethyl acetate (75:25). All solvents used were HPLC grade and filtered prior to use through a 0.2-μm filter. The gradient was 30% A:70% B for 0.5 min and then stepped to 0.1% A:99.9% B for 5.5 min and then to 30% A:70% B for the last 2 min. Column temperature was maintained at 30°C and the temperature of samples at 8°C. Online scanning across the UV/visible range was performed in a continuous manner from 250 to 600 nm, using an extended wavelength photo diode array detector (Waters). Carotenoids were quantified from dose–response curves. The HPLC separation, detection, and quantification of carotenoids, tocopherols, and chlorophylls have been described in detail previously (Fraser et al., 2000).

Lipid Analysis

Lipids were analyzed on high-performance thin layer chromatography silica gel 60 F_{254} plates (Merck) using a solvent system of acetone/toluene/water (91:30:7). They were visualized with iodine vapor and identified by cochromatography with lipids of known composition. For quantitative analysis, individual lipids were isolated from thin layer chromatography plates and extracted in chloroform/methanol (1:1). Then, 50 μg of internal standard (myristic acid D27) was added to the extract prior to drying. To transmethylate the lipids, the samples were resuspended in hexane (2 mL) and methanol (4 mL) plus 1% sulfuric acid and incubated at 85°C for 2 h. Two milliliters of hexane and 1 mL of water plus 5% KCl were then added. The hexane phase was dried and resuspended in 20 μL of methanol for quantification by gas chromatography–mass spectrometry, as described below.

Extraction, Derivatization, and Gas Chromatography–Mass Spectrometry Analysis

Extraction and analysis of polar metabolites was performed as described previously (Enfissi et al., 2010; Jones et al., 2012), with slight modifications. Freeze-dried powder (10 mg) was extracted in methanol (400 μL)/water (400 μL)/chloroform (800 μL). An aliquot (20 μL) was removed from the extract, the internal standard (ribitol, 10 μg) was added to the aliquot, and the samples were dried. Six extractions were performed on each biological replicate. Derivatization was performed by the addition of methoxyamine hydrochloride (30 μL; Sigma-Aldrich) at 20 mg/mL, in pyridine. Samples were incubated at 40°C for 1 h, after which *N*-methyl-*N*-trimethylsilyltrifluoroacetamide (Sigma-Aldrich; 70 μL) was added and the samples incubated for 2 h at 40°C before analysis. Gas chromatography–mass spectrometry was performed as described previously (Enfissi et al., 2010), using a 20:1 split injector. To identify chromatogram components found in the tomato profiles, a mass spectral (MS) library was constructed from in-house standards, as well as the NIST08 MS library. Retention time calibration was performed on all standards to facilitate the determination of retention indices. Using the retention indices and MS, identification was performed by comparison with the MS library. Relative quantification to the internal standard was performed.

Subcellular Fractionation and Cellular Analysis

Electron Microscopy of Intact Chromoplasts

Tomato fruit was cut into 2-mm cubes using a new sharp razor blade in a drop of cold fixative (2.5% glutaraldehyde in 100 mM sodium cacodylate buffer [CAB], pH 7.2) on dental wax. Pieces of tissue were transferred into a glass vial (with a cocktail stick) containing cold fixative (~2 mL). Lids were placed on the vials and tissue was fixed in the fridge (4°C) overnight. Tissue was washed in CAB (2×10 min) and then postfixed in 1% osmium tetroxide in CAB for 1 h at room temp (20°C). Tissue was washed (2×10) min in milliQ water. Tissue was then dehydrated in increasing concentrations of ethanol as follows: 50, 70, and 90% (10 min) and $3 \times 100\%$ (15 min). Tissue was then washed (3×10 min) in the transition solvent propylene oxide. Tissue was then transferred into 50% propylene oxide and 50% agar low-viscosity resin (Agar Scientific) for 30 min. Tissue was then placed in 100% agar low-viscosity resin (2×1.5 h) with a vacuum applied four times during the incubation. Tissue pieces were then placed in labeled silicone molds and polymerized in the oven (60°C) for 24 h. Polymerized blocks were sectioned (70 nm) on a RMC MTXL ultramicrotome, and sections were collected on 400 mesh copper grids. Sections were counterstained with 4.5% uranyl acetate in 1% acetic acid for 45 min and Reynolds lead citrate for 7 min. Sections were viewed in a Jeol 1230 transmission electron microscope with an accelerating voltage of 80 kV. Images were recorded with a Gatan digital camera. The images shown in Figure 5 are representative of three biological replicates for each line, from which 12 sections where taken per biological replicate. Volumes of chromoplasts were measured using ImageJ software.

Electron Microscopy of Subplastidial Components of Chromoplasts

Two previous methods were combined (De Camilli et al., 1983; Angaman et al., 2012). Subchromoplast fractions were pelleted in a microfuge tube and fixed in 2.5% glutaraldehyde in 100 mM phosphate buffer (PB), pH 7.4, for 1 h at room temperature. Fixed subchromoplast components were pelleted in a microfuge and washed (2×10 min) in PB. After the final wash, components were resuspended in PB (100 μL). Aliquots (100 μL) of fixed component were added to tubes immersed in a 54°C water bath. After a 15-s interval, which allowed the suspension to warm up, 100 μL of a solution (at 54°C) containing 3% agarose in 5 mM PB was added to the subchromoplast suspension. The suspension obtained was quickly mixed, while still immersed in the warm water bath, by forcing it up and down through a Pasteur pipette prewarmed in a 60°C oven. Care was taken to prevent foaming. Immediately afterwards, the agarose-subchromoplast suspension was transferred by pipetting into a frame made from two glass slides separated by a shaped acetate gasket and held together by bull dog clips. The frame had also been prewarmed in a 60°C oven. The agarose mixture was then allowed to cool and solidify. At this point, the two glass slides were separated, and the agarose gel, attached to one of the glass slides, was cut into 2-mm squares with a razorblade. The gel squares were then washed off the glass slide into a Petri dish by a stream of 0.1% Alcian blue in 1% acetic acid from a Pasteur pipette. These agarose squares were then transferred to glass vials and washed (2×10 min) in PB to remove stain. The Alcian blue stain made the agarose squares visible and aided subsequent processing and resin embedding. Samples were postfixed in 1% OsO_4 containing potassium ferricyanide (0.8%) in the same PB for 1 h at room temperature. Then, after three washes in milliQ water, transmission electron microscopy was performed as described. Fractions from three technical replicates, which correspond to the mix of ~10 tomatoes, were fixed and photographed. The procedures were repeated independently at least three times. With each *Crt*B+I preparation, an AC control preparation was also performed concurrently and comparative cellular analysis performed.

SUBCELLULAR FRACTIONATION OF CHROMOPLASTS

SYSTEM 1. All procedures were performed at 4°C. Approximately 10 fresh tomatoes (Breaker + 3 to 5 d) were harvested and the pericarp was cut into 1-cm^2 pieces (80 to 150 g) and stored at 4°C overnight. Tomato tissue was added to extraction buffer (0.4 M Suc, 50 mM Tris, pH 7.8, 1 mM EDTA, and 1 mM DTT) and homogenized for 2×3 s in a Waring blender. The

homogenate was filtered through four layers of muslin. Extraction buffer was added to the filtrate in a 500-mL centrifuge tube. Tubes were centrifuged for 10 min at 5000g in a Sorvall RC5C centrifuge (Thermo Scientific) with a GSA-3 rotor. The supernatant was discarded, and the pellet was resuspended in extraction buffer and transferred into 50-mL centrifuge tubes. The tubes were centrifuged for 10 min at 9000g with a GSA-5 rotor. The supernatant was discarded. Pellets were resuspended in 45% Suc buffer (45% [w/v] Suc, 50 mM Tricine, 2 mM EDTA, 2 mM DTT, and 5 mM sodium bisulphite, pH 7.9; 3 mL). The chromoplasts were physically broken using a handheld potter homogenizer (10 times). The solution was then resuspended in 45% Suc buffer (5 mL), and the 8 mL was placed in a 38.5-mL Ultra-Clear centrifuge tube (Beckmann Coulter). Subsequently, other layers of discontinuous Suc gradient were overlaid, consisting of 38% Suc buffer (6 mL), then 20% Suc buffer (6 mL), 15% Suc buffer (4 mL), and 5% Suc buffer (8 mL). Gradients were centrifuged for 17 h at 100,000g and 4°C, using an L7 ultracentrifuge with an SW28 swing out rotor (Beckman Coulter). Fractions (1 mL) were collected, from the top of the gradients using a Minipuls 3 peristaltic pump and FC203B fraction collector (Gilson). Samples were dialyzed overnight against PB (50 mM, pH 7.5) for electron microscopy analysis.

SYSTEM 2. Chromoplasts were isolated as in system 1. However, instead of resuspending the pellets obtained after the centrifugation step at 9000g, they were resuspended in 0.6 M Suc buffer (0.6 M Suc, 50 mM Tris, 1 mM DTT, and 1 mM EDTA, pH 7.8; 3 mL) and homogenized using a handheld potter homogenizer to break the chromoplasts. The solution was then resuspended in 0.6 M Suc buffer to a final volume of 35 mL in 38.5-mL Ultra-Clear centrifuge tubes (Beckmann Coulter). Tubes were centrifuged for 1 h at 100,000g and 4°C, using an L7 ultracentrifuge with an SW28 swing-out rotor (Beckman Coulter). The red supernatants, which correspond to the chromoplast crystals and plastoglobules, were transferred into Eppendorf tubes and stored at −20°C. The pellets were resuspended in 45% Suc buffer (8 mL) and placed in a 38.5-mL Ultra-Clear centrifuge tube (Beckmann Coulter). The same gradient as that used in system 1 was created; subsequently, the same protocol followed as for the system 1. The two systems are represented in Supplemental Figure 5 online.

ISOLATION OF DIFFERENT TYPES OF CHROMOPLASTS

SYSTEM 3. Chromoplast extraction was undertaken in a cold room at 4°C. Fresh tomato fruits (200 g) were harvested from selected plants, cut into pieces of ~1 cm^2, covered in foil, and stored at 4°C overnight to reduce starch content. Tomato tissue was homogenized in prechilled chromoplast buffer A (100 mM Tris-HCl, pH 8.2, 0.33 M sorbitol, 2 mM MgCl$_2$, 10 mM KCl, 8 mM EDTA, 10 mM ascorbic acid, 5 mM L-Cys, 1 mM phenylmethylsulfonyl fluoride, 1% polyvinylpyrrolidone, and 1 mM DTT), twice for 3 s in a small laboratory blender (Waring Products). The resulting slurry was filtered through four layers of muslin cloth and the liquid decanted into a 500-mL screw cap centrifuge tube. Subsequently, tubes were centrifuged for 15 min at 5000g and 4°C in a Sorval RC5C centrifuge (Thermo Scientific) with a GSA-3 rotor. The supernatants were discarded. The pellets were resuspended in buffer B (buffer A without polyvinylpyrrolidone) and transferred into 50-mL centrifuge tubes. The tubes were centrifuged for 15 min at 5000g and 4°C with the GSA-5 rotor. The supernatants were discarded. The pellets were resuspended in 4 mL of buffer B. In 38.5-mL Ultra-Clear centrifuge tubes, a discontinuous Suc gradient (Suc [w/v] in 50 mM Tris-HCl, pH 7.4, supplemented with 1 mM DTT) with the following steps was constituted: 50% (9 mL), 40% (7 mL), 30% (7 mL), and 15% (7 mL) of Suc. The chromoplast solutions (4 mL) were placed on top of the gradients. Gradients were centrifuged for 1 h at 100,000g and 4°C, using an L7 ultracentrifuge with an SW28 swing-out rotor (Beckman Coulter). The chromoplast fractions were recovered with a Pasteur pipette in an Eppendorf tube, washed in 1 volume of buffer B followed by centrifugation at 6000g for 10 min. The supernatants were discarded and the pellets of chromoplasts kept at −20°C.

Protein Analysis

Extraction, separation, immunodetection, and liquid chromatography–mass spectrometry (LC-MS) analysis of proteins were performed following the protocols of Robertson et al. (2012) and Mora et al. (2013).

Extraction, Separation (SDS-PAGE), and LC-MS Analysis of Proteins

Proteins contained in the subplastidial fractions were precipitated with methanol and resuspended in sample buffer solution (0.5 M Tris-HCl, pH 6.8, 10% [v/v] glycerol, 10% [w/v] SDS, 1.4% [v/v] β-mercaptoethanol, and 0.05% [w/v] bromophenol blue). After a heat denaturation step at 95°C for 4 min, a volume of 5 µL of this solution was loaded into a 12.5% acrylamide gel (Laemmli, 1970). The ProteoSilver Silver Stain kit (Sigma-Aldrich) was used to develop the gel after running at 80 V. High-range rainbow molecular weight marker (RPN756E) from GE Healthcare Life Sciences was used.

IN-GEL DIGESTION OF PROTEIN BAND

Stained bands corresponding to the protein of interest were excised using a scalpel and cut into 1 mm^3 and then introduced in centrifuge tubes (0.5 mL) and washed three times for 10 min with 50 mM ammonium bicarbonate, pH 8.0 (50 µL). After that, gel pieces were dried three times with ACN (50 µL) for 10 min. Once the gel pieces shrank and turned opaque, 12.5 ng/µL of trypsin (10 µL) dissolved in 50 mM ammonium bicarbonate, pH 8.0, was added. An additional 15 µL of 50 mM ammonium bicarbonate was added to each tube in order to cover the gel pieces. The tubes were incubated at 37°C overnight, and the supernatant was transferred to a clean Eppendorf tube. Tryptic peptides were sequentially extracted with 25 µL of ACN/water (50:50, v/v) with 0.1% (v/v) trifluoroacetic acid, while sonicating for 10 min (two times). The peptide extracts were combined and dried in a GeneVac Ez-2 Plus rotary evaporator and reconstituted in 5 µL of 0.1% (v/v) trifluoroacetic acid. The peptide samples were cleaned with ZipTip C18 (Millipore) prior to the nano–liquid chromatography–tandem mass spectrometry (nano-LC-MS-MS) analysis, and peptides were eluted with 10 µL of water:ACN (50:50, v/v) with 0.1% (v/v) formic acid.

NANO-LC-MS-MS CONDITIONS

The nano-LC-MS-MS analysis was performed in an Ultimate 3000 rapid separation liquid chromatography nanosystem from Dionex (Thermo Fisher Scientific) coupled to an AmaZon ETD ion-trap mass spectrometer equipped with a nanoelectrospray ionization source (Bruker Daltonik).

Twenty microliters of loading buffer (water:ACN [98:2, v/v] with 0.1% [v/v] formic acid) was added to the sample, and 2 µL was injected into the LC-MS system using the autosampler. Sample was preconcentrated on a Dionex Acclaim PepMap 100 column (100 µm × 2 cm, C18, 5 µm, 100Å) (Dionex, LC Packings) at a flow rate of 4 µL/min and using 0.1% of trifluoroacetic acid as mobile phase. After 3 min of preconcentration, the trap column was automatically switched in-line with a Dionex Acclaim PepMap rapid separation liquid chromatography nanocolumn (75 µm × 15 cm, C18, 2 µm, 100Å) (Dionex, LC Packings). Mobile phases consisted of solvent A, containing 0.1% (v/v) formic acid in water, and solvent B, containing 0.1% (v/v) formic acid in 100% ACN. Chromatographic conditions were a linear gradient from 95 to 60% (v/v) solvent A in 45 min at a flow rate of 0.250 µL/min at 30°C.

The column outlet was directly coupled to a nanoelectrospray ion source. The positive mass spectrum was recorded for a mass-to-charge ratio range of 300 to 2000 followed by MS-MS scans of the three most intense peaks. Typical ion spray voltage was in the range of 2.5 to 3.0 kV, and nitrogen was used as the collision gas. The ion trap was used in ultrascan mode with a maximum accumulation time of 200 ms and an average of 5. Other source parameters and spray positions were optimized with a tryptic digest of BSA protein.

Automated spectral processing and peak list generation were performed using Mascot Distiller v2.4.2.0 software (Matrix Science). The database search was done through Mascot Daemon software in combination with the Mascot interface 2.2 (Matrix Science). Regarding searching parameters, Mascot searches were done with no enzymatic specificity and a peptide tolerance on the mass measurement of 100 ppm and 0.6 Da for MS-MS ions. Carbamidomethylation and oxidation of Met were used as variable modifications. Identification of the protein origin of the identified peptides was done using the UniProt protein database. BLAST was used as a basic local alignment search tool to find regions of local similarity between the identified proteins and the protein sequences of tomato (http://blast.ncbi.nlm.nih.gov/Blast.cgi).

Immunodetection by Immunoblot Analysis

Proteins were separated by SDS-PAGE (12.5%) for 3 h at a constant current of 80 mA. Proteins were transferred onto polyvinylidene difluoride membranes, and immunodetection was performed as described by Fraser et al. (1994).

Statistical Analysis

A minimum of three biological and three technical replicates were analyzed for every experiment unless stated otherwise. Metabolite levels from the different technology platforms were combined. Principal component analysis was performed on these data matrices. SIMCA-P+ software v. 13.0.2 (Umetrics) was used to carry out and display clusters derived from the principal component analysis. GraphPadPrism software v.5 (GraphPad Software) or Excel (Microsoft) embedded algorithms were used to perform Student's t tests or Dunnett's test to determine significant differences between the transgenic lines and the control AC. Where appropriate, P < 0.05, P < 0.01, and P < 0.001 are indicated by one asterisk, two asterisks, and three asterisks, respectively.

Accession Numbers

Sequence data from this article can be found in the GenBank/EMBL databases under the following accession numbers: *Ggpps*-1: DQ267902; *Ggpps*-2: SGNU223568; *Psy*-1: Y00521; *Psy*-2: L23424; *Pds*, X59948; ζ-carotene desaturase, AF195507; carotene isomerase, AF416727; ε-lycopene cyclase, Y14387; *Lcy*-B, AF254793; fruit-specific β-lycopene cyclase, Y18297; *Crt*R-b1, Y14809; *Crt*R-b2, DQ864755; *Zep*-1: Z83835.1; *Crt*E, *Crt*B, and *Crt*I, D90087.2.

Supplemental Data

The following materials are available in the online version of this article.

  Supplemental Figure 1. PCR Confirmation of the Presence of *Crt*E and *Crt*I Genes in the *Crt*E+I Lines.

  Supplemental Figure 2. Chromatographic Profiles of Carotenoids, Chlorophylls, and α-Tocopherol of AC and *Crt*B+I Tomatoes.

  Supplemental Figure 3. Separation of Chromoplast Types on a Sucrose Gradient.

  Supplemental Figure 4. Principal Component Analysis of All Metabolites Detected in AC and *Crt*B+I Tomato Lines.

  Supplemental Figure 5. Schematic Representation of the Systems (1 and 2) Used to Fractionate Chromoplasts and Isolate Their Respective Submembrane Compartments.

  Supplemental Figure 6. Evidence and Importance of the Carotenoid Crystals Embedded in the Chromoplast Membranes.

  Supplemental Table 1. Carotenoid Content in the Pericarp, Jelly, and Columella Tissues of Ripe Fruit Derived from the Genetic Crosses Containing Different Gene Combinations.

  Supplemental Table 2. Changes in the Composition (in Percentage) of Fatty Acids Present in the Lipids Species Found in *Crt*B+I and Control AC.

  Supplemental Table 3. Identification of Proteins from the Isolated Fractions by nESI-LC-MS-MS.

  Supplemental Table 4. Sequences of Primers Used in Real-Time PCR and PCR.

AUTHOR CONTRIBUTIONS

M.N., L.M., P.D.F., and E.M.A.E. performed the experiments. P.D.F., M.N., E.M.A.E., and P.M.B. designed the research program. M.N., P.D.F., P.M.B., and L.M. wrote the article. P.D.F. acquired the funding.

REFERENCES

Angaman, D.M., Petrizzo, R., Hernández-Gras, F., Romero-Segura, C., Pateraki, I., Busquets, M., and Boronat, A. (2012). Precursor uptake assays and metabolic analyses in isolated tomato fruit chromoplasts. Plant Methods **8:** 1.

Atkinson, R.G., Bolitho, K.M., Wright, M.A., Iturriagagoitia-Bueno, T., Reid, S.J., and Ross, G.S. (1998). Apple ACC-oxidase and polygalacturonase: Ripening-specific gene expression and promoter analysis in transgenic tomato. Plant Mol. Biol. **38:** 449–460.

Auldridge, M.E., McCarty, D.R., and Klee, H.J. (2006). Plant carotenoid cleavage oxygenases and their apocarotenoid products. Curr. Opin. Plant Biol. **9:** 315–321.

Barsan, C., Zouine, M., Maza, E., Bian, W.P., Egea, I., Rossignol, M., Bouyssie, D., Pichereaux, C., Purgatto, E., Bouzayen, M., Latché, A., and Pech, J.C. (2012). Proteomic analysis of chloroplast-to-chromoplast transition in tomato reveals metabolic shifts coupled with disrupted thylakoid biogenesis machinery and elevated energy-production components. Plant Physiol. **160:** 708–725.

Beyer, P. (2010). Golden Rice and 'Golden' crops for human nutrition. New Biotechnol. **27:** 478–481.

Cao, H., Zhang, J., Xu, J., Ye, J., Yun, Z., Xu, Q., Xu, J., and Deng, X. (2012). Comprehending crystalline β-carotene accumulation by comparing engineered cell models and the natural carotenoid-rich system of citrus. J. Exp. Bot. **63:** 4403–4417.

Carvalho, L.J.C.B., Lippolis, J., Chen, S., Batista de Souza, C.R., Vieira, E.A., and Anderson, J.V. (2012). Characterization of

carotenoid-protein complexes and gene expression analysis associated with carotenoid sequestration in pigmented cassava (*Manihot esculenta* Crantz) storage root. The Open Biochem. J. **6:** 116–130.

Dall'Osto, L., Fiore, A., Cazzaniga, S., Giuliano, G., and Bassi, R. (2007). Different roles of alpha- and beta-branch xanthophylls in photosystem assembly and photoprotection. J. Biol. Chem. **282:** 35056–35068.

De Camilli, P., Harris, S.M., Jr., Huttner, W.B., and Greengard, P. (1983). Synapsin I (Protein I), a nerve terminal-specific phosphoprotein. II. Its specific association with synaptic vesicles demonstrated by immunocytochemistry in agarose-embedded synaptosomes. J. Cell Biol. **96:** 1355–1373.

Demmig-Adams, B., and Adams, W.W., III., (2002). Antioxidants in photosynthesis and human nutrition. Science **298:** 2149–2153.

Diretto, G., Al-Babili, S., Tavazza, R., Papacchioli, V., Beyer, P., and Giuliano, G. (2007). Metabolic engineering of potato carotenoid content through tuber-specific overexpression of a bacterial mini-pathway. PLoS ONE **2:** e350.

Dogbo, O., Laferriére, A., D'Harlingue, A., and Camara, B. (1988). Carotenoid biosynthesis: Isolation and characterization of a bifunctional enzyme catalyzing the synthesis of phytoene. Proc. Natl. Acad. Sci. USA **85:** 7054–7058.

Egea, I., Barsan, C., Bian, W.P., Purgatto, E., Latché, A., Chervin, C., Bouzayen, M., and Pech, J.C. (2010). Chromoplast differentiation: Current status and perspectives. Plant Cell Physiol. **51:** 1601–1611.

Enfissi, E., et al (2010). Integrative transcript and metabolite analysis of nutritionally enhanced DE-ETIOLATED1 downregulated tomato fruit. Plant Cell **22:** 1190–1215.

Fraser, P.D., and Bramley, P.M. (2004). The biosynthesis and nutritional uses of carotenoids. Prog. Lipid Res. **43:** 228–265.

Fraser, P.D., Enfissi, E.M., and Bramley, P.M. (2009). Genetic engineering of carotenoid formation in tomato fruit and the potential application of systems and synthetic biology approaches. Arch. Biochem. Biophys. **483:** 196–204.

Fraser, P.D., Romer, S., Shipton, C.A., Mills, P.B., Kiano, J.W., Misawa, N., Drake, R.G., Schuch, W., and Bramley, P.M. (2002). Evaluation of transgenic tomato plants expressing an additional phytoene synthase in a fruit-specific manner. Proc. Natl. Acad. Sci. USA **99:** 1092–1097.

Fraser, P.D., Schuch, W., and Bramley, P.M. (2000). Phytoene synthase from tomato (*Lycopersicon esculentum*) chloroplasts—Partial purification and biochemical properties. Planta **211:** 361–369.

Fraser, P.D., Truesdale, M.R., Bird, C.R., Schuch, W., and Bramley, P.M. (1994). Carotenoid biosynthesis during tomato fruit development (evidence for tissue-specific gene expression). Plant Physiol. **105:** 405–413.

Harris, W.M., and Spurr, A.R. (1969). Chromoplasts of tomato fruits. II. The red tomato. Am. J. Bot. **56:** 380–389.

Heinig, U., Gutensohn, M., Dudareva, N., and Aharoni, A. (2013). The challenges of cellular compartmentalization in plant metabolic engineering. Curr. Opin. Biotechnol. **24:** 239–246.

Hirschberg, J. (2001). Carotenoid biosynthesis in flowering plants. Curr. Opin. Plant Biol. **4:** 210–218.

Jones, M.O., Piron-Prunier, F., Marcel, F., Piednoir-Barbeau, E., Alsadon, A.A., Wahb-Allah, M.A., Al-Doss, A.A., Bowler, C., Bramley, P.M., Fraser, P.D., and Bendahmane, A. (2012). Characterisation of alleles of tomato light signalling genes generated by TILLING. Phytochemistry **79:** 78–86.

Kachanovsky, D.E., Filler, S., Isaacson, T., and Hirschberg, J. (2012). Epistasis in tomato color mutations involves regulation of phytoene synthase 1 expression by cis-carotenoids. Proc. Natl. Acad. Sci. USA **109:** 19021–19026.

Kilambi, H.V., Kumar, R., Sharma, R., and Sreelakshmi, Y. (2013). Chromoplast-specific carotenoid-associated protein appears to be important for enhanced accumulation of carotenoids in *hp1* tomato fruits. Plant Physiol. **161:** 2085–2101.

Ko, K., Bornemisza, O., Kourtz, L., Ko, Z.W., Plaxton, W.C., and Cashmore, A.R. (1992). Isolation and characterization of a cDNA clone encoding a cognate 70-kDa heat shock protein of the chloroplast envelope. J. Biol. Chem. **267:** 2986–2993.

Krinsky, N.I., and Johnson, E.J. (2005). Carotenoid actions and their relation to health and disease. Mol. Aspects Med. **26:** 459–516.

Laemmli, U.K. (1970). Cleavage of structural proteins during the assembly of the head of bacteriophage T4. Nature **227:** 680–685.

Li, L., Yang, Y., Xu, Q., Owsiany, K., Welsch, R., Chitchumroonchokchai, C., Lu, S., Van Eck, J., Deng, X.X., Failla, M., and Thannhauser, T.W. (2012). The *Or* gene enhances carotenoid accumulation and stability during post-harvest storage of potato tubers. Mol. Plant **5:** 339–352.

Maass, D., Arango, J., Wüst, F., Beyer, P., and Welsch, R. (2009). Carotenoid crystal formation in *Arabidopsis* and carrot roots caused by increased phytoene synthase protein levels. PLoS ONE **4:** e6373.

Marechal, E., Block, M.A., Dorne, A.J., Douce, R., and Joyard, J. (1997). Lipid synthesis and metabolism in the plastid envelope. Physiol. Plant. **100:** 65–77.

Misawa, N., Masamoto, K., Hori, T., Ohtani, T., Boger, P., and Sandmann, G. (1994). Expression of an erwinia phytoene desaturase gene not only confers multiple resistance to herbicides interfering with carotenoid biosynthesis but also alters xanthophyll metabolism in transgenic plants. Plant J. **6:** 481–489.

Misawa, N., Nakagawa, M., Kobayashi, K., Yamano, S., Izawa, Y., Nakamura, K., and Harashima, K. (1990). Elucidation of the *Erwinia uredovora* carotenoid biosynthetic pathway by functional analysis of gene products expressed in *Escherichia coli*. J. Bacteriol. **172:** 6704–6712.

Misawa, N., Yamano, S., and Ikenaga, H. (1991). Production of beta-carotene in *Zymomonas mobilis* and *Agrobacterium tumefaciens* by introduction of the biosynthesis genes from *Erwinia uredovora*. Appl. Environ. Microbiol. **57:** 1847–1849.

Montero, O., Sánchez-Guijo, A., Lubián, L.M., and Martínez-Rodríguez, G. (2012). Changes in membrane lipids and carotenoids during light acclimation in a marine cyanobacterium *Synechococcus* sp. J. Biosci. **37:** 635–645.

Mora, L., Bramley, P.M., and Fraser, P.D. (2013). Development and optimisation of a label-free quantitative proteomic procedure and its application in the assessment of genetically modified tomato fruit. Proteomics **13:** 2016–2030.

Neta-Sharir, I., Isaacson, T., Lurie, S., and Weiss, D. (2005). Dual role for tomato heat shock protein 21: Protecting photosystem II from oxidative stress and promoting color changes during fruit maturation. Plant Cell **17:** 1829–1838.

Pulido, P., Perello, C., and Rodriguez-Concepcion, M. (2012). New insights into plant isoprenoid metabolism. Mol. Plant **5:** 964–967.

Ravanello, M.P., Ke, D., Alvarez, J., Huang, B., and Shewmaker, C.K. (2003). Coordinate expression of multiple bacterial carotenoid genes in canola leading to altered carotenoid production. Metab. Eng. **5:** 255–263.

Robertson, F.P., Koistinen, P.K., Gerrish, C., Halket, J.M., Patel, R.K.P., Fraser, P.D., and Bramley, P.M. (2012). Proteome changes in tomato lines transformed with phytoene synthase-1 in the sense and antisense orientations. J. Exp. Bot. **63:** 6035–6043.

Römer, S., Fraser, P.D., Kiano, J.W., Shipton, C.A., Misawa, N., Schuch, W., and Bramley, P.M. (2000). Elevation of the provitamin A content of transgenic tomato plants. Nat. Biotechnol. **18:** 666–669.

Rosso, S.W. (1967). An ultrastructural study of the mature chromoplasts of the tangerine tomato (*Lycopersicon esculentum* var. "golden jubilee"). J. Ultrastruct. Res. **20:** 179–189.

Rosso, S.W. (1968). The ultrastructure of chromoplast development in red tomatoes. J. Ultrastruct. Res. **25:** 307–322.

Sandmann, G. (2009). Evolution of carotene desaturation: The complication of a simple pathway. Arch. Biochem. Biophys. **483:** 169–174.

Schweiggert, R.M., Steingass, C.B., Heller, A., Esquivel, P., and Carle, R. (2011). Characterization of chromoplasts and carotenoids of red- and yellow-fleshed papaya (*Carica papaya* L.). Planta **234:** 1031–1044.

Shimada, H., Kondo, K., Fraser, P.D., Miura, Y., Saito, T., and Misawa, N. (1998). Increased carotenoid production by the food yeast *Candida utilis* through metabolic engineering of the isoprenoid pathway. Appl. Environ. Microbiol. **64:** 2676–2680.

Shumskaya, M., and Wurtzel, E.T. (2013). The carotenoid biosynthetic pathway: Thinking in all dimensions. Plant Sci. **208:** 58–63.

Simkin, A.J., Gaffé, J., Alcaraz, J.P., Carde, J.P., Bramley, P.M., Fraser, P.D., and Kuntz, M. (2007). Fibrillin influence on plastid ultrastructure and pigment content in tomato fruit. Phytochemistry **68:** 1545–1556.

Spurr, A.R., and Harris, M. (1968). Ultrastructure of chloroplasts and chromoplasts in *Capsicum annuum* l. Thylakoid membrane changes during fruit ripening. Am. J. Bot. **55:** 1210–1224.

Szilágyi, A., Sommarin, M., and Akerlund, H.E. (2007). Membrane curvature stress controls the maximal conversion of violaxanthin to zeaxanthin in the violaxanthin cycle—Influence of alpha-tocopherol, cetylethers, linolenic acid, and temperature. Biochim. Biophys. Acta **1768:** 2310–2318.

Vasquez-Caicedo, A.L., Heller, A., Neidhart, S., and Carle, R. (2006). Chromoplast morphology and beta-carotene accumulation during postharvest ripening of Mango Cv. 'Tommy Atkins'. J. Agric. Food Chem. **54:** 5769–5776.

Wellburn, A. (1994). The spectral determination of chlorophylls a and b, as well as total carotenoids, using various solvents with spectrophotometers of different resolution. Plant Physiol. **144:** 307–313.

Wrischer, M., Prebeg, T., Magnus, V., and Ljubesic, N. (2007). Crystals and fibrils in chromoplast plastoglobules of *Solanum capsicastrum* fruit. Acta Bot. Croat. **66:** 81–87.

Xiao, Y.M., Savchenko, T., Baidoo, E.E.K., Chehab, W.E., Hayden, D.M., Tolstikov, V., Corwin, J.A., Kliebenstein, D.J., Keasling, J.D., and Dehesh, K. (2012). Retrograde signaling by the plastidial metabolite MEcPP regulates expression of nuclear stress-response genes. Cell **149:** 1525–1535.

Zhong, S., Fei, Z., Chen, Y.R., Zheng, Y., Huang, M., Vrebalov, J., McQuinn, R., Gapper, N., Liu, B., Xiang, J., Shao, Y., and Giovannoni, J.J. (2013). Single-base resolution methylomes of tomato fruit development reveal epigenome modifications associated with ripening. Nat. Biotechnol. **31:** 154–159.
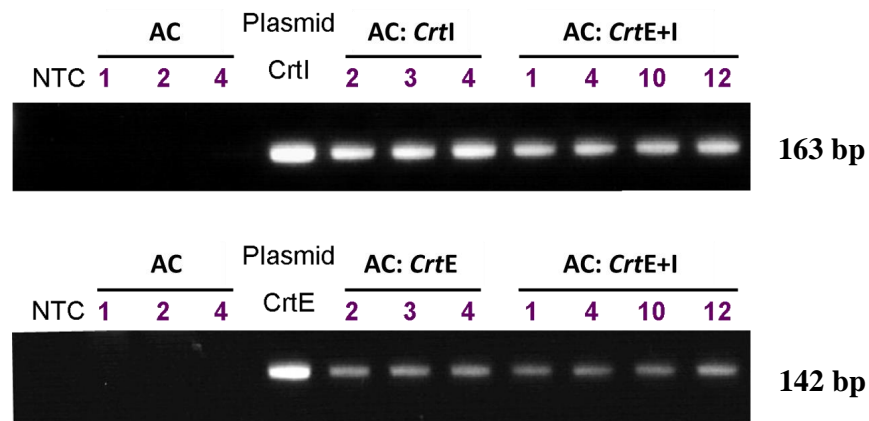
Supplemental Figure 1. PCR confirmation of the presence of *Crt*E and *Crt*I genes in the CrtE+I lines.

Amplication of *Crt*I (163 bp) and *Crt*E (142 bp) was performed by PCR on four plants of the *Crt*E+I genetic cross and visualized with a transilluminator. DNA was extracted from a pool of four representative leaves of each genotype. Purple numbers indicate biological replicates. NTC: non-template control; AC: Ailsa Craig tomato variety (wild type). The same approach was undertaken for *Crt*E+B and *Crt*B+I lines.
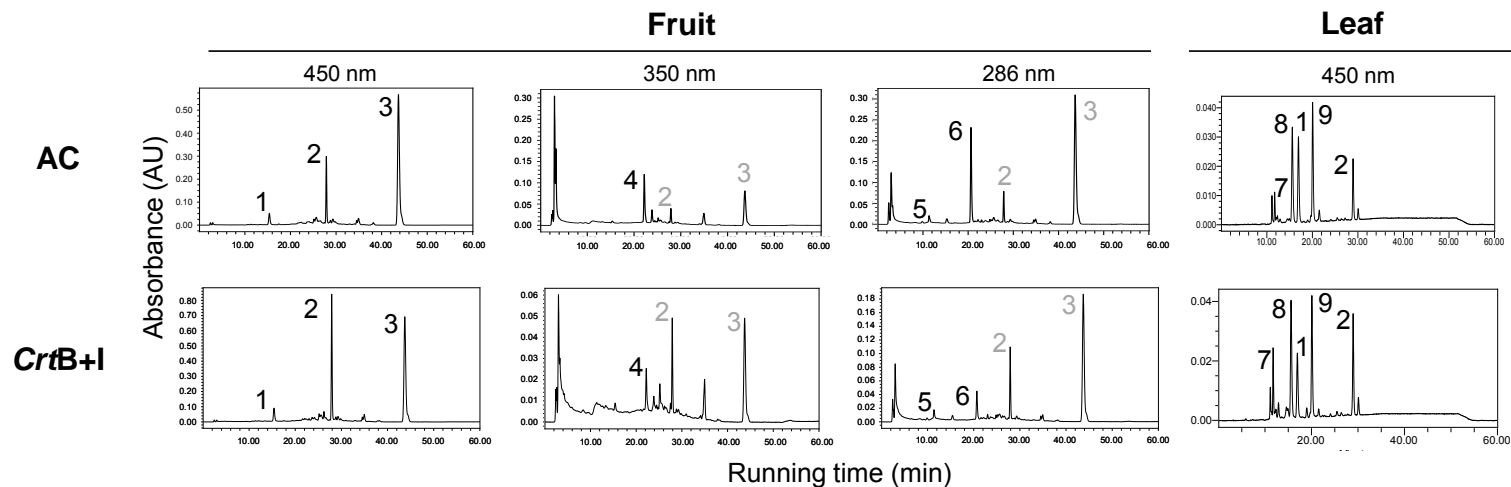
Supplemental Figure 2. Chromatographic profiles of carotenoids, chlorophylls and α-tocopherol of AC and *Crt*B+I tomatoes.

Metabolites were extracted from fruits and leaves as described in Methods and separated by HPLC. Metabolites were identified by their retention times and absorption spectra and quantified by integration of peak areas. 1. lutein; 2. β-carotene; 3. lycopene; 4. phytofluene; 5. α-tocopherol; 6. phytoene; 7. violaxanthin; 8. chlorophyll b; 9. chlorophyll a. Grey numbers indicate peaks, which were not quantified at the wavelength stated. AC is a wild type control line (Ailsa Craig) and the *Crt*B+I genotype contains phytoene synthase (CrtB) and phytoene desaturase (CrtI) in a homozygous state in the Ailsa Craig background.
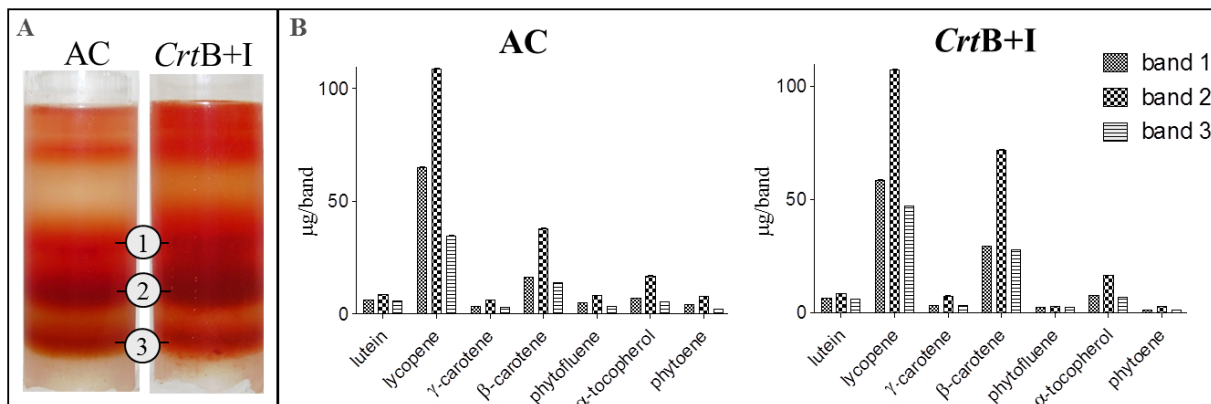
Supplemental Figure 3. Separation of chromoplast types on a sucrose gradient.

(A) Photograph of the sucrose gradient. The numbers 1, 2 and 3 represent the bands of separated chromoplasts.

(B) Carotenoid profile of AC and *Crt*B+I bands 1, 2 and 3.

Carotenoids contents are given as μg/volume of each band (mL). Methods used for determinations are described in Methods. Eight representative fruits from a combination of four plants were used. Three determinations were made per fruit, making eight biological and three technical replicates. The bars represent the mean ± SD. The *Crt*B+I homozygous line was used.

System 1   System 2

Homogenisation of tomatoes	**Chromoplasts isolation**
Filtration	
Addition of extraction buffer to the slurry	
Sedimentation by centrifugation at 5,000 g for 10 min	
Pellet resuspension in extraction buffer	
Sedimentation by centrifugation at 9,000 g for 10 min	

System 1	System 2	
Pellet resuspension in 45 % (w/v) sucrose buffer	Pellet resuspension in 0.6 M sucrose	**Chromoplasts lysis**
Homogenisation with a hand held potter		

System 1	System 2	
Separation on a discontinuous sucrose gradient (45%, 38 %, 20%, 15% and 5% ; w/v)	Sedimentation by centrifugation at 100,000 g for 1h	**Isolation and separation of sub-chromoplast compartments**
Sedimentation by centrifugation at 100,000 g for 17h	Collection of the red-colored supernatant containing plastoglobules and crystals	
Gradient fractions collection	Pellet resuspension in 45% (w/v) sucrose buffer	
	Separation on a discontinuous sucrose gradient (45%, 38 %, 20%, 15% and 5% , w/v)	
	Sedimentation by centrifugation at 100,000 g for 17h	
	Gradient fractions collection	

Supplemental Figure 4. Schematic representation of the systems (1 and 2) used to fractionate chromoplasts and isolate their respective sub-membrane compartments.

The scheme shows the different chromoplasts fractionation systems used. System 1 isolates intact chromoplasts, which are subsequently lysed and their sub-membrane compartments separated over the sucrose density gradient described. System 2 isolates intact chromoplasts initially, and subsequently, the chromoplast membranes (pellet) and the majority of the chromoplasts plastoglobules and crystals (supernatant). The sub-membrane compartments of the chromoplast membranes are then separated over the sucrose density gradient described. Grey rectangles correspond to the steps, which are unique to system 2. Details of the respective methods are provided in the Methods section.

Supplemental Figure 5. Principal components analysis of all metabolites detected in AC and *Crt*B+I tomato lines.

(A) in fruit; (B) in leaves. A minimum of three biological and three technical replicates were analyzed for each independent experiment. Metabolite levels from the different analytical platforms were combined. Lipid values correspond to the sum of the total fatty acid values obtained by GC-MS. The C*rt*B+I homozygous line was used.
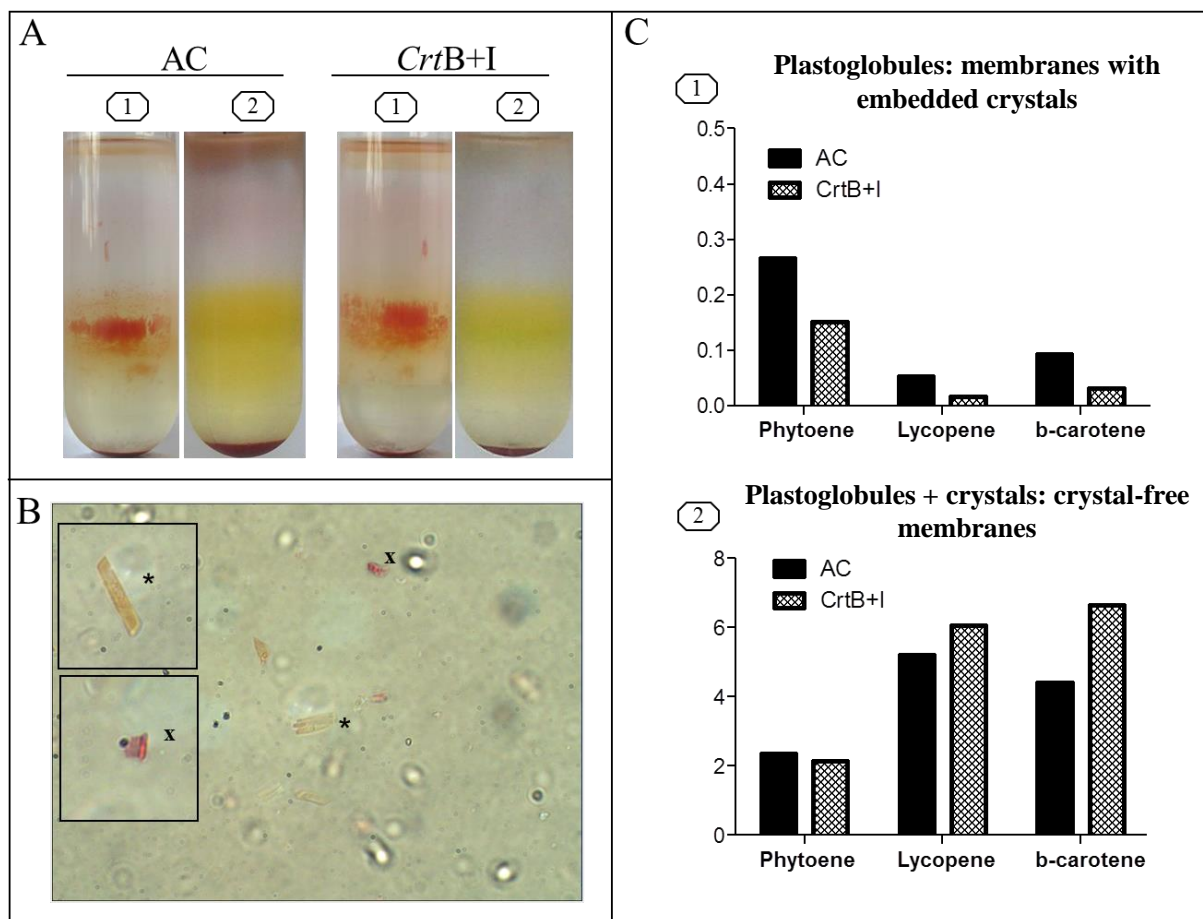
Supplemental Figure 6. Evidence and importance of the carotenoid crystals embedded in the chromoplast membranes.

A. Fractionation of AC and *Crt*B+I chromoplasts using two different systems. The sub-compartments of chromoplasts are separated on a discontinuous sucrose gradient in system 1 (tube 1). In system 2 (tube 2), before separation on the same sucrose gradient, the chromoplast sub-compartments are sedimented by centrifugation in a 0.6 M sucrose solution. A red sector (supernatant containing plastoglobules and crystals) was created at the top of the gradient while the chromoplast membranes pelleted. Only the membranes were separated on the second gradient. The fractionation systems are described in Methods and in Supplemental Figure 4. For both experiments, 150 g of breaker + 3 to 5 day tomatoes were used. B. Light microscopy photographs of the red sector obtained during the first step of the chromoplast fractionation system 2. Magnification 600X. x, membrane-free red crystal (possibly lycopene crystal); *, membrane-free orange crystal (possibly β-carotene crystal). C. Importance of crystals on carotenoid content. Phytoene, lycopene and β-carotene contents have been quantified and compared in different sectors of the gradient from both systems. The analysis was performed on pooled samples from multiple fractionations. The technical error was within 10%. The ratio of plastoglobules to membranes with embedded crystals is determined for each carotenoid studied in system 1. The ratio of plastoglobules plus crystals to crystal-free membranes is then calculated for system 2. The *Crt*B+I homozygous line was used.

Line	Pericarp				Jelly				Columella			
	AC	*Crt*B	*Crt*I	*Crt*B+I	AC	*Crt*B	*Crt*I	*Crt*B+I	AC	*Crt*B	*Crt*I	*Crt*B+I
Lutein	155 ± 5	$\mathbf{133 \pm 1^*}$	151 ± 2	158 ± 3	151 ± 1	146 ± 2	143 ± 6	144 ± 6	128 ± 1	$\mathbf{123 \pm 1^*}$	135 ± 4	133 ± 4
Lycopene	1155 ± 120	$\mathbf{2021 \pm 67^*}$	$\mathbf{1358 \pm 58^*}$	1201 ± 14	226 ± 31	249 ± 28	184 ± 11	192 ± 47	527 ± 26	$\mathbf{1191 \pm 22^{***}}$	491 ± 48	417 ± 60
γ-Carotene	99 ± 4	85 ± 10	89 ± 10	88 ± 4	71 ± 6	61 ± 2	72 ± 5	70 ± 6	90 ± 2	$\mathbf{68 \pm 2^{**}}$	$\mathbf{80 \pm 2^*}$	77 ± 6
β-Carotene	344 ± 21	$\mathbf{246 \pm 8^*}$	$\mathbf{685 \pm 38^*}$	$\mathbf{826 \pm 69^*}$	342 ± 28	302 ± 17	$\mathbf{505 \pm 45^*}$	$\mathbf{541 \pm 44^*}$	304 ± 20	230 ± 12	$\mathbf{658 \pm 18^{***}}$	$\mathbf{775 \pm 70^{***}}$
Phytofluene	188 ± 6	199 ± 16	$\mathbf{67 \pm 3^{***}}$	$\mathbf{67 \pm 1^{**}}$	0 ± 0	0 ± 0	0 ± 0	0 ± 0	113 ± 2	$\mathbf{142 \pm 6^*}$	$\mathbf{66 \pm 3^{***}}$	$\mathbf{67 \pm 11^*}$
Phytoene	177 ± 5	145 ± 8	$\mathbf{54 \pm 5^{***}}$	$\mathbf{60 \pm 5^{***}}$	22 ± 2	21 ± 2	18 ± 1	19 ± 2	99 ± 2	89 ± 11	$\mathbf{40 \pm 7^*}$	$\mathbf{40 \pm 15^*}$
Total CAR	2118 ± 138	$\mathbf{2828 \pm 99^*}$	2403 ± 235	2400 ± 81	811 ± 103	774 ± 16	922 ± 57	965 ± 62	1259 ± 34	$\mathbf{1845 \pm 39^*}$	$\mathbf{1472 \pm 35^*}$	1509 ± 62
α-Tocopherol	309 ± 16	309 ± 5	378 ± 61	$\mathbf{421 \pm 6^*}$	209 ± 17	250 ± 8	274 ± 34	239 ± 20	291 ± 9	248 ± 15	313 ± 59	282 ± 25

Supplemental Table 1. Carotenoid content in the pericarp, jelly and columella tissues of ripe fruit derived from the genetic crosses containing different gene combinations.

Carotenoid contents are presented as µg/g DW. Methods used for these determinations are described in Methods. Determinations were made from three independent pools of three fruits, each pool with three technical replicates. The mean data are presented with ± SD; Dunnett's test was used to determine significant differences between the wild type background (AC) and the transgenic varieties for each compound. Values in bold indicate significant differences. P<0.05, P<0.01 and P<0.001 are designated by *****, ******, and *******, respectively. CAR., carotenoid. The *Crt*B+I homozygous line was used.

| Fatty acid | Ratio % in *Crt* B+I to % in AC | | | | |
	PS/PC	PE	DGDG	MGDG	Triglycerides
12:0	-	-	-	0.48 ± 0.08	1.42 ± 0.61
14:0	0.45 ± 0.07	0.77 ± 0.10	0.68 ± 0.10	0.46 ± 0.08	1.70 ± 1.37
16:0	**1.08 ± 0.03**	1.02 ± 0.05	1.07 ± 0.07	**10***	0.72 ± 0.24
16:1 cis-9	**0.01#**	**0.01#**	-	**10***	7.69 ± 0.48
18:0	1.00 ± 0.20	1.20 ± 0.45	0.83 ± 0.04	0.54 ± 0.18	1.42 ± 0.45
18:1 cis-9	0.64 ± 0.55	**10***	-	3.96 ± 1.92	0.99 ± 0.38
18:1 trans-9	**10***	**10***	-	-	-
18:2 trans-9,12	1.06 ± 0.06	0.94 ± 0.06	1.17 ± 0.22	0.24 ± 0.14	0.95 ± 0.11
20:0	0.86 ± 0.09	**0.67 ± 0.09**	0.89 ± 0.79	1.23 ± 0.98	**1.51 ± 0.39**
22:0	-	-	-	-	2.10 ± 0.37
22:2 cis-13,16	-	-	-	-	1.45 ± 0.05
24:0	0.31 ± 0.03	**0.52 ± 0.10**	-	**0.01#**	1.51 ± 0.46

Supplemental Table 2. Changes in the composition (in percentage) of fatty acids present in the lipids species found in *Crt*B+I and control AC.

Values represent the percentage ratio of each fatty acid in *Crt*B+I compared to the AC background. The ratio data are presented as ± SD. Student's t-test was carried out. The significant changes are shown in bold (p-value < 0.05). Lipids were extracted from a mix of 3 ripe tomato fruits. Lipids were then separated on a TLC plate. Three technical replicates were used. **10***, theoretical value when a fatty acid is unique to *Crt*B+I**; 0.01#**, theoretical value when a fatty acid is unique to AC, - indicates fatty acids not detected in both *Crt*B+I and AC at the sample concentration used; PS/PC, phosphatidylserine/phosphatidylcholine; PE, phosphatidylethanolamine; DGDG; digalactosyldiacylglycerol; MGDG, monogalactosyldiacylglycerol. *Crt*B+I homozygous line was used.

Band number[1]	Acc.No[2]	Protein Name	Score[3]	Location[4]
1	PG1_PEA	Plastoglobulin-1, chloroplastic	73	Chloroplast › plastoglobules periphery
2	LIPC_SOLTU	Light-induced protein, chloroplastic	750	Chloroplast thylakoid membrane
97% similarity with	Q0ZPA3_SOLLC	Plastid lipid associated protein CHRC		Chloroplast
3	ATPB_SOLLC	ATP synthase subunit β	750	Chloroplast thylakoid membrane; Peripheral membrane protein
4	PSAD_SOLLC	Photosystem I reaction center subunit II	187	Chloroplast thylakoid membrane
5	PSBS_SOLLC	Photosystem II 22 kDa protein	331	Chloroplast thylakoid membrane
6	PSBO_SOLLC	Oxygen-evolving enhancer protein 1	170	Chloroplast thylakoid membrane
7	PSBP_SOLLC	Oxygen-evolving enhancer protein 2	853	Chloroplast thylakoid membrane
8	HSP72_SOLLC	Heat shock cognate 70 kDa protein 2	1003	N/A
94% similarity with	HSP7E_SPIOL	70 kDa heat shock-related protein		Chloroplast envelope
9	RUBB_BRANA	RuBisCO large subunit-binding protein subunit β	501	Chloroplast

Supplemental Table 3. Identification of proteins from the isolated fractions by nESI-LC-MS/MS.

The protein band number refers to the number showed in Figure 6, B (i). [1] The homology of bands 2 and 8 with *Solanum lycopersicum* species was studied and the percentage of similarity and accession number of the closest protein are shown. [2] Accession number according to SwissProt protein database. [3] Score obtained in Mascot search. Scores higher than 51 indicate identity or extensive homology (p<0.001).[4] According to UniProt (http://www.uniprot.org/).

Gene ID	Accession number	Primers sequences	
		Forward	Reverse
GGPPS-1	DQ267902	GACAGCATCTGAGTCCGTCA	CTTGGCCAGGACAGAGTAGC
GGPPS-2	SGNU223568	GGGATTGGAAAAGGCTAAGG	AGCAATCAATGGAGCAGCTT
PSY-1	Y00521	TGGCCCAAACGCATCATATA	CACCATCGAGCATGTCAAATG
PSY-2	L23424	GTTGATGGCCCTAATGCATCA	TCAAGCATATCAAATGGCCG
PDS	X59948	GTGCATTTTGATCATCGCATTGA	GCAAAGTCTCTCAGGATTACC
ZDS	AF195507	TTGGAGCGTTCGAGGCAAT	AGAAATCTGCATCTGGCGTATAGA
CRTISO	AF416727	TTTTGGCGGAATCAACTACC	GAAAGCTTCACTCCCACAGC
LCY-E	Y14387	AACACTTGCATTTGGTGCTG	AGTACAGAGGCGCATTTTGG
LCY-B	AF254793	TCGTTGGAATCGGTGGTACAG	AGCTAGTGT CCTTGCCACCAT
CYC-B	Y18297	GTTATTGAGGAAGAGAAATGTGTGAT	TCCCACCAATAGCCATAACATTTT
CRTR-B1	Y14809	CTCGAGGATGAGAAGCTGAAACCTC	GCCAAGCGAGTAGCTAAGATCTGTT
CRTR-B2	DQ864755	TTTCTCAGTCCAAAATCCGCCTCAA	TCATTCTCCAGCACAAAACAAACCG
ZEP-1	Z83835.1	TTGGGGTTTTAGGAGGCAATG	CCCGCAGGTAAAAGTAACCA
CRTE	D90087.2	AACTGCTGGACGATTTGACC	TCACTGGCAAGCTGAAGA
CRTB	D90087.2	CGCCTGTGACCTTGGGCTGG	GGCTCAGCGCCTGACGGTTT
CRTI	D90087.2	AGCCATATGGAAACGACAGG	TCTGCAGTTTGTTGGACTGC

Supplemental Table 4. Sequences of primers used in real-time PCR and PCR.

GGPPS-1, 1-geranylgeranyl pyrophosphate synthase-1; GGPPS-2, 1-geranylgeranyl pyrophosphate synthase-2; PSY-1, phytoene synthase-1; PSY-2, phytoene synthase 2; PDS, phytoene desaturase; ZDS. ζ-carotene desaturase; CRTISO, carotene isomerase; LCY-E, ε-lycopene cyclase; LCY-B, β-lycopene cyclase; CYC-B, β-lycopene cyclase; CRTR-B1, carotene β- hydroxylase 1; CRTR-B2, carotene β-hydroxylase 2; ZEP-1, zeaxanthin epoxidase-1; CRTE, geranylgeranyl pyrophosphate synthase; CRTB, phytoene synthase; CRTI, phytoene desaturase.